7th Conference
of the
International Marangoni Association

June 23–26, 2014

Vienna University of Technology

Scientific Committee

M. Bestehorn (Germany)
C. Dang Vu-Delcarte (France)
A. Gelfgat (Israel)
B. Houchens (USA)
H.C. Kuhlmann (Austria)
Q.-S. Liu (China)
A. Mizev (Russia)
J.M. Montanero (Spain)
K. Nishino (Japan)
A. Oron (Israel)
H. Riegler (Germany)
R. Savino (Italy)
D. Schwabe (Germany)
V. Shevtsova (Belgium)
V. Starov (UK)
I. Ueno (Japan)

Advisory Committee

H.C. Kuhlmann (TU Wien)
A. Oron (Technion, Haifa)
C. Dang Vu-Delcarte (Univ. Paris-Sud 11)

Local Organizing Committee

H.C. Kuhlmann (TU Wien)
F. Romanò (TU Wien)
T. Loimer (TU Wien)
C. Umundum (TU Wien)
K. Cernohorsky (TU Wien)
B. Zerkhold (TU Wien)

Web Page: `http://ima7.conf.tuwien.ac.at/`

Supported by

ERCOFTAC
Magistrat der Stadt Wien

Printed by Grafisches Zentrum HTU GmbH

Contents

Part I

THE CONFERENCE

General Information

Venue

The conference is held at the Vienna University of Technology at the heart of Vienna. Lectures will be given in the *Kuppelsaal* which is located under the roof right above the main entrance of the old main building of the university. The *Kuppelsaal* can be reached by a 3 minutes walk from the subway station *Karlsplatz*.

Contact Address

Prof. Dr. Hendrik Kuhlmann
Institute of Fluid Mechanics and Heat Transfer
Vienna University of Technology
Resselgasse 3/1/2
1040 Vienna
Austria
Phone: +43-1-58801-32224
Fax: +43-1-58801-32298
e-mail: ima7@tuwien.ac.at

Registration Desk

The registration desk is located on the floor just below the *Kuppelsaal* (3rd floor of the main university building, look at the map in the last part). The opening hours will be:

Sunday	June 22	17:00–20:00
Monday	June 23	08:30–12:00
Tuesday	June 24	09:00–12:00
Wednesday	June 25	09:00–12:00
Thursday	June 26	09:00–12:00

Internet and Communication

A guest account will be provided for each participant to have a free wireless connection in Vienna University of Technology. The credential to have access to such accounts should be asked at the registration desk.

Information for Presenting Authors

- Please contact the chairman of your session before the session starts. He must make sure that all presenting authors are present.
- Please stick to the time table. The time available for oral presentations is 15 minutes including discussion, for poster presentation it is 3 minutes.
- For poster presentation, please check the relative board code written in the poster sessions' program.
- If you have a computer presentation, please transfer your presentation to the conference laptop in the *Kuppelsaal*. Please make sure that all features of your presentation are working correctly. You can transfer your presentation to the conference laptop from 08:00 to 08:30 in the morning, or from 13:00 to 14:00. Alternatively, if you want to use your personal laptop, please make sure that it is well adaptable to the projection system in the *Kuppelsaal*. Any delay will reduce your presentation time.

Information for Chairs

- Please reserve 3 minutes for the discussion at the end of each oral presentation.
- Poster presentations do not need to reserve any official time for discussion.
- Please keep the schedule strictly.

Phone Numbers

General

Austria country code: +43
Vienna area code: (0)1
For calls to another country, first dial 00 and then the country code.

Local phone numbers for calls from Vienna

Emergency	144
Police	133
Fire	122
General Hospital (AKH)	40400 - 0
Tourist office	588 660
Vienna University of Technology	58801-0
Porter, Karlsplatz	58801-40001
Porter, Gußhausstrasse	58801-40003
Porter, Freihaus	58801-40004

Airlines

Vienna International Airport and Departure Information: 7007-22233

The following phone numbers are valid for calls from Vienna (number beginning with 7007 refer to offices directly located at Vienna Intl Airport).

Aeroflot	5121501
Air Berlin	0820 737 800
Air China	5868008
Air France	502 222 400
Air One	+39 0912551047
Alitalia	0820 951 051
American Airlines	795 67 156
Austrian Airlines	05 1766 1000
Belavia	7007 36334
British Airways	79567567
China Airlines	813 0156
Delta Air Lines	0820 95 1001
El Al	7007 32400
Emirates	2060 91 999
Iberia	79567722
JAL	5029 17777
KLM	820 420 414
Lufthansa	0810 10 25 80 80
NIKI	0820 737 800
Qatar Airways	2530 22142
Turkish Airlines	0810 222 849

Program Overview

Mon. June 23	08:30–09:00	Registration & Coffee	
	09:00–09:15	Opening Session	
	09:15–10:00	1.1 - Electric-Field Effects	(Chair: Mikishev A.)
	10:00–10:35	1.2 - Posters	(Chair: Kuhlmann H.)
	10:35–11:00	Coffee Break	
	11:00–12:00	1.3 - Droplet Motion and Migration	(Chair: Doumenc F.)
	12:00–14:00	Lunch Break	
	14:00–15:00	1.4 - Thermocapillary Liquid Bridges	(Chair: Schwabe D.)
	15:00–15:35	1.5 - Posters	(Chair: D'Alessio S.)
	15:35–16:00	Coffee Break	
	16:00–17:45	1.6 - Evaporation and Condensation	(Chair: Melnikov D. & Riegler H.)
	17:45–18:00	IMA8 - Presentation	(Bestehorn M.)
	19:30–21:00	Reception at the Mayor's House	
Tue. June 24	09:00–10:00	2.1 - Liquid Film Experiments	(Chair: Mizev A.)
	10:00–10:35	2.2 - Posters	(Chair: Montanero J.M.)
	10:35–11:00	Coffee Break	
	11:00–12:00	2.3 - Contact-Line Dynamics	(Chair: Bestehorn M.)
	12:00–14:00	Lunch Break	
	14:00–15:30	2.4 - Droplet Manipulation	(Chair: Liu Q.-S. & Khayat R.)
	15:30–16:00	Coffee Break	
	16:00–18:00	2.5 - Interfacial Deformation	(Chair: Lyubimova T. & Dietze G.)
Wed. June 25	09:00–10:30	3.1 - Marangoni Instability	(Chair: Imaishi N. & Köllner T.)
	10:30–11:00	Coffee Break	
	11:00–12:00	3.2 - Droplet Coalescence	(Chair: Borcia R.)
	12:00–22:00	Wachau River-Boat Trip	
Thu. June 26	09:00–10:30	4.1 - Long Waves and Heat Transfer	(Chair: Starov V. & Duan F.)
	10:30–11:00	Coffee Break	
	11:00–12:00	4.2 - Solutocapillary Layers	(Chair: Oron A.)
	12:00–14:00	Lunch Break	
	14:00–15:30	4.3 - Surface-Tension-Driven Flows	(Chair: Shevtsova V. & Yiantsios S.)
	15:30–16:00	Coffee Break	
	16:00–18:00	4.4 - Falling Films	(Chair: Schneider W. & Kondic L.)
	18:00–18:20	Adjourn	

Full Program

Sunday, June 22

17:00–20:00 **Arrival, Get Together & Registration**

Monday, June 23

08:30–09:00 **Registration & Coffee**

09:00–09:15 **Opening Session**

09:15–10:00 **Session 1.1 - Electric-Field Effects**
(Chairman: Mikishev A.)

09:15–09:30 Maxwell stress long wave instabilities in a thin aqueous film under time-dependent electro-osmotic flow.
M. Mayur and S. Amiroudine

09:30–09:45 Temperature based weak ac field enhanced patterns formation in vertical deposition of colloids.
R. Aslam, M. Pichumani and W. González-Viñas

09:45–10:00 Experimental investigation of the instability between two immiscible fluids flowing in a microchannel in the presence of an electric field.
P. Eribol and A. K. Uguz

10:00–10:35 **Session 1.2 - Posters**
(Chairman: Kuhlmann H.)

10:35–11:00 **Coffee Break**

11:00–12:00 **Session 1.3 - Droplet Motion and Migration**
(Chairman: Doumenc F.)

11:00–11:15 Numerical simulation of the Marangoni effect on transient mass transfer from a single moving deformable drop.
J. Chen, X. Feng, P. Fan, C. Yang and Z.-S. Mao

11:15–11:30 Control of drop motion by mechanical vibrations.
M. Bestehorn

11:30–11:45 A phase field description of ratchet-like motion of a shaken drop.
R. Borcia, I. D. Borcia and M. Bestehorn

11:45–12:00 Thermocapillary effect on migration of micro-droplet along a non-uniform thermal substrate.
X. Chen, Q.-S. Liu, Z.-Q. Zhu, Y.-N. Sun and Y.-D. Yu

12:00–14:00	**Lunch Break**
14:00–15:00	**Session 1.4 - Thermocapillary Liquid Bridges** (Chairman: Schwabe D.)
14:00–14:15	Instabilities of structured metal films on nanoscale. *L. Kondic, N. Dong, Y. Wu, S. Fu, J. Fowlkes and P. Rack*
14:15–14:30	Time-scale estimates for particle accumulation in thermocapillary liquid bridges. *H. C. Kuhlmann and F. H. Muldoon*
14:30–14:45	Spatial and kinematic topology within an ensemble of particles in a thermocapillary flow in a liquid bridge. *D. Melnikov, T. Watanabe, D. Pushkin, V. Shevtsova and I. Ueno*
14:45–15:00	Particle-size effect in the formation of particle-depletion zones in thermocapillary liquid bridges. *T. Lemee and H. C. Kuhlmann*
15:00–15:35	**Session 1.5 - Posters** (Chairman: D'Alessio S.)
15:35–16:00	**Coffee Break**
16:00–17:45	**Session 1.6 - Evaporation and Condensation** (Chairmen: Melnikov D. & Riegler H.)
16:00–16:15	The stabilizing effect of mass loss on an evaporating thin liquid film due to the vapor concentration gradient. *K. Kanatani*
16:15–16:30	Effect of a constant heat source on evaporative instability in a solid-liquid-vapor system. *A. Karacelik, R. Narayanan and K. Uguz*
16:30–16:45	Jumping pool boiling into mesoscopic structures of monodispersed microspheres. *A. S. Dmitriev, M. A. El Bouz and P. G. Makarov*
16:45–17:00	Coalescing droplets with suspended particles in a tube creeping flow. *M. Muraoka, T. Kamiyama, T. Wada, I. Ueno and H. Mizoguchi*
17:00–17:15	Thermocapillary convection in the evaporation droplets. *B. He and F. Duan*
17:15–17:30	Evolution of thermo-convective flows in liquid bridges due to evaporation. *Y. Gaponenko and V. Shevtsova*
17:30–17:45	Flow regimes in a cylindrical macropore. *P. Beltrame and S. Sammartino*
17:45–18:00	**IMA8 - Presentation** (Bestehorn M.)
19:30–21:00	**Reception at the Mayor's House**

Tuesday, June 24

09:00–10:00 **Session 2.1 - Liquid Film Experiments**
(Chairman: Mizev A.)

09:00–09:15 Experimental study on pulsating heat pipe using self-rewetting fluid as a working fluid (visualization of thin liquid film and surface wave).
K. Fumoto, T. Ishida, K. Yamagami, T. Kawanami and T. Inamura

09:15–09:30 Flow structures in a double free-surface film with small imposed Marangoni numbers.
B. Messmer, T. Lemee, K. Ikebukuro, K. Edwin, I. Ueno and R. Narayanan

09:30–09:45 Foam drainage: experimental study and numerical simulations.
A. Bureiko, N. Kovalchuk, A. Trybala, O. Arjmandi-Tash and V. Starov

09:45–10:00 Dynamic wetting failure and air entrainment: what can thin-film models teach us?
E. Vandre, M. S. Carvalho and S. Kumar

10:00–10:35 **Session 2.2 - Posters**
(Chairman: Montanero J.M.)

10:35–11:00 **Coffee Break**

11:00–12:00 **Session 2.3 - Contact-Line Dynamics**
(Chairman: Bestehorn M.)

11:00–11:15 Salt-induced Marangoni flow in evaporating sessile droplets.
V. Soulié, S. Karpitschka, F. Lequien, T. Zemb, H. Möhwald and H. Riegler

11:15–11:30 Contact line motion of a volatile liquid in an inert gas.
V. Janecek, F. Doumenc, V. Nikolayev and B. Guerrier

11:30–11:45 Self-induced Marangoni flow in alcoholic binary mixtures.
C. Buffone, A. Cecere and R. Savino

11:45–12:00 Convective/capillary deposition of charged nanoparticles directed by receding contact lines: effect of collective diffusion and hydration forces.
D. Noguera-Marin, C. L. Moraila-Martinez, M. A. Cabrerizo-Vilchez and M. A. Rodriguez-Valverde

12:00–14:00 **Lunch Break**

14:00–15:30 **Session 2.4 - Droplet Manipulation**
(Chairmen: Liu Q.-S. & Khayat R.)

14:00–14:15 Impact of complex drops onto surfaces: particle distribution.
V. Grishaev, C. S. Iorio and A. Amirfazli

14:15–14:30 Drops on cylindrical surfaces.
I. D. Borcia, R. Borcia, M. Bestehorn, C. Borcia, N. Dumitrascu and C. Egbers

14:30–14:45 Droplet formation in thin liquid layers under the action of the laser-induced solutocapillary flows.
N. A. Ivanova

14:45–15:00 Deformation of long slender non-newtonian drop in shear flow.
O. M. Lavrenteva, M. Favelukis and A. Nir

15:00–15:15 Non-negligible Marangoni part in convective transport of heavy vapor from a highly volatile pendant droplet on a wafer.
A. Rednikov, S. Dehaeck and P. Colinet

15:15–15:30 Drop transfer between two surfaces.
H.Chen, T.Tang and A.Amirfazli

15:30–16:00 **Coffee Break**

16:00–18:00 **Session 2.5 - Interfacial Deformation**
(Chairmen: Lyubimova T. & Dietze G.)

16:00–16:15 An overview of thermo-vibrational instabilities in near-critical fluids.
G. Gandikota, S. Amiroudine, Chatain D., Lyubimova T. P. and Beysens D.

16:15–16:30 Interfacial instabilities between miscible fluids under horizontal vibrations.
V. Shevtsova, Y. Gaponenko, M. Torregrosa, V. Yasnou and A. Mialdun

16:30–16:45 Dynamical stability of a liquid bridge.
C. Ferrera, J. M. Montanero, M. A. Herrada, M. Torregrosa and V. Shevtsova

16:45–17:00 Two-frequency excitation of single-mode Faraday waves.
W. Batson, F. Zoueshtiagh and R. Narayanan

17:00–17:15 The dynamics of hydraulic jumps in a viscous liquid flowing down an inclined plate.
E. S. Benilov and V. N. Lapin

17:15–17:30 A numerical study of electrohydrodynamic patterning of viscoelastic materials.
G. Karapetsas and V. Bontozoglou

17:30–17:45 On the interplay between inertia and shear thinning for free-surface jet flow near channel exit.
R. E. Khayat

17:45–18:00 Free surface flow simulation with application to bluff body flow control.
S. Kocabiyik and C. Bozkaya

Wednesday, June 25

09:00–10:30 **Session 3.1 - Marangoni Instability**
(Chairmen: Imaishi N. & Köllner T.)

09:00–09:15 Experimental and numerical observations of surface deformation during drying of polymer solutions due to Marangoni phenomena.
S. G. Yiantsios, S. K.Serpetsi, F. Doumenc, S. Mergui and B. Guerrier

09:15–09:30 Wavelet analysis of imperfect symmetries of nonlinear patterns in Marangoni flows.
I. I. Wertgeim and V. G. Zakharov

09:30–09:45 Long-wave Marangoni convection in a binary-liquid layer with Soret effect and surfactant adsorption/desorption.
M. Morozov, A. Nepomnyashchy and A. Oron

09:45–10:00 From linear to highly non-linear steady-state pattern bifurcation diagrams in confined surface-tension-driven-convection.
M. Medale and P. Cerisier

10:00–10:15 Effects of external shield on particle accumulation structure (PAS) due to thermocapillary effect in a half-zone liquid bridge.
M. Gotoda, T. Sano, T. Kaneko and I. Ueno

10:15–10:30 Benard-Marangoni instability in a fluid with a deformable free surface.
D. V. Lyubimov, T. P. Lyubimova, N. I. Lobov and A. E. Samoilova

10:30–11:00 **Coffee Break**

11:00–12:00 **Session 3.2 - Droplet Coalescence**
(Chairman: Borcia R.)

11:00–11:15 Drop coalescence and drop shape: influence of Marangoni flows.
S. Karpitschka and H. Riegler

11:15–11:30 Marangoni instability driving motion, deformation and fission of an oil drop on a surfactant solution.
J. Irvoas, K. Eckert, K. Schwarzenberger, C. Antoine, M. Brost and V. Pimienta

11:30–11:45 Marangoni flow during coalescence of sessile drops: liquids with a precipitation reaction.
M. Jehannin, S. Karpitschka, S. Charton, H. Möhwald, T. Zemb and H. Riegler

11:45–12:00 Interfacial instability arisen on vapor bubble in subcooled pool.
I. Ueno, J. Ando, T. Saiki and T. Kaneko

12:00–22:00 **Wachau River-Boat Trip**

Thursday, June 26

09:00–10:30 **Session 4.1 - Long Waves and Heat Transfer**
(Chairmen: Starov V. & Duan F.)

09:00–09:15 Thermal coupling between two liquid films undergoing long-wavelength instabilities.
M. Vécsei, M. Dietzel and S. Hardt

09:15–09:30 On dynamic excitation of Marangoni instability of deformable liquid layer with insoluble surfactant.
A. B. Mikishev and A. A. Nepomnyashchy

09:30–09:45 Healing of an axisymmetric thin liquid film on a harmonically oscillating horizontal cylindrical surface.
O. Haimovich and A. Oron

09:45–10:00 Creating localized-droplet train by traveling thermal waves.
V. Frumkin, W. Mao, A. Alexeev and A. Oron

10:00–10:15 How to deal with negative surface heat capacities.
W. Schneider

10:15–10:30 Effect of groove angle and distance between grooves on the micro-jet forms.
C. Liu, Q.-J. Feng and X.-H. Liang

10:30–11:00 **Coffee Break**

11:00–12:00 **Session 4.2 - Solutocapillary Layers**
(Chairman: Oron A.)

11:00–11:15 Hierarchical Marangoni roll cells caused by mass transfer: direct numerical simulations and supporting experiments.
T. Köllner, K. Schwarzenberger, K. Eckert, S. Odenbach and T. Boeck

11:15–11:30 Interfacial spreading motions in 2-layer solutal Rayleigh-Marangoni convection: 3D direct numerical simulations and experiments.
T. Köllner, K. Schwarzenberger, T. Boeck and K. Eckert

11:30–11:45 Early Hofmeister series salt solutions: model formulation and linear stability analysis.
J. J. A. Conn, S. K. Wilson, D. Pritchard, B. R. Duffy, P. J. Halling and K. Sefiane

11:45–12:00 Buoyancy driven instabilities in miscible fluids.
J. Carballido-Landeira, P. M. J. Trevelyan, C. Almarcha and A. de Wit

12:00–14:00 **Lunch Break**

14:00–15:30 **Session 4.3 - Surface-Tension-Driven Flows**
(Chairmen: Shevtsova V. & Yiantsios S.)

14:00–14:15 Flow instabilities in annular pool of low Pr fluid.
N. Imaishi, M. Ermakov, W.Y. Shi, Y.R. Li and L. Peng

14:15–14:30 On instability of Marangoni convection on the surface of a surfactant solution.
A. Mizev and A. Trofimenko

14:30–14:45 A drying droplet spreads out its wings: thermo-capillary fingering.
R. De Dier, W. Sempels, J. Hofkens and J. Vermant

14:45–15:00 Space experiment on flow transition of Marangoni convection in liquid bridge with high Prandtl number.
S. Matsumoto and S. Yoda

15:00–15:15 Local corrosion of SiO_2(s) driven by Marangoni convection in the melting liquid surface systems.
Z. Yuan, Y. Wu, K. Mukai and B. Xu

15:15–15:30 Numerical methods for interfacial flows with high density ratios and high surface tension.
F. Denner and B. G. M. van Wachem

15:30–16:00 **Coffee Break**

16:00–18:00 **Session 4.4 - Falling Films**
(Chairmen: Schneider W. & Kondic L.)

16:00–16:15 The effects of variable fluid properties on thin film stability.
S. D'Alessio, C. Seth and J.-P. Pascal

16:15–16:30 Heat and mass transfer between a vertical flat absorbing falling liquid film and a gas flow in a channel.
B. Beladi and H. C. Kuhlmann

16:30–16:45 Dynamics of thin liquid films controlled by thermal fluctuations.
S. Nesic, R. Cuerno, E. Moro and L. Kondic

16:45–17:00 Investigation of the liquid film flows with evaporation by means of new mathematical models based on the general interface conditions.
O. N. Goncharova and E. V. Rezanova

17:00–17:15 Interfacial heat transfer of liquid film flows in narrow channels.
F. Denner, M. Vieweg, C. N. Markides, S. Kalliadasis and B. G. M. van Wachem

17:15–17:30 Direct and model-based simulations of three-dimensional falling liquid films: surface waves and associated flow structures.
G. F. Dietze, W. Rohlfs, K. Nährich, R. Kneer and B. Scheid

17:30–17:45 Thermally induced break-up of regularly excited three-dimensional surface waves on a vertical liquid film.
M. Rietz, W. Rohlfs and R. Kneer

17:45–18:00 An efficient numerical approach to systematically investigate the interfacial heat and mass transfer for wavy falling films.
E. Hofmann and H. C. Kuhlmann

18:00–18:20 **Adjourn**

Poster Sessions

Monday, June 23

10:00–10:35 **Session 1.2 - Posters**
(Chairman: Kuhlmann H.)

10:00–10:03 A1: Study of the acoustic surface waves propagation of porous silicon using different coupling fluids
S. Bouhedja and F. Hamdi

10:03–10:06 A2: Threshold initiation of solutocapillary Marangoni convection near air-bubble surface in horizontal rectangular channel.
M. O. Denisova, K. G. Kostarev, A. L. Zuev and A. Viviani

10:06–10:09 A3: Liquid layered phenomenon and initial droplet size distribution during explosive dispersal process.
Y. N. Shi, T. Hong, C.S. Qin and Q.J. Feng

10:09–10:12 A4: Instabilities of liquid crystal films.
L. Kondic, M. Lam, T.-S. Lin, U. Thiele and L. Cummings

10:12–10:15 A5: Rupture of liquid film placed on solid substrate and on deep liquid under action of thermal beam.
A. Ovcharova and N. Stankous

10:15–10:18 A6: Numerical investigation for the direction of thermocapillary flow in a cooled circular water film.
T. Yamamoto, Y. Takagi, Y. Okano and S. Dost

10:18–10:21 A7: Evolution of the thermocapillarity motion of three liquids in a flat layer.
V. Andreev and E. Cheremnih

10:21–10:24 A8: An index for evaluating the wettability alteration of reservoir rock toward more water wet condition by combined low salinity water and surfactant flooding.
M. Nourani, T. Tichelcamp and G. Øye

10:24–10:27 A9: Study of dynamics of drying processes in Fe_2O_3 and SiO_2 nanocolloid droplets.
A. S. Dmitriev and P. G. Makarov

10:27–10:30 A10: Self-patterning induced by a solutal Marangoni effect in a receding drying meniscus.
F. Doumenc and B. Guerrier

10:30–10:33 A11: Weakly nonlinear stability of Marangoni convection in a half-zone liquid bridge.
K. Fujimura

15:00–15:35 **Session 1.5 - Posters**
(Chairman: D'Alessio S.)

15:00–15:03 B1: Bifurcations of the rotation in the Marangoni layers.
V. A. Batishchev and V. A. Getman

15:03–15:06 B2: Oscillatory Marangoni instability in thin film heated from below.
A. E. Samoilova and N. I. Lobov

15:06–15:09 B3: Large-amplitude Marangoni convection in a binary liquid.
S. Shklyaev, A. A. Nepomnyashchy and A. Ivantsov

15:09–15:12 B4: Influence of surfactants on thermocapillary convection on the confined interfaces.
A. Mizev and A. Shmyrov

15:12–15:15 B5: On locally high-frequency modulated Marangoni convection.
A. B. Mikishev and I. I. Wertgeim

15:15–15:18 B6: Stability of stationary plane-parallel flow over a saturated porous medium.
T. P. Lyubimova, D. Baidina and E. Kolchanova

15:18–15:21 B7: Onset of Benard-Marangoni convection in a two-layer system with deformable fluid interface and fixed heat flux at the external boundaries.
T. P. Lyubimova, D. V. Lyubimov and Y. Parshakova

15:21–15:24 B8: Marangoni convection in liquid layer under alternating heat flux.
B. L. Smorodin and B. I. Myznikova

15:24–15:27 B9: A promising front tracking method with high order of accuracy.
P. Fan and C. Yang

15:27–15:30 B10: Thermocapillary effect on the dynamics of viscous beads on vertical fibre.
R. Liu and Q.-S. Liu

15:30–15:33 B11: Convective structures and diffusion in ternary isothermal liquid and gas mixtures.
V. Kossov, Y. Zhavrin, O. Fedorenko and G. Akylbekova

Tuesday, June 24

10:00–10:35 **Session 2.2 - Posters**
(Chairman: Montanero J.M.)

10:00–10:03 C1: Effect of liquid bridge shape on the oscillatory thermal Marangoni convection.
T. Yano and K. Nishino

10:03–10:06 C2: Experiments on falling water films in interaction with a counter-current air flow.
N. Kofman, S. Mergui and C. Ruyer-Quil

10:06–10:09 C3: Evaporation rate from mesoscopic structures of monodispersed microspheres: experimental and computer simulations.
A. F. Ginevskiy, A. S. Dmitriev and M. A. El Bouz

10:09–10:12 C4: Thermocapillary surface waves – reviewed.
C. Bach and D. Schwabe

10:12–10:15 C5: The effect of heat flux from bottom on the thermal convection of silicon melt in shallow annular pool.
F. Wang and L. Peng

10:15–10:18 C6: Flow instabilities in annular pool of medium Pr fluid effects of Bi_{top}, Bi_{bottom} and Bo_d.
N. Imaishi, M. Ermakov and W.Y. Shi

10:18–10:21 C7: Studying of fast interfacial loading of surfactants by PANDA.
W. Sempels, R. De Dier, J. Hofkens and J. Vermant

10:21–10:24 C8: Concentration Marangoni convection as a factor of self-assembly in evaporating picolitre sessile drop of binary solvent mixture.
P. V. Lebedev-Stepanov

10:24–10:27 C9: Numerical simulation of particle-laden droplet evaporation.
G. Son

10:27–10:30 C10: Janus droplet as a catalytic motor.
S. Shklyaev

10:30–10:33 C11: Numerical simulation of the isothermal dissolution of a single rising bubble in a liquid bath.
A. S. Mohamed, M. A. Herrada, J.M. López-Herrera and A. M. Gañán-Calvo

Social Program

Reception at the Town Hall

The reception will take place in the *Stadtsenatssitzungssaal* of the Town Hall of Vienna on Monday, June 23 at 19:30. The participants should access the *Stadtsenatssitzungssaal* from the street *Felderstrasse* (north side of the building) and enter in the *Feststiege I* (see the map in the last chapter). To get there, take U2 from the *Karlsplatz* and exit after 3 stops at the station *Rathaus*. Alternatively, the walking distance from the *Kuppelsaal* is about 30 minutes. Please note that you can enter the building only with the ticket which you can find in the conference folder.

Wachau River-Boat Trip and visit to a "Heurigen"

Participants joining the excursion on Wednesday, June 25, must gather no later than 12:00 at the bus parking lot on the *Wiedner Hauptrasse* just beside the *Evangelische Mittelschule* (see the map in the last chapter). A bus will take us to the town of Melk where we shall board at about 13:50. We shall go downstream on the Danube river and exit in Dürnstein, a famous picturesque wine village on the banks of the Danube. In a historic baroque ambience we shall enjoy a commented wine tasting and have a rustic traditional meal, characteristic for the type of Austrian guest houses called *Heurigen*. Later on, a bus will take us back to Vienna where we plan to arrive around 21:00.

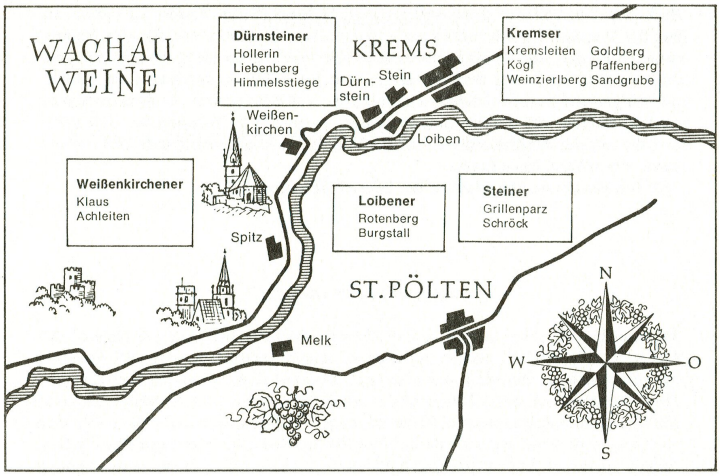

Part II

THE ABSTRACTS

An overview of thermo-vibrational instabilities in near-critical fluids

G. Gandikota,[1] S. Amiroudine,[2] D. Chatain,[1] T. Lyubimova,[3] and D. Beysens[1,4]

[1]*Service des Basses Températures, UMR-E CEA/UJF-Grenoble 1, INAC, 38054 Grenoble Cedex 9, France*
gurunath.sharma@gmail.com, denis.chatain@cea.fr, denis.hitz@cea.fr
[2]*Université Bordeaux 1, Institut de Mécanique et d'Ingénierie - TREFLE, UMR CNRS 5295, 33607 Pessac Cedex, France*
sakir.amiroudine@u-bordeaux1.fr
[3]*Institute of Continuous Media Mechanics UB RAS, 1, Koroleva Str., 614013, Perm, Russia*
lyubimovat@mail.ru
[4]*Physique et Mécanique des Milieux Hétérogènes, UMR 7636, CNRS, ESPCI, Universités Paris6 et Paris7, 75231 Paris, France*
daniel.beysens@espci.fr

The interaction of a thermal boundary layer (TBL) or a liquid-vapour (L-V) interface with vibration is a stimulating problem of fluid physics. Depending on the relative direction of the interface or the boundary layer with respect to vibration, vibrational forces can destabilize an L-V interface leading to Faraday / frozen wave instabilities and similarly a TBL, resulting in parametric / Rayleigh vibrational instabilities. Near the critical point, the above instabilities are emphasized as properties like thermal expansion coefficient, isothermal compressibility etc., diverge, while surface tension and thermal diffusivity vanish. To carry out experimental investigation of these instabilities close to the critical point, zero-g conditions are needed to eliminate density stratification resulting from the hypercompressibility of the near-critical fluid. Experiments / 2D simulations in the supercritical region put in evidence Rayleigh-vibrational [1–3] and parametric instabilities [3] near the walls (see Fig. 1). Experiments have also been carried out using magnetic compensation with Hydrogen approaching its critical point from below the critical temperature (two-phase state). Results (see Fig. 2) have evidenced and explained (i) the mechanism of enhanced dissipation very close the critical point that select rolls instead of squares for Faraday waves and (ii) the link between frozen wave instabilities and the creation of alternate liquid-vapour bands.

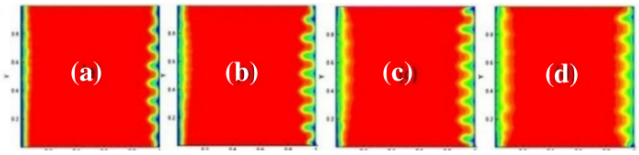

FIG. 1. Parametric instability at 4 consecutive time periods at 14.4 s (a), 14.76 s (b), 15.12 s (c) and 15.48 s (d) for f = 2.78 Hz, a = 20 mm, at 100 mK above the critical point and with a temperature quench of 10 mK at the four walls. The fluid is Hydrogen. In sketches (a) and (c), the form of the waves is the same as the difference in time corresponds exactly to 2/f (Faraday-type instability).

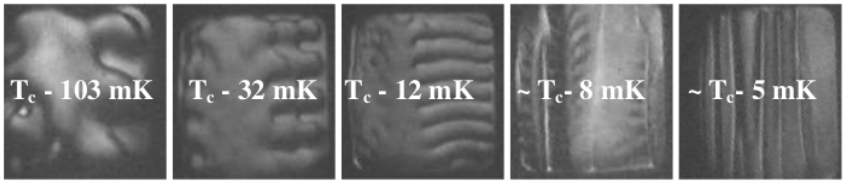

FIG. 2. Squares to rolls patterns of a Faraday wave instability at Tc-T $<$ 12mK and transformation into alternate bands for Tc-T $<$ 8mK. Here f = 40 Hz, a = 0.26 mm and the critical temperature Tc is approached in a square cell of 3mm side filled with H2.

[1] D. Beysens, Y. Garrabos, D. Chatain and P. Evesque, EPL, **86**, 16003 (2009).
[2] S. Amiroudine and D. Beysens, Phys. Rev. E, **78**, 036323 (2008).
[3] G. Gandikota, S. Amiroudine, D. Chatain, T. Lyubimova, and D. Beysens, Phys. of Fluids, **25**, 064103 (2013).

Temperature based weak ac field enhanced patterns formation in vertical deposition of colloids

R. Aslam,[1] M. Pichumani,[2] and W. González-Viñas[1]

[1]*Dept. of Physics and Appl. Math., University of Navarra, Pamplona, Spain*
rmuhammad@alumni.unav.es, wens@unav.es

[2]*Department of Nanotechnology, Sri Ramakrishna Engineering College, Coimbatore, India*
mpichumani@alumni.unav.es

We experimentally study pattern formation in vertical deposition configuration of colloids subjected to weak ac fields at various temperatures. At room temperature, the effect of the field leads to the formation of spatially distributed clusters along the contact line separated by a characteristic length [1] (Fig. 1, Left). Complex flow dynamics involved in the evolution of these clusters is reported. Homogeneous variation of the contact angle by electrowetting becomes unstable and breaks the symmetry at the meniscus. This instability along with capillary force result in accumulation of particles in the form of clusters. We study experimentally the behavior of clusters as a function of increasing initial particle concentration for various field frequencies. The characteristic distance between clusters increases monotonically with an increase in initial particle concentration. For higher concentration, we have clusters even at lower field. At lower concentration, the applied field has to be increased in order to enhance the size of affected basin of attraction to fetch more particles for cluster formation [2]. Moreover, we extend the idea to obtain colloidal dried structures through evaporation at higher temperatures (60 °C) subjected to field. We observe that even at higher temperatures the movement of negatively charged polystyrene colloidal particles is controlled by external fields. Consequently, due to rapid evaporation, particles through capillary action following the applied fields, form dried deposits in the form of columns by convective self-assembly (Fig. 1, Right). We observe how our colloidal suspensions are sensitive to external fields even at higher temperatures [3]. Experimental results on characteristic length of columns as a function of applied field are reported. It is observed that, the width of columns is associated with the field strength. We discuss the complex flow dynamics involved in the evolution of such depositions by electric fields. Also, we observe some order inside these deposits that might be useful for technological applications. In order to make these applications possible, further work is required for exploring the origin and the structure of columns formation mechanisms by external electric fields at higher temperatures.

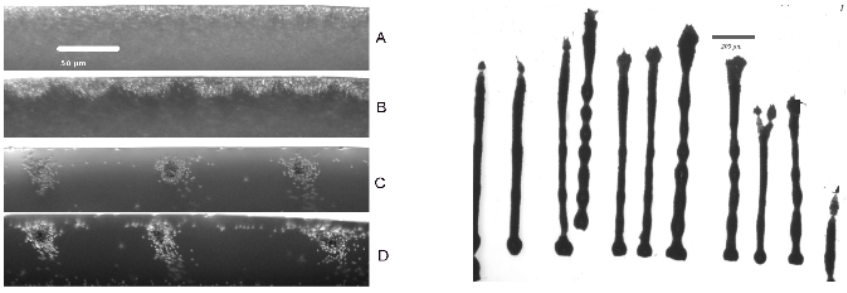

FIG. 1. Pattern formation in colloids by weak ac fields. Left: Clusters at room temperature, scale bar 50 μm; Right: Dried columns of particles at higher temperature, scale bar 200 μm.

[1] M. Pichumani et al., *One-dimensional cluster array at the three-phase contact line in diluted colloids subjected to ac electric fields*, Phys.Rev E, **83**, 047301 (2011)

[2] R. Aslam et al, *Effect of concentration on colloidal pattern formation induced by weak ac fields*, in preparation

[3] R. Aslam et al, *Weak ac field induced columnar pattern formation by temperature controlled evaporation in vertical deposition of colloids*, in preparation

Bifurcations of the rotation in the Marangoni layers

V. A. Batishchev[1] and V. A. Getman[1]

[1]*Southern Federal University, Milchakova 8a, Rostov-na-Donu, Russia*

batishev-v@mail.ru

We study the self-similar fluid flows in the Marangoni layers with the axial symmetry. Such flows are induced by the radial gradients of the temperatures whose distributions along the free boundary obey some power law. The self-similar solutions describe thermo-capillar flows both in the thin layers and in the case of infinite thickness.

We consider both positive and negative temperature gradients. In the former case the cooling of free boundary nearby the axis of symmetry gives rise to the rotation of fluid. The rotating flow concentrates itself inside the Marangoni layer while outside of it the fluid does not revolve. In the latter case we observe no rotating flows at all.

In the layers of infinite thickness the separation of the rotating flow creates two zones where the flows are directed oppositely. Both the longitudinal velocity and the temperature has exactly one critical point inside the boundary layer. It is worth to note that there profiles are monotonic in the case of non-swirling flows. We describe the flow outside the boundary layer with the use of self-similar solution of the Euler equations. This flow is slow and non-swirling.

The introducing of an outer flow gives rise to the branching of swirling flows from the non-swirling ones. There is such the critical velocity of the outer flow that a non-swirling flow exists for supercritical velocities and cannot be extended to the sub-critical velocities. For the positive temperature gradients there are two non-swirling flows. For the negative temperature gradients the non-swirling flow is unique. We determine the critical velocity of the outer flow for which the branching of the swirling flows happens. Fig. 1 displays the radial velocity V on the free boundary versus the velocity of the outer flow (denoted as U). Curves 1 and 2 relate to the basic flows while branch 3 relates to the secondary flow.

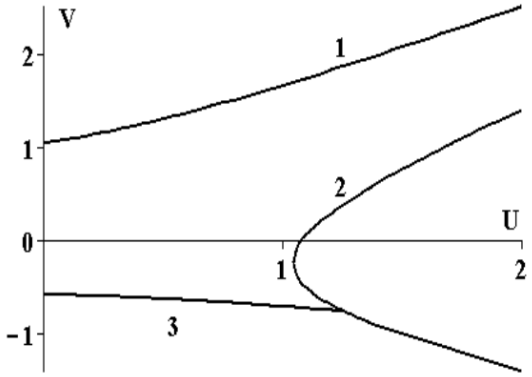

FIG. 1. The radial velocity on the free boundary for the basic flows (1,2) and for the secondary flow (3).

In the case of a thin layer confined within free boundaries we show that the cooling of the free boundaries near the axis of symmetry leads to the separating of the layer and creates two sub-layers with opposite rotations inside. This makes sharp contrast with the case of infinite thickness. We show that such rotation arises provided the thickness of the layer exceed some critical value.

In the case of a thin layer confined within free and rigid boundaries we construct the branching equation and the asymptotic approximation for the secondary swirling flows near the bifurcation point. It turns out that the bifurcation gives rise to one pair of the secondary swirling flows with different directions of swirl.

Two-frequency excitation of single-mode Faraday waves

W. Batson,[1] F. Zoueshtiagh,[2] and R. Narayanan[3]

[1]*Department of Mechanical Engineering, Technion - Israel Institute of Technology, Haifa 32000, Israel*
wbatson@gmail.com

[2]*University of Lille 1, IEMN CNRS 8520, Lille, France*
farzam.zoueshtiagh@univ-lille1.fr

[3]*University of Florida, Dept. Chem. Eng., Gainesville, Florida USA*
ranga@ufl.edu

To date, two-frequency excitation of the Faraday instability has been considered only in the high-frequency regime, typically in the interest of unlocking patterns that are unavailable to single-frequency excitation. In this work, we consider such excitations in the low-frequency regime, where the mode selection is discretized and cell modes can be individually excited. The course of study follows that of Batson $et\ al.$[1], who designed and compared a cylindrical, single-mode experiment with the linear theory of Kumar & Tuckerman[2], to which a stress-free sidewall boundary condition was applied to effect mode discretization. This boundary condition was successfully approximated by judicious choice of the experimental fluids, and, as a result, remarkable agreement was observed between the predicted thresholds and the experimental onsets. A central question to this work therefore is whether or not the same agreement is seen for two-frequency excitation.

The investigation utilizes the two-frequency linear theory of Besson $et\ al.$[3], to which the stress-free boundary condition is again applied. With a substantially increased parameter space owing to the introduction of three degrees of freedom–amplitude, frequency, and phase of the second component–focus is restricted to the case where the two frequencies are of the same order. The model is then used as a guide to explore basic phenomena in the experiment of Batson $et\ al.$ Most notably, the model predicts that a second frequency can produce either significant or insignificant adjustment to the single component threshold amplitude. Whether or not this occurs depends on the frequency ratio, and three different ratios are studied to experimentally verify this prediction. In the nonlinear regime, bifurcation and time series data of the saturated wave response (see figure 1) are used to differentiate the two-frequency and single-frequency cases. Finally, a novel multi-mode excitation, whereby both frequency components excite a cell mode, is highlighted.

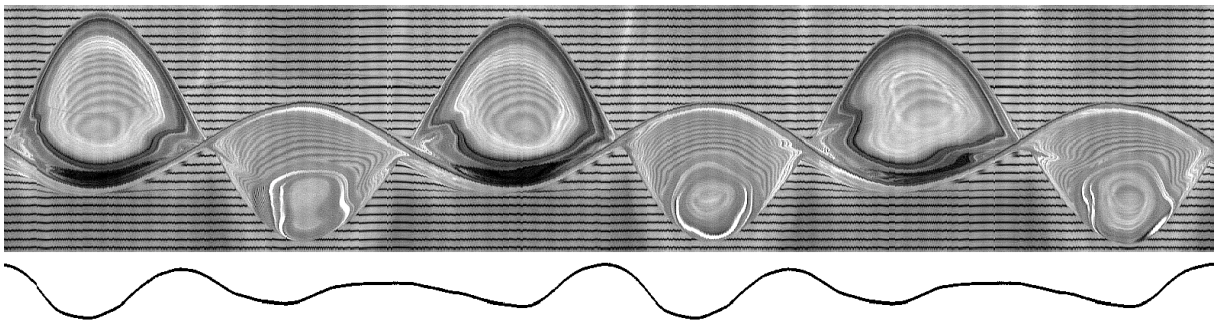

FIG. 1. The saturated response (above) of the fundamental axisymmetric mode for two periods ($2T = 4\pi/\omega$) of a vibrational signal (below) consisting of 3ω and 4ω components.

[1] W. Batson, F. Zoueshtiagh and R. Narayanan, *The Faraday threshold in small cylinders and the sidewall non-ideality*, J. Fluid Mech. **729**, 496–523 (2013).

[2] K. Kumar, L. S. Tuckerman, *Parametric instability of the interface between two fluids*, J. Fluid Mech. **279**, 49–67 (1994).

[3] T. Besson, W. S. Edwards and L. S. Tuckerman, *Two-frequency parametric excitation of surface waves*, Phys. Rev. E **54**, 507–514 (1996).

Heat and mass transfer between a vertical flat absorbing falling liquid film and a gas flow in a channel

B. Beladi[1] and H. C. Kuhlmann[1]

[1]*Institute of Fluid Mechanics and Heat Transfer, TU Wien, Resselgasse 3, 1040 Vienna, Austria*

behnaz.beladi@tuwien.ac.at

Sorption-based air-conditioning devices have a great potential for energy savings compared to conventional systems. In absorption air-conditioning systems, the performance of the absorber is crucial to the overall system performance and system size. Therefore, a focus of current research is to optimize the operating conditions in order to achieve the highest mass transfer by enhancing absorber performance.

The heat and mass transfer in a falling film device is investigated using a simplified model shown in Fig. 1. Only half of the channel is shown. A vertical absorbing falling film flows down along the side wall of the channel. It is exposed to a gas flow perpendicular to the direction of the liquid flow. In a first step we assume that the liquid and the gas flow are not coupled mechanically. Therefore, we can assume a fully developed Nusselt flow in the liquid film and a gas flow which develops downstream from the entry of the channel.

Contrary to the flow being uncoupled at the interface, we consider thermal and chemical coupling and calculate the heat and mass transfer through the phase boundary. In order to find the optimum operating condition, the influence on the heat and mass absorption of the channel height, incoming air velocity, and film thickness is investigated in a dimensional framework.

Two sets of boundary conditions on the vertical wall supporting the liquid film have been investigated. Isothermal and adiabatic wall boundary conditions were tested in order to investigate the cooling effect of the channel side walls on the absorption performance. The problem is solved numerically. The code [1] has been extended by adding a developing channel air flow perpendicular to the Nusselt-film flow. The developing channel flow, serving as input for the heat- and mass-transfer problem, is calculated numerically in advance. The coupled system of linear differential equations with nonlinear boundary conditions for the temperature and concentration fields is then solved numerically using finite difference. We find that most of the absorption takes place in close vicinity of the inlets for the gas as well as the liquid film flow.

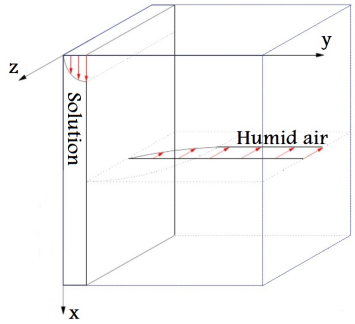

FIG. 1. A simplified model of a vertical falling film (left) exposed to a humid gas flow in a channel. Only half of the channel is shown.

Support by BMVIT through the Klima- und Energiefonds of FFG under grant number 825560 is gratefully acknowledged.

[1] E. Hofmann and H. C. Kuhlmann, *On the optimum mass transfer of flat absorbing falling films*, International Journal of Heat and Mass Transfer, 7686-7697 (2012).

Flow regimes in a cylindrical macropore

P. Beltrame[1] and S. Sammartino[1]

[1]*UMR 1114 EmmaH, UAPV-INRA, F-84914 Avignon, France*

philippe.beltrame@univ-avignon.fr,

stephane.sammartino@univ-avignon.fr

A challenging problem of water transfer in unsaturated soils is the hydraulic function of the macroporosity as opened cracks, earthworm burrows, and channels left by roots. In macropores, free surface flow is a dominant process especially when the soil matrix is saturated or for a matrix permeability reduced by hydrophobic organic coatings. A rich range of flow shapes has been identified: droplets, thin films or rivulets Even if in the last years, there has been a proliferation of conceptual models of film flow (see for instance [1]), they are not able to reproduce the different flow regimes and to explain their emergence.

A novel imaging method, had allowed tracking in space and in time of the water content in an undisturbed soil during water infiltration [2]. It provides new insight for the understanding of the macropore fluid transfer. This contribution aims at modeling flow regimes in a cylindrical macropore in order to understand, at least qualitatively, the observed regimes.

The motion of the three-dimensional liquid film is derived from the Navier-Stokes equation using the long-wave approximation with a free surface (surface tension) [3]. The soil matrix wettability is taking into account using a disjoining and conjoining pressure. Such an approach allows to model contact angle hysteresis if the wettability is not homogeneous [3]. The resulting governing equations are analogous to the lubrication equation. We adapt the numerical code proposed in [4] in order to perform the simulation. For exploring the different regimes we do not only perform time integration but also we employ continuation techniques and tools of dynamical systems. In other words we track the steady-flow regimes in the parameter space as well as the instability threshold. As in [3] and [4] many flow shapes (droplet, rivulets) are found with possible intermittent behaviours. These results are very reminiscent of the observed filling/emptying intermittent behavior of the flow macropore (Fig. 1).

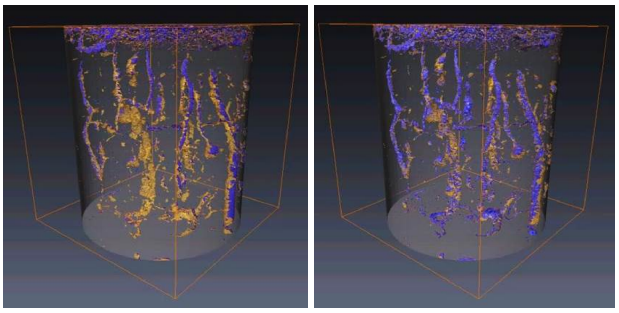

FIG. 1. (Left) Flow in real complex macropore system at the breakthrough of water infiltration. (Right) The same macropore system at the end of the simulated infiltration for an intense rainfall event. The column dimensions are 130 mm diameter and 150 mm height. Macropores are displayed in yellow.

[1] J. R. Nimmo, *Theory for Source-Responsive Free-Surface Film Modeling of unsaturated Flow*, Vadose. Zone. J. **9** (2010).

[2] S. Sammartino, E. Michel and Y. Capowiez, *A novel method to visualize and characterize preferential flow in undisturbed soil cores by using multislice helical CT*, Vadose. Zone. J. **11** (2012).

[3] Ph. Beltrame, E. Knobloch, P. Hänggi and U. Thiele, *Rayleigh and depinning instabilities of forced liquid ridges on heterogeneous substrates*, Phys. Rev. E **83**, 016305 (2011).

[4] Ph. Beltrame and U. Thiele, *Time integration and steady-state continuation for 2d lubrication equations*, SIAM J. Appl. Dyn. Syst. **9**, 484 518 (2010).

The dynamics of hydraulic jumps in a viscous liquid flowing down an inclined plate

E. S. Benilov[1] and V. N. Lapin[2]
[1]*University of Limerick, Limerick, Ireland*
eugene.benilov@ul.ie
[2]*School of Mathematics, University of Leeds, Leeds LS2 9JT, UK*
v.lapin@leeds.ac.uk

We examine the dynamics of a layer of viscous liquid on an inclined plate. If the layers upstream depth h_- exceeds the downstream one h_+, a smooth hydraulic jump (bore) forms and starts propagating down the slope. If the ratio h_-/h_+ and/or the plates inclination angle α are sufficiently large, the bore overturns and no steady solution exists in this case [1]. Surface tension stabilizes the bore for certain values of h_-/h_+ and α, but it cannot do so for larger ones.

We examine the dynamics of bores through numerical simulation and asymptotic analysis of the Stokes equations, as well as those of a heuristic depth-averaged model where the vertical structure of the flow is approximated by a polynomial. It turns out that even the simplest version of the heuristic model (based on the parabolic approximation) is remarkably accurate, producing results which agree, both qualitatively and quantitatively, with those obtained through the Stokes equations. Furthermore, the heuristic model allows one to derive a sufficient criterion of bore overturning,

$$h_-/h_+ > 1 + 3^{1/2}.$$

This criterion is then extended numerically to a sufficient and necessary one, i.e. we compute the boundary of the overturning region on the $(h_-/h_+, \alpha)$ plane.

Physically, the criterion derived reflects the fact that, for large values of h_-/h_+ and/or α, a stagnation point appears on the liquids free surface and stagnation points are generally known to cause instability [2]. To illustrate this effect in the problem at hand, we use the Stokes equations to derive an asymptotic model for a region near the stagnation point and show that disturbances of the free surface there contract horizontally and grow vertically. It can be conjectured that such evolution gives rise to the bore overturning observed in the numerical simulations of the Stokes equations.

---

[1] E. S. Benilov and V. N. Lapin, *Shock waves in Stokes flows down an inclined plate*, Phys. Rev. E, **83**, 066321.15 (2011).
[2] A. Lifschitz and E. Hameiri, *Local stability conditions in fluid dynamics*, Phys. Fluids. A, **3**, 26442651 (1991).

Control of drop motion by mechanical vibrations

M. Bestehorn[1]

[1]*Dep. Theoretical Physics, BTU, 03044 Cottbus, Germany*
bes@physik.tu-cottbus.de

Since the first experimental observations of Michael Faraday in 1831 it is known that a vibrating liquid may show an instability of its flat free surface with respect to oscillating regular surface patterns.

We study thin liquid films on a horizontal substrate in the long wave approximation. The films are parametrically excited by mechanical *horizontal* oscillations. Inertia effects are taken into account and the standard thin film formulation is extended by a second equation for the vertically averaged mass flux. The films can be additionally unstable by Van der Waals forces on a partially wetting substrate, leading to the formation of drops. These drops can be manipulated by the vibrations to move in a desired direction.

Linear results based on a damped Mathieu equation as well as fully nonlinear results using a reduced model will be presented, for more details see [1, 2].

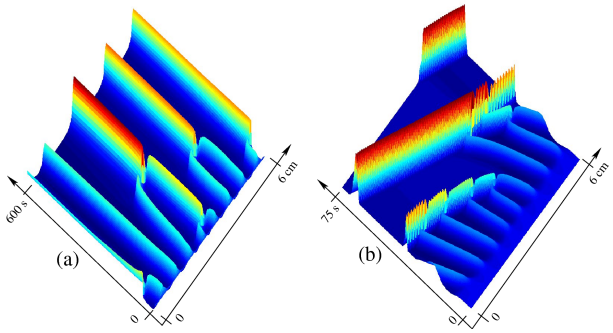

FIG. 1. Space-time plots of the liquid film under lateral vibrations. Left: coarsening leads to a few separated drops. Right: combined action with a normal oscillation drives the drops to the left. From [1].

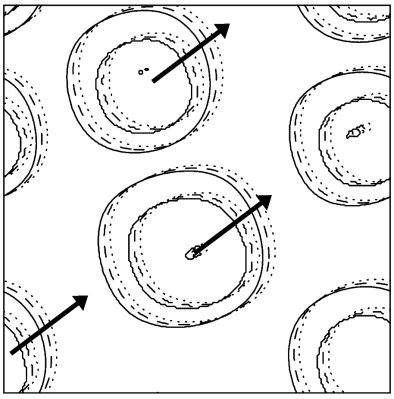

FIG. 2. In 3D, drops start to move, if a horizontal vibration is combined with a normal one. The direction depends on the relative phase of the vibrations. From [2].

[1] M. Bestehorn, Q. Han and A. Oron, *Nonlinear pattern formation in thin liquid films under external vibrations*, Phys. Rev. E, **88**, 023025 (2013).

[2] M. Bestehorn, *Laterally extended thin liquid films under external vibrations*, Phys. Fluids, **25**, 114106 (2013).

Drops on cylindrical surfaces

I. D. Borcia,[1] R. Borcia,[1] M. Bestehorn,[1] C. Borcia,[2] N. Dumitrascu,[2] and C. Egbers[1]

[1]*Brandenburgische Technische Universität Cottbus-Senftenberg, Germany*
borciai@tu-cottbus.de, borciar@tu-cottbus.de,
bes@physik.tu-cottbus.de, egbers@tu-cottbus.de
[2]*Faculty of Physics, "A.I.Cuza" University, 11 Blvd Copou, Iasi, Romania*
cborcia@uaic.ro, nicoleta.dumistrascu@uaic.ro

The aim of this paper is to determine by experiment/phase field simulation static contact angles for liquid droplets resting on different polymer fibers with different curvatures. Due to its flexibility especially when complex interfaces are present, the phase field theory becomes an efficient tool for studying curved surface shapes. This method treats the liquid-vapor system continuously by taking an order parameter to distinguish between the coexisting phases. The most natural phase field function is the fluid density. The fluid density $\rho = 1$ denotes the liquid phase, $\rho \approx 0$ the vapor bulk, $\rho = 0.5$ describes the location of the interface. From a sharp picture of a sessile drop on a cylindrical wire obtained with the experimental set-up sketched in fig. 1, one extracts the light intensity. The equivalent of the 0.5 level from the phase field model will be given by the inflection point in fig. 1-(c). Comparing the drop's contours – from experiment and phase field simulation – we propose a new method for contact angle estimation.

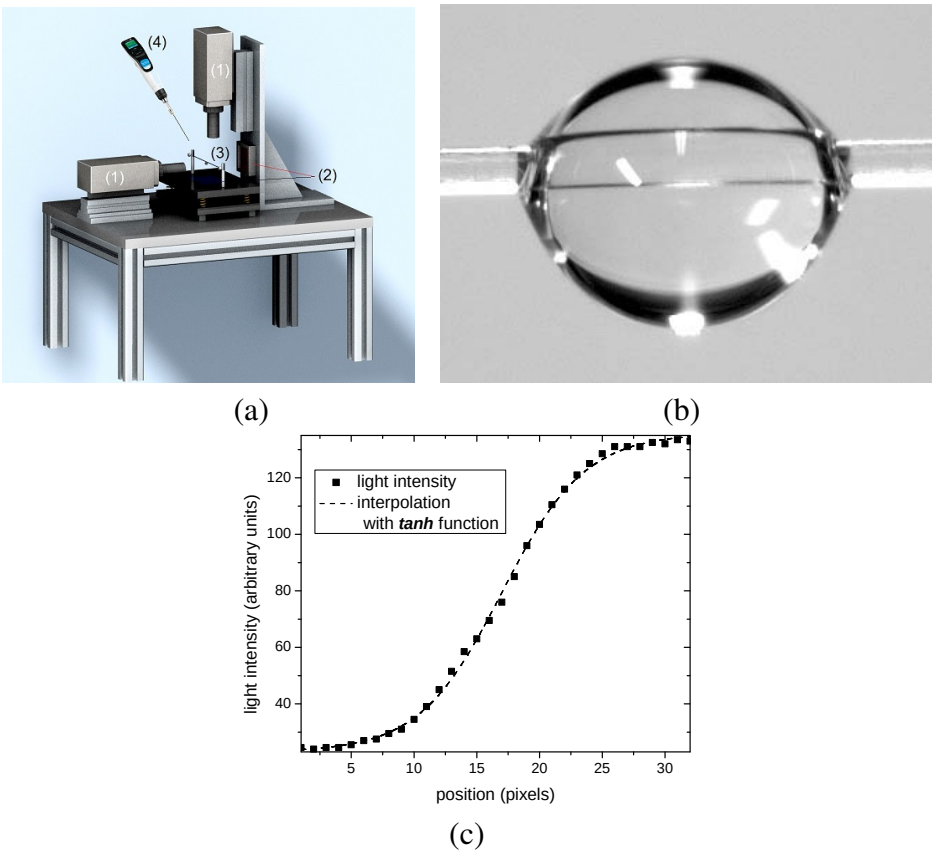

FIG. 1. (a) Experiment scheme containing (1) video cameras, (2) mate back-light LED luminous panels, (3) wire with a liquid droplet, (4) Hamilton syringe with liquid; (b) Photo of an almost symmetric water drop lying on a PA 6 mono-filament with a diameter of 0.15 mm; (c) Example of a light intensity along the drop edge for the photo depicted in (b).

A phase field description of ratchet-like motion of a shaken drop

R. Borcia,[1] I. D. Borcia,[1] and M. Bestehorn[1]

[1]*Brandenburgische Technische Universität Cottbus-Senftenberg, Germany*

borciar@tu-cottbus.de, borciai@tu-cottbus.de, bes@physik.tu-cottbus.de

We study the motion of a drop on a plate simultaneously submitted to horizontal and vertical harmonic vibrations. The investigation will be done via a phase field model earlier developed for describing static and dynamic contact angles [1]. The density field is nearly constant in every bulk region ($\rho = 1$ in the liquid phase, $\rho \approx 0$ in the vapor phase) and varies continuously from one phase to the other with a rapid but smooth variation across the interface. Complicated explicit boundary conditions along the interface are avoided and capturated implicitly by gradient terms of ρ in the hydrodynamic basic equations. The contact angle θ is controlled through the density at the solid substrate ρ_S, a free parameter varying between 0 and 1.

We report on two-dimensional numerical simulations for flow visualization inside a liquid drop under inertial effects induced by the vibrating plate: $v_x(z=0) = V \sin(\omega t)$ and $v_z(z=0) = 0.2\, V \sin(\omega t + \Delta\varphi)$. We investigate the net driven motion Δx by following the location of the drop's mass center:

$$x_{CM} = \frac{\int\int_{\rho \geq 0.99} \rho\, x\, dx\, dz}{\int\int_{\rho \geq 0.99} \rho\, dx\, dz}$$

over some periods, as well as the dependency of Δx on the oscillation frequency ω. A preliminary result concerning the displacement of the droplet center of mass Δx versus phase shift $\Delta\varphi$ is displayed in fig.1.

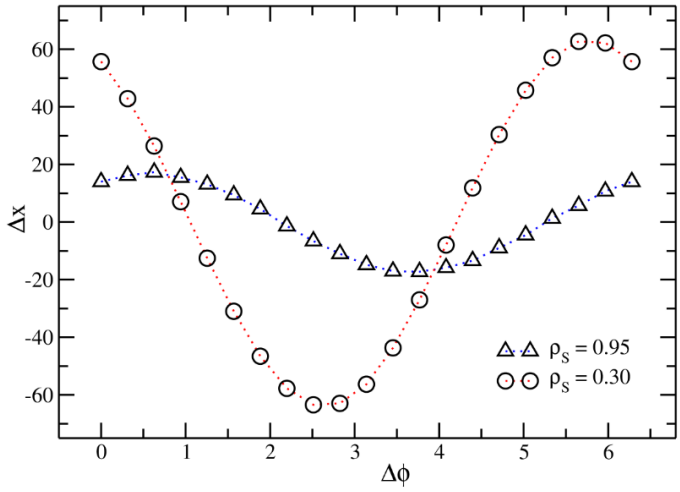

FIG. 1. Net driven displacement Δx versus phase shift $\Delta\varphi$ over 5 periods for hydrophilic ($\rho_S = 0.95, \theta = 10°$) and hydrophobic ($\rho_S = 0.3, \theta = 120°$) surfaces.

[1] R. Borcia, I. D. Borcia and M. Bestehorn, *Drops on an arbitrarily wetting substrate: A phase field description*, Phys. Rev.E **78**, 066307 (2008).

Study of the acoustic surface waves propagation of porous silicon using different coupling fluids

S. Bouhedja[1,2] and F. Hamdi[2]

[1]*Département de Médecine, Université de Constantine 3, BP 125, chalet des pins, Constantine, 25000, Algeria.*
[2]*Laboratoire des Hyperfréquences et Semiconducteurs, département d'Electronique, Faculté des Sciences de la technologie, université de Constantine1, Route Ain El Bey, Constantine, 25017, Algeria.*
bouhedja_samia@yahoo.fr, f_7amdi@yahoo.fr

Non-destructive ultrasonic investigations are based on surface acoustic waves which interact with the elastic properties of a given material which is in contact with the coupling fluid. In this work, we study the effect of the coupling fluid on the surface waves propagation by using acoustic microscopy which is a key technique not only in qualitative microcharacterizations, but also in quantitative measures [1, 2]. In micro-analysis, it can be used to directly determine the mechanical properties of materials via acoustic signature, V(z); this signature is obtained by recording the change in the reflected acoustic signal with the defocusing distance, z, as the sample is moved towards the acoustic lens. It is not only a characteristic of the investigated materials but also influenced by the use of appropriate coupling fluids. We apply our calculations to porous silicon (PSi) with different coupling liquids (Freon, mercury, water and gallium) at 600 MHz.

RESULTS

The obtained results enabled us to study the evolution of acoustic signature curves to find a compromise between the porosity as well as coupling fluids to determine the values of propagating surface acoustic wave velocities of porous silicon.

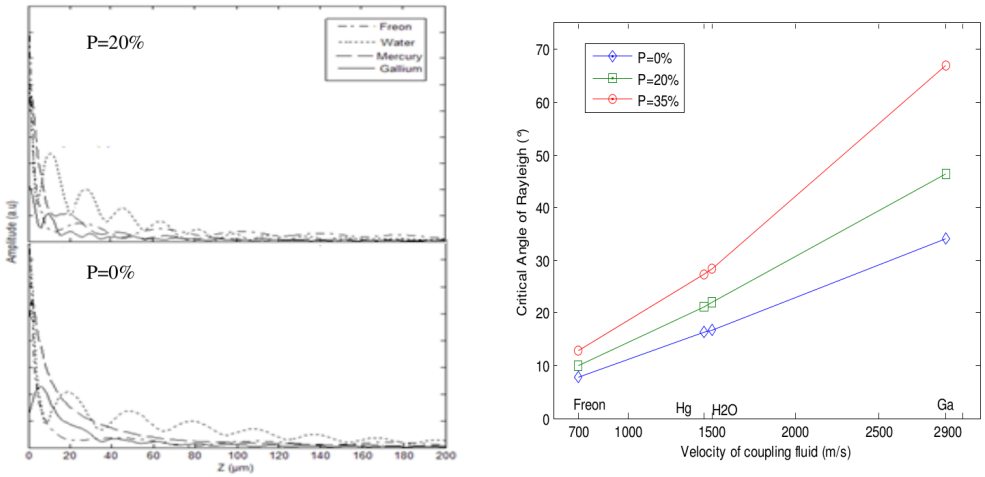

FIG. 1. Left: Variation of V(z) curves as function of coupling fluid and porosity; Right:Variation of critical angle of Rayleigh with coupling fluid in different rates of porosity.

[1] G. A. D. Briggs, O. V. Kolosov, *Acoustic Microscopy*, 2nd edition, Oxford University Press, New York, (2010).
[2] B. Cros, V. Gigot, G. Despaux, *Study of the efficiency of coupling fluids for acoustic microscopy*, Applied Surface Science, **119**, 242-252 (1997).

Self-induced Marangoni flow in alcoholic binary mixtures

C. Buffone,[1] A. Cecere,[2] and R. Savino[2]

[1]*Microgravity Research Centre, Université libre de Bruxelles, Avenue F. Roosevelt 50, 1050 Bruxelles, Belgium*
cbuffone@ulb.ac.be

[2]*Dipartimento di Ingegneria Industriale (DII)-Sezione Aerospaziale, Università degli studi di Napoli Federico II,Piazzale Tecchio, 80 -80125- Napoli, Italy*
anselmocecere@hotmail.com, rasavino@unina.it

The self-induced Marangoni convection in alcoholic solutions (pure ethanol and its mixtures with 5, 10 and 20% of water in weight) is the subject of the present experimental and numerical investigation. Fig. 1 is a superimposition of 20 frames and shows the trajectories of tracer particles near the meniscus interface at the tube mouth; it is evident the presence of two counter rotating Marangoni vortices symmetrical with respect to the tube axis. The characterization of the Marangoni flow in horizontal positioned tubes ranging from 100 to 1,000μm ID cylindrical channels is studied. Dimensions of the Marangoni vortex horizontal cross sections, vortex spinning frequency, average particle tracers velocity and evaporation rate are measured and discussed.

This study found that the evaporation rate increases and the evaporation flux decreases at bigger tube sizes as shown in Fig. 2 in line with previous investigations [1]; pure ethanol has higher evaporation rate and flux than ethanol/water mixtures. The spinning frequency and the average tracer particles velocity decrease for increasing water content in the mixtures. All of these findings are due to evaporative cooling effect which is higher at the meniscus wedge (where the triple-line region is operating) than at the meniscus centre; this causes a difference in temperature between the wedge and the centre that generates a gradient of surface tension which drives for the small tube sizes analysed the vigorous Marangoni convection reported and analysed [2].

The experimental results are explained on the basis of a numerical model including evaporation, vapour diffusion, heat and mass transfer from the liquid to the surrounding ambient and the Marangoni effects following the work on pure liquids presented in [3].

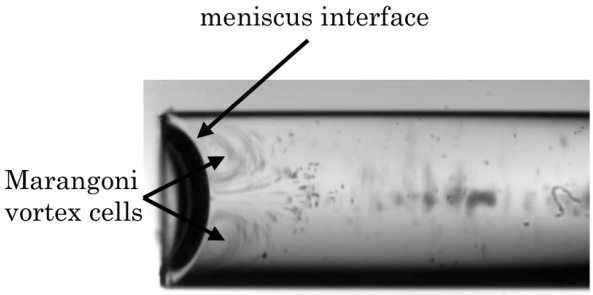

FIG. 1. Superimposition of 20 images of tracers particles unveiling two optical sections of the Marangoni toroidal vortex.

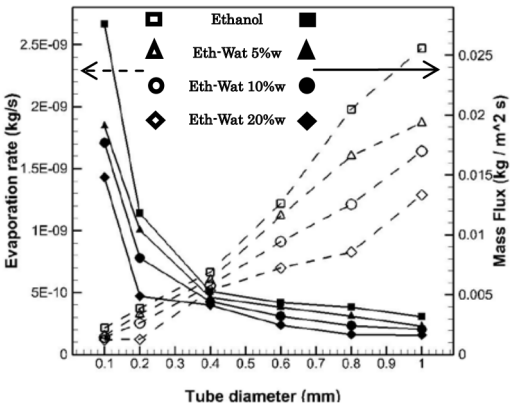

FIG. 2. Evaporation rate and average mass flux as a function of tube diameter, for ethanol-water mixtures.

[1] C. Buffone and K. Sefiane, *Investigation of thermocapillary convective patterns and their role in the enhancement of evaporation from pores*, Int. J. of Multiphase Flow, **30**, 10711091 (2004).

[2] C. Buffone and K. Sefiane, *IR measurements of interfacial temperature during phase change in a confined environment*, Experimental Thermal and Fluid Science, **29**, 6574 (2004).

[3] H. Wang, J. Y. Murthy and S. V. Garimella, *Transport from a volatile meniscus inside an open microtube*, Int. J. of Heat and Mass Transfer, **51**, 3007-3017, (2008).

Buoyancy driven instabilities in miscible fluids

J. Carballido-Landeira,[1] P. M. J. Trevelyan,[1] C. Almarcha,[1] and A. de Wit[1]

[1]*Nonlinear Physical Chemistry Unit, Service de Chimie Physique et Biologie Théorique, Université Libre de Bruxelles, (ULB), CP231, 1050 Brussels, Belgium*

jorge.carballido@gmail.com

We study the hydrodynamic flows induced by buoyancy-driven instabilities in a Hele-Shaw cell caused by miscible fluids both theoretically and experimentally. In a gravitational eld, the horizontal interface between two miscible uids can be destabilized by density or diffusion driven-instabilities [1] We derive the conditions for the existence of the different buoyantly-driven scenarios in the (R, d) parameter plane, where R is the buoyancy ratio between the two solutions and d is the ratio of their diffusion coefcient. In addition to the classical Rayleigh-Taylor (RT) instability (characterized by a deformation of the interface into fingers when the upper solution is denser) and Diffusive Layer Convection (DLC) instability (because of differential diffusion effects once the denser solution is on the bottom [2]) new sort of instabilities may arise between these two regimes. This new dynamical process is originated when the density profiles shows a locally stratifically stable region near the interface delimited by two unstable regions [3], generating new plume-like structures around the initially horizontal interface

---

[1] J. Fernandez, P. Kurowski, P. Petitjeans, and E. Meiburg, J. Fluid Mech., **451**, 239 (2002).
[2] P. M. J. Trevelyan, C. Almarcha, and A. De Wit, J. Fluid Mech., **670**, 38 (2011).
[3] J. Carballido-Landeira, P. M. J. Trevelyan, C. Almarcha, and A. De Wit, Phys. Fluids, **25**, 024107 (2013).

Drop transfer between two surfaces

H.Chen,[1] T.Tang,[1] and A.Amirfazli[2]

[1]*Department of Mechanical Engineering, University of Alberta, Edmonton, AB, T6G 2G8, Canada*
hchen9@ualberta.ca, ttang1@ualberta.ca

[2]*Department of Mechanical Engineering, York University, Toronto, ON, M3J 1P3, Canada*
alidad2@yorku.ca

Drop transfer from one solid surface to another is commonly observed in nature and in many industrial applications. This process typically consists of the deposition of a liquid drop on the donor surface, approach of the acceptor surface to the donor surface, formation and compression of a liquid bridge, and finally stretching and breakage of the liquid bridge. Literature shows that depending on the approaching and separation speed of the surfaces, their wettability and liquid viscosity, the behaviour of the liquid bridge can be categorized into two regimes: quasi-static regime where the surface tension force dominates, and dynamic regime where contributions from viscous and inertia forces are not negligible [2**?**]. In this work, we performed an experimental study of liquid transfer using several types of surfaces with different wettability and liquid with different surface tension and viscosity. The processes of liquid transfer under different approaching and stretching speed were recorded by a high speed camera. By examining the dependence of the transfer ratio (the amount of liquid transferred to the acceptor surface over the total amount of liquid) on the stretching speed, the boundary between the quasi-static and dynamic regimes was determined. When the speed is below a certain threshold, the transfer ratio is insensitive to the changes in speed or viscosity of liquid, but the process is strongly affected by the contact angle and contact angle hysteresis of the solid surfaces. When the speed is above the threshold, the transfer becomes dynamic and the transfer ratio was shown to be strongly dependent on the speed. This threshold, i.e., the boundary between quasi-static and dynamic regimes, can be affected by the viscosity and surface tension of the liquid as well as the surfaces wettability.

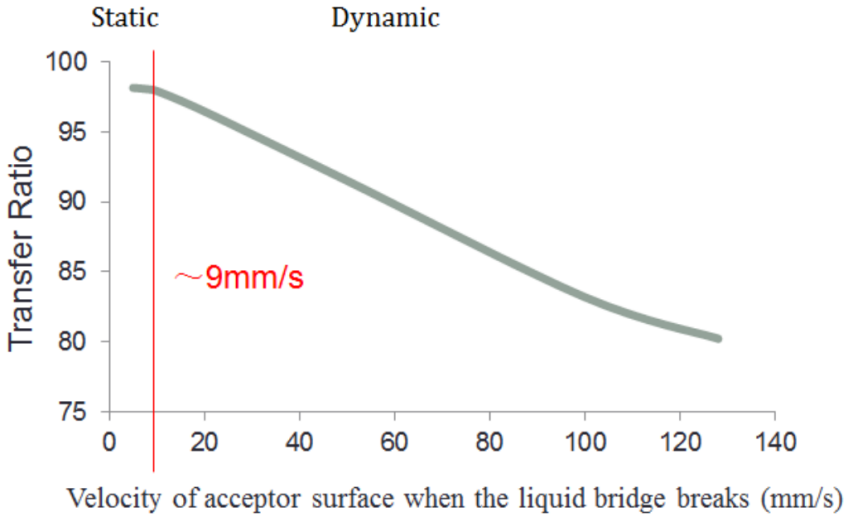

FIG. 1. Relation between transfer ratio and speed of surface of water transferred from an donor surface with contact angle of 50° to an acceptor surface with contact angle of 70°. 9mm is the boundary between quasi-static and dynamic regimes for this specific cases.

[1] A. V. Chadov, E. D. Yakhnin, *Investigation of the transfer of a liquid from one solid surface to another. 1. Slow transfer method of approximate calculation*, Kolloidn. Zh., **41**, 817- 820 (1979).

[2] E. D. Yakhnin, A. V. Chadov, *Investigation of the transfer of a liquid from one solid surface to another. 2. Dynamic transfer*, Kolloidn. Zh., **45**, 1183 1188 (1983).

Numerical simulation of the Marangoni effect on transient mass transfer from a single moving deformable drop

J. Chen,[1] X. Feng,[1] P. Fan,[1] C. Yang,[1] and Z.-S. Mao[1]

[1]*Key Laboratory of Green Process and Engineering, Institute of Process Engineering, Chinese Academy of Sciences, Beijing 100190, China*

chaoyang@ipe.ac.cn

In chemical unit operations, such as liquid-liquid extraction and multiphase chemical reaction, mass transfer between continuous and dispersed phases is often involved. Although hydrodynamic instabilities occur near the interface only, the mass/heat transfer coefficient is dramatically increased. If the hydrodynamic characteristics of such a process were utilized effectively in both optimizing the operation conditions and designing the reaction/separation apparatus, not only the transfer rate would be enhanced, but also the product quality and production efficiency would be improved. This is significant to energy saving and consumption reducing.

It has been discovered about 150 years that surface tension gradient could induce sub-drop scale tangential flow (so-called Marangoni effect). This effect is proved to have a significant influence on mass transfer rate, and hence has attracted more and more attentions in recent years for its potential application on interphase mass transfer related unit operations. Mao and Chen [1] simulated the Marangoni effect for a slowly moving single spherical drop in an axisymmetric boundary-fitted coordinate system. Using the level set method, Wang et al. [2] computed the mass transfer-induced Marangoni effect of a deformable drop. But both results have not been validated by experimental results. Wang et al. [3] found that a substantial difference exists between the 2D numerical simulation and the experimental data on the Marangoni effect induced by mass transfer from/to a deformable drop. Ignoring the impact of deformation, Wegener et al. [4] utilized commercial software STAR-CD to compute the 3-D Marangoni convection dominated toluene-acetone-water system.

It is hard to describe such a process by using empirical or theoretical equations since the process of interphase mass transfer is usually related with the deformation of free interface. Based on a level set framework, in this work we develop a three-dimensional numerical model for studying the Marangoni effect induced by the interphase mass transfer on the free interface of a single drop in an immiscible liquid. The surface tension is involved as an extra volume force by the continuum surface force model. As the Marangoni convection occurs in the three-dimensional space, 3D simulation would be a powerful tool to visualize the development of Marangoni effect and investigate its onset threshold. The present simulation suggests that the Marangoni convection in a 3D scenario is more difficult to be induced as compared with its 2D counterpart, and the Marangoni effect also develops in a faster pace. This work would reveal the real pattern of Marangoni convection in a single drop with mass transfer, and explicate the influence of Marangoni effect on drop deformation.

Acknowledgements. Financial supports from 973 Program (2013CB632601), the National Natural Science Foundation of China (21376243, 21206166) and the National Science Fund for Distinguished Young Scholars (21025627) are gratefully acknowledged.

[1] Z-S. Mao, J. Y. Chen, *Numerical simulation of the Marangoni effect on mass transfer to single slowly moving drops in the liquid-liquid system*, Chem. Eng. Sci., **59**, 1815-1828 (2004).

[2] J. F. Wang, C. Yang, Z-S. Mao, *Numerical simulation of Marangoni effects of single drops induced by interphase mass transfer in liquid-liquid extraction systems by the level set method*, Sci. China. Ser. B-Chem., **51**, 684-694 (2008).

[3] J. F. Wang, Z. H. Wang, P. Lu, C. Yang, Z-S. Mao, *Numerical simulation of the Marangoni effect on transient mass transfer from single moving deformable drops*, AIChE J., **57**, 2670-2683 (2011).

[4] M. Wegener, T. Eppinger, K. Bäumler, M. Kraume, A. R. Paschedag, E. Bänsch, *Transient rise velocity and mass transfer of a single drop with interfacial instabilities-Numerical investigations*, Chem. Eng. Sci., **64**, 4835-4845 (2009).

Evolution of the thermocapillarity motion of three liquids in a flat layer

V. Andreev[1] and E. Cheremnih[1]

[1]*Institute of Computational Modelling SB RAS,*
Akademgorodok, 660036, Krasnoyarsk, Russia
andr@icm.krasn.ru, elena_cher@icm.krasn.ru

We consider the unidirectional motion of three immiscible incompressible viscous heat – conducting liquids in a flat layer. It is assumed that motion arises under the influence of thermocapillarity forces from state of rest.

It follows that the vector of velocity is $\mathbf{u}_j = (u_j(y,t), 0, 0)$ and temperature $\Theta_j = -A_j x + T_j(y,t)$ with the constants $A_j, j = 1,2,3$. Suppose that the coefficient of the surface tension σ on the interface depends on the temperature linearly $\sigma_n(\Theta) = \sigma_n^0 - æ_n\Theta_n, \quad æ_n, \sigma_n^0 = const > 0, n = 1,2$. After the substitution into equations of motion and of heat transfer we obtain three initial boundary value problems for unknowns $u_j(y,t), T_j(y,t)$. These problems can be solved successively. The function $u_j(y,t), T_j(y,t)$ can be called the perturbations of the quiescent state. The following results were obtained:

1. exact stationary solution of the problem;

2. solution of the non-stationary problem in the form of final analytical formulas in the mage using the method of Laplace transformation;

3. by the numerical inversion of Laplace transformation the evolution of the velocity fields and of the temperature perturbation for specific liquids, more exactly for the system of silicon - water - air. It was proved that functions $u_j(y,t), T_j(y,t)$ always tend to stationary state as $t \to \infty$;

4. a priori estimates of convergence of solution to stationary one.

The work is supported by the Russian Foundation for Basic Research #14-01-00067.

Early Hofmeister series salt solutions: model formulation and linear stability analysis

J. J. A. Conn,[1] S. K. Wilson,[1] D. Pritchard,[1] B. R. Duffy,[1] P. J. Halling,[2] and K. Sefiane[3]

[1]*Department of Mathematics and Statistics, University of Strathclyde, Glasgow, Scotland, U. K*
justin.conn@strath.ac.uk

[2]*Department of Pure and Applied Chemistry, University of Strathclyde, Glasgow, Scotland, U. K*

[3]*School of Engineering, Edinburgh University, Edinburgh, Scotland, U. K*

We describe a mathematical model of Marangoni flow in early Hofmeister series salt solutions. These solutions have the anomalous property that in thermodynamic equilibrium the surface tension increases with increasing salt concentrations. Our model differs significantly from existing models of surfactant-driven convection, because these typically do not distinguish between surface concentrations and surface excesses and so cannot consistently represent the anomalous behaviour. We use linear stability analysis of our model to investigate the levelling behaviour of fluid layers, revisiting the classical analysis of Schwartz et al. [1] for these anomalous solutions.

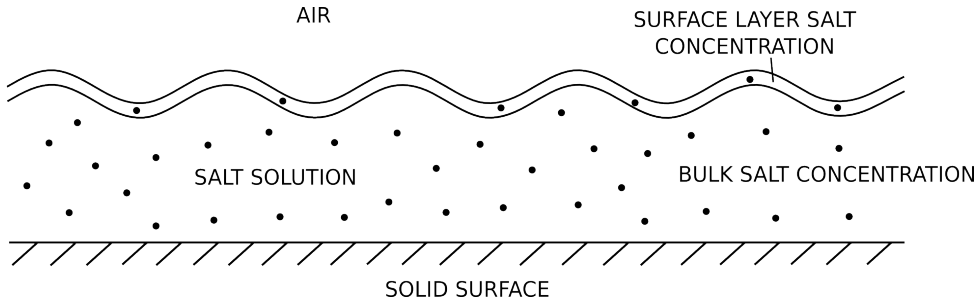

FIG. 1. Schematic diagram of model set up.

[1] L. W. Schwartz, D. E. Weidner and R. R. Eley, An Analysis of the Effect of Surfactant on the Leveling Behaviour of a Thin Liquid Coating Layer, Langmuir **11**, 3690–3693 (1995).

The effects of variable fluid properties on thin film stability

S. D'Alessio,[1] C. Seth,[1] and J.-P. Pascal[2]

[1]*Faculty of Mathematics, University of Waterloo, Waterloo, Ontario, Canada N2L 3G1*
sdalessio@uwaterloo.ca, cjmpseth@uwaterloo.ca

[2]*Department of Mathematics, Ryerson University, Toronto, Ontario, Canada M5B 2K3*
jpascal@ryerson.ca

A theoretical investigation has been conducted to study the impact of variable fluid properties on the stability of gravity-driven flow of a thin film down a heated incline. The incline makes an angle of β with the horizontal and is maintained at a uniform temperature, T_b, which exceeds the temperature of the ambient gas, T_a, above the fluid. The temperature difference $\Delta T = T_b - T_a$ is responsible for heating the thin fluid layer. All fluid properties are allowed to vary linearly with temperature which in dimensionless form are prescribed as follows:

$\frac{\rho}{\rho_0} = 1 - \alpha T$ (density),
$\frac{\mu}{\mu_0} = 1 - \lambda T$ (viscosity),
$\frac{c_p}{c_{po}} = 1 + ST$ (specific heat),
$\frac{K}{K_0} = 1 + \Lambda T$ (thermal conductivity), and
$\frac{\sigma}{\sigma_0} = 1 - \gamma T$ (surface tension).

where $\rho_0, \mu_0, c_{po}, K_0$ and σ_0 denote values of the fluid properties at the reference temperature T_a which in dimensionless form corresponds to $T = 0$.

As with isothermal flow down an incline, it is assumed that long-wave perturbations are most unstable. Based on this, a stability analysis was carried out whereby the governing linearized perturbation equations were expanded in powers of the wavenumber, k, which is a small parameter. The problem is controlled by the following dimensionless parameters: Re (Reynolds number), We (Weber number), Ma (Marangoni number), Pr (Prandtl number), Bi (Biot number), $\Delta T_r = \Delta T/T_a$, S, α, λ, Λ and β. New interesting results illustrating how the critical Reynolds number, Re_{crit}, and perturbation wave speed, c_0, depend on the various dimensionless parameters have been obtained. In a recent study [1] Re_{crit} was determined approximately by resorting to asymptotic expansions which are only valid if certain parameters are taken to be small. In this work exact expressions for Re_{crit} and c_0 have been found with no restrictions on the parameter values. While comparisons between the exact and asymptotic expressions for Re_{crit} reveal good agreement for small parameter values, the results can deviate significantly for arbitrary parameter values. Hence, this contribution represents a major extension of previous research.

---

[1] J. P. Pascal, N. Gonputh and S. J. D. D'Alessio, *Long-wave instability of flow with temperature dependent fluid properties down a heated incline*, International Journal of Engineering Science, **70**, 73–90 (2013).

A drying droplet spreads out its wings: thermo-capillary fingering

R. De Dier[1], W. Sempels[2], J. Hofkens[2] and J. Vermant[1]

[1]*Chemical Engineering, Soft Matter, Rheology and Technology, KU Leuven, W. de Croylaan 46, 3001 Heverlee, Belgium,*
raf.dedier@cit.kuleuven.be

[2]*Chemistry, Laboratory for Photochemistry and Spectroscopy, KU Leuven, Celestijnenlaan 200F, 3001 Heverlee, Belgium*

Patterning of nano- or microparticles on a substrate has received an increasing interest in applications such as the production of nanowires, microsensors, photonic devices and tissue engineering. A simple way of creating these patterns, without the use of an external force, is by evaporation of sessile droplets containing colloidal particles. These particles consequently are deposited in a well-defined macroscopic pattern, controlled by the droplets internal flow due to capillary forces [1]. It has been shown that the internal flow field and the final pattern formation can be modulated by local temperature variations [2] or by a simple addition of surfactants [3].

Here, we report that the addition of surfactants is able to locally depin the contact line of a pinned water droplet at equally spaced positions across the perimeter of the evaporating droplet. The contact line is observed to deform outward and a finger protrudes from the drying droplet, as illustrated in Figure 1. We reveal that, in the present case, temperature variations and associated Marangoni forces exist along the contact line that match the spacing of the undulations and give rise to an interfacial instability and hence the origin of the fingers [4]. The distance between two adjacent fingers can be controlled by conditional parameters and the ability to fine-tune this is key to obtaining different deposition patterns upon drying.

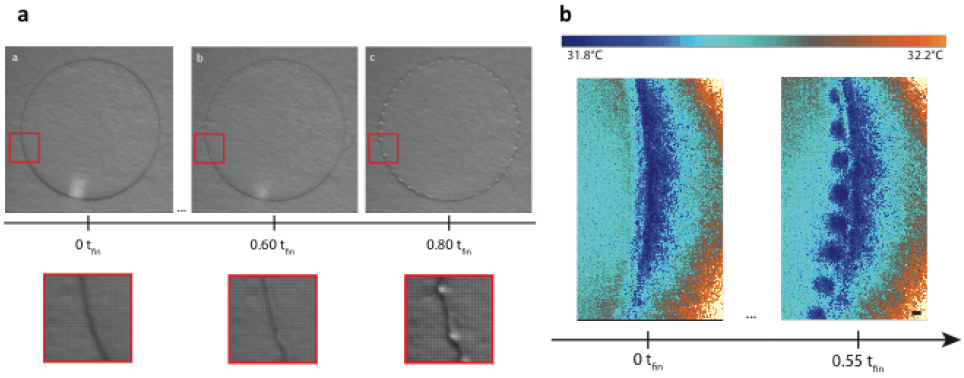

FIG. 1. (a) Top view images of the fingering pattern of an evaporating water droplet containing a high amount of surfactant (Triton X-100) (b) Thermal imaging reveals distinct lateral temperature gradients

[1] R. D. Deegan *et al.*, *Capillary flow as the cause of ring stains from dried liquid drops*, Nature, **389**, 827–829 (1997)

[2] A. M. Cazabat, F. Heslot, S. M. Troian, P. Carles, *Fingering instability of thin spreading films driven by temperature gradients*, Nature, **346**, 824–826 (1990)

[3] W. Sempels, R. De Dier, H. Mizuno, J. Hofkens, J. Vermant, *Auto-production of biosurfactants reverses the coffee ring effect in a bacterial system*, Nat. Commun., **4**, 1757 (2013)

[4] R. De Dier, W. Sempels, J. Hofkens, J. Vermant, *A drying droplet spreads out its wings: Thermo-capillary fingering in water droplets*, submitted (2014)

Interfacial heat transfer of liquid film flows in narrow channels

F. Denner,[1] M. Vieweg,[1] C. N. Markides,[2] S. Kalliadasis,[2] and B. G. M. van Wachem[1]

[1]*Department of Mechanical Engineering, Imperial College London, London, SW7 2AZ, United Kingdom*
f.denner09@imperial.ac.uk, b.van-wachem@imperial.ac.uk

[2]*Department of Chemical Engineering, Imperial College London, London, SW7 2AZ, United Kingdom*

Liquid films flowing in a channel are widely used in heat exchange applications, e.g. microcoolers of electronic devices. Since the heat transfer coefficient of the liquid film is inversely proportional to the film thickness, the application of wavy liquid films, for instance excited by an oscillating mass flow, the substrate topography or hydrodynamic instabilities driven by the thermocapillary Marangoni effect, has great potential to improve the heat transfer in gas-liquid systems. Previous experimental and numerical studies found that circulations in the liquid phase as well as film thinning improve the heat transfer through wavy liquid films [1, 2]. However, the heat transfer across the gas-liquid interface is typically the bottleneck with respect to the heat transfer in gas-liquid systems, due to the lower heat capacity of the gas phase. The resulting limitation in heat transfer is especially problematic around the troughs of wavy films where the heat transfer through the liquid is particularly high because of the reduced film height. An inability to transport the heat away from the gas-liquid interface may cause film rupture and, as a result, a local breakdown in heat transfer.

In our presentation we discuss the results of a comprehensive numerical study on heat transfer at the gas-liquid interface of liquid films in narrow channels, capturing both fluid phases as well as the full capillary and thermocapillary dynamics using our in-house DNS code [3]. For instance, Fig. 1 shows the stream contours in the wave-fixed reference frame of a vertically falling liquid film in a narrow channel with a co-current gas flow. The circulation zones in the gas phase, clearly visible around and upstream the solitary wave, transport the gas from the wave troughs to the gas-sided wall region. Similar flow patterns in co-current gas flows have also been reported by Dietze and Ruyer-Quil [4]. Such circulation zones have the potential to substantially improve the heat transfer across the gas-liquid interface at and near the wave troughs. Furthermore, the closed circulation zones observed in both phases may improve the heat and mass transfer in streamwise direction, as suggested by the study of Camassa *et al.* [5]. Understanding how these flow patterns change the heat transfer in both phases as well as across the gas-liquid interface is pivotal in optimising the application of liquid film flows in heat exchangers. During our presentation we will show the influence of the gas circulation and of thermocapillary motion on the heat transfer across the gas liquid interface. We will also discuss design guidelines for heat exchangers utilising such flows.

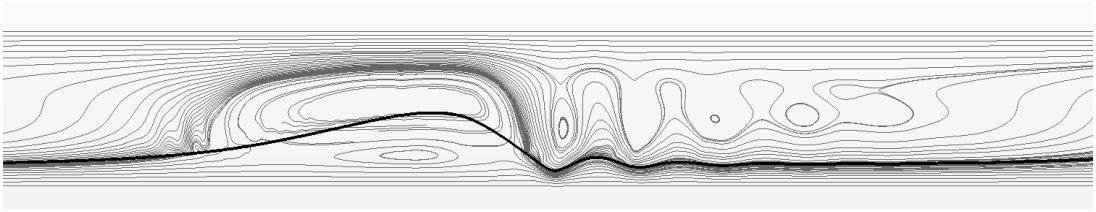

FIG. 1. Stream contours in the wave-fixed reference frame of a vertically falling liquid film flow at $Re = 15$ with a confined co-current gas flow. The gas-liquid interface is depicted in black.

[1] A. Miyara, Heat and Mass Transfer, **35**, 298 (1999).
[2] R. Mathie, H. Nakamura, C. Markides, International Journal of Heat and Mass Transfer, **56**, 819 (2013).
[3] F. Denner, B. van Wachem, Numerical Heat Transfer, Part B: Fundamentals, **65**, 218 (2014).
[4] G. F. Dietze, C. Ruyer-Quil, Journal of Fluid Mechanics, **722**, 348 (2013).
[5] R. Camassa, M. Forest, L. Lee, H. Ogrosky, J. Olander, Physical Review E, **86**, 066305 (2012).

Numerical methods for interfacial flows with high density ratios and high surface tension

F. Denner[1] and B. G. M. van Wachem[1]

[1]*Department of Mechanical Engineering, Imperial College London, London, SW7 2AZ, United Kingdom*
f.denner09@imperial.ac.uk, b.van-wachem@imperial.ac.uk

Although significant research efforts have been dedicated to study and develop numerical methods for two-phase flows, the simulation of surface-tension-dominated flows with large density and viscosity ratios still presents substantial difficulties. Surface tension as well as the difference of density and viscosity between the fluids cause a steep change in momentum at the interface, resulting in ill-conditioned governing equations. This typically leads to limitations of the reliably computable density and viscosity ratios or surface force as well as to unphysical flow pattern in the vicinity of the interface, such as pressure oscillations and parasitic currents.

We have developed a coupled numerical framework that assures an exact balance between the pressure gradient and the acting body forces and provides a strong pressure-velocity coupling, which is particularly desirable for the ill-conditioned set of equations in interfacial flow simulations [1]. Our numerical framework eliminates pressures oscillations at the interface, reliably simulates flows with any practical density and viscosity ratios, is mass conserving and is applicable on structured, unstructured and adaptive meshes [1, 2]. Moreover, parasitic currents are eliminated if the exact curvature value is prescribed at the interface. Figure 1 shows the results for a spherical drop with $d = 1\,mm$ and the surface tension of a water-air system. On the left, the convergence of the residuals is shown as a function of iterations in the first time-step, starting with a $p = 0\,Pa$ throughout the computational domain. Irrespective of the applied density and viscosity ratios, the residuals successfully converge to solver tolerance. On the right of Figure 1, the fully developed pressure profiles after the first time-step are given, showing accurate solutions with no oscillations. The results for the applied density and viscosity ratios are indistinguishable from each other.

In our presentation we will explain our numerical approach and highlight how we solved or mitigated typically encountered difficulties and inaccuracies in interfacial flow simulations, such as the convergence and stability for high density ratios. In addition, we will provide guidelines to practitioners on ways to diminish the impact of some of the most pertinent issues, for instance parasitic currents.

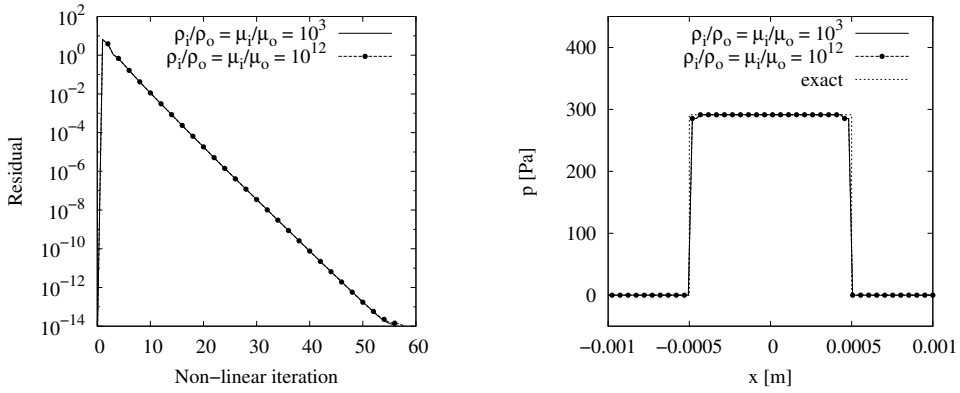

FIG. 1: Convergence and pressure profile for a spherical drop of $d = 1\,mm$

[1] F. Denner, B. van Wachem, Numerical Heat Transfer, Part B: Fundamentals, **65**, 218 (2014).

[2] F. Denner, *Balanced-Force Two-Phase Flow Modelling on Unstructured and Adaptive Meshes*, Ph.D. thesis, Imperial College London (2013).

Direct and model-based simulations of three-dimensional falling liquid films: surface waves and associated flow structures

G. F. Dietze,[1] W. Rohlfs,[2] K. Nährich,[2] R. Kneer,[2] and B. Scheid[3]

[1]*CNRS, Laboratoire FAST, Bât. 502, Campus Universitaire, F-91405 Orsay, France*
dietze@fast.u-psud.fr

[2]*Institute of Heat and Mass Transfer, RWTH-Aachen University, Aachen D-52056, Germany*

[3]*Laboratoire TIPs, Université Libre de Bruxelles, Brussels B-1050, Belgium*

Falling liquid films develop intricately shaped free-surface waves as a result of a gravity-driven instability, which can for instance be observed on an inclined road during a rainy day. After a sufficient development length, these wavy films evolve toward predominantly three-dimensional wave structures that affect a number of yet-to-be fully elucidated features: Firstly, the transition to turbulence in wavy films occurs at relatively low Reynolds number values and is intermittent in nature; secondly, heat and mass transfer is significantly intensified in three- compared to two-dimensional wavy films. To investigate these features in detail, we performed direct numerical simulations (using the VOF and CSF methods) of periodic wave segments for a set of representative falling film scenarios on the supercomputer JUROPA (Forschungszentrum Jülich). These direct numerical simulations (DNSs) enabled a detailed study of the wave-effect on flow structures within the film and gas, while complementary simulations with a low-dimensional Integral Boundary Layer (IBL) model [1] allowed us to investigate wave dynamics at very long times (up to fifty wave periods).

Fig. 1 shows a representative result of the DNS of a water film at relatively high Reynolds number. The free-surface of the film is segregated into a region of large humps surrounded by a very thin film with small capillary waves. Our simulations show that this translates into a corresponding segregation of the flow dynamics within the film: (i) In the large humps, inertia dominates surface tension and the local Reynolds number is up to five times larger than its overall value, explaining the earlier transition to turbulence of falling liquid films. In this region, intricate flow structures carrying streamwise vorticity occur in the trailing hump; (ii) In the thin film region, surface tension and/or viscous forces dominate inertia and the flow is almost entirely governed by pressure variations imposed by changes in free-surface curvature. This generates a three-dimensional cellular flow pattern in the liquid and gas. The vorticity-carrying structures observed in the above-mentioned regions intensify convective transport and, by extension, explain the substantial increase in inter-phase heat/mass transfer in three- dimensional films. Finally, our complementary long-time IBL simulations have shown that the three-dimensional wave structure does not attain a saturated state but oscillates back and forth between three- and more two-dimensional shapes. The onset of these oscillations is visible in the DNSs and we have shown it to result from an interaction between capillary waves and leading large humps, the latter being periodically drained by the former, decreasing their mass and celerity in the process.

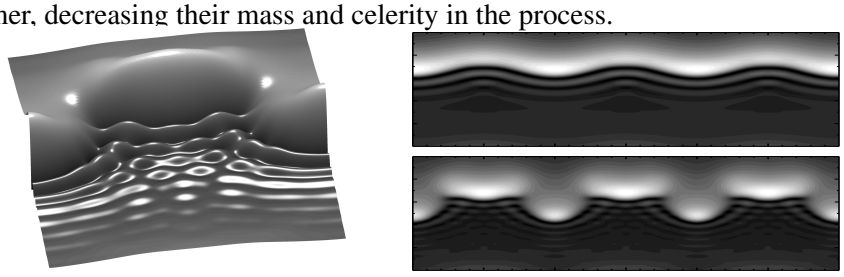

FIG. 1. Wavy water film (Re=59) obtained from direct numerical simulation [2]. Left: Three-dimensional free-surface topology; Right: Time-evolution of surface waves from a small-amplitude initial perturbation.

[1] B. Scheid, C. Ruyer-Quil, P. Manneville, *Wave patterns in film flows: modelling and three-dimensional waves*, J. Fluid Mech., **562**, 183-222 (2006).

[2] G. F. Dietze, W. Rohlfs, K. Nährich, R. Kneer, B. Scheid, *Three-dimensional flow structures in laminar falling liquid films*, J. Fluid Mech., 743, 75-123 (2014).

Self-patterning induced by a solutal Marangoni effect in a receding drying meniscus

F. Doumenc[1] and B. Guerrier[1]

[1]*Univ Paris-Sud, Univ Paris 06, CNRS, Lab FAST, Bât 502, Orsay, F-91405, France,*
doumenc@fast.u-psud.fr

This study explores through numerical simulations the impact of a solutal Marangoni effect on the deposit obtained by drying a polymer solution. A hydrodynamic model with lubrication approximation is used to describe the liquid phase in a dip-coating-like configuration. The studied case considers evaporation in stagnant air (diffusion-limited evaporation), which results in a coupling between liquid and gas phases. Viscosity, surface tension, and saturated vapor pressure depend on solute concentration. When surface tension increases with polymer concentration the Marangoni effect may induce a periodic regime. This results in a self-organized periodic patterning of the dried film in certain control parameter ranges (see Fig. 1). A morphological phase diagram as well as meniscus and dry-deposit shapes are provided as a function of the substrate velocity and bulk solute concentration.

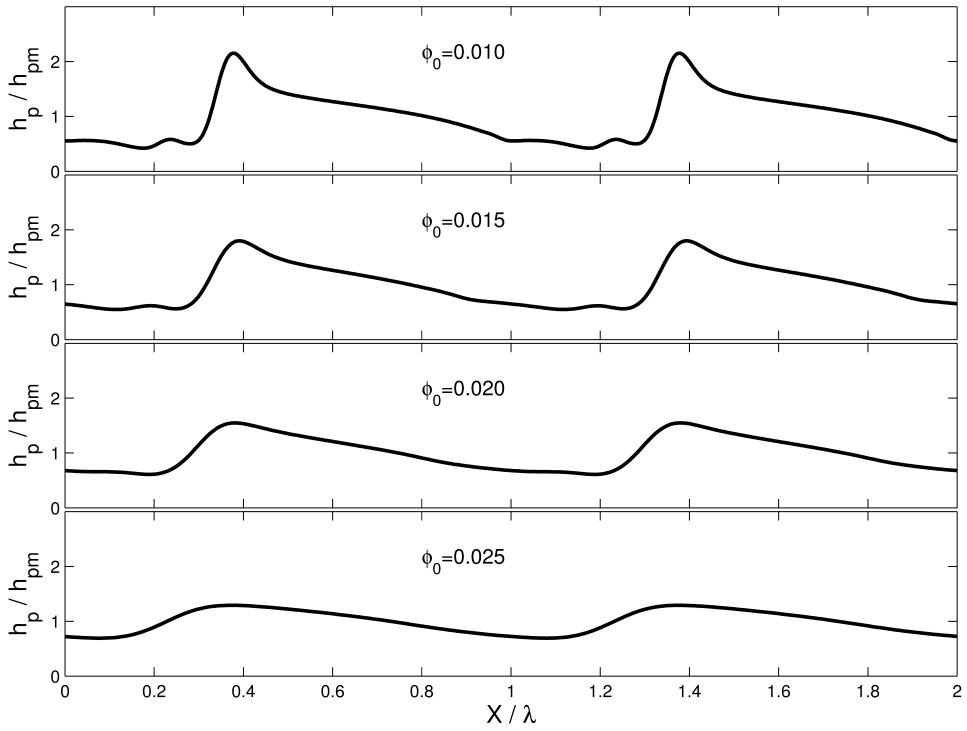

FIG. 1. Deposit shape for a substrate velocity $V_{sub} = 25\mu m/s$ and different initial polymer volume fractions Φ_0. The distance X and the local deposit height h_p are normalized by the wavelength λ and deposit mean thickness h_{pm}, respectively. From top to down:
$\Phi_0 = 0.010,\ \lambda = 314\mu m,\ h_{pm} = 0.158\mu m \quad - \quad \Phi_0 = 0.015,\ \lambda = 300\mu m,\ h_{pm} = 0.243\mu m$
$\Phi_0 = 0.020,\ \lambda = 293\mu m,\ h_{pm} = 0.327\mu m \quad - \quad \Phi_0 = 0.025,\ \lambda = 288\mu m,\ h_{pm} = 0.414\mu m$

Contact line motion of a volatile liquid in an inert gas

V. Janecek[1],F. Doumenc[1], V. Nikolayev[2]and B. Guerrier[1]

[1]*Univ Paris-Sud, Univ Paris 06, CNRS, Lab FAST, Bât 502, Orsay, F-91405, France,*
doumenc@fast.u-psud.fr

[2]*CEA Saclay, Service de Physique de l'Etat Condensé,*
Bât 772, Orme des Merisiers, Gif sur Yvette, F-91191, France,
vadim.nikolayev@cea.fr

For a liquid wedge on a moving substrate, specific approaches are required to model the contact line vicinity in order to relieve the dynamical singularity due to the divergence of the shear stress at the contact line [1, 2]. Among the different mechanisms that are proposed in this context, the present study focuses on the evaporation/condensation phenomena induced by the deformation of the profile close to the contact line (Kelvin effect). Previous studies have been performed for pure vapor and partial wetting [3, 4], or diffusion in an inert gas and total wetting [5, 6]. In a partial wetting configuration (liquid wedge), we develop a model in the framework of lubrication approximation that takes into account diffusion of the vapor in the gas phase and kinetic resistance at the interface. We perform a perturbation analysis assuming a small substrate velocity. The evaporation flux is solution of an integro-differential equation that is solved numerically. This provides quantitative estimations for the local curvature and evaporation flux induced by the substrate motion. This model is valid if the characteristic length of the problem is consistent with hydrodynamic approach. We thus determine the Voinov length for different fluids and wetting properties and analyze the validity domain of the regularization approach based on evaporation/condensation.

---

[1] C. Huh, L. E. Scriven, *Hydrodynamic Model of Steady Movement of a Solid/Liquid/Fluid Contact Line*, Journal of Colloid and Interface Science, **35**, 85-101 (1971).

[2] D. Bonn, J. Eggers, J. Indekeu, J. Meunier, E. Rolley, *Wetting and spreading*, Reviews of Modern Physics, **81**, 739-805 (2009).

[3] A. Rednikov, P. Colinet, *Singularity-free description of moving contact lines for volatile liquids*, Phys. Rev. E, **87**, 010401 (2013).

[4] V. Janecek, B. Andreotti, D. Prazak, T. Barta, V. S. Nikolayev, *Moving contact line of a volatile fluid*, Phys. Rev. E, **88**, 060404 (2013).

[5] J. Eggers, L. M. Pismen, *Nonlocal description of evaporating drops*, Phys. Fluids, **22**, 112101 (2010).

[6] F. Doumenc, B. Guerrier, *A model coupling the liquid and gas phases for a totally wetting evaporative meniscus*, Eur. Phys. J. Special Topics, **197**, 281-293 (2011).

Thermocapillary convection in the evaporation droplets

B. He[1] and F. Duan[1]

[1] *School of Mechanical and Aerospace Engineering Nanyang Technological University, Singapore 639798,* feidua@ntu.edu.sg

Thermocapillary convection is a flow driven by the surface tension gradient at liquid-gas interface. The interfacial temperature variation can be generated the surface tension variation since the surface tension is a function of temperature. Thermocapillary convection is always masked by the buoyancy-driven convection on earth due to the gravitational effect. In recent experiments, the energy balance showed that thermal conduction to the evaporation interface cannot supply the energy for evaporation; the thermocapillary flow can transport energy at interface and distribute the energy along the interface [1, 2]. However, the surface flows were difficult tracked at a curved evaporating interface. A direct velocity recovery method has been applied to recover the vector field at the droplet interface collected by Particle image velocimetry (PIV). The analysis software is developed to obtain actual flow result. From the comparison with the image recovery scheme, the direct velocity recovery method demonstrates a good accuracy on recovering the distorted image. Such method has been applied to recover the flow measurements of a pendant silicon oil droplet during steady state evaporation. The experiments of heated pendant silicon oil droplets were conducted with different base temperature from 30°C to 80°C in ambient conditions. It is found that a higher temperature difference between the apex and the periphery would generate a high convection velocity measured by PIV inside the droplet.

---

[1] F. Duan, *Local evaporation rate effected by thermocapillary convection at evaporating droplet*, J. Phys. D: Appl. Phys, **42**, 102004 (2009).

[2] F. Duan, C. A. Ward, *Investigation of local evaporation flux and vapor-phase pressure at an evaporative droplet interface*, Langmuir, **25**, 7424-7431 (2009).

Evaporation rate from mesoscopic structures of monodispersed microspheres: experimental and computer simulations

A. F. Ginevskiy,[1] A. S. Dmitriev,[1] and M. A. El Bouz[1,2]

[1]*National Research University "MPEI", Moscow, Russia*

asdmitriev@mail.ru

[2]*Mansoura University, Mansoura, Egypt*

mostafa_booz@yahoo.com

In recent decades significant attention has been given to the heat and mass transfer in structures ranging from mesoscopic to nano structures. The study of heat and mass transfer of effective evaporation and boiling in such structures is an important issue [1, 2]. This paper is concerned with mesoscopic structures on the base of monodispersion microspheres with different diameters ranging from d = 50 μm to d = 400 μm.

Evaporation of various fluids in monodisperse systems was investigated experimentally. To perform this experimental study, an experimental test rig was designed and constructed. Two sets of experimental runs were conducted at atmospheric pressure. Firstly, free evaporation of distilled water, alcohol and isooctane without microspheres from test tubes. Secondly, evaporation of distilled water, alcohol and isooctane in the presence of monodisperse microspheres from test tubes. All experiments were carried out at temperatures of 60,70 and 80 $^{\circ}C$ to study the dependence of evaporation rates of various fluids for temperature variations. On the other hand the experiments were carried out for different diameters of microspheres (d = 50 μm to d = 400 μm) to study the effect of microsphere diameter on the process of evaporation. All experiments were repeated in Petri dishes instead of test tubes to obtain a detailed scheme of experiments. Analysis of results, evaporation model with Phoenics [3] software simulation and a comparison with the results of other researchers is carried out.

In mesostructure evaporation is completely different. The experimental results show that, the evaporation in this case, is strongly associated with the influence of the surface of the microspheres, the emergence of "liquid bridges" between the microspheres in the process of evaporation and other effects.

The current investigation is directed at experimentally determining the relational dependence of different parameters and then analyzing the resulting data in order to gain a better understanding of the fundamental parameters that govern the behavior in these types of applications.

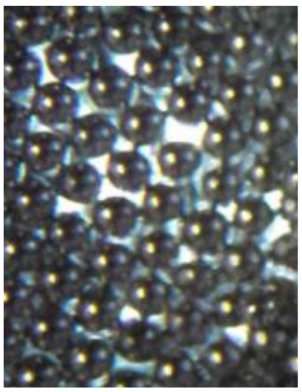

FIG. 1. Microspheres in water.

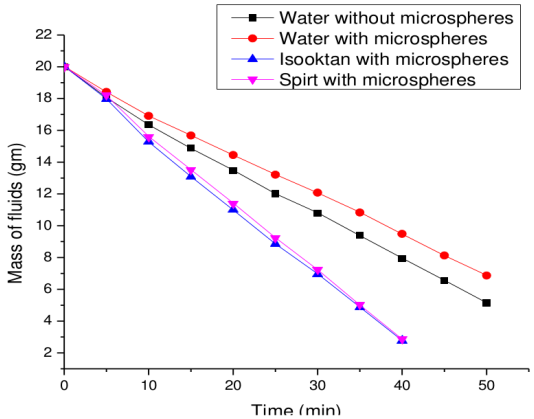

FIG. 2. Variation of mass of different liquids with time.

[1] E. V. Amitistov, A. S. Dmitriev, *Monodispersion systems and technology*, MPEI, **536** (2002).

[2] V. P. Isatchenko, V. A. Osipova, A. S. Sukomel, Heat transfer. M: Energoizdat, **416** (1981).

[3] http://www.cham.co.uk

Experimental investigation of the instability between two immiscible fluids flowing in a microchannel in the presence of an electric field

P. Eribol[1] and A. K. Uguz[1]

[1]*Department of Chemical Engineering, Bogazici University, Bebek, 34342, Istanbul, Turkey,*
pinareribol@gmail.com, kerem.uguz@boun.edu.tr

An electric field may be applied to destabilize the interface between two immiscible fluids flowing in a rectangular microchannel. In this work, the onset of electrohydrodynamic instability of the interface between two Newtonian and immiscible liquids flowing in a microchannel due to a pressure gradient is experimentally investigated. A DC electric field is applied either parallel or normal to the flat interface. Several different liquid combinations and different size microchannels are employed to parametrically investigate the instability. In addition the volumetric flow rates of the fluids are varied to generate different depth ratios of the liquids. The results are qualitatively compared with a leaky-dielectric theory where the fluids are assumed to obey pressure-driven flow and are incompressible. The important theoretical parameters that are analyzed are capillary number, ratios of flow rates, and viscosities of the fluids and the electrical properties of the liquids.

A promising front tracking method with high order of accuracy

P. Fan[1] and C. Yang[1]

[1]*Institute of Process Engineering, Chinese Academy of Sciences,*
No.1 Zhongguancun North Street, 100190, Beijing, China,
pfan@ipe.ac.cn , chaoyang@ipe.ac.cn

Tracking a moving interface is an extremely challenging problem in the computations of free surface (interface) flows appearing in many mathematical and engineering problems and has attracted considerable research interest over the years.

Generally speaking, this problem can be treated by Eulerian and Lagrangian methods. The Eulerian methods (equivalent to the front capturing methods) use an auxiliary scalar field, which is updated by solving a scalar transport equation, to identify different flow domains with respect to a fixed grid and locate the interface. Two typical methods of the front capturing methods are the volume of fluid (VOF) method and the Level-Set (LS) method. The VOF method reconstructs the interface with good mass-preserving properties [1, 2], nonetheless, it is hard to accurately compute the curvature ascribed to that the interface is described by a discontinuous surface at the cells boundaries. The LS method provides a continuous representation of the interface by introducing a Level-Set function and makes the estimation for the most important geometrical features of the interface, such as the local normal vector and the curvature, facilitated. However, the Level-Set function must be often reinitialized which costs an extra computational effort and looses the mass continuously [3].

In summary, the interface reconstruction in the front capturing method is worked completely from a higher dimensional area to a lower dimensional area, which inevitably results in the loss of resolution. Although, the existing front tracking methods track the interface itself and are hence able to perform a better numerical resolution, however the operations for keeping regularity of the boundary element are still too rough to achieve an order higher than 2. This problem will degenerate the numerical results when a flow is dominated by the surface tension which is related to the curvature of the interface. In other words, the numerical results will not higher than second order if the estimated geometric parameters of the interface are not higher than 4^{th} order. These undesirable facts manifest that in spite of the great success of the existing front tracking/capturing methods, further improvements are still indispensable.

In this paper a new front tracking method, called the interface-point-group (IPG) method, is developed, arriving successfully at the goal for high order of accuracy by efficient means. The interface is represented by a series of Lagrangian points groups, taking on a basic feature that the absolute values of the local gradients in each point group are stipulated below 1. The major advantage of this technique is that high quality interpolation formulae can be applied to approximate the local geometrical information of the interface, with the exclusion of any possible multi-valued points which could prevent the use of interpolations. Moreover, for the purpose of enhancing the accuracy and efficiency of this method, effective seeding and de-seeding algorithms are employed to avoid any useless over-scattering and over-clustering of the interface points. The results from some widely used benchmark tests manifest that the present method can achieve a high order of accuracy.

---

[1] W. Rider, D. Kothe, *Reconstructing volume tracking*, J. Comput. Phys., **141**, 112-152 (1998).

[2] R. Scardovelli, S. Zaleski, *Direct numerical simulation of free-surface and interfacial flow*, Annu. Rev. Fluid Mech., **31**, 567-603 (1999).

[3] J. Sethian, P. Smereka, *Level set methods for fluid interfaces*, Annu. Rev. Fluid Mech., **35**, 341-372 (2003).

Creating localized-droplet train by traveling thermal waves

V. Frumkin,[1] W. Mao,[2] A. Alexeev,[2] and A. Oron[3]

[1]*Department of Mathematics, Technion - Israel Institute of Technology, Haifa 32000, Israel,*
valerafr@gmail.com
[2]*Woodruff School of Mechanical Engineering,*
Georgia Institute of Technology, Atlanta, GA 30332, USA,
wmao3@gatech.edu, alexander.alexeev@me.gatech.edu
[3]*Department of Mechanical Engineering, Technion - Israel Institute of Technology, Haifa, IL-32000, Israel,*
meroron@tx.technion.ac.il

Using long-wave theory and direct numerical simulations, we investigate the nonlinear dynamics of a bilayer system consisting of a thin liquid film and an overlying gas layer driven by the Marangoni instability. The bottom solid substrate is heated in the form of periodical thermal waves propagating along the substrate with a constant frequency ω. In the case of a stationary thermal wave, $\omega = 0$, the liquid film rupture takes place with a flattish wide trough when both Marangoni number and the amplitude of the thermal wave are sufficiently large. Regimes in which the film forms a train of localized drops traveling along the substrate arise for sufficiently small, but non-zero ω. In this case, localized traveling drops are interconnected by thin liquid bridges with negligible small flow velocities. We show that the liquid is trapped inside the drops during the drop train motion and the total flow rate is linearly proportional to ω. When the minimal thickness of the bridges between consecutive drops is increased, a faster flow rate can be achieved than in the localized drop-train configuration. In this case, however, fluid in the bridges has the negative (backward) velocity and can migrate from one drop to another, thereby leading to a gradual exchange of the content of drops in the train. Thus, the localized drop-train mechanism can be tuned to allow for the delivery of the entire drop content in the direction of the thermal wave propagation.

Weakly nonlinear stability of Marangoni convection in a half-zone liquid bridge

K. Fujimura[1]

[1]*Department of Applied Mathematics and Physics, Tottori University, Tottori 680-8552, Japan*
kaoru@damp.tottori-u.ac.jp

Marangoni convection in a liquid bridge with finite aspect ratio has been examined on its linear stability during last a quarter century both for half-zone and full-zone models. In contrast, to the author's knowledge, weakly nonlinear stability has not been examined, yet. This can be attributed to the fact that a heavy numerical task is required in the weakly nonlinear analysis. In this paper, we show some recently obtained numerical results on a half-zone liquid bridge on the weakly nonlinear basis. [1]

Assume that a liquid bridge has an interface which is non-deformable and thermally insulating. We ignore the effect of the gravity. We set $h/r_0 = 1$ where h is the height and r_0 is the radius of the liquid bridge. Standard normal mode analysis together with homogeneous boundary conditions yield spatially two-dimensional linear eigenvalue problem. To obtain the basic flow and to solve the eigenvalue problem, we adopted double expansions in Chebyshev polynomials both in r and z-directions. 'Amplitude expansion method' is then utilised to reduce nonlinear PDEs to amplitude equations for slightly supercritical state under O(2)-symmetry. For $P < 0.057$, steady bifurcation sets in, whereas for $P > 0.057$, Hopf bifurcation occurs where P is the Prandtl number. The equation of the amplitude $z(t)$ for steady mode is given by $\dot{z} = z(\mu + \kappa|z|^2)$ where $\mu, \kappa \in \mathbb{R}$. For Hopf bifurcation, equations of amplitudes for counter rotating eigenmodes $z_1(t)$ and $z_2(t)$ are $\dot{z}_1 = z_1(\sigma + \lambda_1|z_1|^2 + \lambda_2|z_2|^2)$ and $\dot{z}_2 = z_2(\sigma + \lambda_2|z_1|^2 + \lambda_1|z_2|^2)$ where $\sigma, \lambda_1, \lambda_2 \in \mathbb{C}$. We summarized the linear critical curve and weakly nonlinear characteristics along it in Fig.1. The results are found to be consistent with those obtained in [5] for $P = 0.02$ and 4.

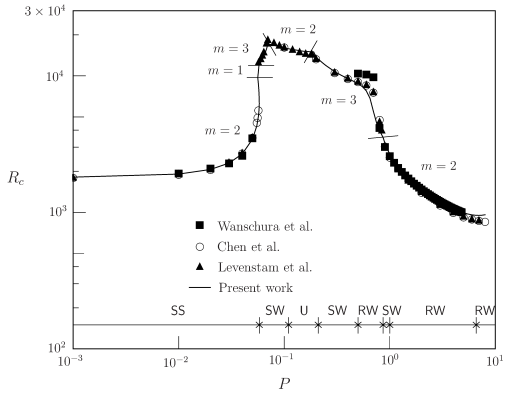

FIG. 1. Linear critical curve for a half-zone liquid bridge and weakly nonlinear characteristics along it for $h/r_0 = 1$ where R_c is the critical Reynolds number. [1] Results of [2–4] are shown for comparison.'SS': stable steady state, 'RW': stable rotating waves, 'SW': stable standing waves, and 'U': absence of stable non-trivial solution.

[1] K. Fujimura, Linear and weakly nonlinear stability of Marangoni convection in a liquid bridge, J. Phys. Soc. Jpn. **82**, 074401 (2013).

[2] M. Wanschura, V. M. Shevtsova, H. C. Kuhlmann and H. J. Rath, Convective instability mechanisms in thermocapillary liquid bridges, Phys. Fluids **7**, 912–925 (1995).

[3] G. Chen, A. Lizée and B. Roux, Bifurcation analysis of the thermocapillary convection in cylindrical liquid bridges, J. Crystal Growth **180**, 638–647 (1997).

[4] M. Levenstam, G. Amberg and C. Winkler, Instabilities of thermocapillary convection in a half-zone at intermediate Prandtl numbers, Phys. Fluids **13**, 807–816 (2001).

[5] J. Leypoldt, H. C. Kuhlmann and H. J. Rath, Three-dimensional numerical simulation of thermocapillary flows in cylindrical liquid bridges, J. Fluid Mech. **414**, 285–314 (2000).

Experimental study on pulsating heat pipe using self-rewetting fluid as a working fluid (visualization of thin liquid film and surface wave)

K. Fumoto,[1] T. Ishida,[1] K. Yamagami,[1] T. Kawanami,[2] and T. Inamura[1]

[1]*Department of Intelligent Machines and Engineering, Hirosaki University, 3 Bunkyo-cho Hirosaki, 0368561, Japan,*
kfumoto@cc.hirosakiu.ac.jp

[2]*Department of Mechanical Engineering, Kobe University 1-1 Rokkodai-cho, Nada-ku, Kobe, 6578501, Japan*

Pulsating (or oscillating) heat pipe (PHP) is a new type of efficient heat transfer device, which was introduced in the mid-1990s by Akachi. PHP can be used for cooling of electronics because of its potential for removing high heat flux. Therefore, PHP has attracted a great deal of attention.

Recently, some studies [1] have been conducted on conventional heat pipes using dilute aqueous solutions of alcohols with a high number of carbon atoms (such as Butanol and Pentanol). These solutions can be considered as self-rewetting fluids because self-rewetting fluids show a non-linear dependence of the surface tension with temperature. In the case of ordinary liquids, the surface tension is a decreasing function of the temperature. By contrast, for self-rewetting fluids, the surface tension takes a minimum value at a certain temperature and there is a range of temperature that surface tension increase with. In addition, some studies [2] have presented self-rewetting fluids as working fluids for PHP. In this study, flow visualization of open-loop pulsating heat pipe (OLPHP) was carried out to investigate flow behavior in the glass tubes.

EXPERIMENTAL SETUP AND RESULTS

The OLPHP was made of pyrex glass tubes with 1.8 mm internal diameter and 3.0 mm external diameter, and the number of turns is 10. The working fluids employed were water, ethanol, and 1-Butanol aqueous solution. The experimental results indicate that OLPHP using Butanol aqueous solutions as working fluids can be observed anomalous liquid film behavior in adiabatic section. For Butanol aqueous solutions, liquid slug easily formed liquid film behind. And the liquid film was very wavy when liquid slug moved to cooling section from heating section (Fig.1). This phenomenon was not observed in other working fluids. The wavy liquid film is caused by peculiar surface tension of the self-rewetting fluid.

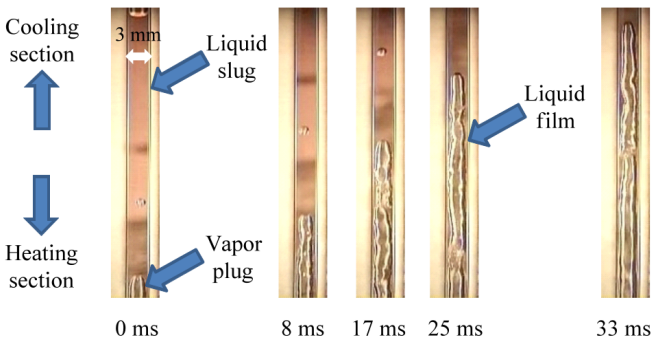

FIG. 1. Flow visualization of adiabatic section.

[1] Y. Abe, Y. Horiuchi, Y. Saito, M. Mochizuki, Proc. 44th National Heat Transfer Symp. of Japan., **Vol. 2**, No. C219 (2007).

[2] K. Fumoto, M. Kawaji, *Improvement in Pulsating Heat Pipes Using a Self-rewetting Fluid (Cases of 1-Butanol and 1-Pentanol)*, Thermal Science & Enginnering, **Vol. 19**, p. 1-7 (2011).

Evolution of thermo-convective flows in liquid bridges due to evaporation

Y. Gaponenko[1] and V. Shevtsova[1]

[1]*Microgravity Research Center, Université Libre de Bruxelles, F. Roosevelt 50, 1050 Brussels, Belgium,*
ygaponen@ulb.ac.be, vshev@ulb.ac.be

The target of present study is to identify the mechanisms that control the evolution of the thermal convection in liquid bridge during the process of its evaporation. We analyze the effects of evaporative cooling on the flow structures and temperature fields during transition from steady to oscillatory convection. This investigation is related to space experiment JEREMI (Japanese European Space Research Experiment on Marangoni Instabilities) which is devoted to the study the influence of a coaxial gas stream on the thermocapillary flows in cylindrical geometry. Gas flows between the liquid bridge and an external wall. This experiment is planned to be performed in the Japanese module on ISS using the dedicated FPEF (Fluid Physics Experiment Facility).

We present results of 2D and 3D numerical simulations in the geometry which corresponds to a liquid bridge, axially placed into an outer cylinder with solid walls. The internal core consists of solid rods at the bottom and top, while the central part is a relatively short liquid zone filled with viscous liquid kept in its position by surface tension. Initially the motionless gas surrounds the quiescent liquid (see Fig.1a). The temperature difference ΔT is imposed between the solid rods. Convective flows in the gas and liquid are produced through a joint action of the two effects, the buoyancy and the thermocapillary effect, and develop in the presence of evaporation through the interface.

It is assumed that convective flow and evaporation do not change the liquids bridge shape. This model corresponds to the experimental conditions with continuous refill of a liquid bridge. The volumes of injected and evaporated liquids are equal and the amount of injected liquid allows determining the evaporation rate. Practically, different evaporation rates can be realized by changing the distance between a liquid and external wall and by the temperature control of the external wall.

Evaporation cools the interface and increases the temperature gradient in middle of the interface, which becomes thermocapillary active on the entire length. At the evaporation rate above a certain value the inversion of temperature gradient occurs, see 3rd-4th curves in Fig 1b. The change of the sign of the temperature gradient causes the flow separation in liquid and gas phases; a vortex with the opposite direction of a circulation appears near the cold wall. Correspondingly, the velocity of a liquid on the interface changes sign as illustrated by Fig.1-(c). This scenario corresponds to the experimental observations reported in [1]. We noted that presence of temperature inversion during cooling of the interface by evaporation is very important factor for onset of 3D oscillatory instability in liquid bridges.

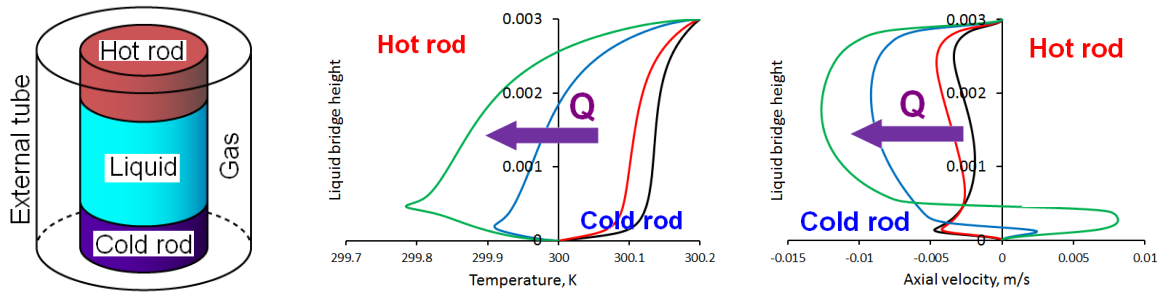

(a) (b) (c)

FIG. 1. (a) Geometry of the problem; (b) temperature profile on the interface with increasing of the evaporation rate; arrow indicates the increase of evaporation rate Q. (c) Interface velocity for the same parameters as the temperature profiles in graph (b).

[1] S. Simic-Stefani, M. Kawaji, S. Yoda, *Onset of oscillatory thermocapillary convection in acetone liquid bridges: The effect of evaporation*, International Journal of Heat and Mass Transfer, **49**, 31673179 (2006).

Investigation of the liquid film flows with evaporation by means of new mathematical models based on the general interface conditions

O. N. Goncharova[1,2] and E. V. Rezanova[1]

[1]*Altai State University, Department of Differential Equations, pr. Lenina 61, 656049 Barnaul, Russia,* gon@math.asu.ru

[2]*Institute of Thermophysics, Russian Academy of Sciences, pr. Lavrentyev 1, 630090 Novosibirsk, Russia*

The processes of convection of the fluids, accompanied by evaporation at the interface, are actively studied in the present time. Mathematical modelling of the convective flows caused by impact of various factors on the fluid media, such as shear flows, gravity and thermocapillary forces, interfacial mass transfer has been presented in [1]. The general conditions to be applied at the interface between two interacting gas and liquid phases result from the strong discontinuity relations for mass, impulse and energy balance when transfer of these quantities occurs through the interface [1, 2]. The additional hypotheses and relations concerning continuity of some flow characteristics, laws of the heat and mass fluxes, phenomenological properties have been assumed in order to obtain the closed problem statements.

In the present paper a film of viscous liquid flowing down an inclined plate is studied using the long-wave approaches (see also [3, 4]). The new mathematical models of flows of the evaporating liquid film constructed on the basis of the Navier-Stokes equations, heat transfer equation and generalized kinematic, dynamic and energetic interface conditions are presented. The equations of thin liquid films in the two-dimensional case are derived in detail for the case of the Reynolds numbers of the order of unity. The dimensionless evolution equation of the film thickness h can be written in the following form:

$$h_t + h_x \left[\left\{ (C_0)_x \frac{h^2}{2} - \gamma_1 \sin\alpha \frac{h^2}{2} + C_1 h \right\} + \epsilon \left\{ (\overline{C_0})_x \frac{h^2}{2} + \overline{C_1} h \right\} \right] -$$

$$\left[-(C_0)_{xx} \frac{h^3}{6} - (C_1)_x h + \epsilon \left\{ -(\overline{C_0})_{xx} \frac{h^3}{6} - \overline{C_1} \frac{h^2}{2} \right\} \right] + (E/\epsilon) J_{ev} = 0.$$

Here the functions $C_0, C_1, \overline{C_0}, \overline{C_1}$ are expressed in terms of h, given substrate temperature and dimensionless parameters such as the Marangoni, Prandtl, Reynolds numbers, capillary and evaporation E numbers, and some other dimensionless parameters; γ_1 is the parameter depending on the Grashof, Reynolds and Boussinesq numbers; J_{ev} denotes a local vapour flux at the interface defined by the Hertz-Knudsen equation; ϵ is a small parameter (a ratio of the transverse and longitudinal characteristic lengths).

The effects of the various forces on the liquid film being under conditions of gravity or microgravity and the effects of an uniform and non-uniform heating of the substrate on the film flows are studied. Numerical investigations and comparison with the results of an alternative modeling of the evaporating falling films [4] are carried out.

Acknowledgments. The research has been supported by the Russian Foundation for Basic Research (Project No. 14-08-00163).

[1] C. S. Iorio, O. N. Goncharova, O. A. Kabov, *Heat and mass transfer control by evaporative thermal pattering of thin liquid layers*, Computational Thermal Sci., **3(4)**, 333-342 (2011).

[2] O. N. Goncharova, *Modeling of flows under conditions of heat- and mass transfer at the interface*, Proceedings of the Altai State University (Izvestiya Altaiskogo universiteta), **1/2(73)**, 12-18 (2012) (in Russian).

[3] A. Oron, S. H. Davis, S. G. Bankoff, *Long-scale evolution of thin liquid films*, Reviews of Modern Physics, **69(3)**, 931 - 980 (1997).

[4] S. Miladinova, S. Slavtchev, G. Lebon, J.-C. Legros, *Long-wave instabilities of non-uniformly heated falling films*, J. Fluid Mech., **453**, 153 - 175 (2002).

Effects of external shield on particle accumulation structure (PAS) due to thermocapillary effect in a half-zone liquid bridge

M. Gotoda,[1] T. Sano,[1] T. Kaneko,[2,3] and I. Ueno[2,3]

[1]*Div. Mechanical Engineering, Graduate School of Fac. Science & Technology, Tokyo Univ. Science, Japan*
a7510049@rs.tus.ac.jp, a7508071@rs.tus.ac.jp

[2]*Dept. Mechanical Engineering, Fac. Science & Technology, Tokyo Univ. Science,*
tkaneko@rs.tus.ac.jp, ich@rs.tus.ac.jp

[3]*Research Institute for Science & Technology, Tokyo Univ. Science,*
2641 Yamazaki, Noda, Chiba 278-8510, Japan

We focus on particle accumulation structure (PAS)[1] due to a thermpcapillary-driven convection induced in a half-zone liquid bridge. It has been known that the PAS emerges in a certain range of the thermocapillary-effect intensity described by the non-dimensional Marangoni number Ma[2, 3]. We pay our special attention to the effects of the size of the ambient gas region on the existing region of the PAS as a function of the intensity of the ambient gas flow, and on the behaviors of the particles on the PAS.

In our experiment, the size and the shape of the liquid bridge are fixed; the height (H) and radius (R) are of 1.6 mm and 2.5 mm, respectively, to maintain the liquid bridge of the aspect ratio $\Gamma(= H/R)$ = 0.64. The volume ratio of the liquid bridge, V/V_0, is kept unity, where V is the volume of the liquid bridge itself, and V_0 is the volume between the coaxial rods (= $\pi R^2 H$). The test fluids are 2-cSt silicone oil for the liquid bridge, whose Prandtl number Pr = 28.1 at 25°C, and the dried air for the ambient gas. We put gold-coated acrylic particle of 15 μm in diameter in the test fluid to visualize the convection in the liquid bridge. We prepare two different external shields whose inner diameters are of 25 mm, and of 10 mm. The corresponding gap distances between the liquid bridge surface and the inner surface of the external shield are of 10 mm (= $4R$) and of 2.5 mm (= R), respectively.

We succeed to realize SL-1 PAS[2] in both cases of the external shields as a function of the intensity of ambient gas flows. Figure 1 indicates the top views of the particle path lines in the rotating frame of reference with the fundamental frequency of the hydrothermal wave under each Ma in the case of null ambient gas flow. In order to determine the existing region of the PAS, we evaluate the intensity of the particle accumulation with the 'accumulation measure' proposed by Kuhlmann *et al.*[4] modified for the experiments.

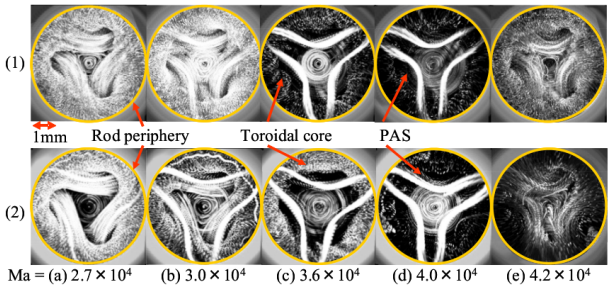

FIG. 1. Typical examples of flow patterns observed from the top under Re_{amb} = 0; the external shield diameters are of (1) 25 mm and (2) 10 mm. Each image is obtained by accumulated for 1 sec. in the frame of reference with the fundamental frequency of the hydrothermal wave.

[1] D. Schwabe, P. Hintz, S. Flank, *New features of thermocapillary convection in floating zone revealed by tracer particle accumulation structure (PAS)*, Microgravity Sci. Technol., **9**, 163-168, 1996.

[2] S. Tanaka, H. Kawamura, I. Ueno, D. Schwabe, *Flow structure and dynamic particle accumulation in thermocapillary convection in a liquid bridge*, Phys. Fluids, **18**, 067103, 2006.

[3] D. Schwabe, A. I. Mizev, M. Udhayasankar, S. Tanaka, *Formation of dynamic particle accumulation structures in oscillatory thermocapillary flow in liquid bridge*, Phys. Fluids, **19**, 072101, 2007.

[4] H. C. Kuhlmann, F. H. Muldoon, *Particle-accumulation structures in periodic free-surface flows: Inertia versus surface collisions*, Phys. Rev. E, **85**, 046310, 2012.

Impact of complex drops onto surfaces: particle distribution

V. Grishaev,[1] C. S. Iorio,[1] and A. Amirfazli[2]

[1]*Microgravity Research Centre, Université Libre de Bruxelles, EP-CP165/62, B-1050, Brussels, Belgium,* vgrishae@ulb.ac.be, ciorio@ulb.ac.be

[2]*Department of Mechanical Engineering, York University, Toronto, ON, M3J 1P3, Canada,* alidad2@yorku.ca

Distribution of particles after the impact of complex drops (liquid and solid particles) onto a substrate is important for many industrial processes, e.g. in additive manufacturing and rail friction management systems. Up to now, the spreading of particle-laden drops was studied mainly on glass (a hydrophilic material) [1]; particle ejection was seen for large particle volume fraction values [2-3]. Drop impact of pure liquids strongly depends on the wettability of a surface [4]. As such, we aim to investigate if the same dependence on surface wettability exists for impact of complex drops and a spatial distribution of solid particles.

Complex drops (diameter - 3.8 mm) were produced using polyethylene microspheres dispersed in deionized water. In the experiments, the particles with diameters 200 and 500μm were used and their volume fraction F_v was varied in the range from 0 to 35%. Glass slides and polycarbonate plates were used as hydrophilic and hydrophobic surfaces, respectively. In the experiments, Reynolds and Weber numbers were varied in the range Re = 7200-16200 and We = 150-725, respectively. The process was studied by using high-speed cameras and image processing methods.

We found that surface wettability strongly influence on the particle distribution. After the impact on the hydrophilic surface, drops with 200μm particles are arranged in 2D annular distribution (Fig. 1, left). With an increase of We, probability of the particle appearance in the centre of the drop decreased. For We = 440$\pm$7, 710$\pm$12 the annular distribution of the particles was wider than for We = 153$\pm$2. For We = 710$\pm$12, with an increase of the particle volume fraction, width of the distribution increased. On hydrophobic surface, 200μm particles formed a rim on the drop contact line (Fig.1, right). When We increased, satellite drops formed from the main drop as a result of the impact. With an increase of the particle volume fraction, the particles covered completely the liquid-air interface of the drops and then deformed it. In the case of 500μm particles on both surfaces, such marked distributions were not observed. Also, mechanisms of distribution formation were elucidated.

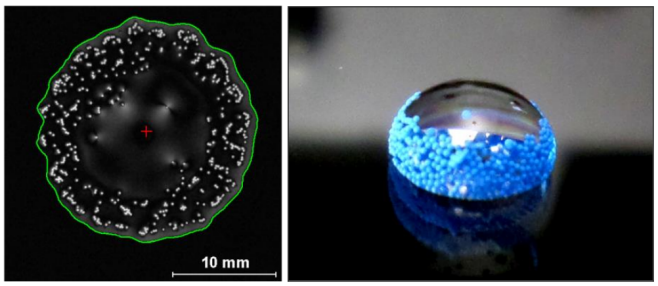

FIG. 1. The distribution of 200μm particles at We = 450. Left: the 2D annular distribution on hydrophilic surface at F_v = 7.0%; Right: the rim on hydrophobic surface at F_v = 5.7%. The green line is the drop contact line; the red cross is the centre of the drop impact.

[1] M. Nicolas, *Spreading of a drop of neutrally buoyant suspension*, J. Fluid Mech., **vol. 545**, 271280 (2005).

[2] I. R. Peters, Q. Xu, H. M. Jaeger, *Splashing Onset in Dense Suspension Droplets*, **PRL 111**, 028301 (2013).

[3] J. O. Marston, M. M. Mansoor, S. T. Thoroddsen, *Impact of granular drops*, Physical Review, **E 88**, 010201(R) (2013).

[4] C. Antonini, A. Amirfazli, M. Marengo, *Drop impact and wettability: From hydrophilic to superhydrophobic surfaces*, Physics of Fluids, **24**, 102104 (2012).

Numerical simulation of the isothermal dissolution of a single rising bubble in a liquid bath

A. S. Mohamed,[1] M. A. Herrada,[1] J.M. López-Herrera,[1] and A. M. Gañán-Calvo[1]

[1]*E.S.I, Universidad de Sevilla, Camino de los Descubrimientos s/n 41092, Spain.*

The evolution of gas bubbles in a liquid under buoyancy forces is a multifaceted multi-phase problem: it does not only involve the obvious fluid mechanical phenomena but also comprises the complex kinetics around the exchange of gases and vapors between the liquid and the bubble. There is a set of quite generic applications where gas exchange is the principal target factor to score performance. For example, in the petroleum industry, in micro algae cultivation tanks or bioreactors.

This work focuses on the total dissolution time and distance traveled by a evolving microbubble, with the idea to make that distance traveled as closer as possible to the distance from the bubble source to the free surface of the liquid. In principle, this would allow an optimal dispersion of the gas throughout the liquid column, with minimal loses at the free liquid surface.

We propose a tracking-interface numerical method to analyze the dissolution of single bubbles in the limit of small Weber numbers. The key elements of the method are the use of a frame of reference moving with the bubble and the application of different meshes to solve the mechanical and mass-diffusion problems. Comparison with experiments has been carried out with success.

RESULTS

The numerical simulations exhibit at great detail the evolution of the flow and the concentration around the sphere at the beginning of the process, before the bubble reaches the quasi-terminal velocity. The correct computation of the boundary layers is critical to get accurate calculation of the bubble radius change with depth (Fig. 1).

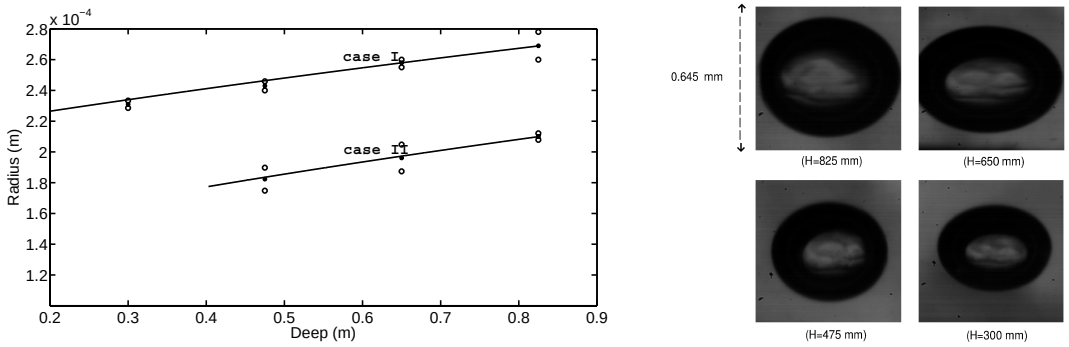

FIG. 1. Left:Radius of the bubble as a function of depth for the two experiments. Solid lines correspond to the simulations, closed (open) circles represent the mean (standard deviation) experimental values.Right:Pictures of the bubbles at different heights.

An efficient numerical approach to systematically investigate the interfacial heat and mass transfer for wavy falling films

E. Hofmann[1] and H. C. Kuhlmann[1]

[1]*Institute of Fluid Mechanics and Heat Transfer, TU Wien, Resselgasse 3, 1040 Vienna, Austria*

h.kuhlmann@tuwien.ac.at

The present contribution is motivated by absorption refrigeration and aims to numerically investigate the influence of a wavy film to the coupled heat and mass transfer. The targeted task is a numerical challenge, since massive computational cost originate from the transient free-surface flow in combination with, typically, vast aspect ratios of the domain. We present a simple but novel approach that allows for a numerically cheap but accurate procedure to investigate the interfacial transfer processes for the wavy falling film.

Our major assumption is one-way coupling (the flow field remains unaffected by the absorption process) so that we are free to solve for the fluid dynamics and for the coupled heat and mass transfer consecutively. To achieve most accurate results, sharp-interface traveling-wave solutions of the Navier–Stokes equations are employed, corresponding to steady states within a co-moving frame of reference. The system of non-linear equations, including the a priori unknown wave celerity and shape of the free surface, is solved by Newton's method in the finite-volume formulation on a staggered grid, similar to [1]. Further, the *constant-height* constraint is substituted by the *constant-flux* constraint, so that our steady states compare excellently with the periodically-forced transient simulations within the laboratory frame of reference of [2]. These solutions are then used to compose a wavetrain that serves as basis for the subsequently solved transient heat and mass transfer. There, the parabolic character of the equations is exploited that justifies a simple marching technique. A proper remedy is used for the treatment of the small backflow regions. A qualitative result is shown in the figure below.

The interface-coupled heat and mass transfer is usually the most difficult task among thermal- and absorbing-film problems which are either wall-sided and/or free-surface sided. Due to the sharp free surface we are able to easily address all these related problems just by adapting the boundary conditions.

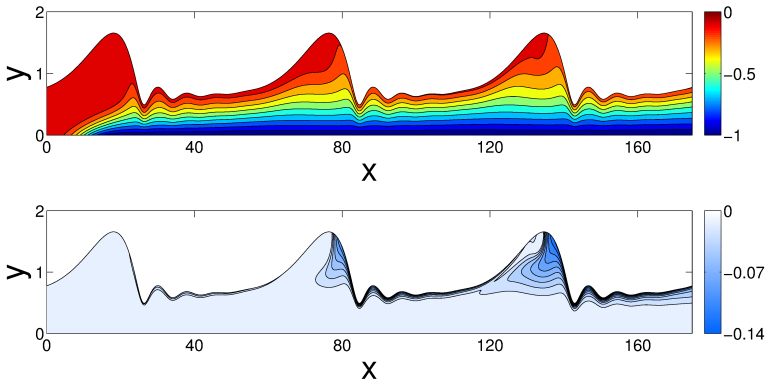

FIG. 1. Qualitative result for the interfacial coupled heat and mass transfer. Top: Temperature $T(x, y, t_0)$; Bottom: Concentration $C(x, y, t_0)$.

[1] T. R. Salamon, R. C. Armstrong, R. A. Brown, *Traveling waves on vertical films: Numerical analysis using the finite element method*, Phys. Fluids, **6**: 2202–2220, 1994.

[2] G. F. Dietze, *Flow separation in falling liquid films.* PhD thesis, RWTH Aachen, 2010.

Flow instabilities in annular pool of medium Pr fluid effects of Bi_{top}, Bi_{bottom}, and Bo_d

N. Imaishi,[1] M. Ermakov,[2] and W.Y. Shi[3]

[1]*Institute for Materials Chemistry and Engineering, Kyushu University, 6-1 Kasuga-koen,Kasuga, 816-8580, Japan,*
imaishi@cm.kyushu-u.ac.jp

[2]*A. Ishlinsky Institute for Problems in Mechanics of the Russian Academy of Sciences, Moscow 119526, Russia,*
ermakov@ipmnet.ru

[3]*College of Power Engineering, Chongqing University, Chongqing, 400044, China,*
shiwy@cqu.edu.cn

A linear stability analysis of thermocapillary and buoyant-thermocapillary flows in annular cavities over a wide range of aspect ratios is conducted for a silicone oil (Pr = ν/α = 6.7) under 0 $\sim$ 1.14G conditions. The cavity is composed of its heated outer wall (Ro = 40mm), cooled inner wall (Ri = 20mm), and its depths d ranges from 0.8mm to 20mm (the aspect ratio Γ = (Ro-Ri)/d ranging from 1 to 25). Heat transfer between the surrounding air and liquid surface, and between the conducting bottom plate and the liquid are also taken into account. We use following non-dimensional expressions $r = R/d$, $z = z/d$, $\mathbf{V} = \mathbf{v}d/\nu$, $\tau = t\nu/d^2$, $P = d^2p/\rho\nu^2$, $\Gamma = \Delta R/d$, $\Theta = \Gamma(T - T_c)/\Delta T$, $Re = \gamma_T \Delta T d^2/\mu\nu\Delta R$, $Gr = g\rho_T \Delta T d^4/\nu^2 \Delta R$, $Bo_d = Gr/Re = g\rho_T d^2/\gamma_T$, $Bi_t = hd/k$, $Bi_b = k_b d/k d_b$. We have reported linear stability analyses at IMA-5 only for adiabatic cases. Several works [1, 2] discussed the effects of thermal boundary conditions at the surface and bottom on the stability of Marangoni convection in annular pools, however, the effects of heat exchanges are not yet clearly understood. In this work, very simple cases will be discussed.

The critical Reynolds number (Re_c) for the onset of hydrothermal wave instability in shallow pool with adiabatic bottom (HTW1) is increased by moderate heat loss from the liquid surface and decreases with heat gain as shown in Fig.1. On the other hand, Re_c for the hydrothermal wave in deep pools first decreases with increasing Bi_t and shows a minimum at a certain value of Bi_t and then starts increasing as shown in Fig.2. Similar Bi dependency is known for half-zone liquid bridge [3]. In heat gain circumstances, Re_c steeply increases with increasing T_a or Bi_t, where $T_a = (T_A - T_C)/\Delta T$ is the non-dimensional ambient temperature. This stabilization was also reported by Sim and Zebib [1].

Bib gives its influences on Re_c mainly via velocity and temperature distributions of the basic flow.

As we reported at IMA-5, flow mode changes from HTW1 to HTW2 and HTW2 to 3D steady flow occur at certain liquid depth d_1^* and d_2^*, respectively. A crude correlation of d_1^* by the Capillary number and that of d_2^* by the dynamic Bond number will be proposed.

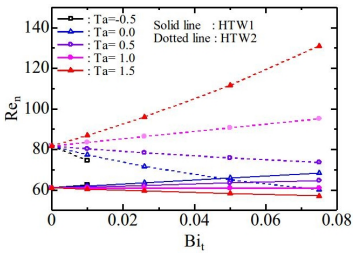

FIG. 1. Effect of Bi_t on the critical Reynolds number for HTW1 and HTW2 in shallow pool (d = 1mm), 0G.

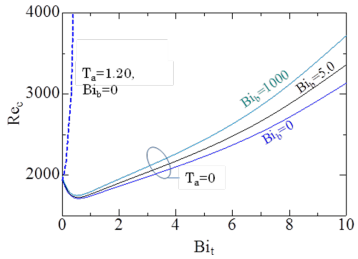

FIG. 2. Effect of Bi_t on the critical Reynolds number for HTW2 in deep pool (d = 20mm), 0G.

[1] B. C. Sim, A. Zebib, D. Schwabe, *Oscillatory thermocapillary convection in open cylindrical annuli*, Part 2. Simulations, J. Fluid Mech., **491**, 259-274 (2003).

[2] S. Hoyas, M. Mancho, H. Herrero, N. Garnier, A. Chiffaudel, *Benard-Marangoni convection in a differentially heated cylindrical cavity*, Phys. Fluids, **17**, 054104 (2005).

[3] Y. Kousaka, H. Kawamura: *Numerical study on the effect of heat loss upon the critical Marangoni number in a half-zone liquid bridge*, Microgravity Sci. Tec., **18**, 141-145 (2006).

Flow instabilities in annular pool of low Pr fluid

N. Imaishi,[1] M. Ermakov,[2] W.Y. Shi,[3] Y.R. Li,[3] and L. Peng[3]

[1]*Institute for Materials Chemistry and Engineering, Kyushu University, 6-1 Kasuga-koen,Kasuga, 816-8580, Japan,*
imaishi@cm.kyushu-u.ac.jp

[2]*A. Ishlinsky Institute for Problems in Mechanics of the Russian Academy of Sciences, Moscow 119526, Russia,*
ermakov@ipmnet.ru

[3]*College of Power Engineering, Chongqing University, Chongqing, 400044, China,*
shiwy@cqu.edu.cn

We reported linear stability analysis and numerical simulations of instabilities of thermocapillary convection in annular pool of low Pr fluid ($Pr = 0.011$) [1]. We extended the model of linear stability analysis to take into account various thermal boundary conditions on the top and bottom of the liquid layer and kinematic and thermal energy balance. In general, thermocapillary flow becomes unstable against 3-D stationary or oscillatory disturbances under temperature differences above certain threshold value. We confirmed two types of oscillatory flow (OSC1 and OSC2) as possible 3D disturbances in annular pool of low Pr fluids ($Pr < 0.0305$) and more than two types of 3-D stationary flow. These 3-D flows are caused by some hydrodynamical mechanisms other than those predicted by Smith and Davis [2]. Fig. 1 shows the critical Marangoni number as a function of Pr for the onset of 3D flow instabilities in an annular pool ($R_o = 40mm$, $R_i = 20mm$ and $d = 1.0mm$, under 0G). Fig.2 shows the contributions of each kinetic energy terms to compensate the viscous dissipation at the critical condition. For medium and high Pr fluids, hydrothermal wave instablity (HTW1) is the most dangerous mode. For low Pr fluids ($Pr < 0.0095$) OSC2 becomes the most dangerous mode. For Pr between 0.0095 and 0.0305 OSC1 is the most dangerous mode. Pattern of OSC1 is somehow similar to HTW1 but the surface fluid flows from colder toward warmer points. In pools of $Pr = 0.011$, OSC2 is dominant in deep pools ($d > 6.173mm$ under 0G, $d > 11.66mm$ under 1G), for other depths OSC1 is dominant. OSC2 is characterized by its unique structure, double stranded vortex, propagating in the clockwise direction. Fig. 3 shows iso-surfaces of temperature disturbance of OSC2 for $Pr = 0.011$ at $Ma_c = 35.03$, $m_c = 13$, $d = 10mm$ under 0G. It should be noted that the bending direction is opposite to that of HTW. In shallow pools, the double stranded structure becomes incomplete and the outer parts becomes blur. In shallow pools, Re_n of 3-D stationary flow is found about 10% above the Re_c.

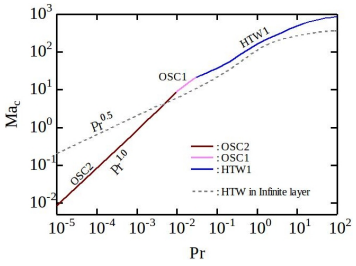

FIG. 1. Critical Marangonin number as a function of Pr for d = 1.0mm under 0G

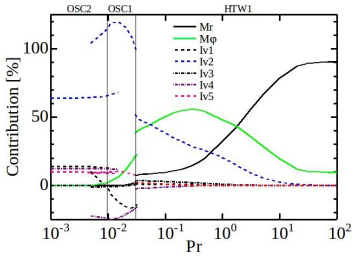

FIG. 2. Contributions of each kinetic energy term at the critical point for d = 1mm, 0G.

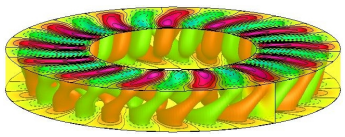

FIG. 3. Two iso-surfaces of temperature disturbance of OSC2 in annular pool of $Pr = 0.011$, at $Ma_c = 38.03$, $m_c = 13$, $d = 10mm$ under 0G and adiabatic condition.

[1] W. Y. Shi, M. Ermakov, Y. R. Li, L. Peng, N. Imaishi, *Influence of buoyancy force on thermocapillary convection instability in the differentially heated annular pools of silicon melt*, Microgravity Sci. Technol., **21**, S280-S297 (2009).

[2] M. K. Smith, S. H. Davis, *Instabilities of dynamic thermocapillary liquid layers. Part 1. Convective instabilities*, J. Fluid Mech., **132**, 119-144 (1983).

Droplet formation in thin liquid layers under the action of the laser-induced solutocapillary flows

N. A. Ivanova[1]

[1]*Institute of Physics and Chemistry, Tyumen State University, Semakova 10, 625003, Tyumen, Russia,* n.ivanova@utmn.ru

Droplet-based microfluidics has recently drawn enormous attention as the promising technology for conducting of biological and chemical assays in lab on chip systems [1]. A modulation of surface tension under the action of the light stimulus is a non-invasive and highly precise method to actuate liquid droplets in microscale. The light energy is released directly in the fluid volume and converted into thermal energy; the light beams can be generated at any wavelength, spatial and time resolutions. Using of the light energy the surface tension gradient which is the driving force for fluid motion can be generated through photochemical, photoelectrochemical and thermal effects [2].

In present work we have studied the formation and growth of droplets in thin layers of aqueous-alcohol mixtures in polystyrene cells controlled by the laser-induced solutocapillary flows [3, 4]. Briefly, mechanism of the drop formation is a competition between mass transfer due to capillary flows related with concentration gradient and mass transfer due to evaporation of volatile component. When the laser beam is incident on the mixture layer thermocapillary flows due to heating arise and result in formation of thermocapillary dip. Simultaneously with thermocapillary spreading of mixture a tiny solitary droplet with an initial contact angle appears on the laser spot, Fig. 1(a). After this moment the droplet shrinks

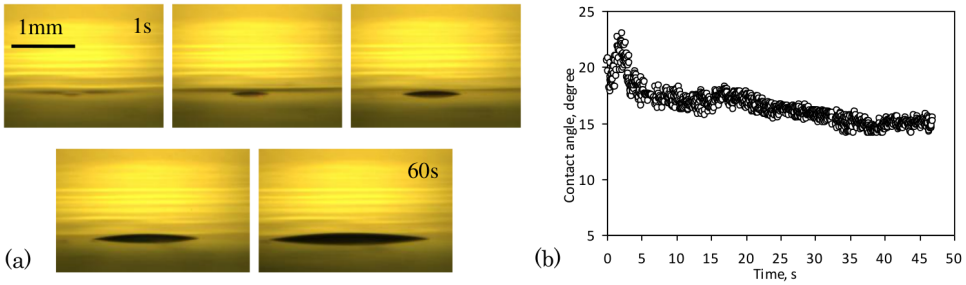

FIG. 1. (a) Time sequence, side view. Droplet growing in 50% water/2-propanol mixture doped with Brilliant green at the radiation power of laser 15 mW (659 nm). (b) Time evaluation of the microscopic contact angle of the droplet growing in the laser beam.

for a few seconds that is reflected in increasing the contact angle, Fig.1(b) and in decreasing the diameter [4]. Further the droplet increases in size continuously under the laser irradiation. However, as it shown in Fig.1(b) the contact angle decreases shortly and reaches more or less constant value, which is retained during the growth process of the droplet.

It was found that in the layers 100-150 microns of thickness, the droplet reaches several micro liters in volume at the laser power 15 mW. The higher concentration of aqueous component in the mixture, the larger volume of droplets is reached.

The solutocapillary flows controlled by the light beam provides a contactless method for creating droplets of required volume with a controlled content of selected substances, thus offering a unique tool for manipulating liquid objects on the microscopic level.

[1] S-Y. Teh, R. Lin, L-H. Hung, A. P. Lee, *Droplet microfluidics*, Lab Chip, **8**, 198–220 (2008).

[2] D. Baigl, *Photo-actuation of liquids for light-driven microfluidics: state of the art and perspectives*, Lab Chip, **12**, 3637–3653 (2012).

[3] B. A. Bezuglyi, N. A. Ivanova, *Creation, transportation and coalescence of liquid drops by means of a light beam*, Fluid Dyn., **41(2)**, 278–285 (2006).

[4] N. A. Ivanova, B. A. Bezuglyi, *Influence of the liquid layer thickness on the growth of droplets controlled by the thermal action of laser radiation*, Tech. Phys. Letter, **35(4)**, 293–295 (2009).

Marangoni flow during coalescence of sessile drops: liquids with a precipitation reaction

M. Jehannin,[1,2] S. Karpitschka,[2] S. Charton,[1] H. Möhwald,[2] T. Zemb,[3] and H. Riegler[2]

[1]*CEA, DEN, DTEC, SGCS, F-30207 Bagnols sur Cèze, France.*
[2]*MPI for Colloids and Interface, Am Mühlenberg, D-14476 Potsdam, Germany.*
[3]*ICSM UMR5257 CEA/CNRS/UM2/ENSCM, F- 30207 Bagnols sur Cèze, France.*

Marangoni flow influences the coalescence behavior of drops containing different liquids. Temporally it can delay the coalescence of sessile drops, even of completely miscible liquids [1, 2]. But it also can increase the mixing/coalescence of freely flowing droplets [3]. Very little is known about the interaction behaviour of drops containing *reactive* species, a key issue in some emulsion based processes [4].

We study the coalescence of sessile drops containing the reactants cerium nitrate and oxalic acid, forming insoluble cerium oxalate upon contact. The reactants are dissolved in water/propandiol mixtures. Thus their concentrations and the surface tension difference between the drops can be adjusted independently. Coalescence/precipitation are imaged from the top and the side [1, 2].

With fixed surface tension difference (3mN/m) and oxalic acid concentration (1.1M), depending on the cerium content, three distinctly different types of coalescence and precipitation behaviors are observed (FIG. 1). To analyze the underlying hydrodynamic and physico-chemical processes the resulting precipitate is studied via optical microscopy, SEM and SAXS. At low initial cerium content, needle-like crystals are found. At high content the precipitate appears as pellets. Most remarkable, at intermediate content, the precipitate unexpectedly forms stripes, supposedly an alternation between the two morphologies.

Currently we perform dedicated experiments and simulations to better understand the nucleation, aggregation and transport processes that lead to the different aggregate morphologies, in particular to the stripe formation. Presumably the stripes result from a feedback between the (Marangoni) transport and the local precipitation reaction, which changes the local composition and the rheological properties and thus influences the transport.

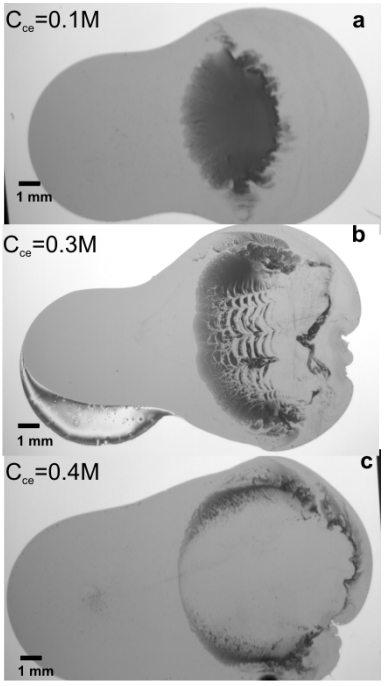

FIG. 1. Top view of coalescing oxalic acid (left) and cerium nitrate drops (right). C_{Ce} refers to the initial concentrations in the cerium nitrate drops. Remarkable is the striped precipitation in the regime of intermediate concentration (b).

[1] S. Karpitschka, H. Riegler, *Quantitative Experimental Study on the Transition between Fast and Delayed Coalescence of Sessile Droplets with Different but Completely Miscible Liquids*, Langmuir, **26**, 11823–11829 (2010).

[2] S. Karpitschka, H. Riegler, *Noncoalescence of Sessile Drops from Different but Miscible Liquids: Hydrodynamic. Analysis of the Twin Drop Contour as a Self-Stabilizing Traveling Wave*, P.R.L, **109**, 066103 (2012).

[3] F. Blanchette, *Simulation of Mixing within Drops due to Surface Tension Variations*, P.R.L, **105**, 074501 (2010).

[4] S. Charton,A. Kacem,A. Amokrane,G. Borda,F. Puel, J. P. Klein, *Actinides oxalate precipitation in emulsion modeling: from the drop scale to the industrial process*, Chem. Eng. Res. Des, **91**, 660–669 (2013).

The stabilizing effect of mass loss on an evaporating thin liquid film due to the vapor concentration gradient

K. Kanatani[1]

[1]*Faculty of Engineering, Yokohama National University, 79-5 Tokiwadai, Hodogaya, Yokohama 240-8501, Japan*
kentaro@ynu.ac.jp

We show that mass loss can stabilize an evaporating thin liquid film owing to the vapor concentration gradient at the liquid-gas interface when an inert gas is present. In order to see what this is, we illustrate in fig. 1 the temperature fields across an evaporating liquid film. The two solid lines correspond to the temperature fields at thicker and thinner parts of the liquid film when the liquid-gas interface is deflected. In the case where an inert gas is present in the gas phase, there is a vapor concentration gradient at the interface. Here the vapor concentration decreases toward the gas phase. Thus the partial pressure of the vapor is smaller at higher locations of the interface. Since the saturation pressure is equal to the partial pressure at thermodynamic equilibrium, the interface temperature also becomes lower for higher positions from the Clausius-Clapeyron relation. If the variation of the interface temperature due to the vapor concentration gradient is sufficiently large, the temperature gradient becomes steeper for thicker portions of the liquid film under the constant wall temperature, as shown in fig. 1. In this case, the evaporation rate is enhanced with the interfacial height and thereby mass loss stabilizes the liquid film.

In contrast to the previous works [1, 2], the vapor concentration gradient is incorporated into the linear stability investigation of an evaporating thin liquid film in this study. We find that a critical temperature exists below which mass loss is stabilizing by the vapor concentration gradient. In fig. 2, the neutral stability curve is depicted in a wavenumber versus film thickness plane at a temperature lower than the critical one. Here the destabilization arises from the Marangoni effect. Figure 2 demonstrates that the flat film becomes stable below a certain thickness due to the mass loss effect.

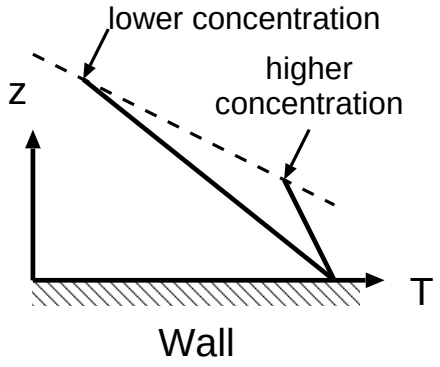

FIG. 1. The temperature fields across a liquid film evaporating into an inert gas when mass loss has a stabilizing effect. The dashed line indicates the relation between the location and temperature of the liquid-gas interface.

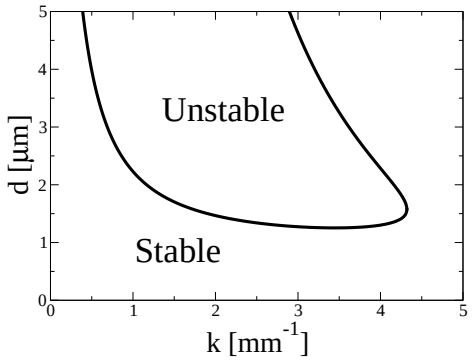

FIG. 2. The neutral stability curve in a dimensional wavenumber versus film thickness plane for the ethanol-nitrogen system at atmospheric pressure. Here the boundary layer depth, ambient vapor concentration and interface temperature have been set to 1 mm, 0 and 300 K, respectively.

[1] E. Sultan, A. Boudaoud and M. Ben Amar, *Evaporation of a thin film: diffusion of the vapour and Marangoni instabilities*, J. Fluid Mech. **543**, 183–202 (2005).

[2] K. Kanatani, *Effects of convection and diffusion of the vapour in evaporating liquid films*, J. Fluid Mech. **732**, 128–149 (2013).

Effect of a constant heat source on evaporative instability in a solid-liquid-vapor system

A. Karacelik,[1] R. Narayanan,[2] and K. Uguz[1]

[1]*Department of Chemical Engineering, Bogazici University, Bebek, 34342, Istanbul, Turkey,*
asli.karacelik@hotmail.com, kerem.uguz@boun.edu.tr

[2]*Department of Chemical Engineering, University of Florida, Gainesville, FL, 32611, USA,*
ranga@ufl.edu

When a liquid underlies its own vapor, convection may arise due to evaporation without gravity or surface tension gradient effects. This process is named as pure evaporative convection. In this study, standard linear stability of a solid-liquid-vapor system considering an evaporative liquid into its own vapor is investigated. A constant heat source is considered in the solid part of the system and the effect of that heat source on the linear stability is studied. Inputs to the system are the heat, the depths of solid, liquid and vapor and the physical parameters, which are assumed to be constant while the output is the temperature difference at which convection starts. The aim is to parametrically analyze this system and compare it with a liquid-vapor evaporative system where the bottom plate is kept at constant hot and upper plate at constant low temperature.

A numerical study of electrohydrodynamic patterning of viscoelastic materials

G. Karapetsas[1] and V. Bontozoglou[1]

[1] *University of Thessaly, Department of Mechanical Engineering, Volos, 38334, Greece*
gkarapetsas@gmail.com, bont@mie.uth.gr

A computational model is developed to study the manufacturing of fine structures using the electrohydrodynamic patterning processes. We consider the flow of a viscoelastic material under the influence of an applied electric field and investigate the non-linear dynamics by carrying out 2D numerical simulations, fully accounting for the flow in both phases. The viscoelastic behavior is modelled using the affine Phan-Thien and Tanner (PTT) constitutive equation [1]. For the numerical solution of the governing equations the mixed finite element method is combined with a quasi-elliptic mesh generation scheme in order to capture the large deformations of the liquid-air interface. We perform a thorough parametric study and investigate the influence of the various rheological parameters, the applied voltage and geometrical characteristics of the mask in order to define the fabrication limits of this process in the case of periodic structures.

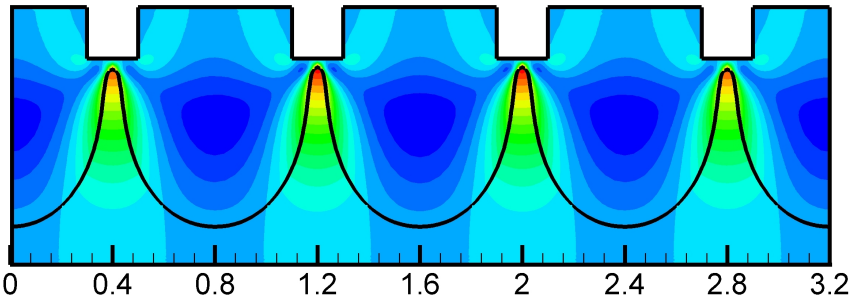

FIG. 1. Contour plots of the vertical velocity component. The black line shows the polymer-air interface as predicted by the non-linear numerical model.

Acknowledgements. The authors would like to acknowledge the financial support by the General Secretariat of Research and Technology of Greece under the Action Supporting Postdoctoral Researchers (grant number: PE8/906), co-funded by the European Social Fund and National Resources.

[1] N. Phan-Thien, *A nonlinear network viscoelastic model*, J. Rheol., **22**, 259–283 (1978).

On the interplay between inertia and shear thinning for free-surface jet flow near channel exit

R. E. Khayat[1]

[1]*Departement of Mechanical and Materials Engineering*
University of Western Ontario, London, Ontario CANADA

The jet flow of a shear-thinning power-law fluid is examined theoretically as it emerges from a channel at moderate Reynolds number. Poiseuille flow conditions are assumed to prevail far upstream from the exit. The problem is solved using the method of matched asymptotic expansions. A similarity solution is obtained in the inner layer near the free surface, with the outer layer extending to the jet centerline. An inner thin viscous sublayer is introduced to smooth out the singularity in viscosity at the free surface, allowing the inner algebraically decaying solutions to be matched smoothly with the solution near the free surface. This treatment is similar to power-law flow near the edge of a boundary layer [1, 2]. A Newtonian jet is found to contract more than a shear-thinning jet. While both the inner-layer thickness and the free-surface height grow with downstream distance, the sublayer thickness is smaller, growing with distance for $n < 0.5$, and decaying for $n > 0.5$, n being the power-law index. The relaxation downstream distance for the jet are found to grow logarithmically with Re. The current work extends our previous study on viscoelastic-inertial jet flow near channel exit [3].

---

[1] J. P. Denier, P. P. Dabrowski, *On the boundary-layer equations for power-law fluids*, Proc R Soc. A, **460**, 3143 (2004).

[2] A. Saffari, R. E. Khayat, *Flow of viscoelastic jet with moderate inertia near channel exit*, J. Fluid Mech., **639**, 65 (2009).

[3] J. Zhao, R. E. Khayat, *Spread of a non-Newtonian liquid jet over a horizontal plate*, J. Fluid Mech., **613**, 411 (2008).

Free surface flow simulation with application to bluff body flow control

S. Kocabiyik[1] and C. Bozkaya[2]

[1]*Memorial University of Newfoundland, Department of Mathematics and Statistics, St. Johns's, NL A1C5S7, Canada*
serpil@mun.ca
[2]*Middle East Technical University, Ankara 06531, Turkey*
bcanan@metu.edu.tr

The interaction of a free surface wave motion with moving cylindrical bodies has been received a great deal of attention owing mainly to its practical significance ([1], see e.g., experimental: [2] and numerical: [3], [4]). However, little fundamental research has been conducted to investigate the link between the wake dynamics of the cylinder, the energy transfers and the properties of fluid forces acting on the cylinder. To better understand the interaction of a free surface wave motion with moving bluff bodies, a two-dimensional numerical study of the forced streamwise oscillation of a circular cylinder beneath a free surface is conducted based on a two-fluid model. Computations are carried out at a Reynolds number of $R = 200$, a fixed displacement amplitude, $A = 0.13$ and the forcing frequency-to-natural shedding frequency ratios, $f/f_0 = 1.5, 2.5, 3.5$. Finite volume discretization of the special integral form of two-dimensional continuity and unsteady Navier-Stokes equations (when a solid body is present) are performed on a fixed Cartesian grid. Improved volume-of-fluid method is used to discretize the free surface. The laminar asymmetric flow regimes in the near wake region and the fluid forces and the total mechanical energy transfer between fluid and the cylinder are analyzed at a fixed Froude number of $Fr = 0.4$ and for submergence depths, $h = 0.25, 0.5, 0.75$. A comparison of the present results with the case in the absence of a free surface ($h = \infty$) is included to illustrate the effects of inclusion of a free surface. The link between the changes in the wake dynamics of the cylinder, and in the properties of fluid forces acting on the cylinder is also discussed.

---

[1] J. Sheridan, J.C. Lin, D. Rockwell, *Flow past a cylinder close to a free surface*, J. Fluid Mech., **330**, 1–30 (1997).

[2] O. Cetiner, D. Rockwell, *Streamwise oscillations of a cylinder in steady current. Part 2. Free-surface effects on vortex formation and loading*, J. Fluid Mech., **427**, 29-59 (2001).

[3] P. Reichl, K. Hourigan, M.C. Thompson, *Flow past a cylinder close to a free surface*, J. Fluid Mech., **533**, 269–296 (2005).

[4] C. Bozkaya, S. Kocabiyik, L.A. Mironova, O.I. Gubanov, *Streamwise oscillations of a cylinder beneath a free surface: Free surface effects on vortex formation modes*, J. Comput. Appl. Math., **235**, 4780–4795 (2011).

Interfacial spreading motions in 2-layer solutal Rayleigh-Marangoni convection: 3D direct numerical simulations and experiments

T. Köllner,[1] K. Schwarzenberger,[2] T. Boeck,[1] and K. Eckert[2]

[1]*Institute of Thermodynamics and Fluid Mechanics,*
Technische Universität Ilmenau, P.O.Box 100565, D-98684 Ilmenau, Germany,
thomas.koellner@tu-ilmenau.de
[2]*Institute of Fluid Mechanics, Chair of Magnetofluiddynamics,*
Measuring and Automation Technology, TU Dresden, D-01062 Dresden, Germany

Mass transfer through a liquid interface may give rise to convection due to buoyancy and interfacial tension gradients. Depending on the substances diverse convective structures can be observed. For instance, roll cell convection under a stabilizing density stratification [1] shows structures that are mainly driven by the Marangoni instability. In a similar chemical system, but with a density-lowering substance transported against the direction of gravity, Marangoni roll cell convection is not amplified. In this situation the interaction of buoyancy instability and Marangoni effect generates persistent spreading events at the interface [2]. We consider this problem for a two-layer system with an organic phase (rich in cyclohexanol) as top layer and an aqueous phase as bottom layer. Isopropanol is dissolved in the aqueous layer. According to Sterling&Scriven [3] this system is stable with respect to the stationary Marangoni instability since isopropanol lowers the interfacial tension and diffuses much faster in the aqueous phase. However, isopropanol lowers density resulting in a Rayleigh instability in both phases. The detaching solutal plumes in the organic phase are the origin of intense spreading events driven by interfacial tension gradients. Our three dimensional simulations reproduce the experimentally observed structures, cf. Fig. 1. The simulations are used for a detailed analysis of the observed complex patterns and their dependence on the initial isopropanol concentration.

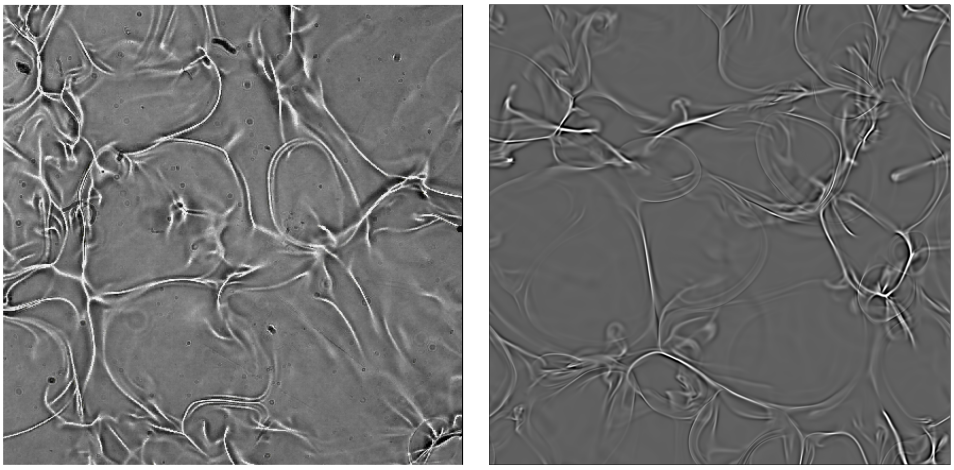

FIG. 1. Shadowgraph image of Rayleigh-Marangoni convection in water+2.5Vol% isopropanol → cyclohexanol. The size is approx. 15 mm for the experimental on the left as well as for the numerical image on the right.

[1] T. Köllner, K. Schwarzenberger, K. Eckert, T. Boeck, *Multiscale structures in solutal Marangoni convection: Three-dimensional simulations and supporting experiments*, Physics of Fluids, **25(9)**, 092109.
[2] E. Schwarz, *Zum Auftreten von Marangoni-Instabilität, Wärme-und Stoffübertragung*, **3.3**: 131-133 (1970).
[3] C. V. Sternling, L. E. Scriven, *Interfacial turbulence: hydrodynamic instability and the Marangoni effect*, AIChE Journal, **5.4**: 514-523 (1959).

Instabilities of structured metal films on nanoscale

L. Kondic,[1] N. Dong,[1] Y. Wu,[2] S. Fu,[2] J. Fowlkes,[3] and P. Rack[2,3]

[1]*Department of Mathematical Sciences, New Jersey Institute of Technology, Newark, NJ, USA,* kondic@njit.edu

[2]*Department of Materials Science and Engineering, The University of Tennessee, Knoxville, TN, USA*

[3]*Center for Nanophase Materials Sciences, Oak Ridge National Laboratory, Oak Ridge, TN, USA*

We consider instabilities of liquid metal films on nanoscale, with particular emphasis on the interplay between the initial geometry and instability properties. In experiments, metal films are deposited lithographically, allowing for precise control of the initial geometry, and then exposed to laser irradiation which liquefies them [1]; the insets in Fig. 1 show two examples of metal film evolution. To start modeling this problem, we consider a Newtonian fluid with time-independent material parameters. Liquid-solid interaction is included using a disjoining pressure model, as considered in similar contexts recently [2, 3]. We carry out fully nonlinear simulations of the resulting nonlinear partial differential equation. Figure 1 shows an example of simulations, where only a small part of the domain is simulated. The figure also illustrates the influence of stochasticity, here considered only on the level of randomly perturbed initial condition, on evolution. The last part of the presentation will concentrate on relevance of Marangoni effects that may be present due to thermal gradients caused by spatially variable heat conduction due to variable metal thickness.

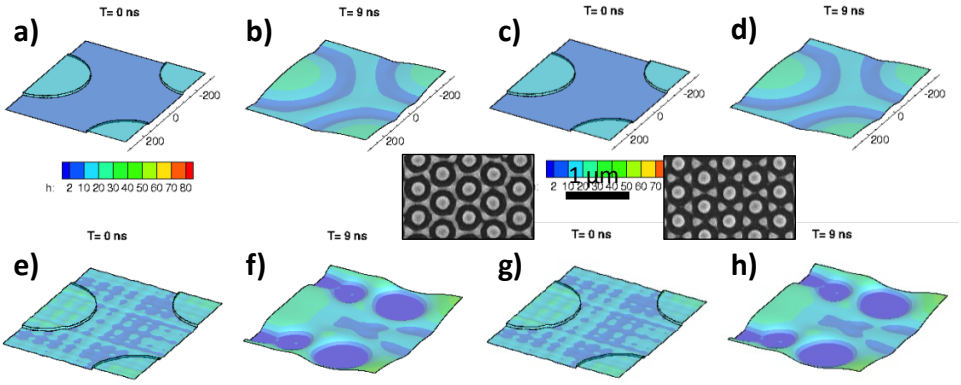

FIG. 1. The insets show experimental snapshots of two stages of liquid film evolution, with metal (light grey) and SiO_2 substrate (dark). The initial geometry consists of 20 nm thick Cu film with 9 nm Cu cylinders on top, as illustrated in the parts a) and c). The radiii and the distance between the cylinders are varied.

Acknowledgements. This work was partially supported by the NSF grants No. CBET-1235710 and CBET-1235651. A portion of this work was conducted at the Center for Nanophase Materials Sciences, which is sponsored at ORNL National Laboratory. by the Office of Basic Energy Sciences, DoE.

---

[1] Y. Wu, N. Dong, S. Fu, J. D. Fowlkes, L. Kondic, M. A. Vincenti, D. de Ceglia, P. D. Rack, *Directed liquid phase assembly of highly ordered metallic nanoparticle arrays*, (submitted) (2014).

[2] L. Kondic, J. A. Diez, P. D. Rack, Y. Guan, J. D. Fowlkes, *Nanoparticle assembly via the deleting of patterned thin metal lines: Understanding the instability mechanisms*, Phys. Rev. E, **79**, 026302 (2009).

[3] A. G. Gonzalez, J. A. Diez, Y. Wu, J. D. Fowlkes, P. D. Rack, L. Kondic, *Instability of Liquid Cu films on a SiO_2 substrate*, Langmuir, **29**, 9378 (2013).

Instabilities of liquid crystal films

L. Kondic,[1] M. Lam,[1] T.-S. Lin,[2] U. Thiele,[3] and L. Cummings[3]

[1]*Department of Mathematical Sciences, New Jersey Institute of Technology, Newark, NJ, USA,* kondic@njit.edu

[2]*Department of Mathematical Sciences, Loughborough University, Leicestershire, LE11 3TU, UK*

[3]*Institut für Theoretische Physik, Westfälische Wilhelms-Universität Münster, Wilhelm Klemm Str. 9, D-48149 Münster, Germany*

Asymptotic analysis finds extensive applications in the field of thin liquid film flows. While plenty of work has been done in the context of Newtonian fluids, this kind of systematic asymptotic treatment of complex fluids, in particular of liquid crystals, has not yet been considered extensively. In our recent works [1, 2], we have formulated asymptotic models applicable to these flows. In the present work, we will outline the methods used, and discuss similarities between the flow of NLC films and of Newtonian thin films destabilized by gravity (hanging films).

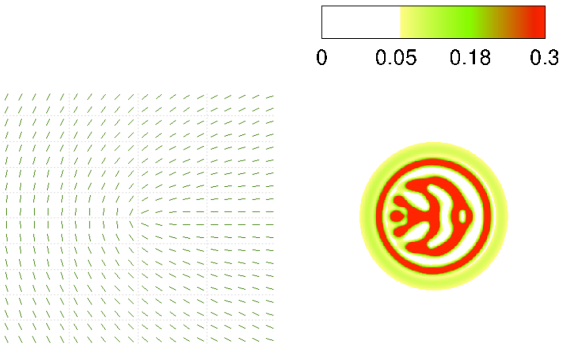

(a)anchoring condition (b)droplet shape at a late time

FIG. 1. Spreading NLC droplet for $s = 1/2$. The color scheme shows drop thickness.

Spreading NLC drops may be influenced by the local director structure, exhibiting "defects". Such defects are specified in terms of their topological winding number, s. Figure 1 shows an example of the results for $s = 1/2$. We can see that the presence of the defect influences the drop shape significantly, leading to development of thinner and thicker zones, with emerging length scales that can be rationalized by carrying out linear stability analysis of a flat film [1].

Flow down an incline. One perhaps surprising feature of the derived evolution equation is that NLC character of the film may have a similar effect to that of destabilizing gravity, such as on a Newtonian film on the underside of an inclined plane. For that problem it is known that surface instabilities may be observed [3] and we will discuss to which degree similar experiments may be expected for NLC films.

Acknowledgements. This work was partially supported by the NSF grant No. DMS-1211713.

---

[1] T-S. Lin, L. Kondic, U. Thiele, L. Cummings, *Modelling spreading dynamics of nematic liquid crystals in three spatial dimensions*, J. Fluid. Mech., **729**, 214 (2013)

[2] T-S. Lin, L. Cummings, A.J. Archer, L. Kondic, U. Thiele, *Note on the hydrodynamic description of thin nematic films: strong anchoring model*, Phys. Fluids, **25**, 082102 (2013)

[3] T-S. Lin, L. Kondic, *Thin film flowing down inverted substrates: two dimensional flow*, Phys. Fluids, **22**, 052105 (2010).

Convective structures and diffusion in ternary isothermal liquid and gas mixtures

V. Kossov,[1] Y. Zhavrin, O. Fedorenko, and G. Akylbekova

[1]*Institute of Experimental and Theoretical Physics, al-Farabi Kazakh National University, al-Farabi av. 71, 050038 Almaty, Kazakhstan,*
kosov_vlad_nik@list.ru

In isothermal state the instability of mechanical equilibrium of binary gas (or liquid) mixture can occur only, when the heavier density environment is over (on). Opposite direction of the gradient density ($\rho < 0$) defines the diffusion. However, the addition of a third component in the mixture provided $\rho < 0$ can lead to instability of the mechanical equilibrium and emergence of convective flows.

EXPERIMENTAL SETUP AND RESULTS

Convective instability in isothermal liquid mixtures has been studied in practice at aqueous solution diffusion of salt and sugar in a vertical plane channel. A set of pictures obtained by Teplers shadow method are shown in Fig. 1. The lower part of the channel is filled with an aqueous salt solution ($\rho = 1.125 g/cm^3$), and the upper part with water solution in 3 parts of salt and 1 part of sugar ($\rho = 1.057 g/cm^3$). Fig. 1a shows the initial mixture in the cell. First, a salt solution is poured, and then along the wall of the cell a lower density of salt and sugar solution is added. At the edges of the cell is clearly observed the boundary of liquids. Diffusion starts, but after 10-15 seconds there can be seen convective instability in the system. Further observation over the system indicates the presence of structured convective flows. More information is got at the result of experiments on studying

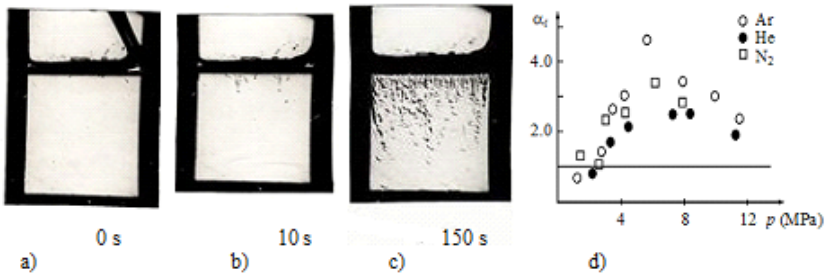

FIG. 1. a) – c): Photographs of instabilities formation. d) Values α_i of rate of flux for various components of a mixture 0.47 He + 0.53 Ar – N2.

the instability of mechanical equilibrium in gases. Two identical flasks were connected by a vertical flat channel. At the top of the flask was a binary mixture of light and heavy components. Average density gas was placed in the lower flask. Concentrations of light and heavy components were chosen so that the mixture in the upper (top) flask was always of lower density of the gas than in the lower (bottom) flask ($\rho < 0$). Pressure is the same in both flasks. The channel connecting the flasks opened. After some time, the channel was blocked and the mixture in both flasks was recorded. Concentrations got at the result of experiments were normalized to the calculated assuming diffusion. Fig. 1d shows the typical dependences thus obtained parameter of pressure for the system 0.47He + 0.53Ar - N2. From Fig. 1d is seen that at a certain critical pressure the parameter exceeds the unit, i.e. mechanical equilibrium of mixture becomes unstable. There occurs gravitational concentration convection. Mathematical description of the effect is based on the linearization of the system equations of continuous mechanics for isothermal ternary systems in ratio to small perturbations. The resulting homogeneous system of linear differential equations with coefficients independent of time has a solution of the following type exp $(-i\omega t)$. If among the found $\omega = \omega_0 + i\omega_1$ there exist such, for which the $\omega_1 > 0$, then the condition will be unstable. For mixture of He + Ar - N2 in terms of Rayleigh numbers were defined the boundaries of regime change of "diffusion – convection concentration".

Time-scale estimates for particle accumulation in thermocapillary liquid bridges

H. C. Kuhlmann[1] and F. H. Muldoon[1]

[1]*Institute of Fluid Mechanics and Heat Transfer, TU Wien, Resselgasse 3, 1040 Vienna, Austria,*
h.kuhlmann@tuwien.ac.at

Particle accumulation in thermocapillary liquid bridges has received increasing interest since its discovery by Schwabe et al. [1]. Small spherical particles suspended in the flow in thermocapillary liquid bridges can rapidly cluster into peculiar shapes, including closed line-like threads and particle-depletion zones.

The particle accumulation can have different causes. Clustering is well known to occur due to particle inertia in turbulent as well as in laminar flows if the density of the suspended particles differs from the density of the liquid [2–5]. A new mechanism proposed by Hofmann and Kuhlmann [6] is the restricted particle motion near a thermocapillary surface (particle–free-surface collision) [7, 8].

In thermocapillary liquid bridges both clustering mechanisms exist for particles heavier than the liquid. In order to assess their relative importance for particle accumulation structures (PAS) the time scale on which accumulation occurs is a crucial criterion. Based on visual observation Schwabe et al. [9] have provided experimental estimates of the time required for particles to accumulate. However, no general correlations exist to date for the PAS formation time which would cover a wide range of parameters. Considering the nature of the flow and the two accumulation mechanisms and analyzing numerical data we propose correlations for the particle-accumulation time for both mechanisms [10]. Under typical conditions [9] the collisional PAS formation is found to be 10 to 100 times faster than the inertial mechanism. Depending on particle size and density, PAS due to the collision mechanism can also have very different shapes than that due to inertia only, with the PAS due to the collision mechanism often being substantially more complicated. Formation-time predictions and shapes of PAS based on the collisional mechanism are in very good agreement with experimental observations.

---

[1] D. Schwabe, P. Hintz, S. Frank. *New features of thermocapillary convection in floating zones revealed by tracer particle accumulation structures (PAS)*, Microgravity Sci. Technol., **9**, 163–168 (1996).

[2] A. L. Yarin, T. A. Kowalewski, W. J. Hiller, S. Koch. *Distribution of particles suspended in convective flow in differentially heated cavity*, Phys. Fluids, **8**, 1130–1140 (1996).

[3] T. Sapsis, G. Haller. *Clustering criterion for inertial particles in two-dimensional time-periodic and three-dimensional steady flows*, Chaos, **20**, 017515–1–017515–11 (2010).

[4] D. O. Pushkin, D. E. Melnikov, V. M. Shevtsova. *Ordering of small particles in One-Dimensional coherent structures by Time-Periodic flows*, Phys. Rev. Lett., **106**, 234501–1–234501–4 (2011).

[5] H. C. Kuhlmann, F. H. Muldoon. *Particle-accumulation structures in periodic free-surface flows: Inertia versus surface collisions*, Phys. Rev. E, **85**, 046310–1–046310–5 (2012).

[6] E. Hofmann, H. C. Kuhlmann. *Particle accumulation on periodic orbits by repeated free surface collisions*, Phys. Fluids, **23**, 0721106–1–0721106–14 (2011).

[7] F. H. Muldoon and H. C. Kuhlmann. *Coherent particulate structures by boundary interaction of small particles in confined periodic flows*, Physica D, **253**, 40–65 (2013).

[8] R. Mukin and H. C. Kuhlmann. *Topology of hydrothermal waves in liquid bridges and dissipative structures of transported particles*, Phys. Rev. E, **88**, 053016–1–053016–20 (2013).

[9] D. Schwabe, A. I. Mizev, M. Udhayasankar, and S. Tanaka. *Formation of dynamic particle accumulation structures in oscillatory thermocapillary flow in liquid bridges*, Phys. Fluids, **19**, 072102–1–072102–18 (2007).

[10] H. C. Kuhlmann, R. V. Mukin, T. Sano, I. Ueno. *Structure and dynamics of particle-accumulation in thermocapillary liquid bridges*, Fluid Dyn. Res. (2014, submitted).

Dynamic wetting failure and air entrainment: what can thin-film models teach us?

E. Vandre,[1] M. S. Carvalho,[2] and S. Kumar[1]

[1]*Department of Chemical Engineering and Materials Science, University of Minnesota, Minneapolis, MN 55455, USA,* kumar030@umn.edu

[2]*Department of Mechanical Engineering, Pontificia Universidade Catòlica do Rio de Janeiro, Rio de Janeiro, RJ, Brazil*

Dynamic wetting is crucial to processes where liquid displaces another fluid along a solid surface, such as the deposition of a coating liquid onto a moving substrate. Numerous studies report the occurrence of dynamic wetting failure and air entrainment past some critical process speed. However, the factors that influence this transition remain poorly understood from an empirical and theoretical perspective. In this talk, I will discuss the results from experiments and hydrodynamic modelling aimed at addressing this issue.

The experiments involve two novel devices that allow for systematic determination of the influence of meniscus confinement. One device consists of a scraped steel roll that rotates into a bath of glycerol. Confinement is imposed via a gap formed between a coating die and the roll surface. Flow visualization is used to record the critical roll speed at which wetting failure occurs. Comparison of the confined and unconfined data shows a clear increase in the relative critical speed as the meniscus becomes more confined. The other device uses high-speed video to record the behaviour of the dynamic contact line as a tape substrate is drawn through a bath of a glycerol/water solution. Air entrainment is identified by triangular air films that elongate from the dynamic contact line above some critical substrate speed.

The hydrodynamic model is evaluated with three distinct approaches: (i) the low-speed asymptotic theory of Cox [1], (ii) a one-dimensional (1D) lubrication approach, and (iii) a two-dimensional (2D) flow model solved with the Galerkin finite element method (FEM). Approaches (ii) and (iii) predict the onset of wetting failure at a critical capillary number Ca^{crit}, which coincides with a turning point in the steady-state solution family for a given set of system parameters. The 1D model fails to accurately describe interface shapes near the three-phase contact line when air is the receding fluid, producing large errors in estimates of Ca^{crit} for these systems.

Analysis of the 2D flow solution reveals that strong pressure gradients are needed to pump the receding fluid away from the contact line. A mechanism is proposed in which wetting failure results when capillary forces can no longer support the pressure gradients necessary to steadily displace the receding fluid. The effects of viscosity ratio, substrate wettability, and fluid inertia are then investigated through comparisons of Ca^{crit} values and characteristics of the interface shape.

Surprisingly, the low-speed asymptotic theory (i) matches trends computed from (iii) throughout the entire investigated parameter space. Furthermore, predictions of Ca^{crit} from the 2D flow model compare favorably to values measured in experimental air-entrainment studies, supporting the proposed wetting-failure mechanism. The implications of these observations for the utility of thin-film modelling and the physical mechanisms of air entrainment will be discussed. Further detail can be found in References [2] and [3].

---

[1] R. G. Cox, *The dynamics of the spreading of liquids on a solid surface. Part 1, Viscous flow.* J. Fluid Mech., **168**, 169-194 (1986).

[2] E. Vandre, M. S. Carvalho, S. Kumar, *Delaying the onset of dynamic wetting failure through meniscus confinement*, J. Fluid Mech., **707**, 496-520 (2012).

[3] E. Vandre, M. S. Carvalho, S. Kumar, *On the mechanism of wetting failure during fluid displacement along a moving substrate*, Phys. Fluids, **25**, 102013 (2013).

Deformation of long slender non-newtonian drop in shear flow

O. M. Lavrenteva,[1] M. Favelukis,[2] and A. Nir[1]

[1]*Chemical Engineering Department, Technion - Israel Institute of Technology, Technion City, 32000, Haifa, Israel,* ceolga@techunix.technion.ac.il

[2]*Dept. of Chemical Engineering, Shenkar - College of Engineering and Design, Ramat-Gan, 52526, Israel,* favelukis@gmail.com

The deformation of a power-law non-Newtonian slender drop in a Newtonian liquid in a simple shear and creeping flow has been studied. The problem is governed by three dimensionless parameters: The capillary number, Ca, the viscosity ratio,λ,and the power-law index of the non-Newtonian drop, n. Following the analysis of a similar problem for a Newtonian drop [1], we assumed circular cross-section and derived a second order system of ordinary differential equation that describes stationary deformation of the drop. This system contains only two governing parameters, n and $\alpha = f(n)\lambda Ca^{3/2}R^2a^{-2}$ with a and R being the equivalent spherical radius and the radius of the cross-section at the center of the drop, respectively. It was shown that, similar to the case of Newtonian drop, the governing equations are singular at the point where the local radius of the cross-section equals $R/\sqrt{2}$. Exact analytical expressions for the local radius near the center and close to the end of the drop are presented. The solution near the end suggests that a stationary slender drop can exist only for cases where $n \leq 1$. As in the case of a Newtonian drop, the non-Newtonian slender drop has pointed ends.

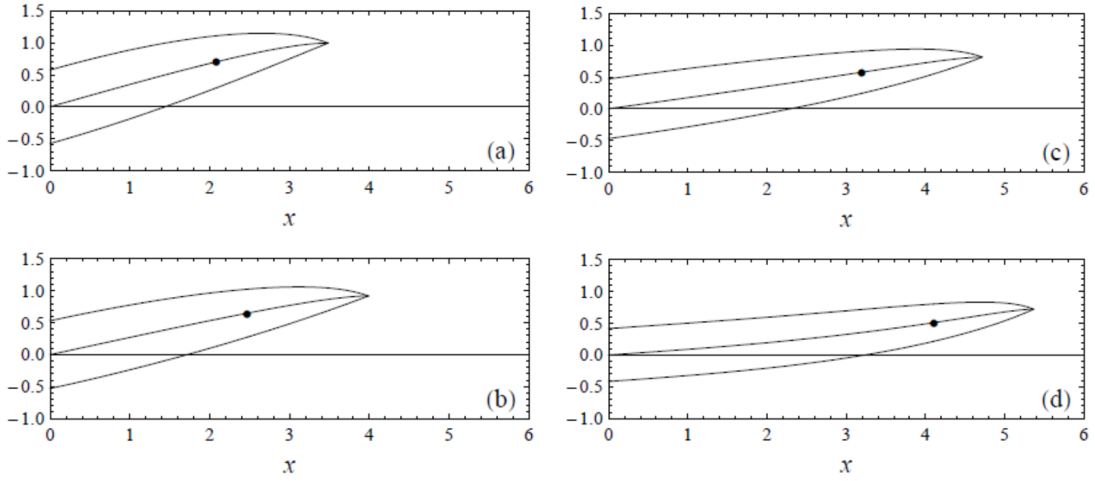

FIG. 1. Examples of steady-state drop shapes for the case n = 0.5. (a) α = 0.01, (b) α = 0.10, (c) α = 0.111, (d) α = 0.119. The solid circle is placed at the singular point.

Steady-state shapes of the drops were obtained via numerically integration of the developed equations for the range of governing parameters. Typical shapes of the drops are presented in the figure. The results of computations show that stationary shapes exists for any strength of the flow and that for the same strength of the flow, Newtonian drops are more elongated than shear thinning drops. A simple approximate is developed and a criterion for the stability of the drop in shear flow is suggested.

---

[1] E. J. Hinch, A. Acrivos, *Long slender drops in a simple shear flow*, J. Fluid Mech., **98**, 305–328 (1980).

Concentration Marangoni convection as a factor of self-assembly in evaporating picolitre sessile drop of binary solvent mixture

P. V. Lebedev-Stepanov[1,2]

[1]*Photochemistry Center, Novatorov St., 7a, Moscow, Russia, 119421,*
petrls@yandex.ru
[2]*National Research Nuclear University "MEPhI". Kashirskoe Shosse St., 31, Moscow, Russia, 115409.*

The evaporating picolitre liquid sessile drop of axis-symmetric shape is an interesting object of theoretical and experimental investigations due to its important fundamental and practice applications. The micro- and nanoparticles self-assembly into picolitre evaporating sessile drop of binary solvent mixture deposited by inkjet device on a flat substrate is considered. Recently, the concentration Marangoni driven migration of particles in such a system was experimentally investigated [1–3]. There was experimentally shown that the polystyrene nanoparticles were moved by toroidal vortex flow acted inside a drop, and the direction of this flow depends on solvent components types (ethanol/water, isopropanol/water, metoxypropanol/water), ratio of mixture, particle size and environmental conditions. In case of picolitre drop, the thermal Marangoni number is small ($Ma_T < 10$), and thermocapillary convection can be neglected, unlike of the concentration driven convection. The concentration Marangoni number $Ma_c = \frac{CR}{D\eta}|\frac{\partial\sigma}{\partial C}|$ (C is concentration of mixture component, R is drop radius, D is diffusion coefficient, is viscosity, is surface tension) reaches more than 10000 for such binary mixture droplet, and the Marangoni instability really takes place. In this report we suggest a new physical model of dissipative particle dynamics (DPD) in picolitre drop of binary solvent mixture as a further development of recently elaborated DPD model of self-assembly into evaporating droplet of pure solvent [4] with account of phenomenological results obtained in [1–3]. The i-th particle acceleration is calculated by the following Langevins equation

$$m_i\frac{d\mathbf{v}_i}{dt} = m_i\left(\frac{d\mathbf{V}}{dt} + (\mathbf{v}_i,\nabla)\mathbf{V}\right) - 6\pi a\eta(\mathbf{v}_i - \mathbf{V}) + \sum\mathbf{F} + \mathbf{F}_{Bi}$$

where m_i and $\mathbf{v}_i$ are an effective mass and velocity of i-th particle with radius of a, the first term of the right part is the hydrodynamic force, $-6\pi a\eta(\mathbf{v}_i - \mathbf{V})$ is a Stokes' viscous force, where $\mathbf{V}$ is a field of hydrodynamic flow in the solution (the sum of Deegan's vortex-free compensative flow and concentration Marangoni driven toroidal vortex flow). The term of $\sum\mathbf{F}$ includes 1) the sum of interaction forces acting to the i-th particle from other j-th particles; 2) interaction force between the i-th particle and substrate; 3) capillary force (interacting with the drop surface); 4) friction force acted due to roughness of the substrate surface, 4) chemoforesis force acted to the particle due to the differential evaporation of each component of binary mixture leads to concentration gradient. $\mathbf{F}_B$ is the Brownian force. The output data include the trajectories of particles during drop evaporation process. The computer modeling results are compared with the previously mentioned experiments.

Author thanks Prof. C.D. Bain (University of Durham, UK) for kind permission to use the experimental results on binary solvent liquid drop obtained in his group and E.L. Talbot for valuable comments to experiment interpretation and fruitful discussion.

[1] E. L. Talbot, A. Berson, L. Yang, C. D. Bain, *Evaporation of picolitre droplets of binary solvent mixtures*, 1-st Int. Workshop on Wetting and evaporation: droplets of pure and complex fluids. Marseilles, France, June 17-20, 2013, Book of Abstracts, 169–170 (2013).

[2] E. L. Talbot, A. Berson, L. Yang, C. D. Bain, *Internal Flows and Particle Transport Inside Picoliter Droplets of Binary Solvent Mixtures*, NIP 29 and Digital Fabrication, Book of Abstracts, 307–312 (2013).

[3] E. L. Talbot, A. Berson, C. D. Bain, *Drying and Deposition of Picolitre Droplets of Colloidal Suspensions in Binary Solvent Mixtures*, NIP 28 and Digital Fabrication, Book of Abstracts, 420–423 (2012).

[4] P. V. Lebedev-Stepanov, K. O. Vlasov, *Simulation of self-assembly in an evaporating droplet of colloidal solution by dissipative particle dynamics*, Colloids and Surfaces A : Physicochem. Eng. Aspects., **432**, 132–138 (2013).

Particle-size effect in the formation of particle-depletion zones in thermocapillary liquid bridges

Thomas Lemee[1] and Hendrik C. Kuhlmann[1]

[1]*Institute of Fluid Mechanics and Heat Transfer, TU Wien, Resselgasse 3, 1040 Vienna, Austria*

thomas.lemee@tuwien.ac.at , h.kuhlmann@tuwien.ac.at

Schwabe et al. [1] have discovered a rapid particle accumulation process in thermocapillary liquid bridges. A particular type of particle accumulation is the rapid removal of particles from a region near the axis of the liquid bridge. This effect leads to peculiar azimuthally periodic zones depleted of particles which have the same wave number as and co-rotate with the hydrothermal wave in high-Prandtl-number liquid bridges [2, 3]. In axisymmetric flows the depletion zone is axisymmetric as well.

Since the time scale on which nearly density-matched particles segregate is smaller [4, 5] than the time scale expected for inertial clustering, we investigate the motion using the particle–free-surface interaction model of [6] in which the particle size is the important parameter. To study the temporal evolution of the particle depletion process we consider the motion of spherical particles in an axisymmetric model flow which is part of the model studied by [7] and [8]. This approach enables an analytical expression of the particle orbit as a function of time and vice versa. Based on time required for a particle to encounter an interaction with the free surface we compute the degree of segregation $K(t)$ defined by [8]. Based on this quantity we can define a particle-depletion time analogous to the PAS-formation time suggested by [5]. We find that the time required to form an axisymmetric depletion zone and its dependence on the particle size is in surprising agreement with the PAS formation time in a three-dimensional flow.

The result suggests, but does not prove, that the particle-depletion zones and also three-dimensional line-like PAS [4] is primarily due to the particle–free-surface interaction. To further consolidate this conjecture, more accurate and innovative experiments are required on the temporal evolution of the particle-depletion process.

---

[1] D. Schwabe, P. Hintz, and S. Frank. New features of thermocapillary convection in floating zones revealed by tracer particle accumulation structures (PAS). *Microgravity Sci. Technol.*, **9**, 163–168 (1996).

[2] I. Ueno, S. Tanaka, and H. Kawamura. Oscillatory and chaotic thermocapillary convection in a half-zone liquid bridge. *Phys. Fluids*, **15**, 408–416 (2003).

[3] S. Tanaka, H. Kawamura, I. Ueno, and D. Schwabe. Flow structure and dynamic particle accumulation in thermocapillary convection in a liquid bridge. *Phys. Fluids*, **18**, 067103–1–067103–11 (2006).

[4] D. Schwabe, A. I. Mizev, M. Udhayasankar, and S. Tanaka. Formation of dynamic particle accumulation structures in oscillatory thermocapillary flow in liquid bridges. *Phys. Fluids*, **19**, 072102–1–072102–18 (2007).

[5] Hendrik C. Kuhlmann, Roman V. Mukin, Tomoaki Sano, and Ichiro Ueno. Structure and dynamics of particle-accumulation in thermocapillary liquid bridges. *Fluid Dyn. Res.*, to appear (2014).

[6] Ernst Hofmann and Hendrik C. Kuhlmann. Particle accumulation on periodic orbits by repeated free surface collisions. *Phys. Fluids*, **23**, 0721106–1–0721106–14 (2011).

[7] H. C. Kuhlmann and F. H. Muldoon. Particle-accumulation structures in periodic free-surface flows: Inertia versus surface collisions. *Phys. Rev.* E, **85**, 046310–1–046310–5 (2012).

[8] F. H. Muldoon and H. C. Kuhlmann. Coherent particulate structures by boundary interaction of small particles in confined periodic flows. *Physica D*, **253**, 40–65 (2013).

Effect of groove angle and distance between grooves on the micro-jet forms

C. Liu,[1] Q.-J. Feng,[1] and X.-H. Liang[1]

[1]*Institute of Applied Physics and Computational Mathematics, Beijing 100094, China*

A hydrodynamics Eulerian code is applied to simulate the micro-jet, which formed from the surface defects such as machined V-grooves under shock loading. The study is focused on the velocity and the mass of micro-jet, when the groove angle and the groove separation changes. The simulation results show: When the groove angle increases, the maximum velocity is decreased linearly, the ejecting factor and mass-velocity distribution of the micro-jet are changed obviously. The maximum velocity is sensitive to the change of groove angle and insensitive to the change of distance between bordered grooves, but the ejecting factor and mass-velocity distribution changes remarkably when the distance between grooves changes. But when the distance between bordered grooves is longer than 5 times of the groove depth, the ejecting factor and mass-velocity distribution of the micro-jet maintain unchanged.

Thermocapillary effect on migration of micro-droplet along a non-uniform thermal substrate

X. Chen,[1] Q.-S. Liu,[1] Z.-Q. Zhu,[1] Y.-N. Sun,[2] and Y.-D. Yu[2]

[1]*Institute of Mechanics, Chinese Academy of Sciences, Bei-Si-Huan-Xi Road, No.15, Beijing, China*
liu@imech.ac.cn
[2]*Institute of Semiconductors, Chinese Academy of Sciences, Qing-Hua-Dong Road, No.35, Beijing, China*

Recently, with the development of microelectronics technology, droplet control technique has become an important direction in microfluidics technology nowadays, gas-liquid, gas-solid and solid-liquid interface effect problem increasingly prominent. Many experimental and theoretical works have been performed to study the drive and control of the droplet, while the mechanisms of migration caused by the temperature gradient are still lack of comprehensive study. The present paper gives a brief presentation of the thermocapillary migration of micro-scale droplets on a non-uniform thermal substrate and tries to explain the cause of the migration of water-solution and paraffin oil droplets that happens in the proceeding of MEMS manufacture. The experimental apparatus is shown in fig.1, by utilizing the SiO_2 as substrate, and paraffin oil, 10 silicon oil and 50 silicon oil as working fluids.

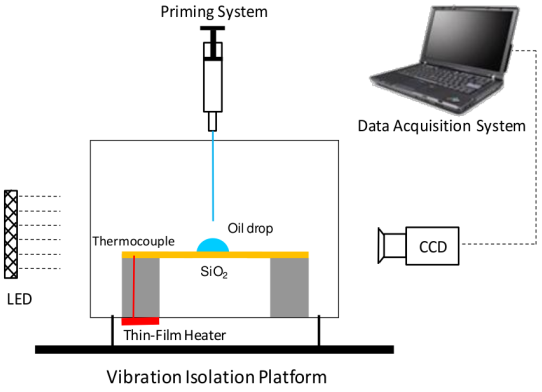

FIG. 1. Schematic setup of the experimental apparatus.

When heating the substrate to gain the temperature gradient, the information of the droplet motion (contact radius, velocity, position) can be observed by CCD camera. From the experimental data, the oil droplet would spread as soon as it was deposited on the SiO_2 substrate owing to the surface free energy effect, which also had some related to the viscosity. In addition, when imposed a temperature gradient on the solid substrate, droplet would flow from the hot side to the cold side with the advent of contact angle hysteresis. This could be illustrated by the impact of the surface tension. When a drop is placed on a solid surface upon which a temperature gradient has been imposed, a corresponding surface tension variation arises at the liquid-vapor interface which generates a flow in the drop and exerts a hydrodynamic force on the solid surface that points in the direction of the applied temperature gradient. Under suitable conditions, it is possible to achieve quasi-steady motion where on the net hydrodynamic force on the drop is zero. It's worth noting that there is a critical radius, regardless of the amount of temperature gradient, the droplet migration would not occur unless the contact radius is greater than the critical value.

Acknowledgements. This research was financially supported by the National Natural Science Foundation of China (Grants No.11072249) and the Strategic Pioneer Program on Space Science, Chinese Academy of Sciences (Grants No.XDA04073000 and No.XDA04020202-02).

Thermocapillary effect on the dynamics of viscous beads on vertical fibre

R. Liu[1] and Q.-S. Liu[1]

[1]*Key Laboratory of Microgravity (National Microgravity Laboratory), Institute of Mechanics, Chinese Academy of Sciences, Beijing, China 100190,*
liurong@imech.ac.cn, liu@imech.ac.cn

The gravity-driven flow of a thin liquid film down a uniformly heated vertical fibre is considered. This is an unstable open-flow that exhibits rich dynamics including the formation of droplets, or beads, driven by a Rayleigh-Plateau mechanism modified by the presence of gravity as well as the variation of surface tension induced by temperature disturbance at the interface. A linear stability analysis and a nonlinear simulation are performed to investigate the dynamic of axisymmetric disturbances.

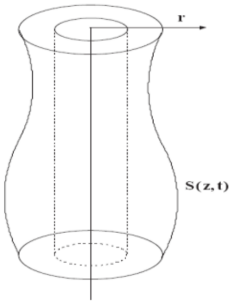

FIG. 1. Sketch of the geometry of fibre flow.

As shown in fig.1, a Newtonian fluid, of constant viscosity μ and density ρ, flows down a vertical fibre of radius $r = a$ under gravity g. The initial radius of the fluid ring measured from the centre of the fibre is $r = R$. The temperatures of the fibre wall and the interface of the film are T_a and T_i. We assume that the radius of the fluid ring, R, is much smaller than the wavelength L. The dynamics of the system is determined by the Bond number $Bo = \rho g R^2/\gamma$, the Bond number $Bo = R/L = \epsilon$, the Marangoni number $Ma = \gamma L \Delta T/\mu V$, the Biot number $Bi = qR/\chi$.

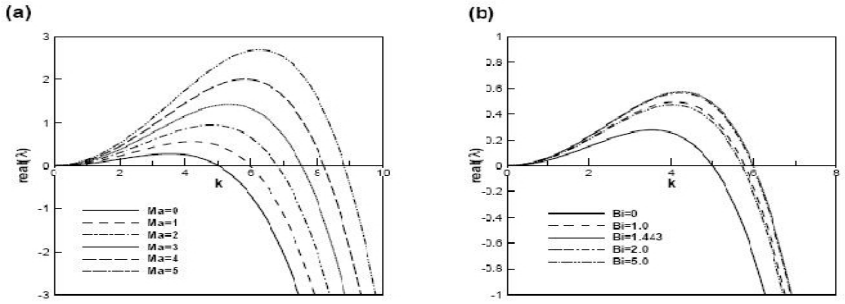

FIG. 2. The dispersion relation of the real growth rate versus the wavenumber. (a) for various Marangoni numbers at $Bi = 1.0$, (b) for various Boit number at $Ma = 1.0$. Other parameters are $\epsilon = 0.2$, $a/R = 0.5$.

Fig.2 plots the dispersion relations of the time growth rate versus the streamwise wavenumber. The result shows that both the Marangoni number and the Biot number influence the stability of the fibre flow. With the increase of Ma, the fibre flow become more unstable.

Stability of stationary plane-parallel flow over a saturated porous medium

T P. Lyubimova,[1,2] D. Baidina,[2] and E. Kolchanova[1]

[1]*Institute of Continuous Media Mechanics UB RAS, Koroleva Str 1., 614013 Perm, Russia,*
lubimova@psu.ru
[2]*Perm State University, Bukireva Str. 15, 614990 Perm, Russia*

When a fluid moves over a porous medium, the flow partially involves the fluid saturating the porous matrix, however, due to the large resistance forces, the sharp drop of the tangential velocity component arises which promotes to the development of instability similar to the Kelvin-Helmholtz instability. The present paper deals with the investigation of linear stability of plane-parallel stationary flow of a viscous incompressible fluid over a porous medium saturated with the same fluid. The layer of the saturated porous medium is bounded from below by the rigid surface and the layer of the pure fluid by the non-deformable free upper surface. The layers are inclined to the horizontal at an angle α. The study is performed in the framework of the Brinkman model taking into account the viscous diffusion of momentum. At the interface between the pure fluid and the saturated porous medium the continuity condition for the velocity and the conditions of the normal and tangential stresses balance are imposed. For the tangential stresses the condition proposed by Oshua - Tapia and Whitaker [1, 2] is used. This condition contains the term having the meaning of the resistance of the porous matrix to the fluid motion in a thin boundary layer near the interface which thickness is of the order of the square root of permeability. The calculations are carried out at different values of the empirical factor of proportionality in this condition. The solutions of the problem for stationary plane-parallel flow at different values of the ratio of layer thicknesses, porosity and permeability of the porous matrix are obtained analytically. The linear stability problem of the stationary plane-parallel flow with respect to the perturbations periodic along the layer is solved numerically by the differential sweep method.

The neutral stability curves are obtained for different values of the parameter $q = Da^{-1/2}$ (Da is the Dacy number) and the ratio d of the thickness of the porous layer to the total thickness. At small q and values of d larger than a certain value, the neutral curves have one minimum. With the increase of q and / or the decrease of d they become bimodal: in addition to the long-wavelength minimum which corresponds to the large-scale perturbations covering the both layers, the shortwave minimum appears in the range of large values of the wave number which corresponds to the perturbations localized in the pure fluid layer. The dependences of the minimal critical Reynolds number and the wave number and frequency of the most dangerous perturbations on q and d are obtained and the structures of the critical perturbations at different q and d are determined. Analysis of the results obtained when the ratio of layer thicknesses is varied and q is fixed shows that at $d > 0.6$ with the increase of d, i.e. with the decrease of the thickness of the liquid layer, the instability threshold increases. This is due to the fact that the instability is determined primarily by the perturbations developing in the pure fluid layer. At $d < 0.6$ the instability threshold increases with the decrease of d. The frequency of perturbations also varies non-monotonically with the change of d. The growth of the parameter q at fixed d leads to the growth of the instability threshold.

The work was made under financial support of Russian Foundation for Basic Research (grant N 12-01-00795).

[1] J. A. Ochoa-Tapia, S. Whitaker, *Momentum transfer at the boundary between a porous medium and a homogeneous fluid - I. Theoretical development*, Int. J. Heat Mass Transfer., **38**, 2635–2646 (1995).

[2] J. A. Ochoa-Tapia, S. Whitaker, *Momentum transfer at the boundary between a porous medium and a homogeneous fluid - II. Comparison with experiment*, Int. J. Heat Mass Transfer., **38**, 2647–2655 (1995).

Onset of Benard-Marangoni convection in a two-layer system with deformable fluid interface and fixed heat flux at the external boundaries

T P. Lyubimova,[1,2] D. V. Lyubimov,[2] and Y. Parshakova[1]

[1]*Institute of Continuous Media Mechanics UB RAS, Koroleva Str 1., 614013 Perm, Russia,* lubimova@psu.ru

[2]*Perm State University, Bukireva Str. 15, 614990 Perm, Russia*

The paper deals with the investigation of the effect of fluid interface deformations on a conductive state stability of a two-layer system subjected to vertical temperature gradient. In the case when the lower fluid density is considerably larger than that of the upper fluid, the gravity suppresses efficiently the interface deformations. Because of that the most interesting case from the viewpoint of the analysis of the deformability effect is the case of fluids of close densities. In this case it is possible to use the conventional equations of thermal buoyancy convection in the Boussinesq approximation, taking into account the density difference (or, more precisely, the difference in hydrostatic pressure gradients) only in the normal stress balance condition at the fluid interface. In the present work, we study the stability of the conductive state of two superposed horizontal layers of immiscible viscous fluids with close densities subjected to the vertical temperature gradient and fixed heat flux at the external boundaries in the framework of the approach described above.

Analysis of the conductive state stability to the longwave perturbations at zero Marangoni number shows that after the loss of the conductive state stability, the through convective flow which covers the entire two-layer system and drags the fluid interface may develop. The instability to the perturbations of the two-floor structure, typical for two-layer systems, becomes more dangerous at large enough values of the modified Galilei number module. At intermediate values of the modified Galilei number the intensive exchange by energy between the perturbations of two types described above takes place which leads to the arising of the oscillatory instability. The boundary of the monotonic longwave instability consists of two branches of hyperbolic type and the oscillatory instability boundary has the form of straight line connecting two branches of the monotonic instability boundary; the stability domain is located between two branches of monotonic instability boundary and oscillatory instability boundary. Analysis of the perturbations with finite wavelength does not introduce qualitative changes to the stability map described above; it results only in the quantitative changes. Besides, the greater the surface tension, the stronger it suppresses the short-wavelength perturbations, which leads to the expansion of the domains where the longwave perturbations are most dangerous.

The study of the conductive state stability to the longwave perturbations at non-zero values of the Marangoni number shows that in the case of heating from above the thermocapillary effect leads to the increase of instability domain to the monotonic longwave perturbations. In the case of heating from below, the thermocapillarity makes stabilizing effect on the longwave perturbations and at some values of the parameters the configuration where more dense fluid is located above less dense one turns out to be stable. However, the analysis of the perturbations with finite wavelength in the presence of thermocapillary effect shows that in the case of heating from below the Rayleigh-Taylor instability is not suppressed. For any values of the parameters the perturbations with finite wavelength turn out to be more dangerous. In this situation the instability domain becomes wider with the increase of the Marangoni number module. In the case of heating from above, for any values of the Marangoni number, at small values of the Rayleigh number module the monotonic longwave perturbations are most dangerous and at large values of the Rayleigh number module - the monotonic perturbations with finite wavelength.

Benard-Marangoni instability in a fluid with a deformable free surface

D. V. Lyubimov,[1] T P. Lyubimova,[1,2] N. I. Lobov,[1] and A. E. Samoilova[1]

[1]*Perm State University, Bukireva Str. 15, 614990 Perm, Russia*
[2]*Institute of Continuous Media Mechanics UB RAS, Koroleva Str. 1, 614013 Perm, Russia*
lubimova@psu

It is known that for small temperature related density inhomogeneities, the deviation of free surface shape from planar one is proportional to the Boussinesq parameter. Because of that, within the framework of the Boussinesq approximation, the interface deformations are generally neglected. In our paper we analyze the Marangoni-Benard instability of a fluid with a deformable free surface. Stability of a conductive state of horizontal fluid layer with free deformable upper surface, subjected to the vertical temperature gradient is considered. The layer is bounded from below by isothermal rigid plate. On the upper boundary, at which the temperature dependent surface tension admits the possibility of the Marangoni convection, the Biot heat transfer condition is imposed. It is assumed that the fluid is isothermally incompressible, i.e. the density depends only on temperature. The dynamic viscosity, thermal conductivity and specific heat are assumed to be constant. The problem is studied in the framework of non-Boussinesq approximation where the density variations are taken into account not only in the buoyancy force, but also in the inertia terms of the momentum equation and in the continuity equation.

Under accepted restrictions the conductive state with flat horizontal free surface and linear temperature distribution along the vertical coordinate is possible, where the density distribution is defined by the state equation and the pressure distribution is defined by the hydrostatics equations.

The long-wave instability is investigated analytically. For linear and exponential state equations, the critical values of the Marangoni number Ma are obtained. Parameter ranges where the long-wave disturbances are most dangerous are defined.

For finite values of the wave number the stability of the conductive state to small disturbances is studied numerically. The state equation with exponential temperature dependence of the density is used. It is found, that at $Ma = 0$ the critical Rayleigh number increases with the decrease of the Galilei number Ga, and at some value of Ga the Rayleigh instability vanishes.

Accounting for the deformations of free surface at fixed small values of the Bond number leads to the following results. For small Ga the long-wave instability mode is the most dangerous at any values of Ra. With the increase of Ga the role of the disturbances with finite wave numbers grows and they become responsible for the stability loss of the conductive state at small values of the Rayleigh number. However at larger Ra the long-wave disturbances remain responsible for the onset of convection. For heating from above the crisis of conductive state is mainly related to the development of long wave disturbances. With further Ga growth the long-wave mode on the Ma – Ra map is shifted upward. The growth of the Bond number leads to the situation, where the long-wave disturbances become most dangerous for the system heated from above. Conventional Boussinesq approximation gives qualitatively different results.

It is found that in the case of negative values of the Boussinesq parameter (which corresponds to the normal thermal expansion) the oscillatory instability mode exists not only when the Marangoni number is negative, but also at $Ma \geq 0$. Moreover, the emergence of the oscillatory instability mode is detected in the case when both thermocapillary effect and gravity are absent. The interpretation of this effect is developed.

Jumping pool boiling into mesoscopic structures of monodispersed microspheres

A. S. Dmitriev,[1] M. A. El Bouz,[1,2] and P. G. Makarov[1]

[1]*National Research University "MPEI", Moscow, Russia,*
asdmitriev@mail.ru
[2]*Mansoura University, Mansoura, Egypt,*
mostafa_booz@yahoo.com

Study of heat and mass transfer in mesoscopic structures is gaining great importance nowadays, both in academic and in practical situations. Boiling liquids in the presence of monodisperse microspheres systems is an important case [1], which requires experimental and theoretical studies. The relevance of these studies for example, technical fluids may often contain various impurities affecting the thermodynamic properties of the fluids. In addition to engineering problems, this topic is of purely academic interest: it is expected that the introduction of liquid metal microspheres will optimize energy consumption and intensify boiling.

For experiments a research stand was collected and prepared. The heat source used was a heating stove ES-HA3040 (300*400) mm 2.2 kW with a temperature-regulated surface (material - stainless steel). Experiments were carried out for distilled water and microspheres (95% lead, 5% antimony) diameter of 100, 200 and 300 microns to study their influence on the process of boiling. All experiments were performed in glass Petri dishes of diameter 93 mm, wall thickness 3.5 mm.

It is obvious that the evaporation and boiling liquids containing monodisperse microspheres, processes different from those for porous media and the free surface [2]. This difference is due, among other effects, additional space, appearing from behind the microspheres, the occurrence of liquid "bridges" (Fig. 1) between the microspheres.

Experimental results showed that the system "fluid - monodisperse microspheres" characterized by a new, hitherto unobserved effect "Jumping bubbles". It is at the initial stage of boiling bubble formed on the bottom of Petri dish captures for a certain amount of the microspheres and the surface begins to rise. But then, without reaching the boundary "liquid-vapor" bubble with microspheres goes back down to the bottom, where, without collapsing, moving up again. The effect is not observed over the entire area of the tank bottom (Fig. 2), and in those areas where the microspheres are packed in a monolayer. It is also seen that it is highly sensitive to a heat flow. Experiments have shown that the liquid with backfilling (monodisperse microspheres) boils faster than without it. Furthermore, the speed depends on the size of boiling microspheres. In general, the observed effect may be a new way of intensification of heat and mass transfer.

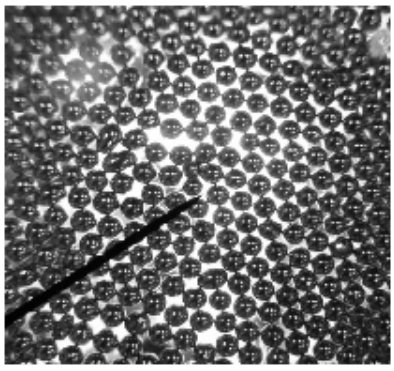

FIG. 1. A monolayer of microspheres (d = $300\mu m$).

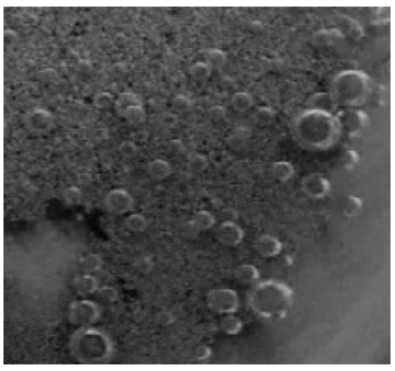

FIG. 2. "Jumping" bubbles coated with microspheres (d = $300\mu m$).

[1] E. V. Amitistov, A. S. Dmitriev, *Monodispersion systems and technology*, MPEI, **– 536** (2002).
[2] V. P. Isatchenko, V. A. Osipova, A. S. Sukomel, *Heat transfer*, M.: Energoizdat, **– 416** (1981).

Study of dynamics of drying processes in Fe_2O_3 and SiO_2 nanocolloid droplets

A. S. Dmitriev[1] and P. G. Makarov[1]

[1]*National Research University "MPEI", Moscow,Russia,*

asdmitriev@mail.ru

This work is devoted to the description of drying processes in droplets of SiO_2 and Fe_2O_3 nanoparticles solutions. It is also devoted to detection of conditions that have influence on forming of ring-shaped patterns (known as "coffee ring effect") that appear after all the fluid has evaporated.

The coffee ring effect is responsible for forming of a capillary-forces-caused pattern left after the droplet of solution with suspended particles has fully dried [1]. In everyday life it can be observed for coffee and red wine.

Relevance of such experiments is due to several reasons. E.g. in many spheres of modern thermal energetics liquids with microparticles suspended in it due to some causes (functional or as a result of contamination) are being used. In nanotechnologies colloids of nanoscale particles of different substances are one of main subjects of inquiry. Experiments aimed at fixation of conditions having effect on forming of specific rings have been held. The extreme case of coffee ring effect cancellation was studied also.

Dynamics of colloids evaporation was studied according to two observing techniques. The first one was based on spectrometric measuring of light transmitted through drying droplets. For these measurements the spectrometer of Avantes production was utilized. The specific feature of both liquids is that baseline stayed constant during all the process of evaporation so drying could be characterized by changing of droplets height but not by compression of the whole droplet. This led to decrease of optical path of light inside of drying droplet and therefore to decrease of the intensity of light transmitted through droplet and registered by the instrument. Most of the time of drying intensity increases uniformly but on the very last stage of drying when major volume of liquid had already evaporated and therefore concentration of suspended substance had increased some specific non-linear changes of intensity were recorded.

The second technique was based on registering of changes of geometrical properties of drying droplets. For these measurements a drop shape analyzer KRÜSS EasyDrop was utilized.

Patterns left by droplets of nanocolloids (Fig. 1) were alike in general collars were formed along the perimeter of initial droplet. According to coffee ring effect a major part of suspended particles assembled in these collars. But reaction of liquids on different influences was also different.

In [2] a realization of self-assembling processes based on coffee ring effect is described. Attempts to organize self-assembling on basis of observable solutions are being undertaken now.

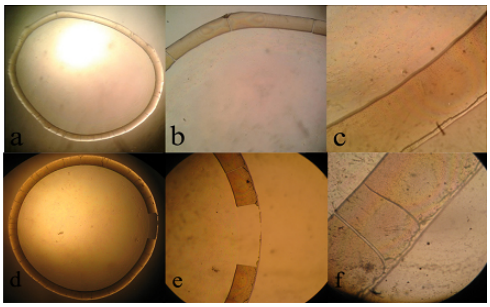

FIG. 1. Microscopic photos of patterns left after all the SiO_2 fluid from droplet has evaporated. a,d) magnification $4x|0.10$; b,e) magnification $10x|0.25$; c,f) magnification $40x|0.65$.

[1] R. D. Deegan, O. Bakajin, T. F. Dupont, G. Huber, S. R. Nagel, T. A. Witten, *Capillary flow as the cause of ring stains from dried liquid drops*, Nature, **389(6653)** (1997).

[2] S. Choi, S. Stassi, A. P. Pisano, T. I. Zohdi, *Coffee-Ring Effect-Based Three Dimensional Patterning of Micro/Nanoparticle Assembly with a Single Droplet*, Langmuir, **26(14)** (2010).

Space experiment on flow transition of Marangoni convection in liquid bridge with high Prandtl number

S. Matsumoto[1] and S. Yoda[2]

[1]*Institute of Space and Astronautical Science, Japan Aerospace Exploration Agency, 2-1-1 Sengen, Tsukuba,Ibaraki Japan,*
matsumoto.satoshi@jaxa.jp

[2]*Institute of Space and Astronautical Science, Japan Aerospace Exploration Agency, 3-1-1 Yoshinodai, Chuo-ku, Sagamihara, Kanagawa, Japan,*
yoda.shinichi@jaxa.jp

It is well known that thermocapillary convection (Marangoni convection) transits from steady to oscillatory, chaotic, finally turbulent flows with increasing the temperature difference at a liquid/gas interface which produces the driving force [1]. However the trasition process is not clear yet. Final goal of this study is to make clear the flow transition on Marangoni convection in liquid bridge configuration and to compare with other flow such as Rayleigh-Bénard convection, Taylor-Couette flow.

In order to observe internal flow of Marangoni convection experimentally, the ultrasonic velocity profiler (UVP) was employed [2]. The ultrasonic transducers were embedded in liquid bridge supporting rod. An ultrasonic bust wave with 8 MHz frequency is emitted at the tip of transducers into liquid bridge. Large diameter liquid bridge is needed to equip the transducers. The liquid bridge of 50 mm diameter was used. A working fluid was silicone oil of 5 mm^2/s viscosity, which Prandtl number is 68. Microgravity condition is needed to form the large liquid bridge, and so the International Space Station (ISS) is utilized.

The echo signals from suspended fine tracer particles (30 μm in diameter) are detected by the same transducers. The signals include the velocity and spatial informations. Therefore, spatio-temporal structure of velocity field can be constructed.

The liquid bridge with aspect ratio (length/diameter) of 0.5 is formed between supporting rods. The one end is heated and other cooled. The temperature difference ΔT is changed up to 50 K. The velocity of thermocapillary convection becomes stronger when ΔT increases. The critical temperature difference ΔT_c was 5.2 K and critical Marangoni number Mac was 24600. Chaotic flow appears when the ΔT is 30.7 K. In that case, the power spectrum of temperature fluctuation near the interface becomes continues spectrum. The spatio-temporal structure of velocity measured by UVP at ΔT = 40.8 K is shown in Fig. 1. Randomly fluctuated velocity profile is appeared in chaotic regime. The characteristics of velocity and temperature fluctuations are compared each other.

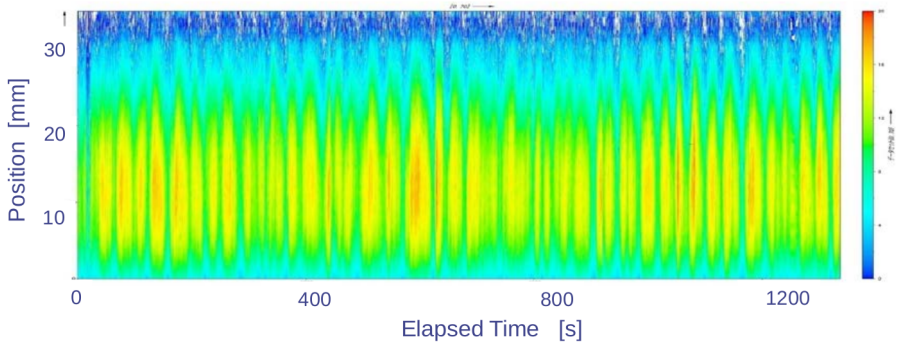

FIG. 1. Measured velocity profile with time by UVP.

[1] H. Kawamura, K. Nishino, S. Matsumoto, I. Ueno, *Report on Microgravity Experiments of Marangoni Convection aboard International Space Station*, Journal of Heat Transfer, **134**, 031005–031018 (2006).

[2] Y. Takeda, W. E. Fischer, J. Sakakibara, *Decomposition of the Modulated Waves in a Rotating Couette System*, Science, **263**, 502–505 (1994).

Maxwell stress long wave instabilities in a thin aqueous film under time-dependent electro-osmotic flow

M. Mayur[1] and S. Amiroudine[2]

[1]*Offenburg University of Applied Sciences, Badstraße 24, 77652 Offenburg, Germany*
manik.mayur@hs-offenburg.de
[2]*Université de Bordeaux, I2M, UMR CNRS 5295,*
16 Av. Pey-Berland, 33607 Pessac, France,
sakir.amiroudine@u-bordeaux.fr

In this study the dynamics and stability of thin [1] and electrically conductive aqueous films is explored under the influence of time-periodic electric field [2] (see Fig.1). With the help of linear stability analysis for long wavelength disturbances, the stability threshold of the system as a function of various electrochemical parameters and transport coefficients is presented. The contributions of parameters like surface tension, disjoining pressure and electric double layer (Debye length and interfacial zeta potential) as well as unsteady Maxwell and viscous stresses are highlighted with the help of appropriate dimensionless groups. The physical mechanisms affecting the stability of thin films are detailed with respect to the above mentioned forces and parametric dependence of stability trends is discussed. Figure 2 shows some typical results of the base-state vorticity profile along the transverse direction and the marginal stability diagram with the variation of two dimensionless parameters: the Debye number which measures the relative thickness of the electric double layer and the Womersley number which expresses the relative strength of temporal inertial force over the viscous dissipation force, while keeping the other parameters fixed.

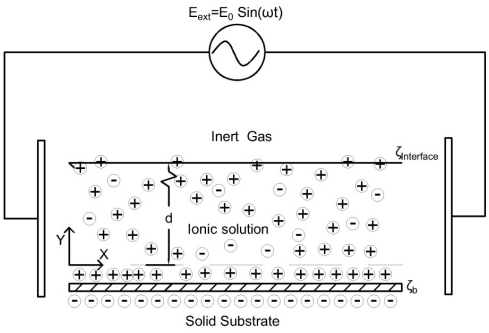

FIG. 1. Schematic of the thin film time-periodic EOF system.

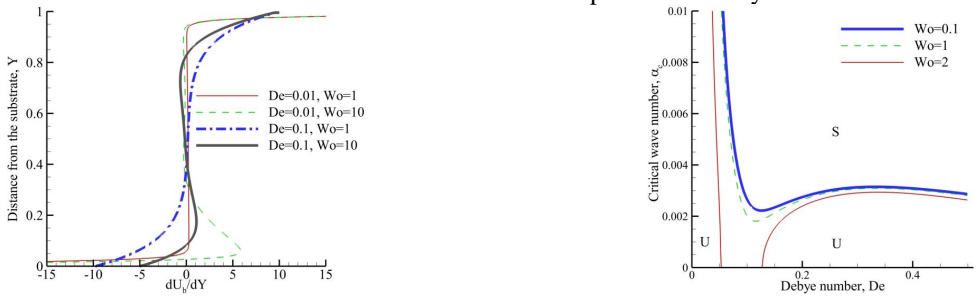

(a) (b)

FIG. 2. (a) Base state vorticity ($\mid \omega \mid = \mid \nabla \text{ x } \mathbf{U}_b \mid$) distribution over the film thickness (b) Marginal stability curves showing the critical wave number as a function of the Debye number (De) with stability trends for different values of Womersley number (Wo).

[1] M. Mayur, S. Amiroudine, D. Lasseux, *Free surface instability in electro-osmotic flows of ultra-thin liquid films*, Phys. Rev. E, **Vol. 85**, Issue 4, 046301, (2012).

[2] M. Mayur, S. Amiroudine, D. Lasseux, S. Chakraborty, *Effect of interfacial Maxwell stress on time periodic electro-osmotic flow in a thin liquid film with a flat interface*, Electrophoresis, DOI: 10.1002/elps.201300236 (2014).

From linear to highly non-linear steady-state pattern bifurcation diagrams in confined surface-tension-driven-convection

M. Medale[1] and P. Cerisier[1]

[1]*Aix-Marseille Université, CNRS, IUSTI UMR 7343, 13013 Marseille, France,*
marc.medale@univ-amu.fr

The numerical model we have developed enables us to investigate both stable and unstable steady-state solutions of surface-tension-driven-convection in confined containers, up to highly non-linear regimes. Few works have previously achieved comparable issue, however, it appears that determining the threshold of convection from experiments could be a quite unreliable process even when one takes a lot of care, e.g., Koschmieder and Prahl [1]. Obviously, experimentally, only stable solutions can be observed. On the other hand, many numerical studies have only concentrated on the threshold of convection and its very close neighbourhood, e.g., Dauby and Lebon [2]. They have therefore ignored so far the very interesting non-linear regime where one can observe pattern evolutions (cell size and shape variations, periodic and non periodic dynamical regimes, etc.).

In the present work, we present some computational results obtained with our continuation algorithm that accurately locates the threshold of convection (primary bifurcation point) and subsequent secondary bifurcations. It is based on an Asymptotic Numerical Method and has been implemented in a high performance computer environment to deal with three-dimensional thermo-convective instability problems [3, 4]. We have performed these computations in square and circular vessels of small-to-moderate aspect ratios ($\Gamma \leq 20$), filled with a high Prandtl number silicon oil ($Pr \approx 900$), with a one layer model, for physical properties in the liquid and air layers corresponding to $Pr = 900$ and $Bi = 0.1$. This numerical study reveals the existence of many steady-state bifurcations in the vicinity of the threshold for small-to-moderate aspect ratios. The patterns inherits the container symmetries at threshold, but progressively looses them as going through subsequent secondary bifurcations, which occur closer to the threshold for higher aspect ratios. Moreover, the nature of these steady-state bifurcations has also been computed and analyzed versus aspect ratio and container shape.

---

[1] E. L. Koschmieder, S. A. Prahl, *Surface-tension-driven bénard convection in small containers*, J. Fluid Mech., **215**, pp. 571-583 (1990).

[2] P. C. Dauby, G. Lebon, *Bénard-Marangoni instability in rigid rectangular containers*, J. Fluid Mech., **329**, pp. 25-64 (1996).

[3] M. Medale, B. Cochelin, *A parallel computer implementation of the Asymptotic Numerical Method to study thermal convection instabilities*, J. Comp. Physics, **228**, pp. 8249-8262 (2009).

[4] B. Cochelin, M. Medale, *Power series analysis as a major breakthrough to improve the efficiency of Asymptotic Numerical Method in the vicinity of bifurcations*, J. Comput. Phys., Vol. **236**, 594–607 (2013).

Spatial and kinematic topology within an ensemble of particles in a thermocapillary flow in a liquid bridge

D. Melnikov,[1] T. Watanabe,[2] D. Pushkin,[3] V. Shevtsova,[1] and I. Ueno[2]

[1]*Université Libre de Bruxelles (ULB), MRC,*
Av. F.D.Roosevelt, 50, CP-165/62, 1050 Brussels, Belgium,
dmelniko@ulb.ac.be, vshev@ulb.ac.be
[2]*Tokyo University of Science, 2641 Yamazaki, Noda, Chiba, Japan,*
a7508151@rs.tus.ac.jp, ich@rs.tus.ac.jp
[3]*Rudolf Peierls Centre for Theoretical Physics, University of Oxford,*
1 Keble Road, Oxford OX1 3NP, United Kingdom,
mitya.pushkin@gmail.com

Experimental and theoretical works have been performed to study the phenomenon of formation of particulate coherent structures (PAS) in a flow driven by the combined effects of buoyancy and thermocapillary forces in a non-isothermal liquid bridge made of n-decane. Formation of a PAS in a thermocapillary flow is possible in a supercritical oscillatory regime. In this regime, the flow can be thought of as a superposition of a main doughnut-like Marangoni vortical flow and a time-dependent azimuthal flow caused by a wave spreading in the transversal direction. It has long been known [1, 2] that a PAS is a collective phenomenon in terms of the evoked identities of individual particles. Each of the PAS-forming particles, in response to the repeatable interaction with the flow, performs an identical periodic motion.

We used solid particles that were denser than the fluid. To explore the long-time behavior of particle trajectories and their dynamical properties in those cases where a PAS is formed, paths of individual members of a particle ensemble population have been recovered from the experimental data and analyzed in depth. Though, for the majority of the particles the interactions with the flow result in that their trajectories become either stable periodic (PAS-forming) or quasi-periodic (torus-forming), see Figs. 1(a),(b) and (c), there is a number of tracers whose trajectories are quasi-stable periodic (Fig. 1(d)). Such "temporarily periodic" orbits are occasionally interrupted by sudden intermittent phase slips before they are attracted back to the periodic orbit. The type of the trajectory a particle is following depends on the physical properties of the particle. We expound the reasons why these types of orbits should be elucidated through the general mechanism of synchronization in dynamical systems [3].

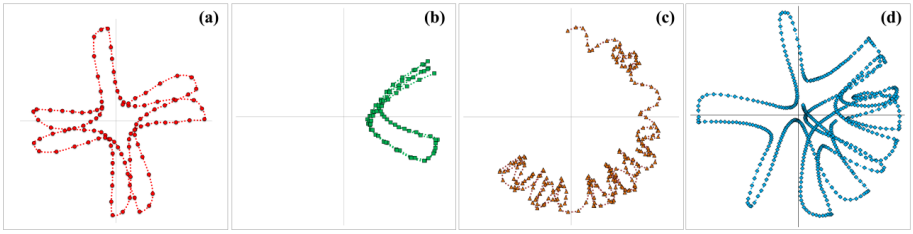

FIG. 1. Top view of single-particle trajectories reconstructed from the experiments.

[1] S. Tanaka, H. Kawamura, I. Ueno and D. Schwabe, *Flow structure and dynamical particle accumulation in thermocapillary convection in a liquid bridge*, Physics of Fluids, **18**, 067103 (2006).

[2] D. E. Melnikov, D. O. Pushkin, V. M. Shevtsova, *Synchronization of finite-size particles by a travelling wave in a cylindrical flow*, Phys. Fluids, **25**, 092108 (2013).

[3] A. Balanov, N. Janson, D. Postnov, O. Sosnovtseva, *Synchronization: From Simple to Complex (Springer Series in Synergetics)*, Springer, Berlin (2009).

Experiments on falling water films in interaction with a counter-current air flow

N. Kofman,[1] S. Mergui,[1] and C. Ruyer-Quil[2]

[1]*Univ Paris-Sud, Univ Paris 06, CNRS, Lab FAST, Bât 502, Orsay, F-91405, France,*
mergui@fast.u-psud.fr

[2]*Univ de Savoie, CNRS, Lab LOCIE, Savoie Technolac, Le Bourget du Lac, F-73376, France*

Falling liquid films flowing in the presence of a co or counter-current gas flow are commonly encountered in a number of industrial applications (cooling of microelectronic equipment, distillation columns in chemical industry, desalination designs ...). The interaction between film and gas flow results in the development of surface waves at the liquid-gas interface responsible for the onset of undesired flooding phenomena. As the optimal operating industrial conditions are generally close to the limit of flooding, it is essential to identify the relevant physical mechanisms with the aim to predict and control its occurrence. Linear stability analyses, nonlinear dynamics of the waves or modelling of two-phase channel flows have been undertaken recently in a number of studies [1, 2] (among others). Until now, very few experiments are available in the literature to quantify the effect of the gas flow on the liquid film.

In the current study, experiments are conducted on water films falling down the bottom plate of an inclined channel in the presence of a counter-current air flow. The dynamics of the film is controlled by applying a temporal forcing at inlet and we focus on the influence of the air flow on the dynamics of solitary waves, characterized by a hump region preceded by a capillary region (see Fig.1). The thickness of the film is measured using both a CCI (Confocal Chromatic Imaging) technique to obtain local temporal measurements and a Schlieren method yielding 2D topographies of the interface [3].

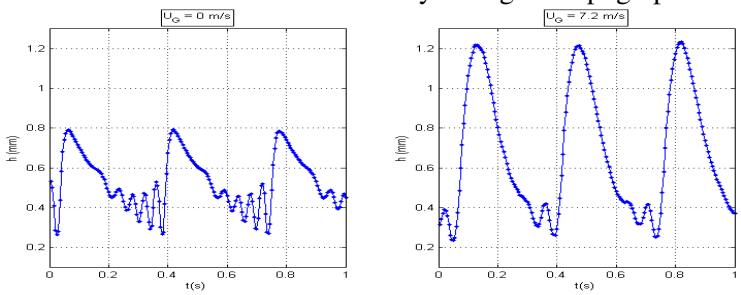

FIG. 1. Film thickness measurements using a CCI technique (time signal). Influence of the gas velocity U_G on the shape and amplitude of 2D quasi solitary waves. Re_L = 44 (related to liquid flow rate), inclination angle β = 5°, forcing frequency f = 2.8 Hz.

First, the influence of the air flow on the shape and amplitude of the 2D waves is investigated. The experiments demonstrate that, with increasing the gas velocity, the capillary region is drastically reduced and the amplitude of the main hump grows significantly even for moderate gas velocity (see Fig.1). Modifications of the wave velocity and the minimum thickness of the film are significant above a specific gas velocity (typically 3 m/s). These results corroborate existing numerical studies. We next focus on the influence of the gas velocity on 3D secondary instabilities of the solitary waves namely rugged or scallop wave patterns generated by the interplay between a short-wave and a long-wave instability mode [4]. The current study shows that the long-wave mode is enhanced by the interfacial shear while the short-wave mode is damped. At small inclination angles, waves going upstream appear for a gas velocity around 8 m/s. At high inclination angles, a rapid development of solitons is observed as the air velocity is increased, preventing flooding occurrence at least in the range of parameters under study.

[1] Y. Y. Trifonov, *Counter-current gas-liquid wavy film flow between the vertical plates analyzed using the Navier-Stokes equations*, AIChE J., **56(8)**, 1975-1987 (2010).

[2] G. Dietze, C. Ruyer-Quil, *Wavy liquid films in interaction with a confined laminar gas flow*, J. Fluid Mech., **722**, 348-393 (2013).

[3] F. Moisy, M. Rabaud, K. Salsac, *A synthetic Schlieren method for the measurement of the topography of a liquid interface*, Exp. In Fluids **46(6)**, 1021-1036 (2009).

[4] N. Kofman, S. Mergui, C. Ruyer-Quil, *Three dimensional instabilities of solitary waves in a falling liquid film*, under consideration in J. Fluid. Mech.

Flow structures in a double free-surface film with small imposed Marangoni numbers

B. Messmer,[1] T. Lemee,[1,2] K. Ikebukuro,[3] K. Edwin,[1] I. Ueno,[3] and R. Narayanan[1]

[1]*University of Florida, Gainesville FL, USA,*
bmessmer@ufl.edu
[2]*Univ Paris-Sud, Orsay, France*
[3]*Tokyo University of Science, Noda, Chiba-Prefecture, Japan*

When a temperature gradient is applied along a fluid surface, there will necessarily be a resulting flow along the interface of that fluid. This interfacial flow can result in a bulk movement of the fluid and, at high enough temperature gradients, can cause instabilities and pattern formation. The flow is referred to as thermo-capillary because it arises due to a change in surface tension with respect to temperature.

In the present work, experiments are performed on a double free-surface film in a rectangular geometry under thermo-capillary forcing. The films show two basic flow structures at low imposed temperature gradients. Infrared and CCD images of these flow structures can be seen in Figure 1. In cellular flow, the fluid leaves the hot source toward the cold wall and, upon reaching the cold wall, returns along the sides in a cellular-like structure. For the case of sheet flow, the fluid leaves the hot boundary, moves as a sheet toward the cool wall and then dips into the fluid returning to the hot source along the interior of the film.

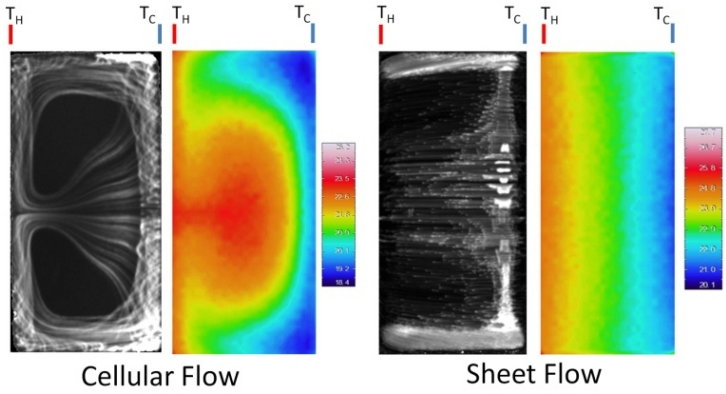

FIG. 1. Difference in flow topologies

Physical reasoning and simple scaling arguments are advanced to show that multiple flow structures arise on account of the lower velocity gradient in the direction of the imposed temperature gradient for various film geometries. This difference in velocity gradients results from inevitable surface deformations. For thin films the effect of surface deformations are magnified because of a larger interfacial-surface-area to volume ratio, whereas thicker films will show less sensitivity to deformations.

The experiment is compared to results from a restricted numerical model which captures the main features of the flow. Good agreement is observed between the experiments and the simulation.

The scientists involved in this work would like to thank the NSF PIRE grant and NASA for their financial support in this research.

On dynamic excitation of Marangoni instability of deformable liquid layer with insoluble surfactant

A. B. Mikishev[1,2] and A. A. Nepomnyashchy[3,4]

[1]*Department of Physics, Sam Houston State University, Huntsville, TX 77341,USA*
amik@shsu.edu
[2]*Embry-Riddle Aeronautical University – Worldwide, Daytona Beach, FL 32114, USA*
[3]*Department of Mathematics, Technion – Israel Institue of Technology, Haifa 32000, Israel*
[4]*Minerva Center for Nonlinear Physics of Complex Systems,*
Technion – Israel Institue of Technology, Haifa 32000, Israel
nepom@technion.ac.il

In our previous work [1] we considered the parametric excitation of Marangoni convection by a periodic flux modulation in a liquid layer with insoluble surfactant absorbed on the non-deformable free surface. Here we investigate the influence of a free surface deformation on this excitation for arbitrary wave numbers of the disturbances. The stability analysis of the convective system is performed. Three response modes of the system to an external periodic stimulation were found synchronous, subharmonic, and quasi-periodic ones. The problem contains a lot of parameters (among them the ratio of the amplitude of the external heat flux modulation to the stationary mean heat flux in the layer, δ, the frequency of the modulation, ω, the capillary number, Σ, the Galileo number, G, the Prandtl number, Pr, the Lewis number, L, the elasticity number, N, the Biot number, B). Depending on the parameters of the problem, one or another of these instability modes can be critical. Some neutral stability curves have two minimum points. Additionally to the neutral curves representing the dependence of Marangoni number on wave number (see Fig. 1) , we present graphs of Marangoni numbers depending on the Galileo number, on the external frequency of modulation and behavior of critical Marangoni numbers depending on different values of Prandtl number (for various media). The obtained numerical estimates can be used in laboratory experiments with real fluids.

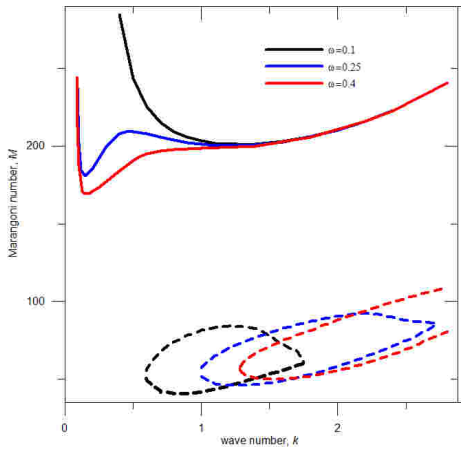

FIG. 1. Typical neutral stability curves for the case Pr = 7, L = 0.001, N = 0.1, B = 0, δ = 1, G = 1000, Σ = 100. Solid lines are for synchronous instability modes, dashed ones are for subharmonic modes. Red lines are for ω = 0.4, blue ones are for ω = 0.25, and black ones are for ω = 0.1.

Acknowledgements. AM was partially supported by research grant ERAU-13353.

[1] A. B. Mikishev, A. A. Nepomnyashchy, *Marangoni instability of a liquid layer with insoluble surfactant under heat flux modulation*, Eur. Phys. J. Special Topics, **219**, 81-88 (2013).

On locally high-frequency modulated Marangoni convection

A. B. Mikishev[1,2] and I. I. Wertgeim[3]

[1]*Department of Physics, Sam Houston State University, Huntsville, TX 77341, USA,* amik@shsu.edu

[2]*Embry-Riddle Aeronautical University-Worldwide, Daytona Beach, FL 32114, USA*

[3]*Institute of Continuous Media Mechanics of UB RAN, Perm 614013, Russia,* wertg@icmm.ru

Recent experimental observations on generation of thermocapillary flows by source of heat, localized near the free surface of a liquid [1, 2] show a variety of spatial-temporal structures near the critical value of Marangoni number. Different methods and parameters of local heating induce different types of structures. One of specific heat forcing methods is the creation of a pulsating thermal spot on the surface of the liquid. Practically this spot is easy to create using a laser beam and it can be used to control on thermocapillary flow stability effects.

Theoretical results [3, 4] contain the asymptotic analysis and numerical simulation of weakly-supercritical thermocapillary convection in deformable thin liquid layer with an inhomogeneous thermal spot, either constant in time or pulsating. Previously there were considered cases of stationary [3] and low-frequency modulated [4] localized heating. The case of high-frequency modulation was not studied in details. Our current investigation is dedicated to this case. As is generally known, modulated external heating creates a thermal skin layer closer to the surface. In case of high frequency modulation this skin layer is significantly smaller compared to the total thickness of the layer. This property provides us with a possibility to introduce a small parameter to the problem (ratio of the thermal skin layer to the thickness of the layer). That permits to use the multi-scale approach and reduce the system to 2D nonlinear equations for disturbances of temperature and distortion of the free surface.

The basic non-stationary localized solutions were found. They preserve the spatial symmetry of inhomogeneous heat flux and contain dependence on heating modulation parameters. The linear stability analysis of the periodic solutions is performed on the base of Floquet method. Nonlinear analysis in the region near the onset of Marangoni instability was performed by numerical integration of 2D nonlinear evolution system using pseudospectral method.

Acknowledgements. AM was partially supported by research grant ERAU-13353, and IW by research grant of the Russian Foundation for Basic Research No. 12-01-00608.

---

[1] A. I. Mizev, *Experimental investigation of thermocapillary convection induced by a local temperature inhomogeneity near the liquid surface. 1. Solid source of heat*, J. Appl. Mechanics and Tech. Physics, **45**, 486–497 (2004).

[2] A. I. Mizev, *Experimental investigation of thermocapillary convection induced by a local temperature inhomogeneity near the liquid surface. 2. Radiation-induced source of heat*, J. Appl. Mechanics and Tech. Physics, **45**, 699–704 (2004).

[3] S. P. Karlov, D. A. Kazenin, B. I. Myznikova, I. I. Wertgeim, *Experimental and numerical study of the Marangoni convection due to localized laser heating*, J. Non-Equilib. Thermodyn., **30**, 283–304(2005).

[4] I. I. Wertgeim, M. A. Kumachkov, A. B. Mikishev, *Periodically excited Marangoni convection in a locally heated liquid layer*, Eur. Phys. J. Special Topics, **219**, 155–165 (2013).

Influence of surfactants on thermocapillary convection on the confined interfaces

A. Mizev[1] and A. Shmyrov[1]

[1]*Institute of Continuous Media Mechanics, Ac, Korolev st. 1, Perm, Russia,*
alex_mizev@icmm.ru, shmyrov@iccm.ru

We present the results of an experimental study of thermocapillary convection induced by a localized heat source in the presence of a surfactant on the interface.

The fluid used in experiments was highly purified water (with conductivity of less than 0.2 μS). The experiments were carried out in the Langmuir trough (Fig.1 a). A final cleaning of the water surface with the help of the barriers of the Langmuir system and aspirator allows us to get "zero" surface with reproducible properties at the beginning of each experiment. The barriers were used also as movable boundaries to separate a part of the interface with a certain area. A platinum Wilhelmy plate partly immersed in water and connected to the a highly sensitive balance was used to control the surface properties at the beginning of each test. Oleic acid was used as a surfactant. Because the use of a solid heater and the application of standard methods for flow visualization (addition of trace particles) can be the source of accidental water contamination with additional impurities including surface active ones the contactless methods were used for both the heating of the interface and the visualization of a flow. Local heating of the water surface was provided by the source of IR radiation. The IR camera was used for temperature profile measurements on the water surface. The analysis of the profile measurements provides evidence for the existence or absence of the convective flow at the interface (Fig.1 b and c).

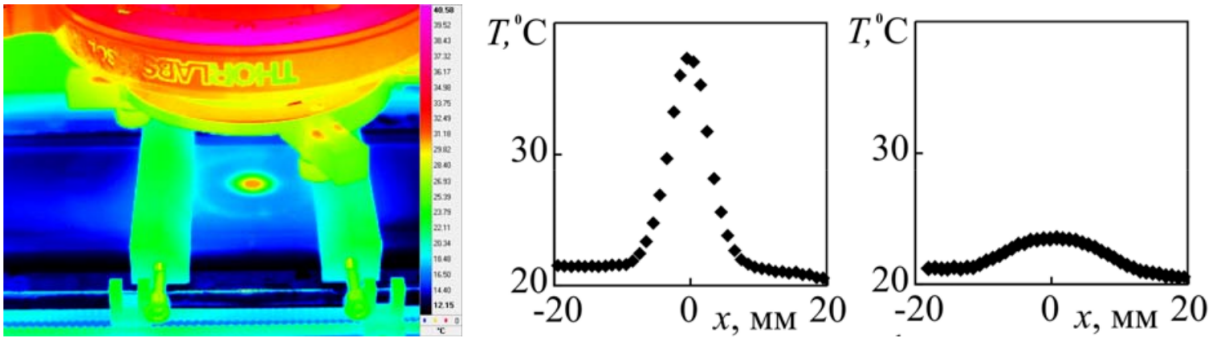

FIG. 1. The external view of the Langmuir barrier system in the IR range (a) and temperature profiles in the radial section of the hot spot in the absence (b) and in the presence (c) of thermocapillary flow.

It has been found that on the clean surface of water, which is free of any impurities, thermocapillary convection develops in the non-threshold manner irrespective of the characteristic dimension of the interface and heat source power. Addition of insoluble surfactant of even very low concentration ($\Gamma/\Gamma_m < 0.1$) to the interface essentially decreases the intensity of the convective flow and reduces the region of its existence. This influence of the surfactant increases with decreasing surface area. It has been shown that at a fixed power of the heat source and surface density of the surfactant there is a certain critical value of the surface area, at which development of the Marangoni convection becomes impossible at all. It was found out that a connection of the separated part of the surface with the surrounding interface which contains the surfactant of the same surface density via even very thin channel results in development of thermocapillary convection. Possible mechanisms of the observed phenomenon are discussed.

On instability of Marangoni convection on the surface of a surfactant solution

A. Mizev[1] and A. Trofimenko[1]

[1]*Institute of Continuous Media Mechanics, Ac, Korolev st. 1, Perm, Russia,*
alex_mizev@icmm.ru, lutsik@icmm.ru

We present the results of the experimental study of the structure and stability of an axisymmetric solutal Marangoni flow initiated at the surface of aqueous solution of a surfactant.

A similar problem was previously investigated [1] for the case of insoluble surfactant (oleic acid at the surface of water). It has been shown that the instability of the convective motion associated with breaking of the axial symmetry by the main flow and formation of the multi-vortex secondary flow is observed even for arbitrarily small amount of the surfactant at the interface. The structure of the multi-vortex flow depends on the surfactant surface concentration and Marangoni number which defines the intensity of the main flow. The mechanism governing the onset of instability has been proposed. In compliance with the approaches used by Levich [2] it is based on the redistribution of the surfactant molecules, which cannot leave the surface, by the flow that leads to appearance of additional tangential stress at the interface. A convective flow generated at the surface is the result of the balance between two tangential stresses caused by the existence of the flow source and non-uniform distribution of the adsorbed surfactant along the interface. In the case of soluble surfactant the situations becomes three-dimensional: the molecules of the surfactant can transfer from the bulk to the surface (adsorption) and revert back (desorption). On the parts of the surface where the adsorbed layer is compressed by the flow the desorption process becomes predominant. And vice verse, near the source where the surface density of the surfactant is lower than the equilibrium value, the molecules are adsorbed from the bulk phase. Thus, the adsorption-desorption mechanisms should lead to dynamically variable boundary conditions at the interface and probably to a nonstationary flow mode.

We performed experiments with water solutions of potassium acetate and potassium laurate which are two members of one homologous series. They differ in the types of kinetics of mass transfer between the bulk and surface phases which results in essential difference in the surface activity and the rates of adsorption-desorption processes. It has been found that axisymmetric Marangoni flow becomes unstable even at very low volume concentrations of surfactants. However, in contrast to the case of insoluble surfactant, a multi-vortex flow initiated at the interface of solutions is non-stationary: the number of vortices changes in a random way at some average value. It has been shown that the results of all experiments can be described with a single relationship using the degree of saturation of the monolayer with surfactant molecules as a quantitative measure of the surfactant content.

---

[1] A. Mizev, A. Trofimenko, D. Schwabe, A. Viviani, *Instability of Marangoni flow in the presence of an insoluble surfactant. Experiments*, Eur. Phys. J. Special Topics, **219**, 89–98 (2013).

[2] V. G. Levich, *Physicochemical Hydrodynamics*, Englewood Cliffs, NJ: Prentice-Hall (1962).

Dynamical stability of a liquid bridge

C. Ferrera,[1] J. M. Montanero,[1] M. A. Herrada,[2] M. Torregrosa,[3] and V. Shevtsova[3]

[1]*Department of Mechanical, Energy, and Materials Engineering, University of Extremadura, Avda. de Elvas s/n, E-06071 Badajoz, Spain*

[2]*Escuela Técnica Superior de Ingenieros, Universidad de Sevilla, Avda. de los Descubrimientos s/n, E-41092-Sevilla, Spain*

[3]*Microgravity Research Center, CP-165/62, Universite Libre de Bruxelles, 50, av. F. D. Roosevelt, B-1050 Brussels, Belgium*

A liquid bridge is a drop of liquid held by surface tension between two solid supports. It can be regarded as the simplest idealization of the configuration appearing in the floating zone technique. Its relationship with this technique endows the study of liquid bridges with great interest not only in fluid mechanics but also in the field of materials engineering. This interest explains why the liquid bridge configuration has been examined several times on board of the International Space Station (ISS) over the last few years (see, e.g., Refs. [1, 2] and references therein).

The experimental analysis of the thermocapillary flows under microgravity conditions is not an easy task. The thermal diffusion characteristic time forces the experimenter to maintain microgravity conditions for relatively long periods of time, only accessible on the ISS. One of the main risks involved in these experiments is the liquid bridge breakup due to g-jitter during both the liquid bridge formation and the course of the experiment. Owing to the centimeter size of the liquid bridge, small mass forces lead to relatively large Bond numbers, which may produce significant free surface oscillations. Because of the obvious limitations on manipulating any experiment in space, the liquid bridge breakage constitutes a tragic outcome. For this reason, it is highly desirable to know *a priori* the magnitude of the g-jitter effects that the liquid bridge can withstand without breaking.

In this contribution, we analyze the dynamical response of an isothermal liquid bridge to a step change in the mass force magnitude by numerically solving the three-dimensional Navier-Stokes equations [3]. We study the free surface oscillations caused by both axial and lateral pulses of the mass force. The values of the noise intensity (dynamical Bond number) above which the liquid bridge breaks up were determined for different liquid bridge slendernesses and volumes. This dynamical stability limit was significantly lower than the static one (i.e., the static Bond number above which the liquid bridge equilibrium shape becomes unstable). The liquid bridge was more sensitive to the lateral perturbation than to the axial one. Finally, the effects of real g-jitter on cylindrical liquid bridges with different slendernesses were analyzed.

---

[1] H. Kawamura, K. Nishino, S. Matsumoto, I. Ueno, *Report on microgravity experiments of marangoni convection aboard international space station*, J. Heat Transfer, **134**, 031005 (2012).

[2] T. Yano, K. Nishino, H. Kawamura, I. Ueno, S. Matsumoto, M. Ohnishi, M. Sakurai, *3-D ptv measurement of Marangoni convection in liquid bridge in space experiment*, Exp. Fluids, **53**, 9-20 (2012).

[3] C. Ferrera, M. A. Herrada, J. M. Montanero, M. Torregrosa, V. Shevtsova, *Dynamical response of liquid bridges to a step change in the mass force magnitude*, Phys. Fluids, in press.

Long-wave Marangoni convection in a binary-liquid layer with Soret effect and surfactant adsorption/desorption

M. Morozov,[1] A. Nepomnyashchy,[1] and A. Oron[2]

[1]*Department of Mathematics, Technion – Israel Institute of Technology, Haifa 32000, Israel,*
mmorozov@technion.ac.il, nepom@technion.ac.il

[2]*Department of Mechanical Engineering, Technion, Haifa, IL-32000, Israel,*
meroron@tx.technion.ac.il

We consider Marangoni convection in a heated layer of binary liquid. Previously, the free surface deformations and the Soret effect were incorporated into the theory. Cases of a prescribed temperature of the solid substrate [1], [2]; a prescribed heat flux at the substrate [3], [4]; and of an arbitrary heat conductivity of the substrate [5] were studied. However, in the papers mentioned above, surface tension was assumed to be a function of the temperature and the bulk concentration of the solution near the free surface. In reality, surface tension depends on the concentration of the solute molecules adsorbed at the interface. If the characteristic time of adsorption/desorption processes is small, the concentration of adsorbed molecules is nearly proportional to the bulk concentration, which leads to the model used in the papers [1–5]. Otherwise, the adsorption/desorption kinetics and advection of the adsorbed molecules along the interface have to be taken into account for determining the local value of surface tension.

The system under consideration is a binary-liquid layer lying on a solid horizontal substrate. We assume that the free surface of the layer is deformable, and the solute molecules can be adsorbed to the surface or leave it due to desorption. Molecules adsorbed at the free surface decrease surface tension; surface tension normally decreases with temperature. Convection is triggered by a given transverse temperature gradient. In the presence of the Soret effect, long-wave linear stability analysis of the quiescent state of the layer reveals a competition between monotonic and oscillatory modes of instability.

We study the system in two distinct limits: in the case of strong surface tension, and in the case of weak gravity (the mean surfactant concentration, and Galileo and Lewis numbers are assumed to be small in the latter case). Nonlinear analysis in both of these cases, brings us to the same set of long-wave evolution equations governing the dynamics of the local layer thickness and local solute concentration. Linear analysis of these equations indicates that they are applicable only in the case of oscillatory instability (just like the respective equations from [4]). We then carry out weakly nonlinear analysis in the vicinity of the oscillatory instability threshold in the case of a 2D layer, and study pattern selection. Finally, we check our theoretical predictions numerically by solving the pertinent nonlinear evolution equations using the method of lines.

This work was supported by grant of the European Union via FP7 Marie Curie scheme Grant PITN-GA-2008-214919 (MULTIFLOW).

---

[1] J. K. Bhattacharjee, *Marangoni convection in binary liquids*, Phys. Rev. E, **50**, 1198-1205 (1994).

[2] S. W. Joo, *Marangoni instabilities in liquid mixtures with Soret effects*, J. Fluid Mech., **293**, 127-145 (1995).

[3] A. Podolny, A. Oron, A. A. Nepomnyashchy,*Long-wave Marangoni instability in a binary-liquid layer with deformable interface in the presence of Soret effect: Linear theory*, Phys. Fluids, **17**, 104104 (2005).

[4] A. Podolny, A. Oron, A. A. Nepomnyashchy, *Linear and nonlinear theory of long-wave Marangoni instability with the Soret effect at finite Biot numbers*, Phys. Fluids, **18**, 054104 (2006).

[5] A. Podolny, A. Oron, A. A. Nepomnyashchy, *Long-wave Marangoni instability in a binary liquid layer on a thick solid substrate*, Phys. Rev. E, **76**, 026309 (2007).

Coalescing droplets with suspended particles in a tube creeping flow

M. Muraoka,[1] T. Kamiyama,[2] T. Wada,[3] I. Ueno,[1] and H. Mizoguchi[1]

[1]*Tokyo University of Science,2641 Yamazaki, Nodashi, Chiba, Japan,*
masa@rs.noda.tus.ac.jp, ich@rs.noda.tus.ac.jp, hm@rs.noda.tus.ac.jp
[2]*Fuji Xerox Co.,Ltd.,0-7-3, Akasaka Minatoku, Tokyo,Japan*
[3]*Takasago Thermal Engineering Co.,Ltd.,4-2-5 Surugadai Kanda Chiyodaku, Tokyo, Japan*

Coalescence phenomena of droplets in a tube creeping flow are expected to be useful for fluid handling technique, controlling chemical reaction and so on. In the case of motion of droplets with suspended particles, Drug delivery system can be cited as one of applications. Coalescence phenomena are also underlying basis on analyzing the flow of multiphase fluids through porous media. Such phenomena can be seen, for instance, in enhanced oil recovery, breaking of emulsions in porous coalescers and so on.

In this experiment, a glass tube of 2.0 mm in inner diameter, 7.0 mm in outer diameter, and 1500 mm in length is used as a test tube. Silicones oil is employed as the test fluid for the droplet. Mixture fluid of glycerol and pure water is used for a surrounding fluid in the tube flow. The density of the droplets is matched to that of the surrounding fluid by adding carbon tetrachloride. An over flow tank is used to keep the flow in the tube steady at a designated averaged velocity. The test tube is surrounded by a tank filled with a temperature-controlled water to keep the temperature of the system constant. Droplets are injected into the test tube using micro-syringes in front of inlet of the tube. Behaviors of droplets and suspended particles are monitored by a digital video camera and high speed cameras placed on a sliding stage. The motion of the stage is electrically controlled to follow the travelling droplets in the test tube. Coalescence time of two droplets is measured. The coalescence time indicates a period between the instant when relative velocity of two droplets becomes zero after their apparent contact and the instant when the coalescence takes place. The coalescence time is compared with semi-theoretical formulas obtained by reference to semi-theoretical equation by Aul R.W. et al [1]. In the formulas, resistance exerted on liquid droplet in a tube creeping flow is used [2]. When relative velocity of two droplets becomes zero after their apparent contact, clearance diameter of clearance area between droplets is also measured. Effect of change in volume concentration of the suspended particles in droplets on coalescence of droplets is discussed.

---

[1] R. W. Aul, W. L. Olbricht, J. Colloid Interface Sci., **145**,pp. 478-492 (1991).
[2] J. J. L. Higdon, G. P. Muldowney, J. Fluid Mech., **298**,pp. 193-210 (1995).

Large-amplitude Marangoni convection in a binary liquid

S. Shklyaev,[1] A. A. Nepomnyashchy,[2] and A. Ivantsov[1]

[1]*Institute of Continuous Media Mechanics, UB RAS, 614013 Perm, Russia*
[2]*Technion – Israel Institute of Technology, 32000 Haifa, Israel,*
nepom@techunix.technion.ac.il

Longwave convection in a layer of a binary liquid was analyzed in [1]: both monotonic and oscillatory modes were found and studied. Finite-amplitude regimes were investigated for small supercriticality (small deviation of the Marangoni number from the stability threshold): the perturbations of temperature and concentration were finite, whereas typical convective velocity was small. For the monotonic mode the dynamics is governed by a nonlinear partial differential equation; for the oscillatory mode the amplitude equations are nonlocal, the nonlinear evolution is determined by the solvability conditions for a certain linear nonhomogeneous problem.

For the monotonic instability the competition of two modes with the critical wavenumbers proportional to $B^{1/2}$ and $B^{1/4}$ was found [2] with B being the Biot number governing the heat flux from the free surface. While the latter mode is conventional, the former one is inherent to the convection in a binary liquid only. Nonlinear dynamics for this mode was studied recently in [3].

We consider a large-amplitude convection at finite supercriticality (finite deviation of the Marangoni number from the stability threshold), when the perturbations of the temperature and solute concentration are large, whereas the longitudinal components of the velocity are finite. The characteristic horizontal lengthscale is proportional to $B^{-1/2}$. The set of two partial differential equations is derived under those assumptions; it is valid for both monotonic and oscillatory instabilities. Nonlinear terms are cubic, neither quadratic nor higher order terms contribute to these amplitude equations. This set of equations coincides up to the rescaling with the set of equations derived within the restitution procedure (see [4] for the buoyancy convection). In the limit of small supercriticality it matches the appropriate limit of the prior studies [3, 5]. In particular, for the oscillatory mode alternating rolls are selected, whereas for the monotonic mode both squares and hexagons are stable. It is worth noting that the selection between up- and down- hexagons and triangles can be performed only accounting for the quintic nonlinearity within the above-mentioned set of equations.

We also performed numerical simulations for one-dimensional monotonic mode. Steady solutions of a fixed spatial period are found and their stability is studied, including the stability with respect to the perturbations with incommensurable wavenumbers. The so-called Busse balloons—domains of stability of perfectly periodic solutions—are plotted.

A.I. and S.Sh. is partially supported within the grant of RFBR N 14-01-96027a.

---

[1] A. Oron, A. A. Nepomnyashchy, *Long-wavelength thermocapillary instability with the Soret effect*, Phys. Rev. E, **69**, 016313 (2004).

[2] A. Podolny, A. Oron, A. A. Nepomnyashchy, *Long-wave Marangoni instability in a binary-liquid layer with deformable interface in the presence of Soret effect: Linear theory*, Phys. Fluids, **17**, 104104 (2005).

[3] S. Shklyaev, A. A. Nepomnyashchy, *Longwave Marangoni convection in a binary liquid layer heated from above: Weakly nonlinear analysis*, Fluid Dyn. Res. (2014) (submitted for publication).

[4] T. Clune, M. C. Depassier, E. Knobloch, *Long wavelength oscillatory instability in binary fluids*, in Instabilities and Nonequilibrium Structures V, eds. E. Tirapegui and W. Zeller, 75–84, Kluwer Acdemic Publishers, Dordrecht (1996).

[5] S. Shklyaev, A. A. Nepomnyashchy, A. Oron, *Oscillatory longwave Marangoni convection in a binary liquid: Rhombic Patterns*, SIAP, **73**, 2203–2223 (2013).

Dynamics of thin liquid films controlled by thermal fluctuations

S. Nesic,[1] R. Cuerno,[1] E. Moro,[1] and L. Kondic[2]

[1]*Grupo Interdisciplinar de Sistemas Complejos (GISC) and Departamento de Matemáticas, Universidad Carlos III de Madrid, Avenida de la Universidad 30, E-28911 Leganés, Spain,* snesic@math.uc3m.es

[2]*Department of Mathematical Sciences, New Jersey Institute of Technology, Newark, New Jersey, United States*

In the presence of thermal fluctuations the dynamics of a thin fluid film is given by the equation [1, 2]

$$\frac{\partial h}{\partial t} = \nabla \cdot \left(h^3 \nabla\, p\right) \,+\, \sqrt{2\sigma}\,\nabla \left[h^{3/2}\epsilon(x,t)\right],$$

where p is the generalized pressure term accounting for the effects of surface tension, gravity, and van der Waals (vdW) attraction. The second term on the RHS represents thermal fluctuations, where ϵ is a zero-mean white noise. In the case of complete wetting in two dimensions ($2D$), the droplet width ℓ [see fig. 1(a)] obeys Tanner's law [3], $\ell \sim t^{1/7}$. When thermal fluctuations are considered and in the absence of gravity and vdW attraction, the stochastic force takes over the dynamics of the system and introduces a new enhanced spreading law, $\ell \sim t^{1/4}$ [1].

Motivated by this important result we present simulations of the $1D$ equation using a finite-difference scheme [4]. We show that the same enhanced spreading law holds in gravity-dominated systems. Meanwhile, the interplay of vdW and surface tension forces introduces a finite contact angle [5, 6]. We show that [see fig. 1(b)] on average there is a small change in the droplet width in the region where the latter has saturated, when the noise is introduced. In general, fluctuations combined with surface tension tend to smear out the droplet which is leading to a small correction in the Young-Laplace condition.

Finally we study the problem of dewetting in the presence of fluctuations. Specifically in $2D$, fluctuations accelerate breakup when a flat thin film is slightly perturbed [2, 6]. The final aim of our work is the study of the dynamics of such films in more realistic $3D$ setups [7], where deterministic approach may fail to reproduce the time scales and the shapes experimentally observed.

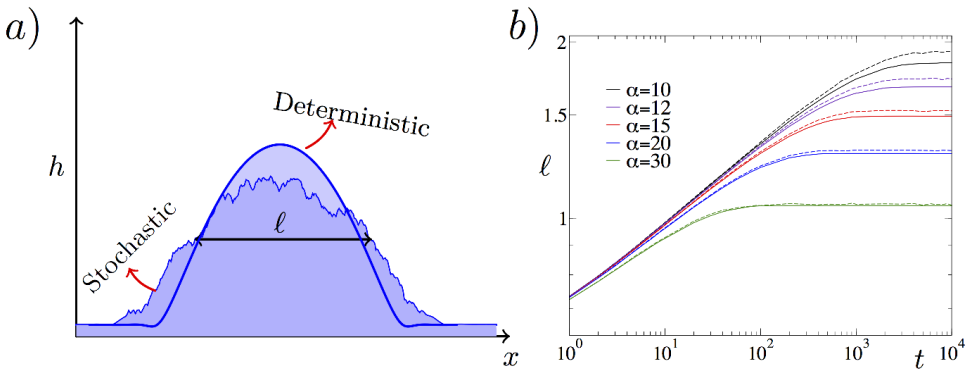

FIG. 1. a) Stochastic and deterministic droplet surface. b) Width of a droplet as a function of time for a given contact angle. Dashed lines represent stochastic films while continuous lines represent deterministic films.

[1] B. Davidovitch, E. Moro, H. Stone, Phys. Rev. Lett., **95**, 244505 (2005).
[2] G. Grun, K. Mecke, M. Rauscher, J. Stat. Phys., **122**, 1261 (2006).
[3] L. Tanner, J. Phys. D, **95**, 1473 (1979).
[4] J. A. Diez, L. Kondic, A. Bertozzi, Phys. Rev. E, **63**, 011208 (2000).
[5] D. Bonn, J. Eggers, J. Indokeu, J. Meunier, E. Rolley, Rev. Mod. Phys., **81**, 0034 (2009).
[6] J. A. Diez, L. Kondic, Phys. Fluids, **19**, 072107 (2007).
[7] A. G. Gonzlez, J. A. Diez, Y. Wu, J. D. Fowlkes, P. D. Rack, L. Kondic, Langumir, **29**, 2378 (2013).

Convective/capillary deposition of charged nanoparticles directed by receding contact lines: effect of collective diffusion and hydration forces.

D. Noguera-Marin,[1] C. L. Moraila-Martinez,[1]
M. A. Cabrerizo-Vilchez,[1] and M. A. Rodriguez-Valverde[1]

[1]*Biocolloid and Fluid Physics Group, Applied Physics Department, Faculty of Sciences, University of Granada, E-18071 Granada (Spain).*
dnogue@ugr.es, marodri@ugr.es

A better control of colloidal assembly by convective deposition is particularly helpful for nanolithography, particle templating and design of "smart surfaces". However, knowledge about the different factors that can alter colloidal patterning mechanisms is still insufficient. It is well established that, inside evaporating sessile drops, an outward convective flow is created due to the liquid loss at the contact line where the evaporation rate is divergent [1]. On the other hand, the motion of electrically charged particles in confined regions and subjected to an evaporation-driven capillary flow might be ruled by collective diffusion rather than self-diffusion. When the local gradient of particle concentration increases, the Ficks law establishes that an inward flow is created by particle cooperative diffusion. In absence of other signicant flows of different origin, the competition between both convective and diffusive flows might dictate the final deposit shape [4]. In this work, we examined experimentally the role of the collective diffusion of charge-stabilized nanoparticles in the convective deposition. We performed sessile drop experiments using the controlled shrinking sessile drop method [3] where the receding contact line is guided to emulate the contact line dynamics of a free evaporating drop. Moreover, to decouple the sustained evaporation from the contact line motion, we used a set-up similar to the dip-coating technique based on a meniscus formed between two parallel substrates and driven by pumping out of the reservoir liquid [2]. For each method, we fixed the receding contact line velocity and the nanoparticle concentration, and we explored a variety of substrate-particle systems where the particle-particle electrostatic interaction was changed (via pH) as well as the relative humidity and the receding contact angle using different smooth substrates: glass, PMMA, and Titanium oxide. To test the relevance of hydrophobic/hydrophilic forces in the morphology of nanoparticle deposits we used particles with different polar character. We found that when the evaporation flow is weak, deposition can be suppressed if the long-range interparticle repulsion becomes important and the diffusion overcomes the particle transport by convection before reaching the triple line. Furthermore, using PMMA particles, it is possible to enhance the particle deposition by hydrophobic forces, regardless of the substrate contact angle.

---

[1] R. D. Deegan, O. Bakajin, T. F. Dupont, G. Huber, S. R. Nagel, T. A. Witten, *Capillary flow as the cause of ring stains from dried liquid drops*, Nature, vol.**389**, 827-829 (1777).

[2] H. Bodiguel, F. Doumenc, B. Guerrier, *Stick-Slip Patterning at Low Capillary Numbers for an Evaporating Colloidal Suspension*, Langmuir, vol.**26(13)**, 10758-10763 (2010).

[3] C. L. Moraila-Martínez, M. A. Cabrerizo-Vílchez, M. A. Rodríguez-Valverde, *The role of the electrostatic double layer interactions in the formation of nanoparticle ring-like deposits at driven receding contact lines*, Soft Matter, vol.**9(5)**, 1664–1673 (2013).

[4] D. Noguera-Marin, C. L. Moraila-Martínez, M. A. Cabrerizo-Vílchez, M. A. Rodríguez-Valverde, *Impact of the collective diffusion of charged nanoparticles in the convective/capillary deposition directed by receding contact lines*, Soft Matter, submitted.

An index for evaluating the wettability alteration of reservoir rock toward more water wet condition by combined low salinity water and surfactant flooding

M. Nourani,[1] T. Tichelcamp,[1] and G. Øye[1]

[1]*Ugelstad Laboratory, Department of Chemical Engineering, Norwegian University of Science and Technology (NTNU) Kjemiblokk V, Sem Sælandsvei 4, NTNU Gløshaugen Trondheim, Norway,*
meysam.nourani@ntnu.no

The efficiency of surfactant flooding methods in enhanced oil recovery (EOR) is often related to the reduction of oil/water interfacial tension (IFT), while wettability changes of the reservoir rock from oil wet to more water wet conditions are considered to play an important role in microscopic oil displacement. As most oil reservoirs are inhomogeneous and consist of layers of different rock types, it might in practice be difficult to nominate a proper surfactant blend to a given reservoir.

The wettability of solid surfaces can be compared by measuring liquid/liquid/solid or air/liquid/solid contact angles. The theoretically derived relationships between air-water, oil-water, and air-oil contact angles have been experimentally verified for diverse surfaces recently. [1, 2] In this study, an index for evaluating the wettability alteration toward more water wet conditions by applying combined low salinity water and surfactant flooding is presented. The index is obtained by intercept analysis of linear relationships between the cosines of air/water ($\cos\theta_{aw}$) and oil/water ($\cos\theta_{ow}$) contact angles at $\cos\theta_{ow} = -1$. The contact angles were measured after ageing the silicone dioxide crystal with one of four different crude oils and after applying a low salinity surfactant solution flood. The proposed theoretically and experimentally based index may help designing suitable insensitive surfactant formulations to the rock types, while the needed interfacial and surface tension data are all easy to measure.

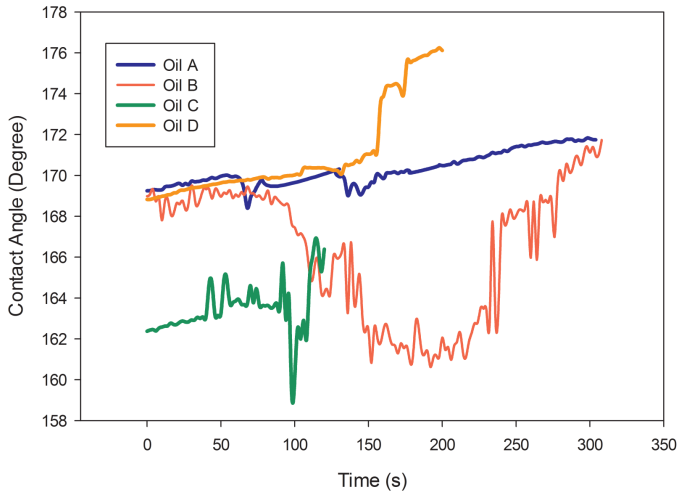

FIG. 1. Dynamic contact angle-aged oils ABCD-High Sal.-Low Sal/1000 ppm SDBS.

[1] J. W. Grate, K. J. Dehoff, M. G. Warner, J. W. Pittman, T. W. Wietsma, C. Zhang, M. Oostrom, *Correlation of Oil-Water and Air-Water Contact Angles of Diverse*, Langmuir, **28**, 7182 – 7188, (2012).

[2] M. I. J. van Dijke, K. S. J. Sorbie, *The relation between interfacial tensions and wettability in three-phase systems: consequences for pore occupancy and relative permeability*, Pet. Sci. Eng., **33**, 39 – 48, (2002).

Healing of an axisymmetric thin liquid film on a harmonically oscillating horizontal cylindrical surface

O. Haimovich[1] and A. Oron[1]

[1]*Department of Mechanical Engineering, Technion, Haifa, IL-32000, Israel,*
orivich@tx.technion.ac.il, meroron@tx.technion.ac.il

Investigation of the nonlinear dynamics of a thin axisymmetric liquid film on a horizontal circular cylinder subjected to harmonic axial oscillation was recently carried out in the cases of both isothermal[1] and non-isothermal[2] harmonic forcing, and that of the double-frequency isothermal forcing[3]. These theories were based on the assumptions of the long-wave theory[4]. It was found that it is possible to arrest the capillary long-time film rupture typical to the case of a static cylinder, if the substrate is forced with a sufficiently high amplitude and/or frequency. The critical curve demarcating between the ruptured and non-ruptured regimes of the system is determined by the value of the product of the dimensionless amplitude and frequency of forcing and whether this value is smaller or larger than a critical constant depending solely on the liquid properties and the geometrical parameter. Recently, Rohlfs *et al.*[5] showed the existence of such critical curve based on direct numerical simulations of Navier-Stokes equations.

In this research, based on the long-wave theory[4]. we extend the study to the case where the chosen initial condition are characterized by a large amplitude compared with the initial mean film thickness, The initial conditions for the numerical simulations are obtained from various states of a corresponding unforced system on its path to rupture, which yield patterns of large-amplitude droplets. We find that near-rupture configuration of the film may be healed by applying harmonic forcing of the substrate with a sufficiently large forcing amplitude. We also reveal that for large forcing delay times the critical forcing amplitude is well correlated with the linear combination of the inverse and squared inverse dimensionless forcing frequencies.

We have shown that for saturated flows the minimal film thickness oscillates around the same non-zero value, as long as the film rupture does not take place for fixed forcing and geometrical parameters for several different types of initial conditions. Therefore, axial harmonic forcing is thus proposed as a mechanism for healing thin axisymmetric liquid films placed on a horizontal cylindrical surface even for their near-rupture configurations that result from the film evolution on a static surface starting from a nearly uniform coating.

The research was partially supported by the European Union via the FP7 Marie Curie scheme [PITN-GA-2008-214919 (MULTIFLOW)] and by the Jewish Communities of Germany Research Fund.

---

[1] O. Haimovich, A. Oron, Phys. Fluids, **22**, pp. 032101-1-032101-14, 2010.
[2] O. Haimovich, A. Oron, Phys. Rev. E, **84**, pp.061605-1-061605-9, 2011.
[3] O. Haimovich, A. Oron, Phys. Rev. E, **87**, pp.052403-1-052403-11, 2013.
[4] A. Oron, S. H. Davis, S. G. Bankoff, Rev. Mod. Phys., **69**, pp. 931-980, 1997.
[5] W. Rohlfs, M. Binz, R. Kneer, Phys. Fluids, in press, 2014.

Rupture of liquid film placed on solid substrate and on deep liquid under action of thermal beam

A. Ovcharova[1] and N. Stankous[2]

[1]*Lavrentyev Institute of Hydrodynamics SB RAS, Novosibirsk, Russia,*
ovcharova@hydro.nsc.ru

[2]*National University, La Jolla, CA, 92037, USA,*
nstankous@nu.edu

We investigate a film rupture and a liquid flow pattern at the film which occur under action of a thermal beam on the film free surface. We consider the cases when the film is placed on the solid substrate and on the deep liquid and make a comparison of the flow characteristics under identical thermal load. The film has length L and thickness h_0 . At initial moment of time the film is in the rest. We also assume that the deep liquid is motionless and it does not affect any process in the film. In order to investigate those processes, the two-dimensional mathematical model based on the Navier-Stokes equations in the variables ψ (stream function) and ω (vorticity) was applied.

The action of the thermal beam is modeled as the prescribed temperature on the film-gas free surface in the form: $\theta(x,t) = \theta^*$, if $L/2 - mh_0 \le x \le L/2 + mh_0$. At the rest of the film surface $\theta(x,t) = 0$. On the lower boundary of the film $\partial\theta/\partial n = 0$. Here, m is a positive number which determines the width of the thermal beam acting on the free surface of the film. To reveal the character of the film rupture we performed computational investigations using parameters $Re = 1$; $Ca = 0.025$; $Mn = 15$;

$Pr = 1$. The ratio of the film length to its thickness $L/h_0 = 90$, $m = 3$, that means that the width of the thermal beam $d = 6h_0$. The boundary conditions on the lower boundary for the film placed on the solid substrate are nonslip conditions; for the film placed on deep liquid they are: $\psi = 0$, $\omega = kMn\partial\theta/\partial s$. A detailed derivation of those conditions can be found in [1].

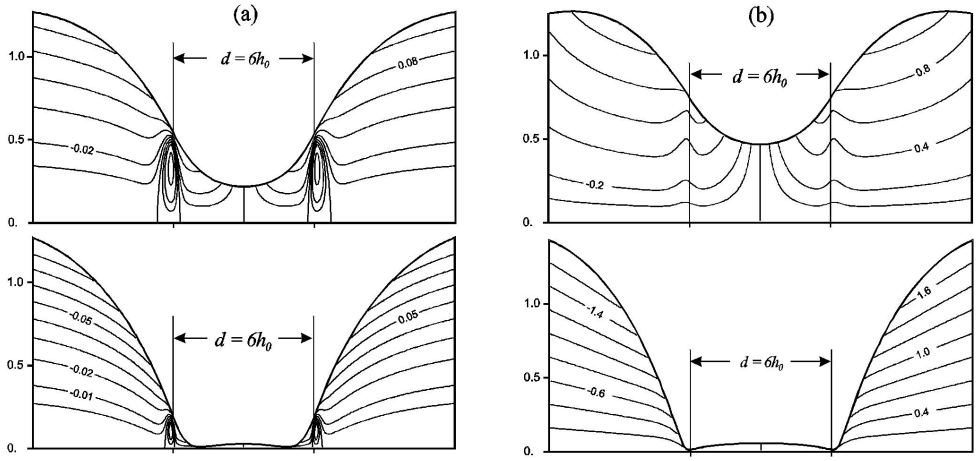

FIG. 1. Evolution of the flow and the rupture of the film at $\theta^* = 0.25$. (a): the pattern of the flow in the film placed on solid substrate; the dimensionless lifetime of the film is $t^* = 35.3$. (b): the pattern of the flow in the film placed on deep liquid; the dimensionless lifetime of the film is $t^* = 4.5$, $k = 0.5$

The investigations have shown essential distinctions in the film flow pattern and the lifetime of the film depending on the conditions by the lower boundary of the film even under identical thermal load.

[1] A. S. Ovcharova, *Features of the Behavior of a Liquid Film Heated from Above and Placed over Deep Liquid*, J. Comput. Mathem. and Mathem. Phys., vol. **53** No. **12**, 1900–1907 (2013)

Marangoni instability driving motion, deformation and fission of an oil drop on a surfactant solution

J. Irvoas,[1] K. Eckert,[2] K. Schwarzenberger,[2] C. Antoine,[3] M. Brost,[1] and V. Pimienta[1]

[1]*Université de Toulouse, UPS, IMRCP, 118 route de Narbonne, F-31062 Toulouse,*
pimienta@chimie.ups-tlse.fr

[2]*Technische Universität Dresden, Institute for Fluid Mechanics, D-01062 Dresden, Germany*

[3]*LPTMC,Université Pierre et Marie Curie, 4place Jussieu, 75005 Paris, France*

Surface tension or buoyancy-driven instabilities are at the origin of shape modifications and motion of drops. They result from the coupling of physico-chemical processes among which evaporation, solubilization, solute transfer, surfactant adsorption, aggregation and chemical reactions are the most frequent. Desired processes can be selected by the choice of chemicals and experimental conditions.

A dichloromethane droplet deposited on a CTAB solution shows a remarkable succession of regimes controlled by the concentration of surfactant. The diagram in Figure 1 shows a variety of complex drop shapes and dynamics that we identified to be the most characteristic ones. The evolution of the dynamics with surfactant concentration reveals three main types of spatio-temporal regimes. At low surfactant concentration, they are related to spreading and dewetting. A film, arising from the droplet, spreads on the water surface and induces steady or pulsating radial spreading, oscillatory and circular motion. Dewetting (i.e. break-up of the oil film at the water surface) appears through the observation of rings and lines of droplets emitted from the edge of the film as in the Rayleigh-Plateau instability. At intermediate concentrations, rotational motion becomes predominant. The drop transforms into an elongated structure with two or sometimes three or four sharp tips emitting smaller droplets reminiscent of tip streaming. At the highest concentration, dichloromethane drops have a polygonal rim featuring several small tips. These tips move erratically along the drop boundary and mediate changes in its shape. A single small droplet is ejected in the radial direction when two tips collide.

Special attention has been paid to the induction period. We have analyzed its duration as a fonction of surfactant concentration and volume of the drop. PIV experiments have shown that convective flows are generated around the drop and that the direction of convective cells is inversed during this phase. This effect is correlated to the evolution of the drop shape (contact angle, higth and diameter). Surface thermography has been used in order to evaluate the contribution of thermal effects.

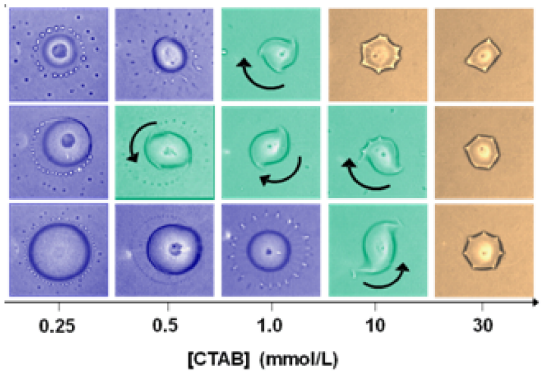

FIG. 1. Qualitative description of the drop evolution in the CH2Cl2/CTAB system at five different concentrations of the surfactant CTAB. The time axis is not to scale as the diagram emphasizes distinct, successive states in the drop evolution. Blue: spreading/dewetting; green: rotation; orange: polygonal regime.

[1] V. Pimienta, M. Brost, N. Kovalchuk, S. Bresch, O. Steinbock, Angew, Chem. Int., **Ed 50**, 10728 (2011).

Non-negligible Marangoni part in convective transport of heavy vapor from a highly volatile pendant droplet on a wafer

A. Rednikov,[1] S. Dehaeck,[1] and P. Colinet[1]
[1]*TIPs, ULB, CP 165/67, 1050 Brussels, Belgium,*
aredniko@ulb.ac.be

In our recent paper [1], we have shown how a modern refinement of digital holographic interferometry can lead to reliable quantitative characterization of evaporating droplets. This most notably includes measurements of the vapor concentration field around the droplet and of the local-evaporation-rate and temperature distributions along the droplet interface. The study has been carried out in the ambient atmosphere for a pendant droplet (axisymmetic, freely receding, initial contact radius $R_c \sim 2\,\mathrm{mm}$, contact angle $\sim 35^\circ$) of the 3M$^{\text{TM}}$ Novec$^{\text{TM}}$ HFE-7000 liquid deposited on the lower face of a flat silicon wafer (pendant counterpart of a sessile droplet). HFE-7000 is a highly volatile liquid (saturation pressure $\sim 0.6\,\mathrm{atm}$ at room temperature) with a large molecular weight ($200\,\mathrm{g/mol}$). Under such circumstances, the gas-phase Grashof number Gr is estimated at $Gr \sim 10^3$ and thus an essential buoyancy-driven convection is expected. This is what is observed in the measured form of the vapor cloud, shown in fig. 1(left), with a plume along the symmetry axis. Clearly, the evaporation rate is thereby increased as compared to the corresponding pure diffusion regime (by about 4 times globally, as revealed by the measurements). Furthermore, this also leads to an essential temperature fall at the droplet interface, as represented in fig. 1(center), even if the silicon-substrate temperature is shown not to significantly deviate from the ambient one. A full modeling of the problem is currently not available. However, in order to facilitate the interpretation of the experimental results, various kinds of partial modeling (viz. adopting certain data from the experiment to carry out the computations) have been undertaken in [1], which will be the focus of this presentation. In particular, adopting the interfacial temperature (and hence the interfacial vapor concentration, related to the former with the help of the known saturation pressure data) from the experiment, an axisymmetric and quasi-stationary (at each moment during the droplet evaporation) problem for the buoyancy convection in the gas phase is resolved numerically, as well as that for the Marangoni flow inside the droplet. We note that the problem in the gas is treated in the boundary-layer approximation (large Gr limit) in the framework of a non-Boussinesq formulation (the density and other properties vary significantly). Quite surprisingly, the Marangoni velocity, see fig. 1(right), proves to be so large that it is comparable with the buoyancy-induced velocity in the gas. Accounting for the Marangoni velocity when modeling the gas flow brings to higher evaporation rates (by $\sim 30\%$ in terms of the global ones) and to a better agreement with the measurements.

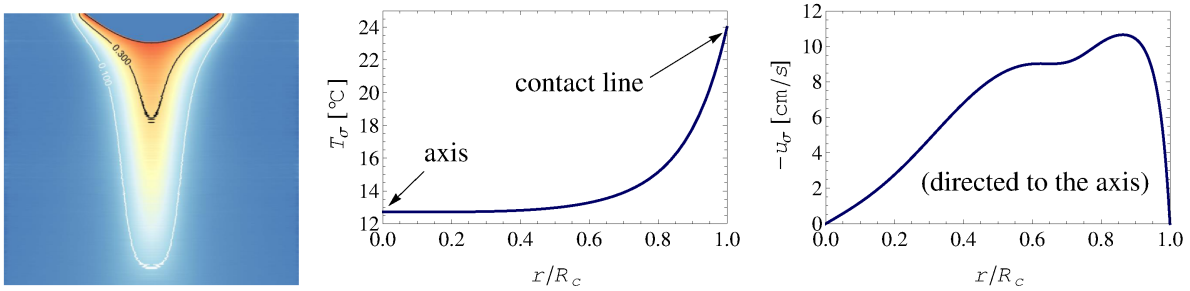

FIG. 1. Left: Measured vapor cloud (molar fraction); Center: Fitting (adopted in the computations) of the measured interfacial temperature distribution extrapolated to the ambient temperature at the contact line for $R_c = 1.81\,\mathrm{mm}$ (r distance to the axis); Right: Computed tangential Marangoni velocity at the droplet interface for $R_c = 1.81\,\mathrm{mm}$.

[1] S. Dehaeck, A. Ye. Rednikov and P. Colinet, *Vapour-based interferometric measurement of local evaporation rate and interfacial temperature of evaporating droplets*, Langmuir, Accepted (2014).

Drop coalescence and drop shape: influence of Marangoni flows

S. Karpitschka[1] and H. Riegler[1]

[1]*MPI for Colloids and Interface, Am Mühlenberg, D-14476 Potsdam, Germany.*

Surface tension gradients due to locally different surface compositions can induce Marangoni flows. These can have dramatic effects on the coalescence behavior of sessile drops consisting of different (miscible) liquids. Analogous effects are also observed if single drops consist of mixtures of liquids with different volatilities because the nonuniform evaporation/adsorption of drops can also create substantial local surficial composition gradients.

We present an overview on recent experimental data and the theoretical analysis on this topic.

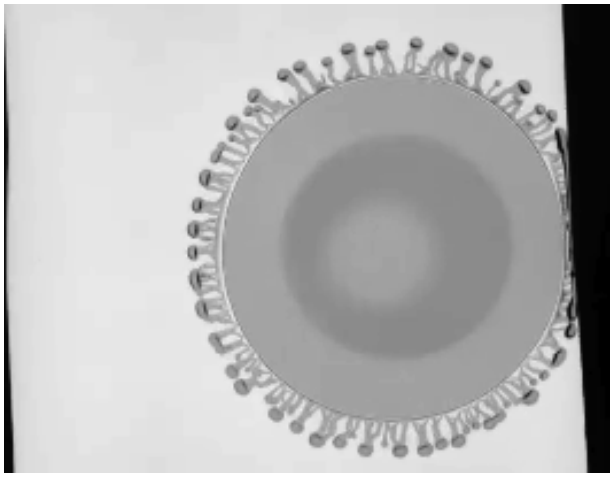

FIG. 1. Top view of a sessile drop with a mixture of components with different volatilities and surface tensions. Satellite droplets appear if evaporation sufficiently enriches one liquid component close to the contact line. The local surface tension gradient eventually can destabilize the drop perimeter.

[1] S. Karpitschka, H. Riegler, *Quantitative Experimental Study on the Transition between Fast and Delayed Coalescence of Sessile Droplets with Different but Completely Miscible Liquids*, Langmuir, **26**, 11823–11829 (2010).

[2] R. Borcia, S. Menzel, M. Bestehorn, S. Karpitschka, H. Riegler, *Delayed coalescence of droplets with miscible liquids: Lubrication and phase field theories*, Eur. Phys. J. E, **34**, 24 (2011)

[3] S. Karpitschka, H. Riegler, *Noncoalescence of Sessile Drops from Different but Miscible Liquids: Hydrodynamic Analysis of the Twin Drop Contour as a Self-Stabilizing Traveling Wave*, Phys. Rev. Lett, **109**, 066103 (2012).

[4] S. Karpitschka and H. Riegler, *Sharp Transition between Coalescence and Noncoalescence of Sessile Drops: Interplay between Marangoni Flow and Local Topography*, Submitted to J. Fluid Mech.

[5] S. Karpitschka, C. Hanske, A. Fery, H. Riegler, *Coalescence and Noncoalescence of Sessile Drops: Impact of Surface Forces*, submitted to Langmuir.

Thermally induced break-up of regularly excited three-dimensional surface waves on a vertical liquid film

M. Rietz,[1] W. Rohlfs,[1] and R. Kneer[1]

[1]*Institute of Heat and Mass Transfer, RWTH Aachen University, Augustinerbach 6, 52056 Aachen, Germany*

rohlfs@wsa.rwth-aachen.de

The wave topology of falling liquid films under non-isothermal conditions is strongly influenced by the presence of thermo-capillary (Marangoni) forces at the interface which leads to destabilization of the film flow and to appearance of rivulets, as presented in [1, 2]. As a consequence, film rupture might occur, possibly damaging the heater or temperature sensitive fluids. Previous experimental studies by the authors have focused on the investigation of the surface topology of regularly excited surface waves influenced by the presence of thermo-capillary and electrostatic surface forces [3, 4], showing an unstable behavior of the three-dimensional waves. In order to gain more insights in the break-up mechanisms for the case of non-isothermal conditions, additional information on the distribution of the surface temperature is required. Therefore, the present study extends the previous investigations by providing additional thermal images of the wavy surface as well as extended measurements of the film thickness development. The employed measurement setup enables the excitation of regular three-dimensional surface waves on a vertical falling liquid film. This is realized by way of an upstream loudspeaker, imposing a constant streamwise wavelength and equidistant needles which impose a spanwise wavelength. A copper plate is mounted in the hydrodynamically established region, where a wall side heat flux is imposed through embedded heating cartridges. Using this setup, different film flow regimes, e.g. solitary waves ($Re = 4.5; f = 12\mathrm{H}z$) and sinusodial ($Re = 6; f = 18\mathrm{H}z$) are investigated by means of their response to thermo-capillary forces. Film thickness measurements were performed by the confocal-chromatic imaging technique and surface temperature distributions have been visualized by IR-thermography. Due to the good repeatability of the excited surface waves, three-dimensional images of the film topology where reconstructed from pointwise measurements. Combining the film thickness and surface temperature information (see. Fig. 1) interactions of hydrodynamics and thermo-capillary forces are revealed. These include among others the formation of rivulets, critical film thinning and period doubling in spanwise direction.

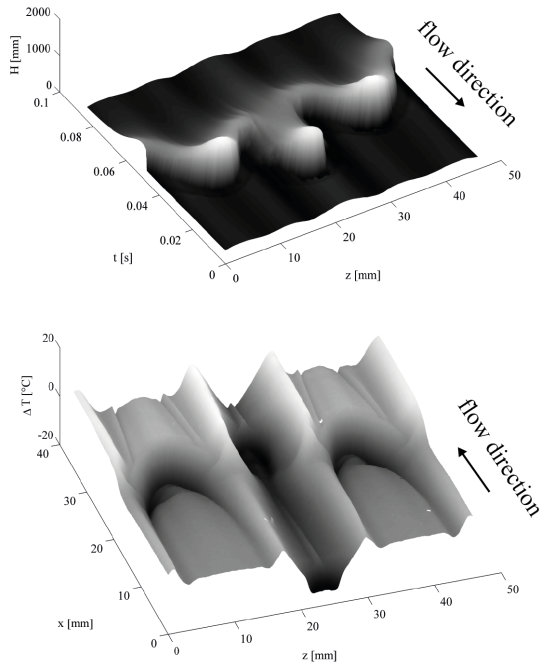

FIG. 1. Surface topology (top) and surface temperature (bottom) of the liquid film for Re=4.5; f=12Hz

[1] B. Scheid, S. Kalliadasis, C. Ruyer-Quil, P. Colinet, Phys. Rev. E, **78**, 066311, 2008.

[2] V. V. Lel, A. Kellermann, G. Dietze, R. Kneer, A. N. Pavlenko, Exp. Fl., **44 (2)**, pp. 341-354, 2008.

[3] W. Rohlfs, G. F. Dietze, H. D. Haustein, O. Y. Tsvelodub, R. Kneer, Exp. Fl., **53**, pp. 1045-1056, 2012.

[4] W. Rohlfs, G. F. Dietze, H. D. Haustein, R. Kneer, Eur. Phys. J. ST, **219**, pp. 111-119, 2013.

Oscillatory Marangoni instability in thin film heated from below

A. E. Samoilova[1] and N. I. Lobov[1]

[1]*Department of Theoretical Physics, Perm State University, Bukirev str. 15, 614990 Perm, Russia,*
annsomeoil@gmail.com

We consider the classic problem of the Marangoni convection in a liquid layer with a deformable free surface atop a substrate heated from below. Substrate is assumed to be insulated for perturbations: a normal component of the heat flux is fixed there. We suppose that the unperturbed layer thickness is so small that the buoyancy is neglected but not too small and the free surface deformation is important. The linear stability analysis is performed numerically in order to extend the recent asymptotic results [1] to finite wavenumbers of perturbations.

Since the pioneering work of Pearson [2] the detailed analysis of the Marangoni convection was provided by many researchers. However, first in [1] it was found that the longwave oscillatory mode is critical for heating from below within a certain range of parameters. Namely, it is possible when the capillary number is high and the Biot number, which characterizes the heat flux from the free surface, is small keeping their product finite. Additionally, the Galileo number is not too large. We have confirmed the existence of this novel oscillatory mode. The neutral stability curve for the monotonic mode is derived, whereas the oscillatory mode is examined numerically. Numerical simulations indicate that the oscillatory instability occurs in a wider range of problem parameters than it is predicted within the asymptotic analysis.

For a sake of simplicity in a single layer computations we use the Newton law of cooling that governs the heat flux from the free surface. This assumption does not allow one to reproduce the experimental conditions in a realistic manner. Besides it is well known that such a boundary condition can even lead to wrong results, see e.g. [3]. Thus, we additionally consider the longwave Marangoni instability of liquid-gas system with a deformable interface. The liquid layer is atop a substrate of a finite thickness of low but finite thermal conductivity; the substrate is heated from below. The gas layer is sufficiently thick; the viscosity and the density of the gas are small, but the heat conduction there is of importance. Assuming the capillary number is high we derive a set of the amplitude equations similar to that obtained in [1]. Linear stability analysis within this set demonstrates the emergence of the oscillatory mode.

Dealing with this liquid-gas system we succeed in realistic estimates for possible future experiments where the novel oscillatory mode would found.

The work is supported by the Russian Foundation for Basic Research (Grant No. 14-01-00148).

---

[1] S. Shklyaev, M. Khenner, A. A. Alabuzhev, *Long-wave Marangoni convection in a thin film heated from below*, Phys. Rev. E, **85**, 016328 (2012)

[2] J. R. A. Pearson, *On convection cells induced by surface tension*, J. Fluid Mech. 4, 489–500 (1958)

[3] A. A. Golovin, A. A. Nepomnyashchy, L. M. Pismen, *Pattern formation in large-scale Marangoni convection with deformable interface*, Physica D, **81**, 117–147(1995)

How to deal with negative surface heat capacities

W. Schneider[1]

[1]*Institute of Fluid Mechanics and Heat Transfer, TU Wien, Resselgasse 3, 1040 Vienna, Austria,*
wilhelm.schneider@tuwien.ac.at

When the surface of a liquid is treated as a thermodynamic system, as it is commonly done in classical macroscopic thermodynamics, one faces the problem of negative surface heat capacities that are observed for many liquids, at least in certain temperature regimes. Since thermodynamic stability of a system requires positive heat capacities, it is usually argued in the thermodynamic literature that the surface must not be considered as an "autonomous" system, but rather ought to be treated together with the liquid that forms the surface. This, however, is sometimes easier said than done. In the literature on thermo-capillary fluid flow, on the other hand, the surface heat capacity is commonly not taken into account, based on the - often tacit - assumption that the effect will be small.

With the aim of clarifying the role of negative surface heat capacities, the energy balance of a moving surface is formulated. It contains terms with the following physical meaning: rate of change of internal energy; net convective flux of internal energy; work done by surface tension; work done by shear stresses; net heat flux. In problems of heat transfer and/or fluid flow with temperature changes, the energy balance of the surface plays the role of a boundary condition for the field equations. As a consequence, negative surface heat capacities may lead to instabilities, even if the non-dimensional parameters characterizing the effect of the surface heat capacity are very small.

As a first example, a semi-infinite liquid body with horizontal, adiabatic surface is considered, and the temporal development of small, spatially periodic temperature perturbations is investigated. The liquid is taken to be at rest initially, but velocity perturbations due to thermo-capillary effects are allowed. Depending on the value of a non-dimensional parameter, instabilities may occur for common fluids, but the perturbations are confined to an extremely thin layer near the surface.

As an example of instabilities that are not confined to a thin layer, a heat pulse applied to the horizontal surface of a semi-infinite liquid body, which is at rest, is considered. A solution in closed form is given for the temperature distribution in the liquid as a function of time. In case of negative surface heat capacities it turns out that the temperature of the surface as well as the temperature in the bulk of the liquid decays beyond bounds even after the supply of heat has been terminated. The cause of the unconfined instability is a mechanism of self-amplification: As the temperature of the surface with negative surface heat capacity drops to balance the supply of heat, heat is conducted from the bulk of the liquid to the surface, leading to a further reduction of the surface temperature.

Another example of an instability that extends to the whole system is the stretching of a liquid film in a wire frame. Accounting for heat conduction due to temperature differences between the surface and the bulk of the liquid, one obtains that the deviation of the mean bulk temperature from the surface temperature grows beyond bounds with increasing time if the surface heat capacity is negative. This result is, of course, in contrast to the common assumption of local thermodynamic equilibrium.

To deal with instabilities associated with negative surface heat capacities it is proposed to introduce a thin surface layer whose (finite) thickness is defined solely in terms of macroscopic thermodynamic quantities. Guided by various molecular models, the surface tension divided by the cohesive pressure that appears in the van der Waals equation is identified as a suitable scale of the layer thickness. Since heat capacities are extensive quantities of state, the heat capacity of the liquid contained in the thin surface layer is added to the (possibly negative) surface heat capacity to obtain a positive total heat capacity of the surface layer. Finally, a few thermodynamic properties of the proposed macroscopic model of a surface layer are discussed, in particular concerning the point whether a stretched surface layer ought to be considered as an open system.

Thermocapillary surface waves – reviewed

C. Bach[1] and D. Schwabe[1]

[1] *Physikalisches Institut der Justus-Liebig-Universität Giessen, 35398 Giessen, H.-Buff-Ring 16, Germany,*
dietrich.schwabe@physik.uni-giessen.de

We report on experiments which claim to have identified thermocapillary surface waves (TSWs). The TSWs occur in differentially heated shallow liquid layers at larger Marangoni number Ma. These TSWs differ from the well known hydrothermal (thermocapillary) waves (HTWs), termed such after a paper of Smith and Davis [1]. These authors investigated the instabilities of thermocapillary flow (with return flow) in a model system (infinitely extended liquid layer with free and rigid upper surface which is subjected to a linear temperature gradient). We note the three constraints in the model, chosen by Smith and Davis; (i) infinite extension, (ii) rigid free surface, (iii) imposed linear temperature gradient. In spite of these deviations from reality, instabilities similar to HTWs and many features of HTWs predicted by this analysis have been identified in experiments.

The existence of the HTW is not coupled to a movement of the free surface. However, Smith and Davis extended their analysis to a second paper [2] where they allowed for the flexibility of the free surface. They predicted the existence of themocapillary surface waves (TSWs), with their existence intimately coupled to the movement of the free surface. These TSWs are rather unknown, presumably because they appear only at higher Ma and under special conditions.

We expect a stronger surface modulation for the TSWs compared to the HTWs. Deviations of the features of the TSWs from theoretical predictions are expected in the experiments mainly because of the limited extension of the free surface and from non-constant temperature gradients.

In two experiments with shallow annular gaps TSWs have been observed besides HTWs. The TSWs displayed a much larger dynamic surface deformation and larger wavelength and were preferred over HTWs for liquid depth $d > 1.4mm$, whereas the latter were preferred for $d < 1.4mm$ [3]. The TSW can travel in radial direction for Ma slightly above the threshold for onset and travel later with an azimuthal component. These findings have been corroborated by experiments with the same shallow annular gap, however, with an adiabatic bottom [4], a boundary condition much nearer to theory [2]. The critical properties of the wave, observable only for d between $1.8mm$ and $4.1mm$, are in good agreement with the theoretical TSWs. It was speculated that TSWs can be only observed in layers with sufficient extension, a condition which is not given for the rather short liquid bridges.

In a rectangular cuvette with differentially heated end-walls we could observe the separation of flow driven by thermocapillarity in the fluid meniscus at the cold side [5]. The convection in the bulk was driven mainly by buoyancy with a separated upper layer with thermocapillary-driven flow. For a certain range of meniscus shapes we observed a resonance between oscillations in this meniscus region with gravity surface waves in the free surface in the cuvette [5]. Most likely, TSWs of a frequency that is in resonance with gravity surface waves could excite and sustain macroscopic standing gravity surface waves. The faint surface oscillations of a TSW in the liquid meniscus are able to provide the energy for the excitation of standing gravity surface waves in the whole surface. The resonance was demonstrated, by detuning the gravity surface waves (other dimension of the cuvette) and by detecting frequencies of the TSWs in the meniscus region which could be the exciting ones. Fine tuning of the resonance was possible by either changing the meniscus shape or by changing Ma.

[1] M. K. Smith, S. H. Davis, J. Fluid Mech., **132**, pp. 119-144 (1983).
[2] M. K. Smith, S. H. Davis, J. Fluid Mech., **132**, pp. 145-162 (1983).
[3] D. Schwabe, U. Moeller, J. Schneider, A. Scharmann, Phys. Fluids A, **4**, pp. 2368-2381 (1992).
[4] J. Schneider, D. Schwabe, A. Scharmann, Microgravity Sci. Technol., **9**, pp. 86-94 (1996).
[5] C. Bach, *Resonanz von Oberflaechenwellen mit thermokapillaren Instabilitäten in einem Meniskus*, PhD-thesis, Justus-Liebig-Universitaet Giessen (2000).

Hierarchical Marangoni roll cells caused by mass transfer: direct numerical simulations and supporting experiments

T. Köllner,[1] K. Schwarzenberger,[2] K. Eckert,[2] S. Odenbach,[2] and T. Boeck[1]

[1]*Institute of Thermodynamics and Fluid Mechanics, TU Ilmenau, P.O.Box 100565, 98684 Ilmenau, Germany*
[2]*Institute of Fluid Mechanics, Chair of Magnetofluiddynamics, Measuring and Automation Technology, TU Dresden, 01062 Dresden, Germany,*
karin.schwarzenberger@tu-dresden.de

We consider the diffusion of the weakly surface-active butanol from cyclohexanol into water, which is sensitive to stationary Marangoni instability according to [1]. In the temporal evolution of this system, hierarchical Marangoni roll cells appear. The system is modeled as two immiscible layers separated by a plane and undeformable interface where the partition of butanol is governed by Henry's law. Highly resolved simulations based on a pseudospectral method and associated validation experiments are conducted for two different system geometries. Firstly, cuvettes of rectangular cross-section are used, corresponding to a cubical computational domain for the 3D simulations. Secondly, the liquid-liquid system is placed in a Hele-Shaw configuration, so that 2D simulations with a parabolic velocity profile over the gap width can be performed. The multiscale flow observed in the experiments is successfully reproduced by the simulations, cf. Fig. 1. Furthermore, it can be shown that the pattern evolution proceeds in a self-similar way with respect to different initial butanol concentrations when length and time are appropriately rescaled and buoyancy effects are negligible [2]. Horizontal length scales of the hierarchical roll cells agree well with our experimental data from shadowgraph images for the 3D case. However, larger differences are obtained when comparing the vertical length scales observed in the Hele-Shaw configurations. Nevertheless, qualitative tendencies of the pattern characteristics in the vertical/horizontal position of the Hele-Shaw cell are consistent with simulations including/neglecting gravity influence. The influence of wall friction on the hierarchical structures is studied by a variation of the Hele-Shaw gap width.

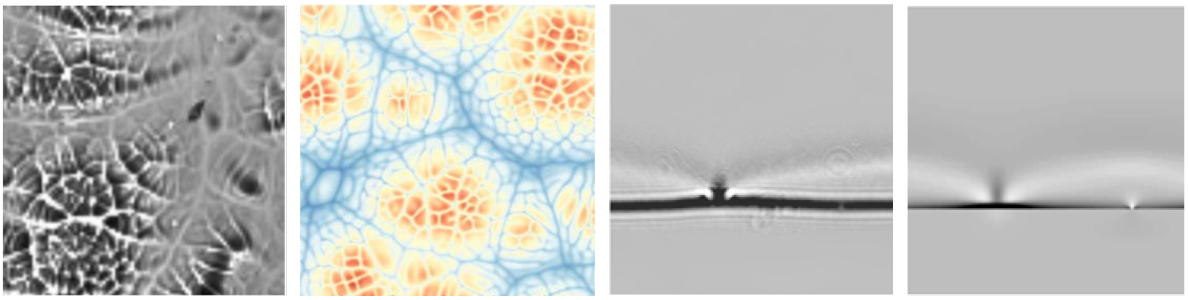

FIG. 1. Horizontal flow structures (3D case) from shadowgraph records in the experiment (left) and from simulated concentration distribution at the interface (middle left). Vertical flow structures (2D case) from shadowgraph records in the experiment (middle right) and from synthetic shadowgraph images of the simulations (right).

[1] C. V. Sternling and L. E. Scriven, *Interfacial turbulence: hydrodynamic instability and the Marangoni effect*, AIChE J., **5**, 514–523 (1959).

[2] T. Köllner, K. Schwarzenberger, K. Eckert, T. Boeck, *Multiscale structures in solutal Marangoni convection: Three-dimensional simulations and supporting experiments*, Phys. Fluids, **25**, 092109 (2013).

[3] K. Schwarzenberger, T. Köllner, H. Linde, T. Boeck, S. Odenbach, K. Eckert, *Pattern formation and mass transfer under stationary solutal Marangoni instability*, Adv. Colloid Interface Sci. (2013).

Studying of fast interfacial loading of surfactants by PANDA

W. Sempels,[1] R. De Dier,[2] J. Hofkens,[1] and J. Vermant[2]

[1]*Departement of Chemistry, KULEUVEN, Celestijnenlaan 200F, 3001 Heverlee, Belgium,*
wouter.sempels@chem.kuleuven.be
[2]*Chemical engineering, KULEUVEN, W. de Croylaan 46, 3001 Heverlee, Belgium*

I. OSCILLATING PENDANT DROPS: INDIRECT IMAGING OF SURFACE TENSION

Surfactant molecules are important in household, industrial procedures and in biological [1] and micro-organism related studies [2]. Pendant drop experiments measure dynamic surface tensions, yet are slow due to inertia. Hence, the fast dynamics of surfactant interfacial ad/desorption cannot be probed.

II. FAST SURFACTANT DYNAMICS: DOMINATE FLOWS AND TIME SCALE

A volume of air was trapped into the surfactant solution (see Fig. 1) in an oscillating pendant droplet. This scheme with improved temporal resolution is nicknamed PANDA (Pressure Assisted Nucleation of a Droplet of Air). A systematic study of concentration and surfactant types was done, together with a complementary confocal study of the flow in geometrical identical drops (see Fig. 2, left). Astonishingly (even above CMC) time and concentration influence the flow and deposition pattern of the (bio)colloidals. Experiments in surfactant producing bacteria (P. aeruginosa) show similar flows.

The internal flow of evaporating droplets was influenced by the soluble surfactants; and their ad/desorption dominate the observed time scale in the oscillating flow behaviour (see Fig. 2, right). The PANDA technique proves the importance of the dynamics of surfactant molecules.

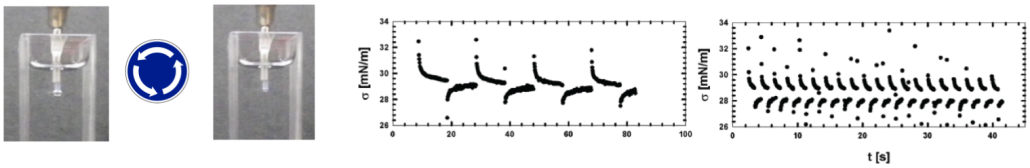

FIG. 1. PANDA oscillating pendant "droplet of air" in an aqueous surfactant solution. Left: Expansion and compression of air bubble. Right: Data set from PANDA, probing of adsorption of surfactants to the interface.

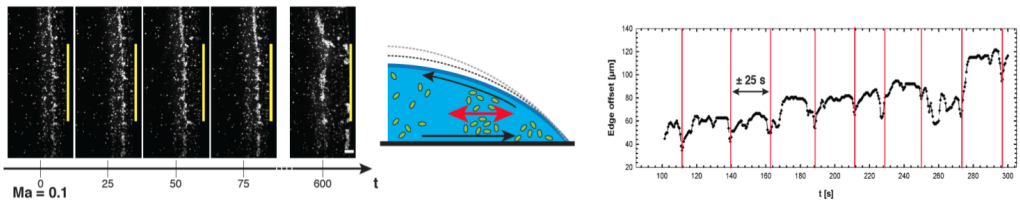

FIG. 2. Complementary measurements via confocal microscopy probe an excisting time scale due to the surfactant loading of the interface. Left: Time evolution of surfactant loaded droplet, with Triton X-100 and eGFP E. Coli. The bacterial front oscillates periodically. Left, time (in s), 30 μm scale bar and in yelow the contact line, with a side profile sketch the of the oscillating motion. Right, Oscillation of bacterial front by surfactants.

[1] E. Hermans, J. Vermant, *Interfacial shear rheology of DPPC under physiologically relevant conditions*, Soft Matter, **10(1)**, 175-186, (2014).

[2] W. Sempels, R. De Dier, H. Mizuno, J. Hofkens, J. Vermant, *Auto-production of biosurfactants reverses the coffee ring effect in a bacterial system*, Nat. Commun., **4**, 1757 (2013).

Interfacial instabilities between miscible fluids under horizontal vibrations

V. Shevtsova,[1] Y. Gaponenko,[1] M. Torregrosa,[1] V. Yasnou,[1] and A. Mialdun[1]

[1]*Microgravity Research Center, Université Libre de Bruxelles, CP–165/62, Av. F.D. Roosevelt, 50, B–1050 Brussels, Belgium,*
vshev@ulb.ac.be

Interfacial instabilities occurring between two fluids are of fundamental interest in fluid dynamics, biological systems and engineering applications such as liquid storage, solvent extraction, oil recovery and mixing. Horizontal vibrations applied to stratified layers of immiscible liquids may generate spatially periodic waving of the interface, stationary in the reference frame of the vibrated cell, referred to as a "frozen wave"[1]. We are aware of only single previous experimental study with miscible fluids where liquids viscosities differ by 70 and 1000 times [2].

The formation and progress of perturbations at the interface between two horizontally vibrated miscible liquids is investigated experimentally and numerically. Two superimposed layers of ordinary liquids, water-alcohol of different concentrations, are placed in a closed cavity of 7.5 mm$\times$5 mm$\times$ 15mm, in a gravitationally stable configuration. The density and viscosity contrasts between these two fluids are $\rho = \rho_2/\rho_1 = 0.92$, $\nu = \nu_2/\nu_1 = 2.35$ and the aspect ratio is $L/H = 2$. The bottom fluid (#1) is more dense and less viscous.

The experiments were performed inside an airplane during the 59th ESA Parabolic Flight campaign. 60 experimental runs were conducted under reduced gravity and several tests were executed between parabolas in normal gravity. For the clarification of some observations we have performed 2D and 3D numerical analysis[3].

We present experimental evidence that frozen wave instability exists between two ordinary miscible liquids of similar densities and viscosities and this finding is illustrated by the first three snapshots in Fig. 1. Similar to the immiscible fluids this instability has a threshold. When the value of forcing is increased the amplitudes of perturbations grow continuously displaying a saw-tooth structure, see the snapshots at t=3.9 s in Fig. 1. the last snapshot shows the results of computer simulations for the same set of parameters. We have noted that for the liquids with comparable viscosity the amplitude and wavelength of frozen waves are sensitive to a small variation of the viscosity contrast. Unlike a sine shape of frozen waves on the immiscible interface reported in literature, the observed shape is triangle. The decrease of gravity drastically changes the structure of frozen waves.

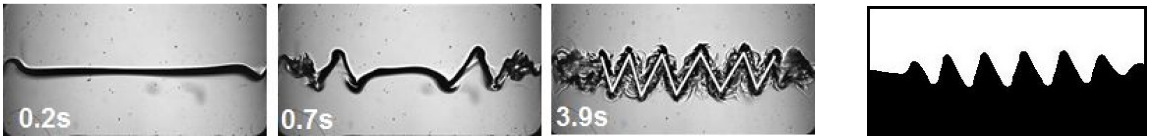

FIG. 1. Development of frozen waves in miscible liquids under horizontal vibrations with amplitude A=11 mm and frequency f=12 Hz. First three snapshots on the left show the experimental results at Earth gravity while the last one corresponds to numerical simulations

[1] G. H. Wolf, *The Dynamic Stabilization of the Rayleigh-Taylor Instability and the Corresponding Dynamic Equilibrium*, Z. Physik 227, **227** 291 (1969)

[2] M. Legendre, P. Petitjeans, P. Kurowski, *Instabilités à l'interface entre fluides miscibles par forçage oscillant horizontal*, C. R. Méc., **331**, 617 (2003).

[3] Y. Gaponenko, V. Shevtsova, *Effects of vibrations on dynamics of miscible liquids*, Acta Astronautica, **66**, 174 (2010).

Liquid layered phenomenon and initial droplet size distribution during explosive dispersal process

Y. N. Shi,[1] T. Hong,[1] C.S. Qin,[1] and Q.J. Feng[1]

[1]*Institute of Applied Physics and Computational Mathmatics, Beijing 100094, P. R. China,*
shyn@iapcm.ac.cn

It is one of the important stages during aerosol cloud formation process, that liquid outer interface happen to disperse and break up. In the process of liquid dispersion driven by explosion, the liquid characteristics and dispersion feature may be directly affected by the propagation of explosion shock wave in liquid and the interaction in the gas-liquid interface[1, 2]. An experimental device for liquid dispersed by center explosive is set up. The high-speed framing photography is applied to observe liquid interface developing process of explosion scattering. And the experimental results show that it can be divided into three stages: jet integral injection, interface appearing in flocculent and breaking, small water droplets forming, as shown in fig. 1.

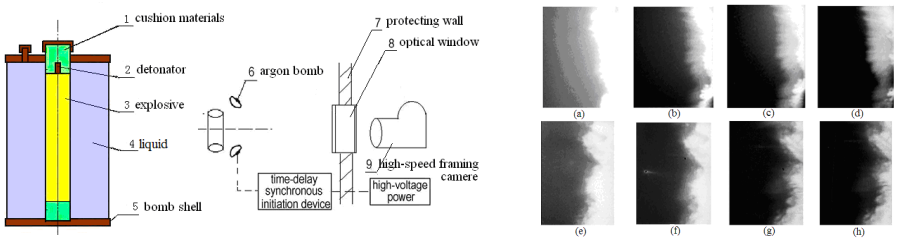

FIG. 1. the liquid dispersal experiment. Left: the dispersal device; Right:Framing photographs of water interface

The flow fields driven by explosive detonation are simulated by using the Euler code, with dimensional split algorithm. Young's method is employed to deal with the interface in the mixing mesh. It is verified that liquid ring is not a uniform continuous, but happens to the density layered phenomenon. The cavitations phenomenon occurs near the interface.

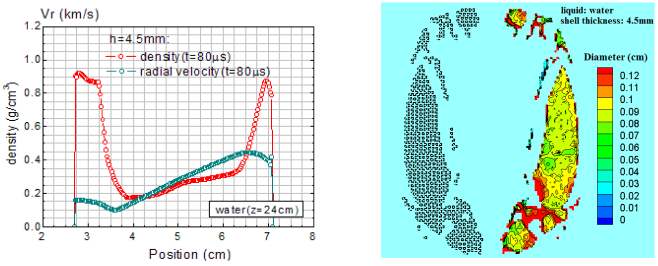

FIG. 2. the calculated results. Left: Liquid radial density and velocity disturbance; Right: Initial droplet size

The possible mechanisms of initial droplet formation are attributed to jet breakup and liquid dynamic fragmentation. The difference primary breakup models are built. The initial droplet size distributions are shown by fig. 2. The drop diameter scale is mm, and liquid jet mass is about 15% of the total mass.

---

[1] Z. H. Jiang, X. P. Long, H. Yong, et al, *Experimental studies on shell fracturing and jet forming and developing process driven by detonation*, Chin. J. Eng. Mater., **03**, 321–324 (2011).

[2] Y. N. Shi, C. S. Qin, *Instability and breakup of stretching metallic jets*, Chin. J. Theo. Appl. Mech., **41**, 361–369 (2009).

Janus droplet as a catalytic motor

S. Shklyaev[1]

[1]*Institute of Continuous Media Mechanics, UB RAS, 614013 Perm, Russia,*
shklyaev@yandex.ru

One of the challenges in modern microtechnology is a design a cheap, biocompatible, easy-to-control, and efficient nanomotor, an artificial particle which demonstrates the self-propulsion. The so-called "catalytic motor" [1] is among the other promising strategies in this field; this is a microparticle that triggers a chemical reaction on a part of its surface, thus creating the nonuniform distribution of the reactant. Via phoretic mechanisms (electrophoresis, diffusiophoresis, or even thermophoresis) this nonuniformity results in a translational motion of the motor.

The surface-tension-driven convection is a well-known source of motion at small scales, therefore an idea to design a catalytic motor that works using the variation of the surface tensions is promising. Such motors moving along the interface/free surface are well-known (e.g. a camphor boat); but a self-propulsion in a bulk is often needed for applications. The autonomous motion of a droplet due to a chemical reaction was found in a series of theoretical papers, see the review in [3]. However, for a single-fluid active droplet the self-propulsion emerges as a result of symmetry breaking bifurcation, a certain stability threshold should be exceeded; this makes almost impossible scaling down such motors below the size of $100\ \mu\mathrm{m}$. In contrast, for a compound drop the fore-aft symmetry is absent. Thus, similarly to self-phoretic motion of catalytic motors [1], a compound droplet creates the gradient of concentration along its surface and this gradient then pushes the drop in a manner discovered in [2].

In this work the self-propulsion of a Janus droplet in a solution of surfactant is considered. The Janus droplet comprises two hemispherical domains occupied by different liquids; the interfacial tensions on both external surfaces of the Janus droplet decrease linearly with the concentration of the surfactant. The surfactant experiences the zero order chemical reaction—the mass flux of the surfactant is fixed—at the contact with one of the internal liquids. The difference in the surfactant concentration triggers the solutocapillary convection, which, in turn, drags the droplet.

The variation of the self-propulsion velocity with the problem parameters (viscosities of internal liquids, variations of both interfacial tensions with the surfactant concentration) is investigated. It is shown that the maximum velocity takes place if the mean viscosity of the droplet is small in comparison with that of the ambient liquid, whereas the internal viscosities differ as much as possible.

This publication is based on work supported by Award No. RUP1-7078-PE-12 (joint grant with Ural Branch of the Russian Academy of Sciences) of the U.S. Civilian Research & Development Foundation (CRDF Global) and by the National Science Foundation under Cooperative Agreement No. OISE-9531011.

---

[1] D. Patra, S. Sengupta, W. Duan, H. Zhang, R. Pavlick, A. Sen, *Intelligent, self-powered, drug delivery systems*, Nanoscale, **5**, 1273–1283 (2013).

[2] N. O. Young, J. S. Goldstein, M. J. Block, *The motion of bubbles in a vertical temperature gradient*, J. Fluid Mech., **6**, 350–356 (1959).

[3] M. G. Velarde, A. Y. Rednikov, Y. S. Ryazantsev, *Drop motions and interfacial instability*, J. Phys.: Condens. Matter, **8**, 9233-9247 (1996).

Marangoni convection in liquid layer under alternating heat flux

B. L. Smorodin[1] and B. I. Myznikova[2]

[1]*Perm State University, 614990, Perm, Russia,*
bsmorodin@yandex.ru
[2]*Institute of Continuous Media Mechanics of Ural Branch of Russian Academy of Sciences, 614013 Perm, Russia,*
myz@icmm.ru

The pattern formation and transport phenomena in open liquid layers caused by the thermal nonuniformity of surface tension under modulated external conditions were investigated in the case of a deep, or more precisely, semi-infinite liquid layer [1].

In this presentation we will discuss the excitation of the Marangoni instability in a horizontal liquid layer is in the case of a heat flux periodically varying at the i) flat and ii) deformable upper surface. The neutral stability curves are presented for a variety of external conditions. Convection thresholds are determined. The critical Marangoni number and the critical wave number are expressed as functions of frequency. The cellular and long-wave instability thresholds are compared. It is shown that the long-wavelength mode can give rise to the instability prior to the cellular mode within the definite range of parameters.

Two response modes of the convective system to an external periodic action, subharmonic and synchronous ones, are found. It is shown that contrary to the classical parametric resonance, the synchronous disturbances may become most dangerous for the stability of the base state. This happens in the case when the Prandtl number slightly exceeds the unit.

The spatiotemporal behavior and the bifurcation properties of nonlinear oscillating convection flows in the case of flat upper surface is investigated with finite difference numerical simulations. The dependences of flow intensity on the Marangoni number are examined for the subharmonic and synchronous resonance regions. The numerical results agree with the stability boundaries of the base state predicted by linear theory.

Acknowledgements. This work was partially supported by the Russian Basic Research Foundation (No. 14-01-96027).

---

[1] G. Z. Gershuni, A. A. Nepomnyashchy, M. G. Velarde, *On dynamic excitation of Marangoni instability*, Phys. Fluids A, **4**, 2394-2398 (1992).

Numerical simulation of particle-laden droplet evaporation

G. Son[1]

[1]*Sogang University, Seoul 121-742, South Korea,*
gihun@sogang.ac.kr

The evaporation of a particle-laden droplet, which can be utilized for fabrication of microstructures, has been extensively studied in the last decade [1]. However, the past efforts to develop a general predictive model for the droplet evaporation were suffered from the complexity of the process involving the liquid-gas interface motion with phase change and its interaction with the vapor concentration and the particle distribution as well as the liquid-gas flow and temperature fields. Numerical simulation of the evaporation of a droplet with or without particles were performed in several studies using FEM and moving grid methods, but the Lagrangian methods are not straightforward to implement for breaking or merging of the interface. In this study, an Eulerian interface tracking method, which can easily handle the interface with change in topology, is developed for computation of particle-laden particle evaporation. The present numerical approach is based on the sharp-interface level-set (LS) formulation for the evaporation of a pure droplet developed in our previous work [2] and extended for the evaporation of a particle-laden droplet. The liquid-gas interface is tracked by the LS function ϕ, which is defined as a signed distance from the interface. The conservation equations of mass, momentum, energy and vapor mass fraction for the liquid-gas region are solved employing a calculation procedure for the coupled interface conditions for the temperature, vapor fraction, particle concentration and evaporative mass flux $\dot{m}$. In order to treat the particle distribution in an evaporating droplet, we introduce the particle concentration, Y_p. The conservation equation of particle concentrtion can be expressed as

$$\rho_l \left(\frac{\partial Y_p}{\partial t} + \mathbf{u}_l \cdot \nabla Y_p \right) = \nabla \cdot \rho_l \hat{D}_l \nabla Y_p \quad if \phi > 0; \quad -\mathbf{n} \cdot \rho_l \hat{D}_l \nabla Y_p = \dot{m} Y_p \quad if \phi = 0.$$

The present method is first tested through the computation of one-dimensional case of particle-laden droplet evaporation in a stationary air layer of infinite extent. The velocity and mass fraction fields computed from the LS method are observed to be comparable to the exact solution obtained from the coordinate transformation method. Numerical simulation is performed for the evaporation of a microdroplet with nanoparticles on a heated surface. The results are plotted in Fig. 1. The computation demonstrates droplet evaporation and particle accumulation near the contact line, which results in coffee-ring formation. This indicates that the LS formulation is applicable to investigating the evaporation of a particle-laden droplet.

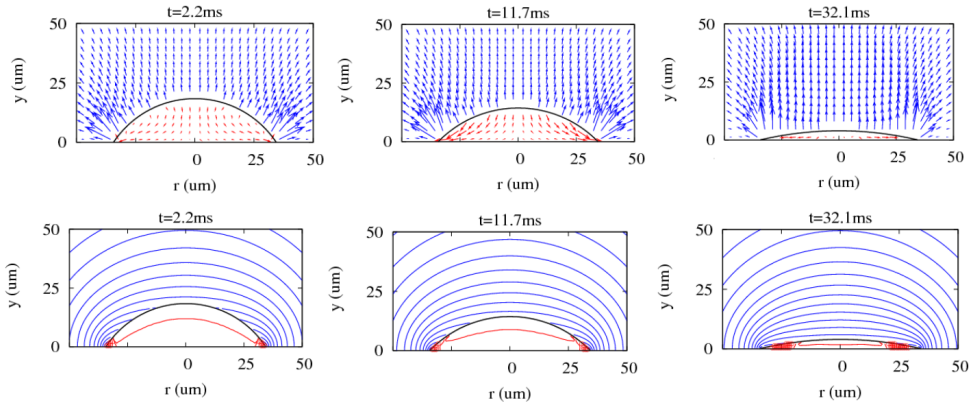

FIG. 1. (a) Evaporation of a particle-laden droplet: velocity fields and vapor and particle fraction fields.

[1] A. F. Routh, *Drying of thin colloidal films*, Rep. Prog. Phys., **76**, 046603 (2013).

[2] G. Son, *Numerical simulation of microdroplet impact and evaporation on a solid surface*, J. Heat Transfer, **134**, 101502 (2012).

Salt-induced Marangoni flow in evaporating sessile droplets

V. Soulié,[1,2] S. Karpitschka,[1] F. Lequien,[2] T. Zemb,[3] H. Möhwald,[1] and H. Riegler[1]

[1]*Max Planck Institute of Colloids and Interfaces, 14424 Potsdam-Golm, Germany,*
virginie.soulie@mpikg.mpg.de
[2]*CEA, DEN, DPC, SCCME, Laboratoire d'Etude de la Corrosion Non Aqueuse, 91191 Gif-sur-Yvette, France*
[3]*ICSM, UMR 5257 (CEA/CNRS/UM2/ENSCM), Bagnols-sur-Cèze, France*

The evaporation behavior of a sessile drop is rather complicated because of the subtle issues arising from its description such as the non-uniform evaporative flux. The evaporation at the contact line region is enhanced, which induces a capillary flow towards the edge (leading to the "coffee-ring" effect [1]). For complex fluids the evaporation behavior becomes even more complex, because the non-uniform evaporative flux will lead to an inhomogeneous distribution of the fluid constituents within the drop. This can induce a surface tension gradient, which in turn may lead to a Marangoni flow [2] in addition to the capillary flow.

We study the evaporation of sessile drops from aqueous sodium chloride solutions on solid planar surfaces. The diverging evaporative flux locally enriches NaCl at the droplet edge (Fig 1.a). Since chaotrope salts are depleted from the air-water interface, the surface tension locally increases in the edge region. This can lead to a Marangoni flow in the same direction as the capillary flow, *i.e.* towards the contact line. Diffusive dilution resulting from the salt concentration gradient will reduce the evaporation-induced gradient (Fig 1.b).

We investigate how the flows within the drop and, in particular the Marangoni flow along its surface, are related and affected by: (i) the initial NaCl concentration, (ii) the contact angle, (iii) the drop size and (iv) the evaporation rate. To this end the shape and the contact angle of the drop are analyzed by simultaneous optical imaging from the top and the side [3] and the liquid flow is studied by particle tracking velocimetry (PTV) with polystyrene particles.

We find that the flow behavior is strongly affected by the initial NaCl concentration. At low initial NaCl concentrations, PTV experiments reveal only a flow towards the contact line. This may arise from the capillary flow compensating for the local evaporative losses, possibly increased by a Marangoni flow component (Fig 1.b). However, above 10^{-3}M NaCl, the surface tension gradient respectively Marangoni flow leads to a such strong flow towards the drop edge that the capillary pressure in this region increases. Therefore, the compensating capillary flow is now directed inward and we observe a convection roll near the drop edge (Fig 1.c). Experiments reveal that the flow patterns are also affected by the ambient vapor pressure, the drop size and contact angle.

To conclude, the flow behavior of an evaporating drop of a saline solution is dominated by a solely outward flow (combination of Marangoni and capillary forces) at low salt concentrations. At high salt concentrations, the flow behavior changes drastically and is governed by compensating Marangoni and capillary flows that lead to convection rolls.

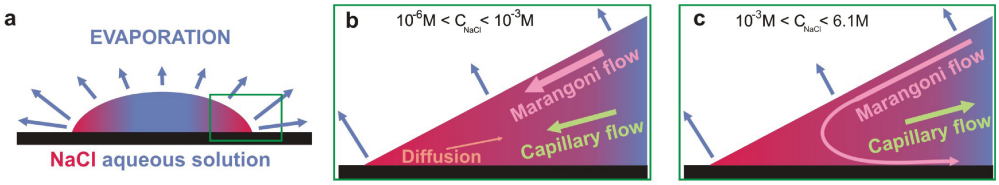

FIG. 1. (a) Evaporation behavior of a sessile drop from aqueous sodium chloride solutions. Locally varying evaporation rate and resulting concentration gradient: below (b) and above (c) 10^{-3}M NaCl.

[1] R. D. Deegan, O. Bakajin, T. F. Dupont, G. Huber, S. R. Nagel, T. A. Witten, *Capillary flow as the cause of ring stains from dried liquid drops*, Nature, **389**, 827–829 (1997).
[2] L. E. Scriven, C. V. Sternling, *The Marangoni effects*, Nature, **187**, 186–188 (1960).
[3] S. Karpitschka, H. Riegler, *Study on the Transition between Fast and Delayed Coalescence of Sessile Droplets with Different but Completely Miscible Liquids*, Langmuir, **26**, 11823–11829 (2010).

Foam drainage: experimental study and numerical simulations

A. Bureiko,[1] N. Kovalchuk,[2,3] A. Trybala,[2] O. Arjmandi-Tash,[2] and V. Starov[2]

[1]*Procrtor & Gamble, USA*
[2]*Department of Chemical Engineering, Loughborough University, UK*
[3]*Institute of Biocolloid Chemistry, Kiev, Ukraine*

Foams are widely used in food, cosmetics, pharmacy etc [1, 2]. stabilised by surfactants, but during the last decade polymers (polyelectrolytes) become a frequently used additives to foaming solutions [3]. Polymers often increase considerably the viscosity of foaming liquids and in this way affect the foam drainage kinetics.

We present the results of experimental study on drainage of foams produced from solutions of commercially available polymers Aculyn^{TM} 22 and Aculyn^{TM} 33 broadly used in cosmetic industry. In particular the influence of bulk and the surface rheology of foaming solutions on the drainage kinetics is addressed.

For many applications, particularly in pharmacy and cosmetics, the interaction of foam with substrate is of considerable importance. This interaction can affect, for example, the kinetics of the release of acting substances from foam and therefore have to be taken into consideration for finding optimal formulations.

Often the surfaces where foam is applied are porous (skin, hair). To identify the methods to control the kinetics of liquid release in this case we performed direct numerical simulations of foam drainage on the porous substrate. The mathematical model developed combines the foam drainage equation with the equation describing the penetration of liquid in the model porous substrate of prescribed structure coupled with appropriate boundary conditions at foam/substrate interface.

The performed numerical simulations have shown that depending on the liquid viscosity, bubble size, foam height, substrate porosity and wetting conditions two different scenarios are possible with and without the formation of continuous liquid layer between the foam and porous substrate. Kinetics of foam drainage and penetration of liquid into porous substrate is considered in details for both scenarios depending on the properties of foaming liquid and substrate.

Acknowledgements. This research was supported by Procrtor & Gamble, USA; CoWet project, EU; EPSRC, UK and PASTA project, European Space Agency.

---

[1] L. H. Kircik, J. Bikobski, Vehicles Matter, Supplement to Practical Dermatology, **1**, 3-18 (2012).
[2] A.Arzhavitina, H. Steckel, Int. J. Pharmaceutics, **394**, 1-17 (2010).
[3] R. Von Klitzing, H.-J. Muller, COCIS, **7**, 42-49 (2002).

Interfacial instability arisen on vapor bubble in subcooled pool

I. Ueno,[1] J. Ando,[1] T. Saiki,[1] and T. Kaneko[1]

[1]*Dept. Mechanical Engineering, Fac. Science & Technology, Tokyo University of Science, 2641 Yamazaki, Noda, Chiba 278-8510, Japan,*
ich@rs.tus.ac.jp

We pay a special attention to the collapsing processes of vapor bubble injected into a subcooled pool; we have tried to extract the vapor-liquid interaction by employing a vapor generator that supplies vapor at designated flow rate to the subcooled pool instead of using a immersed heated surface to realize a vapor bubble by boiling phenomenon [1]. This system enables ones to detect a spatio-temporal behavior of a single bubble of superheated vapor exposed to a subcooled liquid. We indicate that an abrupt condensation of the injected vapor results in a fine disturbance over the vapor bubble surface before the collapse stage of the bubble (Fig. 1). The wave number is sharply dependent on the degree of subcooling of the pool. Correlation between such a fine disturbance formation over the bubble and the dynamic behavior of the vapor bubble will be illustrated.

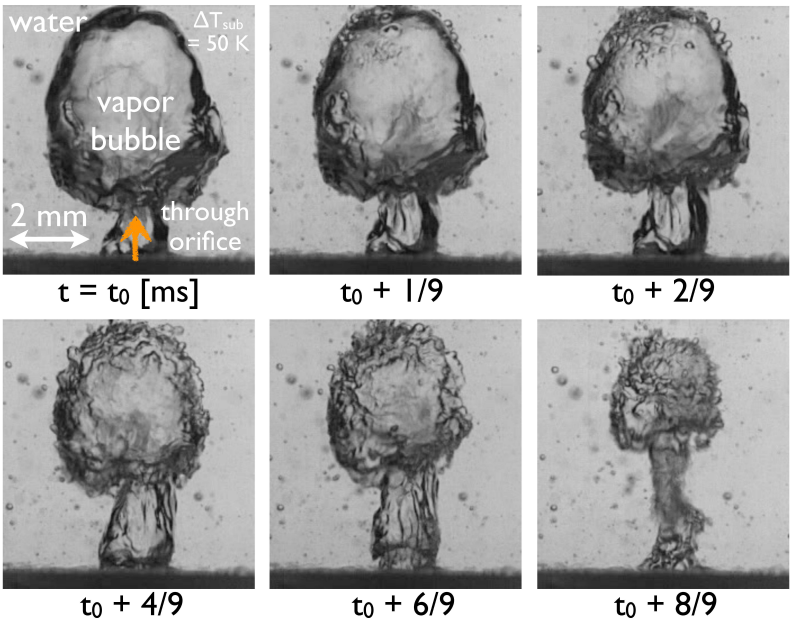

FIG. 1. Typical example of successive images of the condensing/collapsing vapor bubble formed in the pool of 50 K in the degree of subcooling ΔT_{sub} through the orifice.

[1] I. Ueno, Y. Hattori, R. Hosoya, *Condensation and collapse of vapor bubbles injected in subcooled pool*, Microgravity Science & Technology, **23**, 73 - 77 (2011).

Thermal coupling between two liquid films undergoing long-wavelength instabilities

M. Vécsei,[1] M. Dietzel,[1] and S. Hardt[1]

[1]*Center of Smart Interfaces, TU Darmstadt, Alarich-Weiss-Str. 10, D-64287, Darmstadt, Germany*

In this study the effects of coupling between two self-organizing systems are analyzed. Two thin liquid films are placed opposite to each other on flat substrates, which are maintained at different temperatures T_1 (lower substrate) and T_2. The films are separated by a gaseous layer and affected by thermocapillary and gravitational stresses. Without the presence of the respective other film, in previous works it has been shown that if $T_1 > T_2$ the upper film undergoes a long-wave thermocapillarity-stabilized Rayleigh-Taylor (RT) instability while the lower one is susceptible to a long-wave gravity-stabilized Bénard-Marangoni (BM) instability [1–3]. Inspired by [4], the thermal coupling between these two instabilities is analyzed at hand of the triple layer configuration schematically shown in Fig. 1.

The deformation of one film changes the surface temperature of the other one, altering the thermocapillary forces along its interface. Since the viscosity of the gaseous medium can be neglected, there is no direct mechanical connection between the liquids. This simplifies the analysis, as the evolution equation of the film height used in systems with one liquid layer can be directly applied, and the coupling only needs to be considered in the energy equations.

In the analysis it was assumed that the liquids have identical material properties and similar initial thicknesses. Full numerical calculations and a linear stability analysis of the evolution equations were conducted. In comparison to the individual systems investigated before, it has been found that the coupling changes the stability properties of the system. Depending on the dimensionless groups of the films, regimes with different degrees of coupling were identified. In those with weaker coupling, only one of the films is inherently unstable, while triggering a deformation also in the stable one. In regimes with stronger coupling the joint system may be stable, but within a certain parameter range a qualitatively different instability appears on both surfaces where the emerging patterns undergo lateral movement (Fig. 2). It can be shown that such behavior cannot occur for the isolated RT and BM instabilities. The numerical simulations of the non-linear evolution equations agree well with the analytical predictions. In essence, equivalent to the circumstance that the coherent behavior of a single self-organizing system is more than just the sum of the individual properties characterizing the isolated building blocks, it is found that the coupled system has considerably enhanced properties compared to the individual systems.

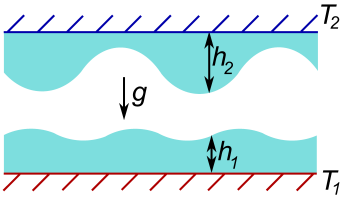

FIG. 1: Two thermally coupled liquid films under the influence of gravity and thermocapillarity.

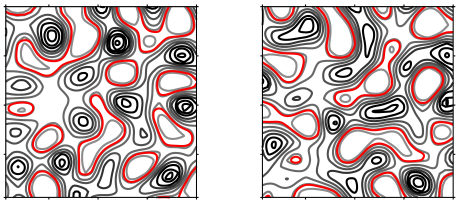

FIG. 2: Contour plots of the pattern on the lower liquid film at two consecutive timesteps with highlighted contours at a selected liquid thickness.

[1] A. Oron, S. H. Davis, S. G. Bankoff, *Long-scale evolution of thin liquid films*, Rev. Mod. Phys., **69**, 931 (1997).

[2] S. J. VanHook, M. F. Schatz, J. B. Swift, W. D. McCormick, H. L. Swinney, *Long-wavelength surface-tension-driven Benard convection: experiment and theory*, Journal of Fluid Mechanics, **345**, 45 (1997).

[3] J. M. Burgess, A. Juel, W. D. McCormick, J. B. Swift, H. L. Swinney, *Suppression of Dripping from a Ceiling*, Phys. Rev. Lett., **86**, 1203 (2001).

[4] S. Srivastava, D. Bandyopadhyay, A. Sharma, *Embedded Microstructures by Electric-Field-Induced Pattern Formation in Interacting Thin Layers*, Langmuir, **26**, 10943 (2010).

The effect of heat flux from bottom on the thermal convection of silicon melt in shallow annular pool

F. Wang[1] and L. Peng[1]

[1]*College of Power Engineering, Chongqing university, Chongqing 400044, China*
wf20061002010@hotmail.com

Surface tension gradient generated by temperature inhomogeneity results in Marangoni-thermocapillary convection, it exists and plays a very important role in nature and many engineering technology fields, such as thin-film coating, evaporation and single crystal growth from melt. According to geometry relation between free surface and temperature gradient, the convection induced by surface tension gradient was categorized into two types: one is Marangoni convection induced by temperature gradient perpendicular to the free surface. The other is thermocapillary convection induced by temperature gradient parallel to the free surface. Many researchers have studied these two convections separately [1, 2], however, normal and tangential temperature gradients often coexist in nature and engineering field. Therefore, in this paper we study Marangoni-thermocapillary convection of silicon melt in annular layer with numerical simulation method under the condition of bidirectional temperature gradients coexistence and focus on the effect of heat flux from bottom. Tangential temperature difference is fixed at 6K while heat flux from bottom varies. The results show melt state goes through three stages with heat flux increases: steady while the minimum temperature in melt is lower than crystallization temperature, steady while the minimum temperature in melt is higher than crystallization temperature and unsteady while the minimum temperature in melt is higher than crystallization temperature. Two critical heat flux values exist in this stage change process, melt state skips to the next stage when heat flux exceeds critical value. The first critical value is between $32950w/m^2$ and $33000w/m^2$. The second critical value gotten by linear extrapolation method is $41511w/m^2$. Uneven distribution of temperature enhancessurface temperature increases and flow becomes stronger with increase of heat flux when melt is steady. When melt is unsteady, the temperature of monitoring point is oscillatory.

---

[1] M. F. Schatz, G. P. Neitel, *Experiments on thermocapillary instabilities*, Annu Rev.Fluid Mech., **33**, 93 – 129 (2001).

[2] Y. R. Li, N. Imaishi, T. Azami, et al, *Three-dimensional oscillatory flow in a thin annular pool of silicon melt*, J. Crystal Growth, **260**, 28 – 42 (2004).

Wavelet analysis of imperfect symmetries of nonlinear patterns in Marangoni flows

I. I. Wertgeim[1] and V. G. Zakharov[1]

[1]*Institute of Continuous Media Mechanics, Ural Branch RAS, Acad. Korolyov St. 1, 614013, Perm, Russia,*
wertg@icmm.ru, victor@icmm.ru

The nonlinear processes in unstable hydrodynamic flows frequently show the formation of different kinds of spatial structures, and at growing supercriticality value, lead to patterns starting from simple ones, formed by regular rolls, hexagons or rectangles, changing by more complex, organised as domains with defects, and then by strongly irregular patterns.

Well known examples are patterns on the fluid surface due to nonlinear development of the instability of Marangoni and thermogravitational convection, Faraday ripples, magnetic domains, large-scale structure of the Universe etc. [1]. These patterns usually can be described as obtained by applying some global deformation and including local defects to the regular structure arising above the instability threshold. In the almost regular case these patterns could be characterized by the some spatially dependent macroscopic order parameters, like amplitude and local wave-vector field, and the continuous wavelet transform supplies a convenient method to extract them from microscopic field variables [1]. The possibility of description of sufficiently irregular spatial structures and their evolution by means of continuous two-dimensional wavelet transform was shown earlier [2]. This method is based on using directional wavelets such as Morlet or Cauchy wavelet [3], which have additional rotation parameter, except the usual translations and dilations. Main tool for analyzing symmetries of the structure is its scale-angle measure [2, 3] which may be considered as a partial energy density in the scale and angle variables. Directional wavelets allow to determine rotation-dilation symmetries of patterns, even approximate or local ones. This technique could also be used for uncovering hidden symmetries of structures (like quasicristal symmetries). The wavelet transform allows also to directly compute important characteristics of the patterns, including the wavenumber histograms, correlation lengths, and provides also an effective way to detect and to locate point singularities of the structure. It is possible to compute topological quantities like twist and circulation in order to classify the types of singularities.

Main focus in this report will be on Marangoni convection flows, which show at growing Marangoni number the sequence of instabilities of ground states leading to complex patterns, including mixing structures of hexagons, rolls and squares and to irregular large-scale structures of Voronoi tesselation type [4, 5]. In the present study our main goal is to determine contribution of patterns of different symmetries, like hexagons, rectangular cells etc. to the whole structure, to reveal hidden symmetries of these specific structures and to find the global characteristics of pattern symmetry.

This work was supported by the grant of Russian Foundation for Basic Research No. 12-01-00608.

---

[1] C. Bowman, A. C. Newell, *Natural patterns and wavelets*, Rev. Mod. Phys., **70**, 289–301 (1998).

[2] V. G. Zakharov, I. I. Wertgeim, *Wavelet scale-angle analysis of hydrodynamic irregular patterns similar to Voronoi tesselations*, Advances in Turbulence IX - Proceedings of the Ninth European Turbulence Conference, CIMNE , Barcelona, 103–106 (2002).

[3] J.-P. Antoine, R. Murenzi, *Two-dimensional directional wavelet and the scale-angle representation*, Signal Processing, **52**, 259–281 (1995).

[4] A. Juel, J. Burgess, M. W. D. McCormick, J. B. Swift, H. L. Swinney, *Surface tension-driven convection patterns in two liquid layers*, Physica D, **143**,169–186 (2000).

[5] M. F. Schatz, G. Paul Neitzel, *Experiments on thermocapillary instabilities*, Annu. Rev. Fluid Mech., **33**, 93–127 (2001).

Numerical investigation for the direction of thermocapillary flow in a cooled circular water film

T. Yamamoto,[1] Y. Takagi,[1] Y. Okano,[1] and S. Dost[2]

[1]*Department of Materials Engineering Science, Osaka University, 1-3 Machikaneyama, Toyonaka, Osaka 560-8531, Japan,*
okano@cheng.es.osaka-u.ac.jp

[2]*Crystal Growth Laboratory, University of Victoria, British Columbia V8W 3P6, Canada,*
sdost@uvic.ca

Dr. D. Pettit conducted a thermocapillary flow experiment in a water film sustained in a circular wire on the International Space Station (ISS) in 2003. In the experiment the developed flow in the film was towards the heated section of the wire, which is contrary to what is usually observed in thermocapillary flows [1]. The direction of such flows was investigated experimentally in a rectangular film in 2010 [2], in space experiment in 2011-2012 [3], and numerically in 2013 [4]. It was found that the ratio of the liquid film volume to that of the flat liquid film is related to the flow direction. In the rectangular film experiment conducted by Ueno *et al.* [2], one side of the frame was heated and the other side was cooled. To have a better understanding and validate the mechanism proposed in Yamamoto *et al.* [4], it was considered necessary to study the phenomena occurring on the cooled side of the film. In the present study, the direction of thermocapillary flow in a water film sustained in a circular ring was numerically simulated when a part of the water film was cooled. Details of the numerical procedure can be found in our previous study [4]. In the present simulation only the boundary condition was different from that of [4], namely the negative heat flux was applied instead of the positive heat flux.

The computed streak lines and temperature distribution at 5 s are shown in Fig. 1. As seen, the developed flow direction depends on the free surface shape even in the cooled water film section. However, the developed flow direction in the cooled film was opposite to that in the heated film. In the case of a concave film ($V/V_0 < 1$), the developed flow was towards the cooled area, in the case of a flat film ($V/V_0 = 1$), no flow developed in the center region, and in the case of a convex film ($V/V_0 > 1$), the developed flow was towards the center of the water film. Results show that the flow direction is related to the free surface shape even in the cooled water film, which explains the mechanism proposed in [4].

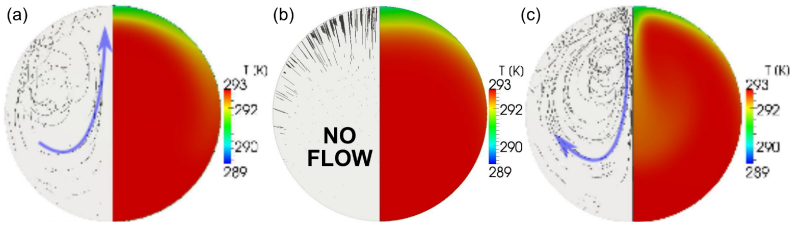

FIG. 1. Streak lines (left) and temperature distribution (right) at 5 s; (a) concave, (b) flat, and (c) convex film.

[1] D. Pettit, *Staturday Morning Science*, (see http://mix.msfc.nasa.gov/IMAGES/QTVR/0601211.mov) (2003).
[2] I. Ueno, T. Katsuta, T. Watanabe, *Flow patterns induced by thermocapillary effect in thin free liquid film accompanying with static/dynamic deformations*, Proceedings of the 2nd European Conference on Microfluidics, 10-203 (2010).
[3] D. Pettit, *Thin Film Physics*, (see http://physicscentral.com/explore/sots/episode3.cfm) (2011).
[4] T. Yamamoto, Y. Takagi, Y. Okano, S. Dost, *Numerical investigation for the effect of the liquid film volume on thermocapillary flow direction in a thin circular liquid film*, Phys. Fluids, **25**, 082108 (2013).

Effect of liquid bridge shape on the oscillatory thermal Marangoni convection

T. Yano[1] and K. Nishino[1]

[1] *Yokohama National University, 79-5 Tokiwadai, Hodogaya-ku,Yokohama, Japan,*
yano-taishi-rn@ynu.jp, nish@ynu.ac.jp

Instability and associated flow structures of thermal Marangoni convection in liquid bridge depend on various factors (e.g. liquid bridge shape, ambient gas conditions, physical properties of working fluid). A liquid bridge of high Prandtl number fluid is suspended between two coaxial disks heated differentially, and the aspect ratio, AR, and the volume ratio, VR, are commonly used to characterize the shape of liquid bridge, where AR is the ratio of the liquid bridge height to the disk diameter and VR is the ratio of the liquid volume to the cylindrical gap volume. It is well known that both AR and VR strongly affect the instability and flow structures of Marangoni convection [1, 2], but their effectiveness is considered separately in the previous studies. In the present study, onset conditions of oscillatory Marangoni convection are measured for various combinations of AR and VR to clarify their interrelated effects on the onset of instability.

Silicone oils with the kinematic viscosity of 2 or 5cSt at 25°C (Shin-Etsu Chemical Co., Ltd., KF-96) are used as a working, which is seeded with small tracer particles within the concentration of 0.05volume%. A liquid bridge is formed between a cooled aluminum disk and a transparent heated sapphire disk. Both temperature of the cooled and the heated disks is feedback controlled with the accuracy of 0.5K. Three CCD cameras observe the liquid bridge shape and flow field, one is mounted above the heated disk and the others are mounted on the side. Onset of oscillatory flow is detected by using particle image and temperature signal, the former is obtained by the top view CCD camera and the latter is obtained by the temperature signal of a fine thermocouple sensor placed near the liquid surface. Note that the liquid bridge is surrounded by a rectangular plastic box to avoid the disturbance from ambient.

Figure 1 shows the relationship between critical Marangoni number, Ma_{cH} $(= |\sigma_T|\Delta T H/(\rho\nu\alpha))$, and VR for various AR, where σ_T is the temperature coefficient of surface tension, ΔT the temperature difference between disks, H the disk distance, ρ the density, ν the kinematic viscosity and α the thermal diffusivity. The present data indicate that Ma_{cH} has a local peak at a certain VR and its position shifts to larger VR with increasing AR. To understand the relation between AR and VR, a new dimensionless quantity, $SDR(= L/D_0)$ is proposed. It is the ratio of liquid bridge surface length, L, to the liquid bridge neck diameter, D_0. Figure 2 shows the plot of Ma_{cL} as the function of SDR. Note that L is used as the characteristic length in Ma_{cL} instead of H. All results from different AR fall onto a single curve, thus suggesting that the relation between AR and VR can be specified by using SDR.

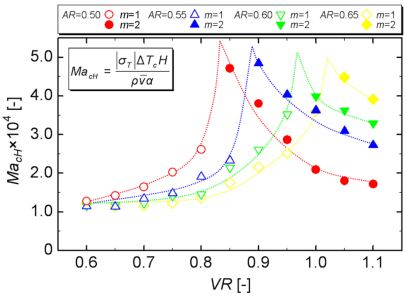

FIG. 1: Ma_{cH} vs. VR.

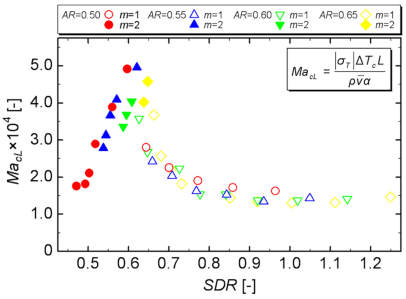

FIG. 2: Ma_{cL} vs. SDR.

[1] R. Velten, D. Schwabe, A. Scharmann, *The periodic instability of thermocapillary convection in cylindrical liquid bridge*, Phys. Fluids A, **3**, 267–279 (1991).

[2] W. R. Hu, J. Z. Shu, R. Zhou, Z. M. Tang, *Influence of liquid bridge volume on the onset of oscillation in floating zone convection I. Experiments*, J. Cryst. Growth, **142**, 379–384 (1994).

Experimental and numerical observations of surface deformation during drying of polymer solutions due to Marangoni phenomena

S. G. Yiantsios,[1] S. K.Serpetsi,[1] F. Doumenc,[2] S. Mergui,[2] and B. Guerrier[2]

[1]*Department of Chemical Engineering, Aristotle University of Thessaloniki, Univ. Box 453, GR 541 24, Thessaloniki, Greece,*
yiantsio@auth.gr

[2]*Univ Paris-Sud, Univ Paris 06, CNRS, Lab FAST, Bât 502, Orsay, F-91405, France,*
doumenc@fast.u-psud.fr

Experimental observations [1, 2] on the drying of polymer solution films under conditions of controlled evaporation of the volatile solvent are analyzed. The physicochemical and transport properties of the solutions are strongly dependent on polymer concentration, most notably the solution viscosity which increases by several orders of magnitude over the course of the experiments. Over a range of conditions, namely for relatively, yet not overly, small initial film thicknesses and evaporation rates, the dynamics is dominated by solutocapillary driving forces and wrinkling of the films takes place during a final stage. During this stage the interfacial polymer concentration approaches a certain threshold marking a significant reduction in the evaporation rate and the cessation of fluid motion. It has been observed qualitatively that the final dried films are accordingly patterned. The objective of the study is to find out the involved mechanisms for the selection of wavelengths and pattern amplitudes, through in-situ observation of the free surface deformation during drying (see FIG. 1) and through numerical simulations. Numerical simulations of the solutocapillary phenomena are performed taking into account the variability of the transport properties and the deformation of the film interface [3]. The simulations suggest that at relatively low Marangoni numbers the mechanism of Overdiep [4] may be responsible for the final film wrinkling, whereas at sufficiently high Marangoni numbers the fine cellular structure of the Pearson mechanism dominates [5, 6] but interfacial deformation is inhibited by strong capillary pressure forces. Yet, this mechanism results in nonuniform distribution of the solute along the thin film. Hence, the numerical simulations corroborate the analysis of the experimental observations in the suggestion that the cellular instability is responsible for the uneven distribution of the solute and for the uneven profile of the dried polymeric deposit.

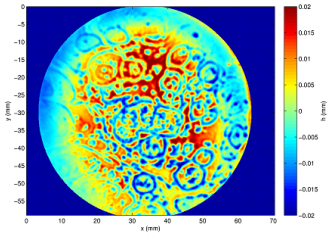

FIG. 1. Visualisation of the free surface deformation using a Schlieren method [7, 8]. Image corresponding to the end of drying for a PIB/toluene solution, with initial conditions h_0 = 1.1mm, Φ_{P0} = 0.05 Δ h_{max} (red to dark blue colors)$\sim$ 40 μm.

[1] F. Doumenc, E. Chénier, B. Trouette, T. Boeck, C. Delcarte, B. Guerrier, M. Rossi, *Free convection in drying binary mixtures: solutal versus thermal instabilities*, IJHMT, **63**, 336-350 (2013).

[2] N. Bassou, Y. Rharbi, *Role of Bénard-Marangoni Instabilities during Solvent Evaporation in Polymer Surface Corrugations*, Langmuir, **25**, 624-632 (2009).

[3] S. K. Serpetsi, S. G. Yiantsios, *Stability characteristics of solutocapillary Marangoni motion in evaporating thin films*, POF, **24** (2012).

[4] W. S. Overdiep, *The leveling of paints*, Prog. Org. Coatings, **14**, 159-175 (1986).

[5] J. R. A. Pearson, *On convection cells induced by surface tension*, J. Fluid Mech., **4**, 489-500 (1958).

[6] P. G. de Gennes, *Instabilities during the evaporation of a film: Non-glassy polymer+ volatile solvent*, Eur. Phys. J. E, **6**, 421 (2001).

[7] F. Moisy, M. Rabaud, K. Salsac, *A Synthetic Schlieren method for the measurement of the topography of a liquid interface*, Exp. Fluids, **46(6)**, 1021-1036 (2009).

[8] P. Cavadini, J. Krenn, P. Scharfer, W. Schabel, *Investigation of surface deformation during drying of thin polymer films due to Marangoni convection*, Chem. Eng. Proc., **64**, 24-30 (2013).

Local corrosion of SiO_2(s) driven by Marangoni convection in the melting liquid surface systems

Z. Yuan,[1] Y. Wu,[1] K. Mukai,[1] and B. Xu[1]

[1]*Department of Energy and Resources Engineering, College of Engineering, Peking University, 5 Yi He Yuan Road, Haidian District, Beijing 100871, China,*
zfyuan@pku.edu.cn

As reported that the cross section shape of silica prism solids will maintain the original square or become round after a certain duration of dipping and corrosion in certain melts, the two kinds of phenomena along with their mechanism driven by Marangoni convection was proposed in this paper. The corrosion rate of local corrosion was calculated to explain the mechanism of Marangoni convection. There are two typical solid-liquid systems attributed by their motion patterns as a result of Marangoni flow: one is that silica prism solid dipped in Fe_xO-SiO_2 slag or silicon melt maintains its original square shape during its corrosion and dissolution with the liquid surface moving down-and-up almost simultaneously on the four lateral faces; the other is that silica prism solid dipped in PbO-SiO_2 slag transforms the cross section shape of the sample from the original square to the near round while the melts surface has the up-and-down motion that the liquid climbs mainly along the edges and meets on the lateral faces, returning to the bulk. It is Marangoni effect that results in such phenomena and difference: in the former pattern, the beginning surface tension of the liquid near the solid prism is larger than that of the bulk, Marangoni flow caused by surface tension gradient of molten SiO_2 dominates that by axial concentration gradient caused by different corrosion rate; while in the latter one the beginning situation of the surface tension and axial concentration gradient is just the opposite, the former makes for liquid film downward motion, wettability and axial concentration gradient is responsible for the upward motion.

Threshold initiation of solutocapillary Marangoni convection near air-bubble surface in horizontal rectangular channel

M. O. Denisova,[1] K. G. Kostarev,[1] A. L. Zuev,[1] and A. Viviani[2]

[1]*Institute of Continuous Media Mechanics UB RAS, Acad. Korolev Str. 1, 614013 Perm, Russia,*
zal@icmm.ru

[2]*Seconda Università di Napoli, via Roma 29, I-81031 Aversa, Italy,*
antonio.viviani@unina2.it

It is generally assumed that the surface of a Newtonian fluid under the action of the capillary forces begins to move at any arbitrarily small shear stress. However, our previous experiments show that in fact the solutocapillary fluid flow was initiated by a certain (threshold) gradient of the surface tension occurring on the surface [1, 2]. The value of surface tension gradient increases rapidly with decreasing surface area of the fluid. A threshold nature of the Marangoni convection leads to delay in its development in case when the surfactant distribution along the interface becomes inhomogeneous. Such an abnormal behavior can be caused by the adsorption of uncontrolled surface-active impurities initially contained in the fluid. These impurities form the "solid" adsorption film exhibiting rheological (viscoplastic) properties. The composition and amount of impurities absorbed on the surface are dependent on the degree of purification of the fluid and the value of its surface tension. Under such conditions the capillary motion occurs only in the case of applying a rather high shear stress capable of removing film from a part of the fluid surface by way of its deformation or destruction.

In this study, we performed a series of experiments in order to analyze the peculiarities of the fluid flow developed under such conditions [3]. The threshold initiation of the oscillatory modes of the solutal Marangoni convection near a stationary air bubble was investigated. In the experiments, the bubble was placed in a horizontal channel of small cross-section filled with an aqueous solution of a surfactant with non-uniform concentration stratification. As a surfactant, we used several monoatomic alcohols, which made it possible to investigate the influence of their physicochemical characteristics, such as surface activity (the value of concentrational coefficient of the surface tension) and solubility in water. These characteristics affected the frequency of onsets of the capillary convection near the bubble, convection intensity, the ratio of the capillary to buoyancy flow times, duration of the oscillatory mode, the threshold stress value, and the relevant critical Marangoni number. It has been found that the value of the threshold difference in surfactant concentration adjoined to the bubble lateral surface decreases with an increasing level of water purification. The increase of alcohol initial concentration as well as the growth of the surface activity of monoatomic alcohols with the length of its molecule also reduces the threshold value. On the contrary, the threshold difference rapidly grows with the decrease of the characteristic dimensions of the free surface. Subdivision of the oscillation period into two intervals associated with different driving mechanisms of motion led us to conclusion that the oscillatory mode terminates with a transition to a monotonic flow, not to a quiescent state, as we previously suspected proceeding from the analysis of interferograms in [1].

The work was supported by Russian Foundation for Basic Research (grant # 12-01-00656), collaborative project of SB, UB and FEB of RAS # 12-C-1-1006 and the Program for International Research Teams of the Ministry of Science and Education of Perm region (project # -26/210).

[1] R. V. Birikh, A. L. Zuev, K. G. Kostarev, R. N. Rudakov, *Convective self-oscillations near air-bubble surface in horizontal rectangular channel*, Fluid Dynamics, **41**, 514–520 (2006).

[2] A. Mizev, M. Denisova, K. Kostarev, R. Birikh, A. Viviani, *Threshold onset of Marangoni convection in narrow channels*, Eur. Phys. J. Special Topics, **192**, 163–173 (2011).

[3] M. O. Denisova, K. G. Kostarev, *Initiation of motion in a fluid with a free surface of small area*, Procedia IUTAM, **8**, 75–84 (2013).

Part III

INDICES & MAPS

List of Participants

Amiroudine, Sakir
University of Bordeaux
12M-Site ENSCBP, 16 Avenue Pey Berland
33607, Pessac, France
sakir.amiroudine@u-bordeaux.fr

Aslam, Raheema
University of Navarra
Department of Physics and Applied Mathematics
Pamplona, Spain
rmuhammad@alumni.unav.es

Batishchev, Vladimir A.
Southern Federal University
Milchakova 8a, Rostov-na Donu
Russia
batishev-v@mail.ru

Batson, William R.
Department of Mechanical Engineering
Technion-Israel Institute of Technology
Haifa 32000, Israel
wbatson@gmail.com

Beladi, Behnaz
Technical University Wien
Institute for Fluid Mechanics and Heat Transfer
Resselgasse 3
1040, Wien, Austria
behnaz.beladi@tuwien.ac.at

Beltrame, Philippe
Université d'Avignon
Department of Physique / UMR EmmaH
33 rue Pasteur
84000, Avignon, France
philippe.beltrame@univ-avignon.fr

Benilov, Eugene
University of Limerick
Department of Mathematics and Statistics
29 Salmon Wier, Annacotty, Limerick, Ireland
eugene.benilov@ul.ie

Bestehorn, Michael
BTU Cottbus-Senftenberg
Department of Theoretical Physics
Erich-Weinert-Straße 1
03046, Cottbus, Deutschland
bes@physik.tu-cottbus.de

Borcia, Ion Dan
BTU Cottbus-Senftenberg
Erich-Weinert-Straße 1
03046, Cottbus, Germany
borciai@tu-cottbus.de

Borcia, Rodica
BTU Cottbus-Senftenberg
Erich-Weinert-Straße 1
03046, Cottbus, Germany
borciar@tu-cottbus.de

Bouhedja, Samia
Université de Constantine
Faculté des Sciences de la Technologie
Laboratoire des Hyperfréquences
et Semiconducteurs
Département d'Electronique
Route Ain El Bey
25017, Constantine, Algeria
bouhedja_samia@yahoo.fr

Carballido-Landeira, Jorge
Université Libre de Bruxelles
Nonlinear Physical Chemistry Unit
Service de Chimie Physique
et Biologie Théorique CP231
1050, Bruxelles, Belgium
jorge.carballido@gmail.com

Chen, Huanchen
University of Alberta
Department of Mechanical Engineering
4-9 Mechanical Engineering Building
University of Alberta Edmonton
AB, T6G 2G8, Canada
hchen9@ualberta.ca

Cheremnih, Elena
Siberian Branch
of the Russian Academy of Sciences
Institute of Computational Modelling
Akademgorodok, 660036, Krasnoyarsk, Russia
elena_cher@icm.krasn.ru

D'Alessio, Serge
University of Waterloo
Faculty of Mathematics
200 University Avenue West, Waterloo
N2L 3G1, Canada
sdalessio@uwaterloo.ca

Buffone, Cosimo
Université Libre de Bruxelles
Microgravity Research Centre
Avenue F. Roosevelt 50
1050, Bruxelles, Belgium
cbuffone@ulb.ac.be

Cerisier, Pierre
Aix-Marseille University
5 rue Enrico Fermi
13453, Marseille, France
cerisier@polytech.univ-mrs.fr

Chen, Jie
Chinese Academy of Sciences
Key Laboratory of Green Process
and Engineering
Institute of Process Engineering
100190, Beijing, China

Conn, Justin
University of Strathclyde
Department of Mathematics and Statistics
26 Richmond Street
G1 1XH, Glasgow, Scotland, UK
justin.conn@strath.ac.uk

De Dier, Raf
Katholieke Universiteit Leuven
Soft Matter, Rheology and Technology
Chemical Engineering
Willem de Croylaan 46
3001, Heverlee, Belgium
raf.dedier@cit.kuleuven.bc

Denner, Fabian
Imperial College London
Department of Mechanical Engineering
Thermofluids Section
Exhibition Road, SW7 2AZ
London, United Kingdom
f.denner09@imperial.ac.uk

Dietze, Georg F.
Chargé de Recherche CNRS
Laboratoire FAST
Bât 502. Campus Universitaire
F-91405, Orsay, France
dietze@fast.u-psud.fr

Doumenc, Frédéric
University Pierre and Marie Curie
Campus Universitaire Bât 502
91405, Orsay, France
doumenc@fast.u-psud.fr

Duan, Fei
Nanyang Technological University
School of Mechanical and Aerospace Engineering
50 Nanyang Avenue
639798, Singapore
feidua@ntu.edu.sg

El Bouz, Moustafa Aly
National Research University"MPEI"
Energeticheskaya st. 14-4
111116, Moscow, Russia
mostafa_booz@yahoo.com

Eribol, Pinar
Bogazici University
Department of Chemical Engineering
Bebek
34100, Istanbul, Turkey
pinareribol@gmail.com

Fan, Ping
Chinese Academy of Sciences
Institute of Process Engineering
Zhongguancun North Street 1
100190, Beijing, China
pfan@ipe.ac.cn

Frumkin, Valeri
Technion-Israel Institute of Technology
Department of Mathematics
Haifa 32000, Israel
valerafr@gmail.com

Fujimura, Kaoru
Tottori University
Department of Applied Mathematics and Physics
Tottori 680-8552, Japan
kaoru@damp.tottori-u.ac.jp

Fumoto, Koji
Hirosaki University
Department of Intelligent Machines
and Engineering
3 Bunkyo-cho
0368561, Hirosaki, Japan
kfumoto@cc.hirosakiu.ac.jp

Gaponenko, Yuri
Université Libre de Bruxelles
Microgravity Research Center
Avenue F.D. Roosevelt 50
1050, Brussels, Belgium
ygaponen@ulb.ac.be

Goncharova, Olga
Altai State University
Department of Differential Equations
pr. Lenina 61
656049, Barnaul, Russia
gon@math.asu.ru

Gotoda, Masakazu
Tokyo University of Science
Division of Mechanical Engineering
Graduate School of Faculty of Science
& Technology
2641 Yamazaki, Noda
278-8510, Chiba, Japan
a7510049@rs.tus.ac.jp

Herrada, Miguel A.
E.S.I, University of Seville
Camino de los Descubrimientos s/n
41092, Seville, Spain
herrada@us.es

Imaishi, Nobuyuki
Kyushu University
Institute for Materials Chemistry & Engineering
Room 110, Building E
6-1 Kasugakoen, Kasuga City
818-8580, Kasuga, Japan
imaishi@cm.kyushu-u.ac.jp

Jehannin, Marie
MPI of Colloids and Interfaces& CEA
MPIKG, Am Mühlenberg 1
14476, Potsdam, Germany
marie.jehannin@cea.fr

Karacelik, Asli
Bogazici University
Department of Chemical Engineering
Nispetiye Cad. Peker S. No 54 D13, 1. Levent
34330, Istanbul, Türkey
asli.karacelik@hotmail.com

Khaleghi, Mohammad Reza Akhavan
Mashhad,Iran
rfemcfd@gmail.com

Grishaev, Victor
Universitè Libre de Bruxelles
Microgravity Research Centre EP-CP165/62
1050, Brussels, Belgium
vgrishae@ulb.ac.be

Hofmann, Ernst
Technical University Wien
Institute of Fluid Mechanics and Heat Transfer
Resselgasse 3
1040, Wien, Austria

Ivanova, Natalia
Tyumen State University
Department of Radiophysics
Semakova 10
625003, Tyumen, Russia
n.ivanova@utmn.ru

Kanatani, Kentaro
Yokohama National University
Faculty of Engineering
79-5 Tokiwadai, Hodogaya
240-8501, Yokohama, Japan
kentaro@ynu.ac.jp

Karapetsas, George
University of Thessaly
Department of Mechanical Engineering
38334, Volos, Greece
gkarapetsas@gmail.com

Khayat, Roger
University of Western Ontario
Department of Mechanical
and Materials Engineering
990 Waterloo
N6A 3X5, London, Ontario, Canada
rkhayat@uwo.ca

Kocabiyik, Serpil
Memorial University St. John's
Department of Mathematics and Statistics
230 Elizabeth Evenue, St. John's
NL A1C 5S7 ,Canada
serpil@mun.ca

Kofman, Nicolas
Laboratory FAST, Bt 502, Rue du Belvédère
Campus Universitaire d'Orsay
91405, Orsay Cedex, France
kofman@fast.u-psud.fr

Köllner, Thomas
Technische Universität Ilmenau
Institute of Thermodynamics and Fluid Mechanics
Am Helmholtzring 1, Haus M
98693, Ilmenau, Deutschland
thomas.koellner@tu-ilmenau.de

Kondic, Lou
New Jersey Institute of Technology
Department of Mathematical Sciences
3 Christopher Ct.
07042, Montclair, USA
kondic@njit.edu

Kossov, Vladimir
al-Farabi Kazakh National University
Institute of Experimental and Theoretical Physics
al-Farabi av. 71
050038, Almaty, Kazakhstan
kosov_vlad_nik@list.ru

Kuhlmann, Hendrik
Technical University Wien
Institute of Fluid Mechanics and Heat Transfer
Resselgasse 3
1040, Wien, Austria
h.kuhlmann@tuwien.ac.at

Kumar, Satish
University of Minnesota
Department of Chemical Engineering
and Materials Science
55455, Minneapolis, MN,USA
kumar030@umn.edu

Lavrenteva, Olga
Technion-Israel Institute of Technology
Technion City
32000, Haifa, Israel
ceolga@techunix.technion.ac.il

Lebedev-Stepanov, Peter
Photochemistry Center of
Russian Academy of Science
Novatorov St. 7a/1
119421, Moscow, Russia
petrls@yandex.ru

Lemee, Thomas
Technical University Wien
Institute of Fluid Mechanics and Heat Transfer
Resselgasse 3
1040, Wien, Austria
thomas.lemee@tuwien.ac.at

Liu, Chao
Institute of Applied Physics
and Computational Mathematics
Beijing 100094, China

Liu, Qiu-Sheng
Chinese Academy of Sciences
Institute of Mechanics
Bei-Si-Huan-Xi Road No.15
Beijing, China
liu@imech.ac.cn

Liu, Rong
Chinese Academy of Sciences
Key Laboratory of Microgravity
(National Microgravity Laboratory)
Institute of Mechanics
100190, Beijing, China
liurong@imech.ac.cn

Makarov, Peter G.
National Research University "MPEI"
Moscow, Russia

Mayur, Manik
Offenburg University of Applied Sciences
Badstraße 24.
77652, Offenburg, Germany
manik.mayur@hs-offenburg.de

Melnikov, Denis
Université Libre de Bruxelles, MRC
F.D.Roosevelt 50, CP-165/62
1050, Brussels, Belgium
dmelniko@ulb.ac.be

Messmer, Brad
University of Florida
1245 SW 9th Road, Apt. 103
32608, Gainesville FL, USA
bmessmer123@gmail.com

Mizev, Aleksey
Institute of Continuous Media Mechanics
Ural Branch of Russian Academy of Science
Acad. Koroleva Str 1
614013, Perm, Russia
alex_mizev@icmm.ru

Lyubimova, Tatyana
Ural Branch of the Russian Academy of Science
Institute of Continuous Media Mechanics
Koroleva Str.
614013, Perm, Russia
lubimova@psu.ru

Matsumoto, Satoshi
Japan Aerospace Exploration Agency
Institute of Space and Astronautical Science
2-1-1 Sengen, Tskuva, Ibaraki
3058505,Japan
matsumoto.satoshi@jaxa.jp

Medale, Marc
Université Aix-Marseille and CNRS
5 rue Enrico Fermi
13453,Marseille,France
marc.medale@univ-amu.fr

Mergui, Sophie
University of Paris-Sud
University Paris 06, CNRS
Lab FAST, Bât 502Orsay, France
mergui@fast.u-psud.fr

Mikishev, Alexander
Sam Houston State University
Department of Physics
5550 N. Braeswood apt. 65
Houston, Texas, 77096, USA
amik@shsu.edu

Montanero, José Maria
University of Extremadura
Department of Mechanical, Energy
and Materials Engineering
Avda. de Elvas s/n
06006, Badajoz, Spain
jmm@unex.es

Morozov, Matvey
Technion - Israel Institute of Technology
Klibanov 28-9
32000, Haifa, Israel
mmorozov@technion.ac.il

Muraoka, Masahiro
Tokyo University of Science
2641 Yamazaki, Nodashi
278-8510, Noda, Japan
masa@rs.noda.tus.ac.jp

Nepomnyashchy, Alexander
Technion - Israel Institute of Technology
Department of Mathematics
Technion City
32000, Haifa, Israel
nepom@techunix.technion.ac.il

Noguera-Marin, Diego
University of Granada
Faculty of Sciences, Biocolloid
and Fluid Physics Group
Applied Physics Department
Avenue De Fuentenueva s/n
18071, Grenada, Spain
dnogue@ugr.es

Oron, Alex
Technion - Israel Institute of Technology
Department of Mechanical Engineering
Haifa, 32000, Israel
meroron@tx.technion.ac.il

Pimienta, Véronique
University Paul Sabatier
IMRCP Toulouse, Bordeneuve
11320, Montmaur, France
pimienta@chimie.ups-tlse.fr

Muhammad Aslam, Rabeema
University of Navarra
Department of Physics and Applied Mathematics
c/Irunlarrea 1
31008, Pamplona, Navarra, Spain
rmuhammad@alumni.unav.es

Narayanan, Ranga
University of Florida
7914 SW 37th Pl.
32608, Gainesville, FL, USA
ranga@ufl.edu

Nesic, Svetozar
Universidad Carlos III de Madrid
Grupo Interdisciplinar de
Sistemas Complejos(GISC)
and Departamento de Matematicas
Avenida de la Universidad 30
28911, Leganés, Spain
snesic@math.uc3m.es

Nourani, Meysam
Norwegian University of Science and Technology
Ugelstad Laboratory
Department of Chemical Engineering (NTNU)
Kjemiblokk V, Sem Sælandsvei 4
NTNU Gløshaugen Trondheim, Norway
meysam.nourani@ntnu.no

Ovcharova, Alla
Siberian Branch
of the Russian Academy of Sciences
Lavrentyev Institute of Hydrodynamics
Novosibirsk, Russia
ovcharova@hydro.nsc.ru

Rednikov, Alexey
Université Libre de Bruxelles
TIPs, ULB, CP 165/67
1050, Brussels, Belgium
aredniko@ulb.ac.be

Riegler, Hans
MPI of Colloids and Interface
Am Mühlenberg
14476, Potsdam, Germany
hans.riegler@mpikg.mpg.de

Rietz, Manuel
RWTH Aachen University
Institute of Heat and Mass Transfer
Augustinerbach 6
52056, Aachen, Germany
rietz@wsa.rwth-aachen.de

Rohlfs, Wilko
RWTH Aachen University
Institute of Heat and Mass Transfer
Augustinerbach 6
52056, Aachen, Germany
rohlfs@wsa.rwth-aachen.de

Romanò, Francesco
Technical University Wien
Institute of Fluid Mechanics and Heat Transfer
Resselgasse 3
1040, Wien, Austria
francesco.romano@tuwien.ac.at

Roushangar, Kiyoumars
University of Tabriz
Civil Engineering Department
9841151388, Iran
roshangari@tabrizu.ac.ir

Samoilova, Anna
Perm State University
Department of Theoretical Physics
Krasnovodskaya 24-249
614067, Perm, Russia
annsomeoil@gmail.com

Schneider, Wilhelm
Technical University Wien
Institute of Fluid Mechanics and Heat Transfer
Resselgasse 3
1040, Wien, Austria
wilhelm.schneider@tuwien.ac.at

Schwabe, Dietrich
Physikalisches Institut der
Justus-Liebig-Universität Giessen
Fontaneweg 20
35398, Giessen, Germany
dietrich.schwabe@
physik.uni-giessen.de

Schwarzenberger, Karin
Technical University Dresden
Institute of Fluid Mechanics
01062, Dresden, Germany
karin.schwarzenberger@
tu-dresden.de

Sempels, Wouter
Katholieke Universiteit Leuven
Departement of Chemistry
Celestijnenlaan 200F
3001, Heverlee, Belgium
wouter.sempels@chem.kuleuven.be

Serraiocco, Luigi
Yara International
Yara Technology Centre, B92
P.O. Box 1130
3905, Porsgrunn, Norway
luigi.serraiocco@yara.com

Shevtsova, Valentina
Université Libre de Bruxelles
MRC, EP CP - 165/62
Avenue F.D. Roosevelt 50
1050, Brussels, Belgium
vshev@ulb.ac.be

Shi, Yi-Na
Institute of Applied Physics
and Computational Mathematics
100094, Beijing, P.R. China
shyn@iapcm.ac.cn

Smorodin, Boris
Perm State University
Bukirev str. 15
614990, Perm, Russia
bsmorodin@yandex.ru

Soulié, Virginie
MPI of Colloids and Interfaces
14424, Potsdam-Golm, Germany
virginie.soulie@mpikg.mpg.de

Starov, Victor
Loughborough University
Department of Chemical Engineering
Ashby Rd., Loughborough, UK
v.m.starov@lboro.ac.uk

Uguz, Kerem
Bogazici University
Department of Chemical Engineering
Bebek
34342, Istanbul, Turkey
kerem.uguz@boun.edu.tr

Wang, Fei
Chongqing University
College of Power Engineering
400044, Chongqing, China
wf20061002010@hotmail.com

Shklyaev, Sergey
Ural Branch of Russian Academy of Science
Institute of Continuous Media Mechanics 1
Ak. Korolev str.
614013, Perm, Russia
shklyaev@yandex.ru

Son, Gihun
Sogang University 121742
Seoul, South Korea
gihun@sogang.ac.kr

Stankous, Nina
National University, US
11255 N Torey Pines Rd.
92037-1011, La Jolla, CA, USA
nstankous@nu.edu

Ueno, Ichiro
Tokyo University of Science
Department of Mechanical Engineering
Faculty of Science& Technology
2641 Yamazaki, Noda
278-8510, Chiba, Japan
ich@rs.tus.ac.jp

Vécsei, Miklós
Technical University Darmstadt
Center of Smart Interfaces, Nano-
and Microfluidics Group
Am Klingacker 7
64295, Darmstadt, Germany
vecsei@csi.tu-darmstadt.de

Ward, Kevin
University of Florida
134 SW 62nd Street, Apt. 618
32607, Bainesville, USA

Wertgeim, Igor
Ural Branch of Russian Academy of Science
Institute of Continuous Media Mechanics
Acad. Korolyov St. 1
614039, Perm, Russia
wertg@icmm.ru

Wu, Yan
Peking University
Department of Energy & Resources Engineering
College of Engineering 5
Yi He Yuan Road, Haidian District
100871, Bejing, China
zfyuan@pku.edu.cn

Xu, Bing Sheng
Peking University
Department of Energy & Resources Engineering
College of Engineering
5 Yi He Yuan Road, Haidian District
100871, Beijing, China
dengdaitiangingdeyu@126.com

Yamamoto, Takuya
Osaka University
Deptartment of Materials Engineering Science
1-3 Machikaneyama
560-8531, Toyonaka, Osaka, Japan
y-takuya@cheng-cs.osaka-u.ac.jp

Yano, Taishi
Yokohama National University
79-5 Tokiwadai, Hodogaya-ku
240-8501, Yokohama, Kanagawa, Japan
yano-taishi-rn@ynu.jp

Yiantsios, Stergios
Aristotle University of Thessaloniki
Department of Chemical Engineering
University Box 453
541 24, Thessaloniki, Greece
yiantsio@auth.gr

Yuan, Zhang Fu
Peking University
Department of Energy &
Resources Engineering
College of Engineering
5 Yi He Yuan Road, Haidian District
100871, Beijing, China
zfyuan@pku.edu.cn

Zuev, Andrew L.
Ural Branch of Russian Academy of Science
Institute of Continuous Media Mechanics
Acad. Korolev Str. 1
614013, Perm, Russia
za1@icmm.ru

Authors' Index

Maps


U-Bahn-Linie
S-Bahn-Linie
City Airport Train
Lokalbahn Wien–Baden
Kundenzentrum der Wiener Linien (U3-Station Erdberg)
Informationsstelle der Wiener Linien
Vorverkaufsstelle der Wiener Linien
Park & Ride
Gerasdorf
Leopoldau
Süßenbrunn
Brettenleer Straße
Hausfeldstraße
Hirschstetten
Erzherzog-Karl-Straße
Stadlau
Lobau
Prater Kai
Haidestraße
Simmering
Zentralfriedhof
Kaiserebersdorf
Schwechat
Kledering
Großfeldsiedlung
Aderklaaer Straße
Rennbahnweg
Kagraner Platz
Kagran
Siemensstraße
Floridsdorf
Brünner Straße
Strebersdorf
Jedlersdorf
Neue Donau
Alte Donau
Kaisermühlen-Vienna Int. Centre
Donauinsel
Vorgartenstraße
Messe Prater
Praterstern
Stadion
Kriau
Handelskai
Traisengasse
Dresdner Straße
Friedensbrücke
Roßauer Lände
Schottenring
Taborstraße
Nestroyplatz
Schwedenplatz
Stubentor
Stadtpark
Oper
Karlsplatz
Taubstummengasse
Südtiroler Platz
Südbahnhof
Keplerplatz
Reumannplatz
Landstraße (Wien Mitte)
Rochusgasse
Kardinal-Nagl-Platz
Schlachthausgasse
Erdberg
Gasometer
Zippererstraße
Enkplatz
Rennweg
St. Marx
Geiselbergstr.
Grillgasse
Jägerstraße
Franz-Josefs-Bahnhof
Schottentor
Rathaus
Herrengasse
Museumsquartier
Kettenbrückengasse
Philharmonikerstraße
Matzleinsdorfer Platz
Nußdorf
Heiligenstadt
Spittelau
Nußdorfer Straße
Währinger Straße-Volksoper
Michelbeuern-Allg. Krankenhaus
Alser Straße
Josefstädter Straße
Thaliastraße
Burggasse-Stadthalle
Westbahnhof
Zieglergasse
Volkstheater
Neubaugasse
Niederhofstraße
Philadelphiabr.
Meidling
Schedifkaplatz
Schöpfwerk
Gutheil-Schoder-G.
Inzdf. Personenbhf.
Neu Erlaa
Schönbrunner Allee
Vösendorf-Siebenhirten
Tschertteggasse
Am Schöpfwerk
Alterlaa
Erlaaer Straße
Perfektastraße
Siebenhirten
Oberdöbling
Krottenbachstr.
Cottage
Hutteldorfer Straße
Hütteldorfer Straße
Johnstraße
Schweglerstraße
Gumpendorfer Straße
Längenfeldgasse
Meidlinger Hauptstraße
Hietzing (Tiergarten)
Braunschweiggasse
Unter St. Veit
Ober St. Veit
Hütteldorf
Hadersdorf
Penzing
Breitensee
Hernals
Ottakring
Cottage
Cersthof
Speising
Hetzendorf
Inzersdorf
Atzgersdorf
Blumental
Liesing
Purkersdorf Sanatorium
Wolfingau

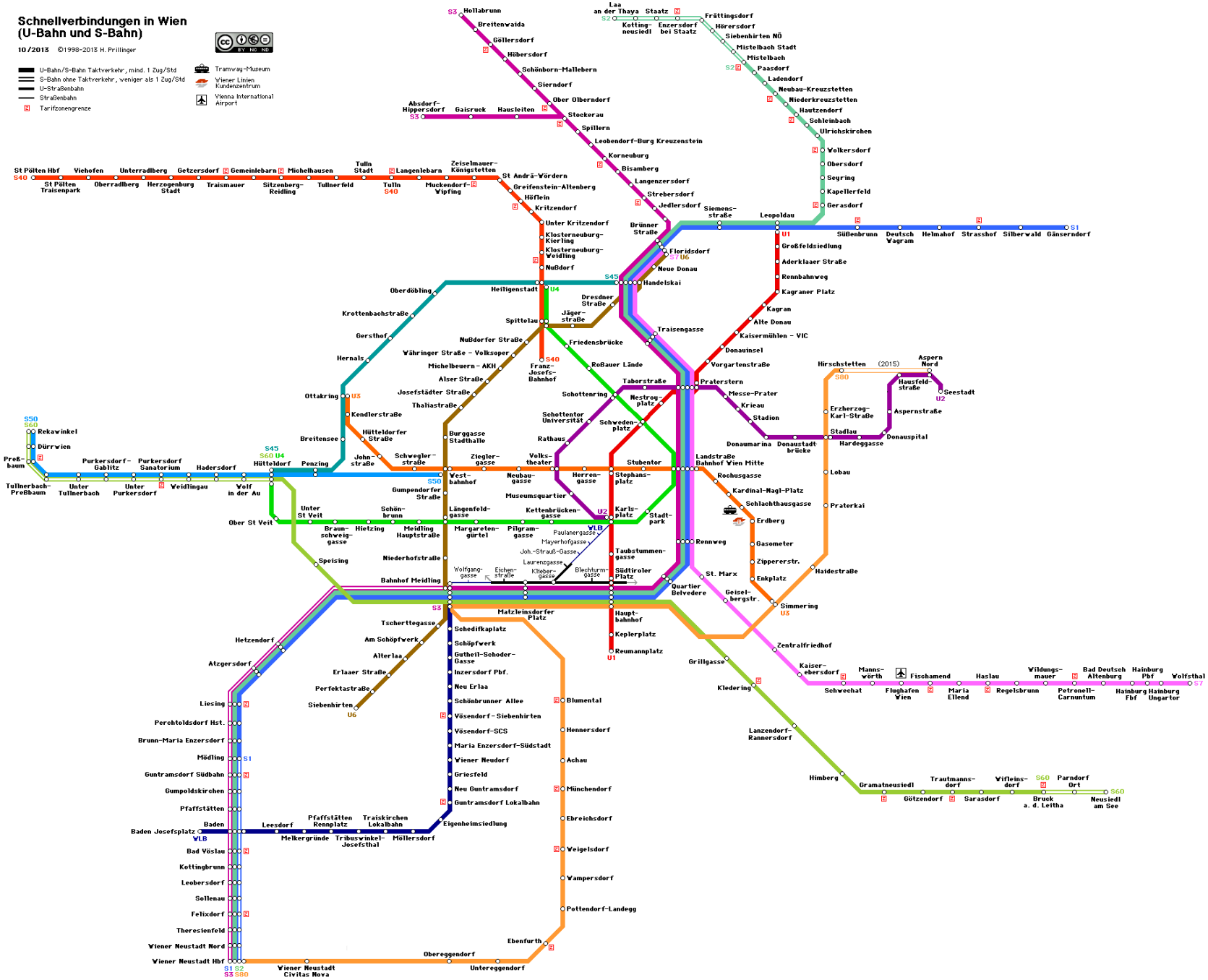
Schnellverbindungen in Wien
(U-Bahn und S-Bahn)
10/2013 ©1998-2013 H. Prillinger
U-Bahn/S-Bahn Taktverkehr, mind. 1 Zug/Std
S-Bahn ohne Taktverkehr, weniger als 1 Zug/Std
U-Straßenbahn
Straßenbahn
Tarifzonengrenze
Tramway-Museum
Wiener Linien Kundenzentrum
Vienna International Airport
S3 Hollabrunn
Breitenwaida
Göllersdorf
Höbersdorf
Schönborn-Mallebern
Sierndorf
Ober Olberndorf
Stockerau
Spillern
Leobendorf-Burg Kreuzenstein
Korneuburg
Bisamberg
Langenzersdorf
Strebersdorf
Jedlersdorf
Absdorf-Hippersdorf
Gaisruck
Hausleiten
Laa an der Thaya
S2 Kotting-neusiedl
Staatz
Enzersdorf bei Staatz
Frättingsdorf
Hörersdorf
Siebenhirten NÖ
Mistelbach Stadt
Mistelbach
Paasdorf
Ladendorf
Neubau-Kreuzstetten
Niederkreuzstetten
Hautzendorf
Schleinbach
Ulrichskirchen
Wolkersdorf
Obersdorf
Seyring
Kapellerfeld
Gerasdorf
St Pölten Hbf
S40 St Pölten Traisenpark
Viehofen
Unterradlberg
Oberradlberg
Getzersdorf
Herzogenburg Stadt
Gemeinlebarn
Traismauer
Michelhausen
Sitzenberg-Reidling
Tullnerfeld
Tulln Stadt
Tulln S40
Langenlebarn
Zeiselmauer-Königstetten
Muckendorf-Wipfing
St Andrä-Wördern
Greifenstein-Altenberg
Höflein
Kritzendorf
Unter Kritzendorf
Klosterneuburg-Kierling
Klosterneuburg-Weidling
Nußdorf
Siemens-straße
Leopoldau
Brünner Straße
Floridsdorf
S7 U6
Neue Donau
Handelskai
S45
U1
Süßenbrunn
Deutsch Wagram
Helmahof
Strasshof
Silberwald
Gänserndorf
S1
Großfeldsiedlung
Aderklaaer Straße
Rennbahnweg
Kagraner Platz
Kagran
Alte Donau
Kaisermühlen - VIC
Donauinsel
Vorgartenstraße
Oberdöbling
Heiligenstadt
U4
Dresdner Straße
Krottenbachstraße
Spittelau
Jäger-straße
Traisengasse
Gersthof
Nußdorfer Straße
Friedensbrücke
Währinger Straße - Volksoper
Roßauer Lände
Hernals
Michelbeuern - AKH
Alser Straße
S40 Franz-Josefs-Bahnhof
Taborstraße
Praterstern
Hirschstetten (2015)
S80
Aspern Nord
Hausfeld-straße
Seestadt
U2
Aspernstraße
Josefstädter Straße
Thaliastraße
Ottakring
U3
Schottenring
Nestroyplatz
Messe-Prater
Krieau
Stadion
Erzherzog-Karl-Straße
Kendlerstraße
Schottenter Universität
Schwedenplatz
Donaumarina
Donaustadtbrücke
Stadlau
Hardeggasse
Donauspital
S50
S60
Rekawinkel
Dürrwien
Breitensee
Hütteldorfer Straße
Burggasse Stadthalle
Rathaus
Preßbaum
Purkersdorf-Gablitz
Purkersdorf Sanatorium
Hadersdorf
S45
S60 U4
Hütteldorf
Penzing
John-straße
Schwegler-straße
Ziegler-gasse
Volks-theater
Stubentor
Landstraße Bahnhof Wien Mitte
Rochusgasse
Tullnerbach-Preßbaum
Unter Tullnerbach
Unter Purkersdorf
Weidlingau
Wolf in der Au
S50 West-bahnhof
Neubau-gasse
Herren-gasse
Stephans-platz
Kardinal-Nagl-Platz
Lobau
Gumpendorfer Straße
Museumsquartier
Schlachthausgasse
Praterkai
Unter St Veit
Ober St Veit
Schön-brunn
Längenfeld-gasse
Kettenbrücken-gasse
U2
Karls-platz
Stadt-park
Erdberg
Braun-schweig-gasse
Hietzing
Meidling Hauptstraße
Margareten-gürtel
Pilgram-gasse
VLB
Paulanergasse
Mayerhofgasse
Joh.-Strauß-Gasse
Laurenzgasse
Gasometer
Rennweg
Taubstummen-gasse
Zippererstr.
Speising
Niederhofstraße
Wolfgang-gasse
Eichen-straße
Kliebergasse
Blechturm-gasse
Südtiroler Platz
Enkplatz
Haidestraße
Bahnhof Meidling
St. Marx
Quartier Belvedere
Geisel-bergstr.
Simmering
U3
S3
Matzleinsdorfer Platz
Haupt-bahnhof
Keplerplatz
Reumannplatz
U1
Zentralfriedhof
Kaiser-ebersdorf
Manns-wörth
Fischamend
Haslau
Wildungs-mauer
Bad Deutsch Altenburg
Hainburg Pbf
Wolfsthal
S7
Schwechat
Flughafen Wien
Maria Ellend
Regelsbrunn
Petronell-Carnuntum
Hainburg Pbf
Hainburg Ungarter
Tscherttegasse
Schedifkaplatz
Schöpfwerk
Gutheil-Schoder-Gasse
Inzersdorf Pbf.
Neu Erlaa
Schönbrunner Allee
Vösendorf-Siebenhirten
Vösendorf-SCS
Maria Enzersdorf-Südstadt
Wiener Neudorf
Griesfeld
Neu Guntramsdorf
Guntramsdorf Lokalbahn
Eigenheimsiedlung
Hetzendorf
Am Schöpfwerk
Alterlaa
Erlaaer Straße
Perfektastraße
Siebenhirten
U6
Atzgersdorf
Liesing
Perchtoldsdorf Hst.
Brunn-Maria Enzersdorf
Mödling
S1
Guntramsdorf Südbahn
Gumpoldskirchen
Pfaffstätten
Baden
Baden Josefsplatz
VLB
Leesdorf
Pfaffstätten Rennplatz
Traiskirchen Lokalbahn
Melkergründe
Tribuswinkel-Josefsthal
Möllersdorf
Bad Vöslau
Kottingbrunn
Leobersdorf
Sollenau
Felixdorf
Theresienfeld
Wiener Neustadt Nord
Wiener Neustadt Hbf
S1 S2 S3 S80
Wiener Neustadt Civitas Nova
Blumental
Hennersdorf
Achau
Münchendorf
Ebreichsdorf
Weigelsdorf
Wampersdorf
Pottendorf-Landegg
Ebenfurth
Obereggendorf
Unteregendorf
Grillgasse
Kledering
Lanzendorf-Rannersdorf
Himberg
Gramatneusiedl
Trautmanns-dorf
Wifleins-dorf
S60
Parndorf Ort
Götzendorf
Sarasdorf
Bruck a. d. Leitha
S60
Neusiedl am See

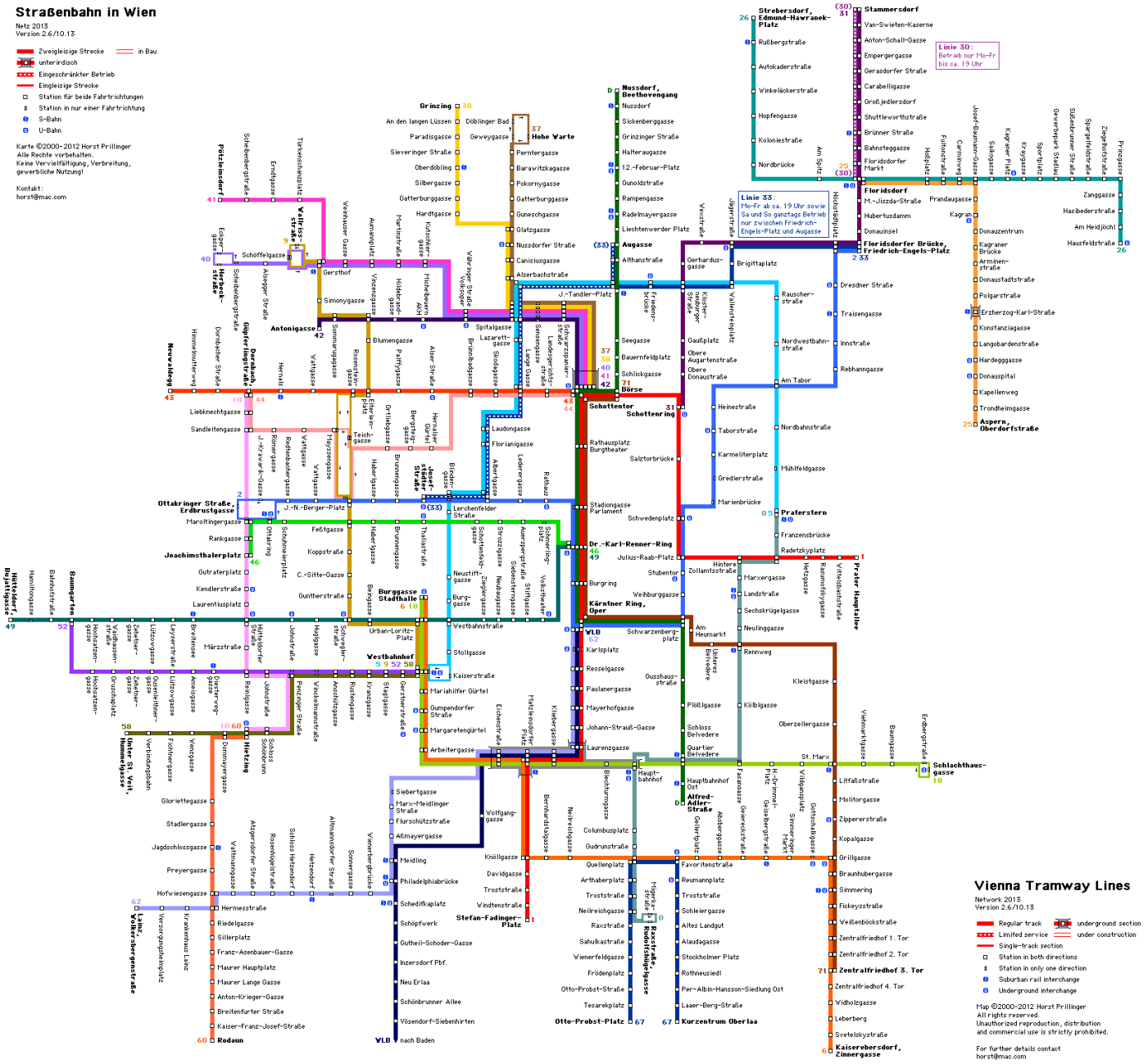
Straßenbahn in Wien
Netz 2013
Version 2.6/10.13
Zweigleisige Strecke
in Bau
unterirdisch
Eingeschränkter Betrieb
Eingleisige Strecke
Station für beide Fahrtrichtungen
Station in nur einer Fahrtrichtung
S-Bahn
U-Bahn
Karte ©2000-2012 Horst Prillinger
Alle Rechte vorbehalten.
Keine Vervielfältigung, Verbreitung, gewerbliche Nutzung!
Kontakt:
horst@mac.com
Linie 30:
Betrieb nur Mo-Fr bis ca. 19 Uhr
Linie 33:
Mo-Fr ab ca. 19 Uhr sowie Sa und So ganztags Betrieb nur zwischen Friedrich-Engels-Platz und Augasse
Vienna Tramway Lines
Network 2013
Version 2.6/10.13
Regular track
underground section
Limited service
under construction
Single-track section
Station in both directions
Station in only one direction
Suburban rail interchange
Underground interchange
Map ©2000-2012 Horst Prillinger
All rights reserved.
Unauthorized reproduction, distribution and commercial use is strictly prohibited.
For further details contact
horst@mac.com

TU Wien

Kuppelsaal: 1040, Karlsplatz 13, 4. Stk.

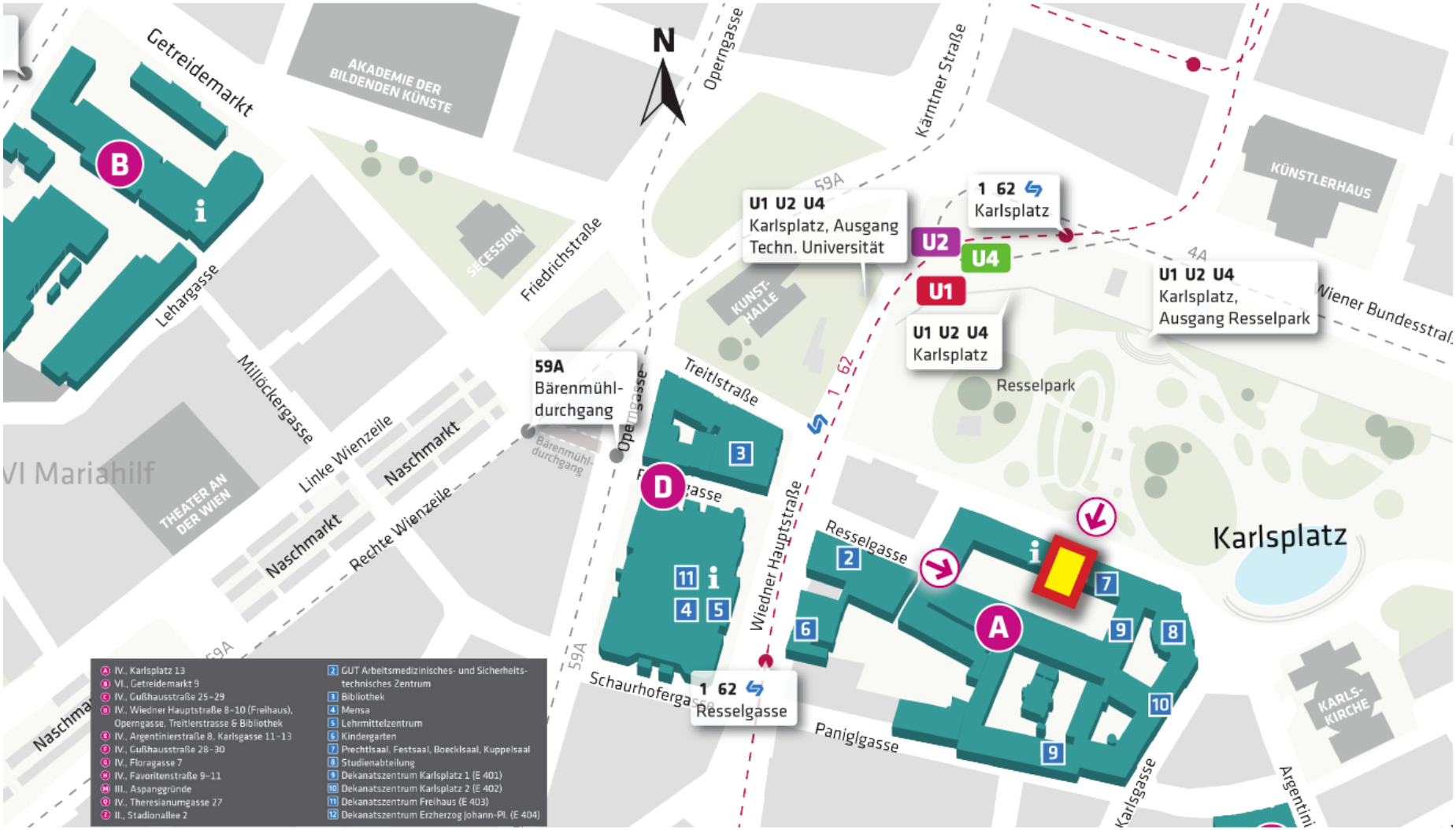

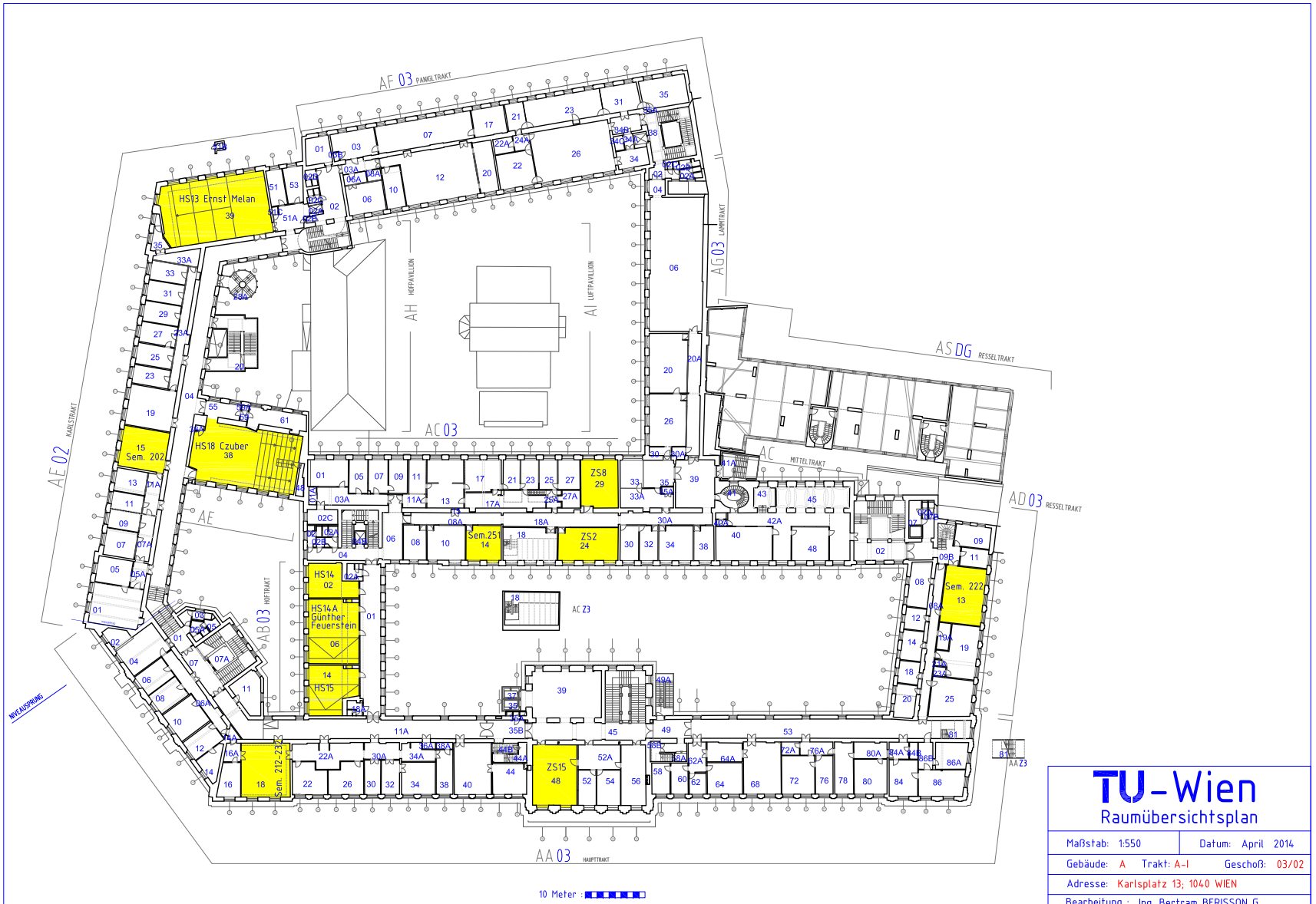

TU-Wien
Raumübersichtsplan

Maßstab: 1:550	Datum: April 2014
Gebäude: A Trakt: A-I	Geschoß: 03/02
Adresse: Karlsplatz 13; 1040 WIEN	
Bearbeitung : Ing. Bertram BERISSON G. bberisson@gut.tuwien.ac.at	

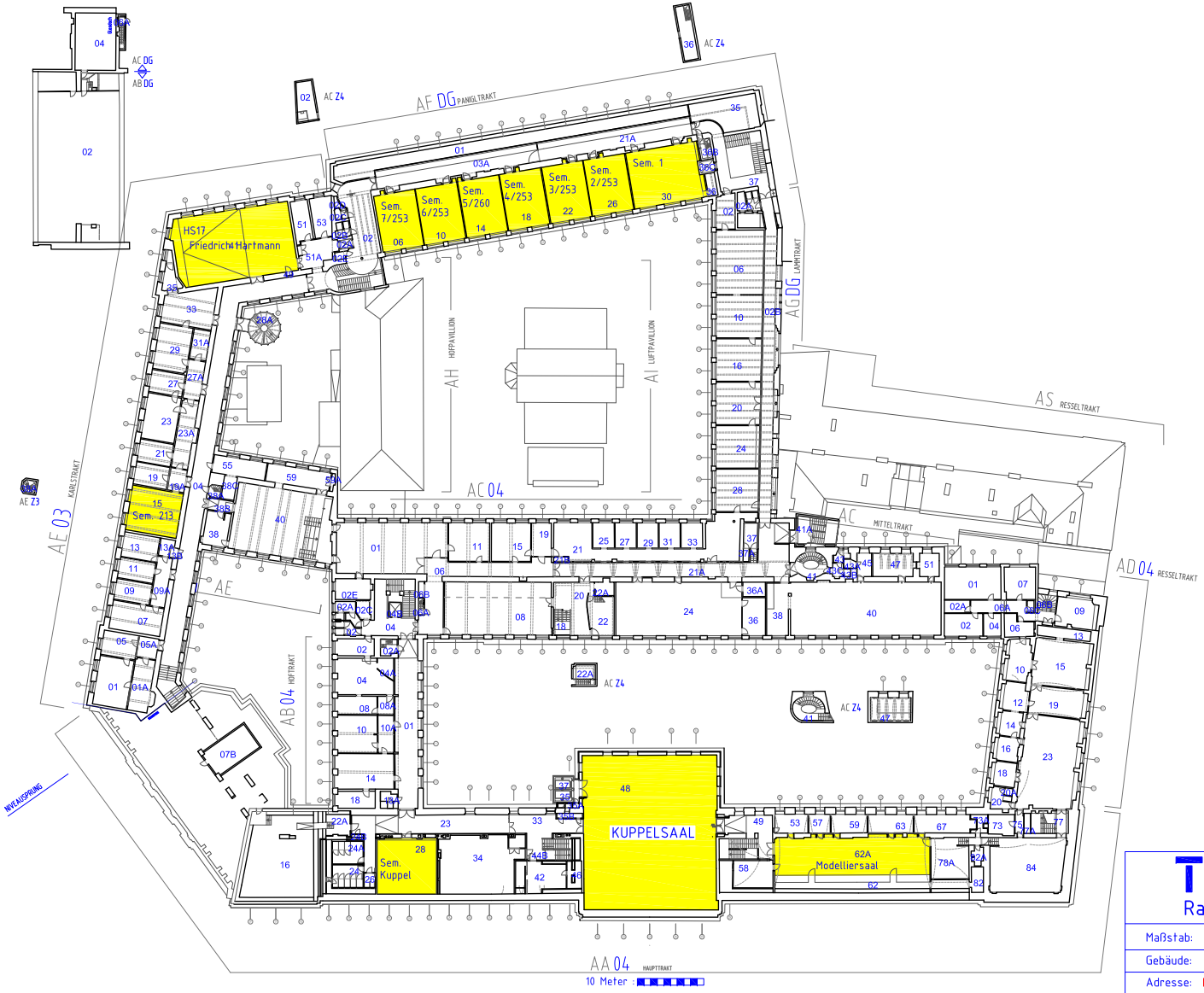

TU-Wien
Raumübersichtsplan

Maßstab: 1:550	Datum: Dez. 2013
Gebäude: A Trakt: A-I	Geschoß: 04/03
Adresse: Karlsplatz 13; 1040 WIEN	
Bearbeitung : Ing. Bertram BERISSON G. bberisson@gut.tuwien.ac.at	

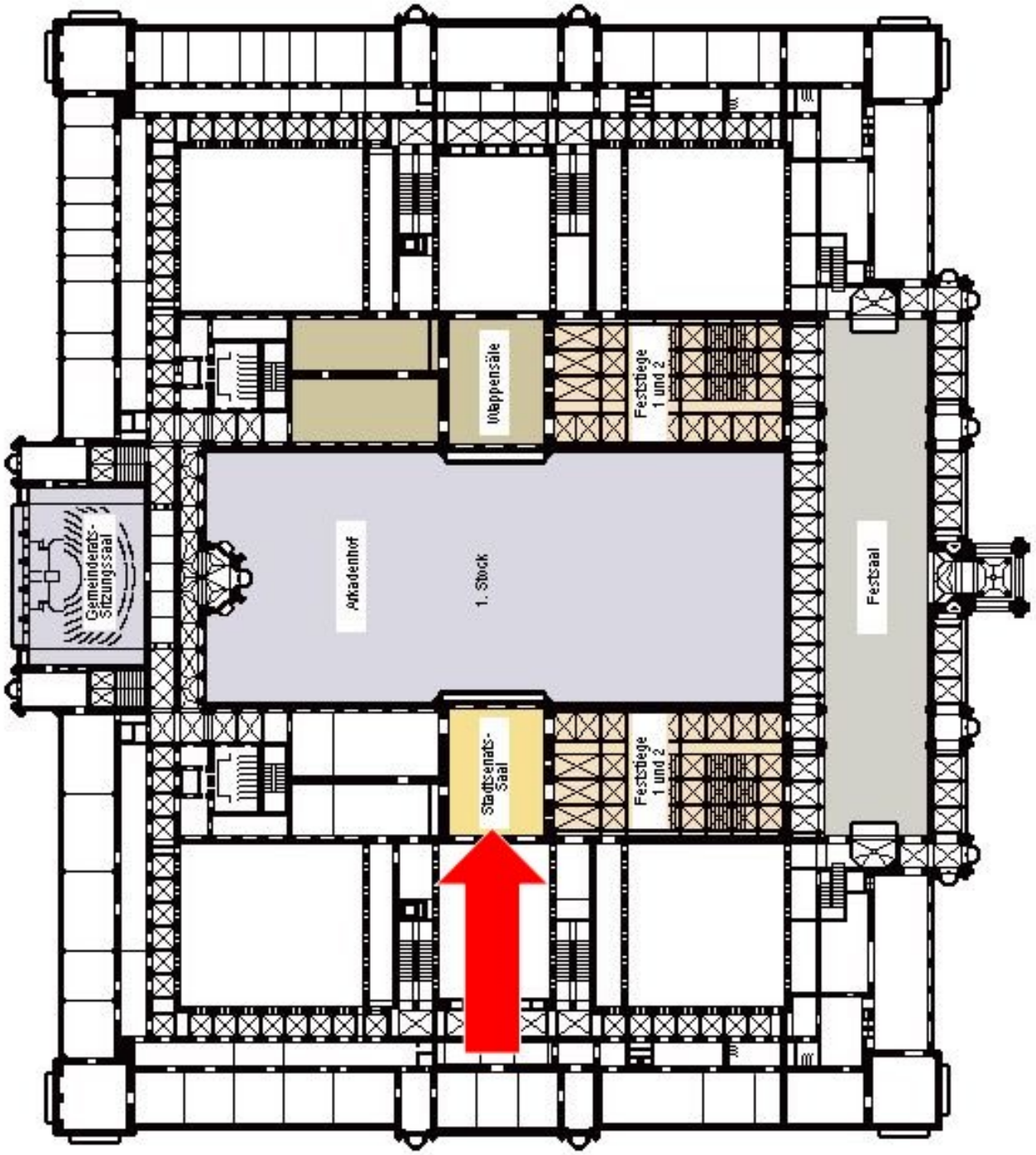
Gemeinderats-Sitzungssaal
Arkadenhof
1. Stock
Wappensäle
Feststiege 1 und 2
Festsaal
Stadtsenats-Saal
Feststiege 1 und 2


Mayor's House
Rathaus
Herrengasse
Stephansplatz
INNERE STADT
VIENN
Volkstheater
ST ULRICH
NEUBAU
Museumsquartier
LAIMGRUBE
Karlsplatz
Naschmarkt
Wachau Meeting Point
TU Vienna
Neubaugasse

Sponsors

The organizers gratefully acknowledge financial support through:

European Research Community on Flow,
Turbulence and Combustion (ERCOFTAC)

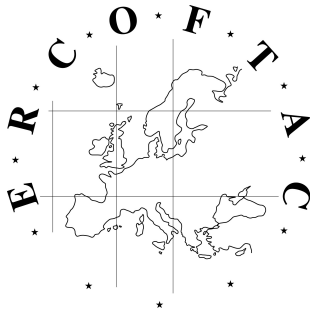

Magistrat der Stadt Wien